



THE UNIVERSITY *of* EDINBURGH

This thesis has been submitted in fulfilment of the requirements for a postgraduate degree (e.g. PhD, MPhil, DClinPsychol) at the University of Edinburgh. Please note the following terms and conditions of use:

This work is protected by copyright and other intellectual property rights, which are retained by the thesis author, unless otherwise stated.

A copy can be downloaded for personal non-commercial research or study, without prior permission or charge.

This thesis cannot be reproduced or quoted extensively from without first obtaining permission in writing from the author.

The content must not be changed in any way or sold commercially in any format or medium without the formal permission of the author.

When referring to this work, full bibliographic details including the author, title, awarding institution and date of the thesis must be given.

Mast Cell Recruitment and Activation as Measures of Cyathostomin Burden

Ruth Jocelyn Muriel Clements

A thesis submitted for the requirements of Doctor of Philosophy degree registered by
the College of Medicine and Veterinary Medicine, University of Edinburgh.

Research conducted at Moredun Research Institute

Table of Contents

Declaration	vii
Acknowledgements	viii
Abstract	ix
Figures	xi
Tables	vii
List of Abbreviations.....	xxvii
1 General Introduction	1
1.1 Equine Gastrointestinal Parasites	1
1.2 Cyathostominae.....	2
1.2.1 Life cycle.....	3
1.2.2 Mucosal Larval Stages	4
1.2.3 Current Control Strategies	5
1.2.4 Anthelmintic Resistance	6
1.2.5 Clinical Significance	7
1.3 Mast cells in Gastrointestinal Parasitism	9
1.3.1 Mast Cell Overview	9
1.3.2 Mast Cells in Nematode infections	11
1.3.3 Mast Cell Serine Proteinases.....	14
1.3.4 Mast Cell Serine Proteinases in Nematode Infections	20
1.4 Diagnostic Approach to Cyathostomin Infection.....	21
1.5 Thesis aims.....	24
2 Investigation of Recruitment of Large Intestinal Mast Cells in Response to Cyathostomin Infection	25

2.1	Introduction	25
2.2	Materials and Methods	27
2.2.1	Sampling Protocol.....	27
2.2.2	Abattoir Sampling Protocol	27
2.2.3	R(D)SVS Sampling Protocol	27
2.2.4	Serum Samples.....	29
2.2.5	Faecal Samples.....	29
2.2.6	Rectal Samples	29
2.2.7	Luminal Contents for Parasite Enumeration	30
2.2.8	Tissue Samples for Parasite and Mast Cell Enumeration and Mast Cell Proteinase Quantitation	31
2.2.9	Faecal Egg Count	31
2.2.10	Luminal Cyathostomin Enumeration	32
2.2.11	Transmural Illumination to Detect Mural Cyathostomins	32
2.2.12	Peptic Digestion	32
2.2.13	Mast Cell Staining.....	33
2.2.14	Mast Cell Enumeration	34
2.2.15	Haemotoxylin and Eosin Staining.....	34
2.2.16	Carbol Chromotrope Staining	34
2.2.17	DAB Staining for Eosinophils	35
2.2.18	Enumeration of Eosinophils.....	35
2.2.19	Data Analysis	35
2.3	Results	37
2.3.1	Sample Cohort.....	37
2.3.2	Comparison of Location of Sample Collection.....	41

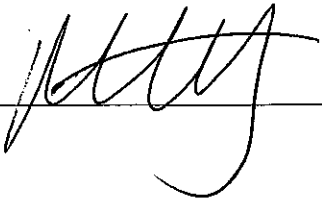
2.3.3	Cyathostomin Recovery	43
2.3.4	Parasitology.....	47
2.3.5	Mast Cell Response.....	60
2.3.6	Correlations between Mast Cell Counts at Different Mucosal Sites	64
2.3.7	Eosinophil Populations	68
2.3.8	Mast Cells and Cyathostomin Burdens	70
2.4	Discussion	77
3	Characterisation of Large Intestinal Mast Cell Activation in Response to Cyathostomin Infection	86
3.1	Introduction	86
3.2	Materials and Methods	90
3.2.1	Purified Proteinase Verification and Validation	90
3.2.2	IgG Purification from Rabbit Sera	90
3.2.3	Biotinylation of anti eqMCP-1 Rabbit IgG.....	91
3.2.4	Tissue Samples for Parasite and Mast Cell Enumeration and Mast Cell Proteinase Quantitation	91
3.2.5	Immunohistochemistry.....	92
3.2.6	Single Immunohistochemistry using DAB Substrate	93
3.2.7	Serum Collection and Storage for ELISA.....	94
3.2.8	Tissue Preparation for ELISA.....	95
3.2.9	Optimisation of Serum and Tissue ELISAs for eqTRYP and eqMCP-1.	95
3.2.10	Data Analysis	106
3.3	Results	107
3.3.1	Validation of eqTRYP and eqMCP-1	107
3.3.2	Dual-Immunofluorescence.....	109

3.3.3	Immunohistochemistry.....	110
3.3.4	Analysis of Equine Tissue eqMCP-1 and eqTRYP Concentrations Measured by ELISA.....	144
3.4	Discussion	153
4	Exploration of Novel Equine Mast Cell Proteinases.....	163
4.1	Introduction	163
4.2	Materials and methods	167
4.2.1	Sample Selection for Proteomic analysis.....	167
4.2.2	Liquid Chromatography- Electrospray Ionisation– Tandem Mass Spectrometry (LC-ESI-MS/MS)	167
4.2.3	Proteomic Analysis of MS/MS Data.....	168
4.2.4	MALDI-TOF-MS for Recombinant Protein Identification	169
4.2.5	Proteinase Sequence Analysis and Selection	169
4.2.6	Processing and Storage of Tissue Material	169
4.2.7	RNA Extraction from Equine Tissue	170
4.2.8	RNA Validation	170
4.2.9	Complementary DNA Production.....	171
4.3	Design of Primers.....	171
4.3.1	Primer Validation and PCR Amplicon Sequencing.....	173
4.3.2	House Keeping Gene Selection.....	174
4.3.3	Probe Design for Quantitative PCR for Genes of Interest.....	176
4.3.4	Probe design for Quantitative PCR housekeeping genes.....	180
4.3.5	Generation of Plasmid Standards for Quantitative PCR.....	180
4.3.6	Probe Verification	180
4.3.7	Quantitative PCR of Equine Tissue Samples.....	181

4.3.8	Re-annotation of Equine Genome.....	181
4.3.9	Data Analysis	182
4.4	Results	183
4.4.1	Sequence Selection for Identification of Additional Proteinases.....	183
4.4.2	Sequence Analysis of PCR Products	193
4.4.3	Reference Gene Selection	199
4.4.4	Probe Validation	201
4.4.5	Quantitative PCR Efficiency.....	202
4.4.6	Tissue Transcript Levels from Quantitative PCR	204
4.4.7	Relationship between Mast Cell Proteinase Transcripts and Mucosal Cyathostomin Burdens	211
4.4.8	Relationship between Tissue Transcript Expression and Mast Cell Populations.....	213
4.5	Relationship between Tissue Transcript Levels and Tissue Proteinase Concentration	217
4.6	Relationship between Tissue Transcript Levels and Serum Proteinase Concentration	220
4.7	Discussion	224
5	General Discussion.....	235
6	References	245
7	Appendix A: Additional Data	269
8	Appendix B: Nucleotide and Protein Sequences	279
9	Appendix C: General Laboratory Solutions and Procedures.....	282

Declaration

The work presented in this thesis is my own work, unless otherwise stated, and has not been submitted for any other degree or professional qualification.

 Ruth Clements

Acknowledgements

I would like to start by formally thanking my supervisors, Jacqui Matthews, Tom McNeilly, John Keen and Kirstie Pickles for all their help, patience and support throughout my journey. Each of you provided me with valuable guidance and I will be forever grateful for the time you invested in my work and development. In addition, I would like to wholeheartedly thank Darren Shaw and Alan Pemberton for their guidance, insight and support throughout. I am also very grateful to the Horserace Betting Levy Board for their funding and interest in my research. This work would not have been possible without the staff at the R(D)SVS and CES. I would like to thank them for helping me collect the necessary clinical samples. I hope this work goes some way to fulfilling my goal of improving equine health.

There are a number of scientists who I would also like to thank. In particular, my fellow PhD cohort at the Moredun Research Institute. Each one of you has individually helped me along the way and I have enjoyed sharing this chapter of our lives together. Also, within Moredun I would especially like to thank Jeanie Finlayson, Neil Inglis, Kevin Mclean and Mairi Mitchell for teaching me new techniques, helping with my experiments and offering me such sound advice.

Most importantly I would like to thank my parents, family and friends for your constant and unwavering support. In particular my amazing partner, Dan Tipney, who always believes in me, and whose kindness, understanding and love has been my rock throughout.

Finally, I would like to dedicate this work to the memory of my wonderful mother, Dr. Elizabeth Clements (1957-2011); the most incredible and inspiring role model, with formidable energy.

I could never have started this without you; but I finished it for you.

Abstract

Cyathostomins are potentially life threatening parasitic nematodes of adult horses and are highly prevalent worldwide. Infected animals may be asymptomatic or show clinical signs of weight loss, diarrhoea and colic. Third and fourth stage larvae spend a large proportion of their lifecycle encysted in the large intestinal wall where they cannot currently be detected ante mortem. Mast cells are commonly found at interfaces to the external environment, such as the rectum, and these cells and the proteinases they produce have been implicated in protective host immune responses against nematode infection in animals. Previous studies have demonstrated an increase in caecal mast cell proteinase expression during cyathostomin infection. Prior to this study, there were two known equine mast cell proteinases, which had been purified and characterised from a mastocytoma (equine tryptase [eqTRYP] and equine mast cell proteinase-1 [eqMCP-1]). However, as many mammalian species express multiple closely-related chymases it was hypothesised that other equine mast cell proteinases exist that have not yet been characterised and which may be more closely associated with the level of worm burden. The primary objective of this study was to investigate the recruitment of mast cells to the large intestine in cyathostomin infected horses and the expression of mast cell proteinases in response to infection. A further aim was to evaluate the potential of associated mast cell proteinase assays or rectal biopsy mast cell enumeration for utility in diagnostic tests to estimate cyathostomin mucosal burden. A secondary objective was to explore the existence of further mast cell proteinases and the relationship of these enzymes to cyathostomin mucosal burden. Optimised sampling protocols, parasitological, histological and immunohistochemistry techniques were performed to enumerate cyathostomin mucosal burden and to characterise the mast cell populations in the caecum, right ventral colon (RVC) and rectum of naturally infected horses (n=28). Mast cell populations correlated throughout the intestine, providing further evidence of the common mucosal system. EqMCP-1 and eqTRYP labelled mast cells were identified throughout the large intestine. Significant positive linear relationship existed between rectal proteinase-labelled mucosal mast cell populations and both the combined total cyathostomin mucosal burden (CTMB; eqMCP-1, $p=0.018$; eqTRYP, $p=0.048$) and

the combined total luminal burden (CTLB; eqMCP-1, $p=0.009$; eqTRYP, $p=0.007$). Concentrations of eqMCP-1 and eqTRYP in (i) serum, (ii) local serum from venous blood draining the large intestine, and (iii) large intestinal tissue homogenates were assessed using ELISA. There was no significant correlation identified between local and peripheral serum proteinase concentrations suggesting that peripheral serum proteinase levels are not representative of the local proteinase response. There was however a significant negative relationship between peripheral serum eqMCP-1 concentrations and the CTMB, which could relate to the activation and sequestering of proteinases within the gut lumen. Concentrations of eqMCP-1 and eqTRYP measured in local serum did not significantly positively correlate with cyathostomin mucosal burden. There was a significant association observed between intestinal tissue levels of eqMCP-1 and eqTRYP and the CTMB in the RVC ($p<0.023$), providing support for their role in the immune response. Four proteinase sequences, equine tryptase (TLP1), Granzyme B-like (GZMBL), putative equine Mast Cell Proteinase-1 (CLP1) and Granzyme(BGH)-like (GZM(BGH)L), were sequenced and the local transcription levels of each of these enzymes assessed using quantitative reverse-transcription PCR. The expression of TLP1 was closely correlated with GZMBL expression, and there was a significant positive relationship observed between TLP1 and GZMBL transcript levels and combined total mucosal burden in the RVC. Both GZM(BGH)L and CLP1 transcript levels were also positively correlated with each other, but the levels of these transcripts were not statistically correlated to any of the cyathostomin parasitological measures assessed here.

This work has provided the basis for further rectal biopsy studies to examine the important dynamics of the mast cell response to cyathostomin infection. The results from this thesis, with the demonstration of novel proteinases, are encouraging for further investigation into equine mast cell proteinases and their role in cyathostomin infections.

Figures

Figure 1.1: Cyathostomin life cycle	3
Figure 2.1: Schematic of protocol for processing of samples from the R(D)SVS and equine abattoir	28
Figure 2.2: Individual value plot of $\log_{10}+1$ transformed total luminal cyathostomin counts from abattoir and R(D)SVS horses for comparison of sample location.	42
Figure 2.3: Individual value plot of $\log_{10}+1$ transformed CTMB counts from abattoir and R(D)SVS horses for comparison of sample location	42
Figure 2.4: Image of developing larvae	43
Figure 2.5: Images of larvae released from tissue.....	43
Figure 2.6: Image from Transmural Illumination of areas suggestive of empty cysts. A: AB16 Caecum. B: AB3 Right ventral colon.....	44
Figure 2.7: Rectal mucosal larvae at varying stages of development	45
Figure 2.8: Individual Value Plot of $\log_{10}+1$ transformed CTMB grouped according to presence or absence of rectal mucosal larvae.....	45
Figure 2.9: Image of a clinical case of larval cyathostominosis, horse DV3, at post mortem	46
Figure 2.10: Image of inflamed, hyperaemic and oedematous tissue from the right ventral colon of Horse DV3, a case of larval cyathostominosis	46
Figure 2.11: Barchart of average faecal egg count of all horses sampled (AB1-16 and DV1-12)	47
Figure 2.12: Image of luminal cyathostomins stained with iodine	48
Figure 2.13: Scatterplot of $\log_{10}+1$ transformed RVC luminal versus caecal luminal counts coloured according to sample location	49

Figure 2.14: A: Individual $\log_{10}+1$ transformed value plot of caecal and RVC luminal counts. B: Graph of individual values of caecal and RVC luminal counts	49
Figure 2.15: Image of evidence of developing larvae at various stages on Transmural Illumination from the caecum of horse AB6.....	50
Figure 2.16: Scatterplot of $\log_{10}+1$ transformed RVC DL versus caecal DL counts coloured according to sample location.....	51
Figure 2.17: A: Individual value plot of $\log_{10}+1$ transformed caecal and RVC DL counts. B: Graph of individual values of $\log_{10}+1$ caecal and RVC DL counts	51
Figure 2.18: Image of encysted third stage larvae released from tissue through pepsin digest and stained with iodine.	52
Figure 2.19: Scatterplot of $\log_{10}+1$ transformed caecal EL3 versus RVC EL3 counts coloured according to sample location.....	52
Figure 2.20: A: Individual value plot of $\log_{10}+1$ transformed caecal and RVC EL3 counts. B: Graph of individual values of $\log_{10}+1$ caecal and RVC EL3 counts	53
Figure 2.21: A: Scatterplot of $\log_{10}+1$ transformed caecal DL from TMI versus caecal DL from DIG counts. B: Scatterplot of $\log_{10}+1$ transformed counts of RVC DL from TMI versus RVC DL from DIG	54
Figure 2.22: A: Individual $\log_{10}+1$ transformed value plot of caecal DL from TMI and caecal DL from DIG counts. B: Graph of individual values of $\log_{10}+1$ caecal DL from TMI and caecal DL from DIG counts.....	54
Figure 2.23: A: Individual $\log_{10}+1$ transformed value plot of RVC DL from TMI and RVC DL from DIG counts. B: Graph of individual values of $\log_{10}+1$ RVC DL from TMI and RVC DL from DIG counts.....	55
Figure 2.24: A: Individual $\log_{10}+1$ transformed value plot of caecal TMB and RVC TMB. B: Graph of individual values of $\log_{10}+1$ caecum and RVC TMB	56

Figure 2.25: Matrix scatterplot of log10+1 transformed data for total (caecum and RVC combined) luminal, total DL, total EL3, CTMB and average FEC grouped according to sample location.....	58
Figure 2.26: Scatterplot of average cell count per field of MMC from RS versus RB	61
Figure 2.27: A: Individual value plot of average cell count per field of RS and RB MMC counts. B: Graph of individual values of RS and RB MMC counts	61
Figure 2.28: A: Individual value plot of average cell count per field of RS and RB submucosal mast cell counts. B: Graph of individual values of RS and RB SMMC counts	62
Figure 2.29: Image of caecal tissue section from horse AB9 stained with Toluidine Blue	63
Figure 2.30: Image of caecal tissue section from horse DV3 stained with Toluidine Blue	63
Figure 2.31: Image of right ventral colon mucosal tissue from horse DV3 stained with Toluidine Blue	64
Figure 2.32: Scatterplot of caecal MMC versus caecal SMMC.....	64
Figure 2.33: Scatterplot of RVC SMMC versus RVC MMC	65
Figure 2.34: Scatterplot of RB SMMC versus RB SMMC.....	65
Figure 2.35: Matrix scatterplot of counts for caecal, RVC and RB MMC	66
Figure 2.36: Matrix scatterplot of counts for caecal, RVC and RB SMMC.....	67
Figure 2.37: A: Image of a caecal tissue section fixed in Carnoy's and stained with H&E. B: Image of a caecal tissue section fixed in formalin and stained with H&E	68
Figure 2.38: Individual Value Plot of A: caecal MMC and B: caecal SMMC	69
Figure 2.39: Individual Value Plot of A: RVC MMC and B: RVC SMMC Cells grouped according to presence or absence of Tapeworm	70

Figure 2.40: Individual Value Plot of A: RB MMC and B: RB SMMC Cells grouped according to presence or absence of Tapeworm	70
Figure 2.41: Boxplot of the 28 horses divided into 4 groups according to CTMB....	72
Figure 2.42: Boxplots A: Caecal TB MMC counts B: Caecal TB SMMC counts	72
Figure 2.43: Boxplots A: RVC TB MMC counts. B: RVC TB SMMC counts.....	72
Figure 2.44: Boxplots A: RB TB MMC counts. B: RB TB SMMC counts	73
Figure 2.45: Relationship between log ₁₀ +1 transformed CTMB and Caecal MMC	73
Figure 2.46: Relationship between log ₁₀ +1 transformed CTMB and Caecal SMMC	74
Figure 2.47: Relationship between log ₁₀ +1 transformed CTMB and RVC MMC ..	74
Figure 2.48: Relationship between log ₁₀ +1 transformed CTMB and RVC SMMC.	75
Figure 2.49: Relationship between log ₁₀ +1 transformed CTMB and RB	75
Figure 2.50: Relationship between log ₁₀ +1 transformed CTMB and RB SMMC ...	76
Figure 3.1: EqMCP-1 serum ELISA: Graph of serum dilution curves of four horses (DV1, DV2, DV3 and DV8)	98
Figure 3.2: EqTRYP serum ELISA: Graph of serum dilution curves from two horses (DV9 and AB16) and the pooled serum of cyathostomin-negative horses.....	100
Figure 3.3: EqMCP-1 caecal tissue ELISA: Graph of tissue homogenate dilution curves from three horses (DV2, AB1 and DV9).....	101
Figure 3.4: EqTRYP tissue homogenate ELISA: Graph of caecal tissue homogenate dilution curves from three horses (DV2, AB1 and DV9)	102
Figure 3.5: Graph of OD readings at 492nm for serum and tissue samples for eqTRYP ELISA with two different capture antibodies, rabbit anti eqTRYP IgG and rabbit IgG	103
Figure 3.6: Barchart of samples for eqTRYP ELISA with three different blocking solutions	104

Figure 3.7: Validation of equine mast cell proteinases. Scanned image of a Simple Blue stained SDS-PAGE gel.....	107
Figure 3.8: Validation of equine mast cell proteinases. Scanned image of a Western blot	108
Figure 3.9: Validation of anti-equine albumin removal from anti eqMCP-1 antiserum. Scanned image of Western blots	109
Figure 3.10: Image of caecal mucosa demonstrating immunolabelled cells. A: eqTRYP at 2µg/ml and B: eqMCP-1 at 2µg/ml.....	110
Figure 3.11: Images of caecal tissue dual-immunolabelled with negative control antibodies	110
Figure 3.12: Image of a section of caecal tissue from horse AB9 at labelled with A: rabbit anti eqMCP-1 IgG at 0.2µg/ml. B: rabbit IgG at 0.2µg/ml	111
Figure 3.13: Image of a section of caecal tissue from horse AB9 at x 400 magnification labelled with A: rabbit anti eqTRYP IgG at 0.2µg/ml. B: rabbit IgG at 0.2µg/ml	111
Figure 3.14: A: Graph of individual values of caecal mucosal eqMCP-1- counts and eqTRYP-labelled mast cell counts B: Graph of individual values of caecal submucosal eqMCP-1 counts and eqTRYP-labelled mast cell counts	113
Figure 3.15: A: Graph of individual values of RVC mucosal eqMCP-1- and eqTRYP-labelled mast cell counts. B: Graph of individual values of RVC submucosal eqMCP-1+ and eqTRYP-labelled mast cell counts	113
Figure 3.16: A: Graph of individual values of rectal mucosal eqMCP-1- and eqTRYP-labelled mast cell counts B: Graph of individual values of rectal submucosal eqMCP-1- and eqTRYP-labelled mast cell counts	114
Figure 3.17: A: Graph of individual values from caecal mucosal TB counts and eqMCP-1 counts. B: Graph of individual values from caecal submucosal TB counts and eqMCP-1 counts	115

Figure 3.18: A: Graph of individual values from RVC mucosal TB counts and eqMCP-1 counts. B: Graph of individual values from RVC submucosal TB counts and eqMCP-1 counts	115
Figure 3.19: A: Graph of individual values from rectal mucosal TB counts and eqMCP-1 counts B: Graph of individual values from rectal submucosal TB counts and eqMCP-1 counts	116
Figure 3.20: Matrix scatterplot of log ₁₀ + 1 transformed counts for caecal Toluidine blue, eqMCP-1 and eqTRYP MMC and SMMC	119
Figure 3.21: Matrix scatterplot of log ₁₀ + 1 transformed counts for RVC Toluidine blue, eqMCP-1 and eqTRYP MMC and SMMC	120
Figure 3.22: Matrix scatterplot of log ₁₀ + 1 transformed counts for Rectal Toluidine blue, eqMCP-1 and eqTRYP MMC and SMMC	121
Figure 3.23: Relationship between log ₁₀ +1 transformed CTMB and RB eqMCP-1 MMC	125
Figure 3.24: Relationship between log ₁₀ +1 transformed CTMB and RB eqTRYP MMC	125
Figure 3.25: Barchart of eqMCP-1 concentrations of serum samples stored at -20 °C and -80 °C	127
Figure 3.26: A: Scatterplot of eqMCP-1 concentrations from local and peripheral serum. B: Bland-Altman plot of eqMCP-1 concentrations from local and peripheral serum.....	128
Figure 3.27: A: Individual value plot of eqMCP-1 serum concentrations (ng/ml) from local and peripheral sites. B: Graph of individual values of eqMCP-1 serum concentrations	128
Figure 3.28: Barchart of eqTRYP concentrations of serum samples stored at -20 °C and -80 °C	130
Figure 3.29: Scatterplot of eqTRYP concentrations from local and peripheral serum B: Bland-Altman plot of eqTRYP concentrations from local and peripheral serum	131

Figure 3.30: A: Individual value plot eqTRYP serum concentration from local and peripheral sites. B: Graph of individual values of eqTRYP serum concentrations from local and peripheral sources	131
Figure 3.31 A: Scatterplot of local serum results eqMCP-1 versus eqTRYP serum. B: Scatterplot of peripheral serum results eqMCP-1 versus eqTRYP serum ..	132
Figure 3.32: A: Relationship between log10+1 transformed CTMB and local serum eqMCP-1 concentrations. B: Relationship between log10+1 transformed CTMB and local serum eqTRYP concentrations	135
Figure 3.33: A: Relationship between log10+1 transformed CTLB and local serum eqMCP-1 concentrations. B: Relationship between log10+1 transformed CTLB and local serum eqTRYP concentrations	135
Figure 3.34: A: Relationship between log10+1 transformed CTMB and peripheral serum eqMCP-1 concentrations B: Relationship between log10+1 transformed CTMB and peripheral serum eqTRYP concentrations	136
Figure 3.35: A: Relationship between log10+1 transformed CTLB and peripheral eqMCP-1 concentrations B: Relationship between log10+1 transformed CTLB and peripheral serum eqTRYP concentrations.....	136
Figure 3.36: Boxplot of the 16 horses with serum samples divided into four groups according to CTMB.....	137
Figure 3.37: Local eqMCP-1 serum concentrations of the 16 horses with serum samples divided into four groups according to CTMB.....	137
Figure 3.38: Local eqTRYP serum concentrations of the 16 horses with serum samples divided into four groups according to CTMB.....	138
Figure 3.39: Scatterplots of eqMCP-1 and eqTRYP tissue concentration.....	145
Figure 3.40: Graphs of individual horse eqMCP-1 and eqTRYP tissue concentrations	146
Figure 3.41: Boxplot of Caecal log10+1eqMCP-1 tissue concentrations.....	148
Figure 3.42: Boxplot of Caecal log10+1 eqTRYP tissue concentrations	149

Figure 3.43: Boxplot of RVC log10+1 eqMCP-1 tissue concentrations	149
Figure 3.44: Boxplot of RVC log10+1 eqTRYP tissue concentrations	149
Figure 3.45: Boxplot of RB log10+1 eqMCP-1 tissue concentrations	150
Figure 3.46: Boxplot of RB log10+1 eqTRYP tissue concentrations.....	150
Figure 3.47: Relationship between log10+1 transformed CTMB and RVC eqMCP-1 tissue concentration	151
Figure 3.48: Relationship between log10+1 transformed CTMB and RVC eqTRYP tissue concentration	152
Figure 4.1: Alignment of the four amplicons of interest with primers and probe for TLP1 highlighted	178
Figure 4.2: Alignment of relevant equine proteinase predicted sequences from blastn of granzyme B-like (GZMBL) amplicon (<i>E. caballus</i>) with highlighted primer sequences and selected probe sequence	178
Figure 4.3: Alignment of both equine proteinase predicted sequences from blastn of CLP1 amplicon (<i>E. caballus</i>) with highlighted primer sequences and selected probe sequence	179
Figure 4.4: Alignment of relevant equine proteinase predicted sequences from blastn of Granzyme(BGH)-like amplicon (<i>E. caballus</i>) with highlighted primer sequences and selected probe sequence	179
Figure 4.5: A: EqTRYP SDS PAGE gel showing the three slices each lane was divided into. B: The corresponding Western blot probed with rabbit IgG anti- eqTRYP and developed with ECL.....	184
Figure 4.6: A: EqMCP-1 SDS PAGE gel showing the three slices each lane was divided into. B: The corresponding eqMCP-1 western blot probed with rabbit IgG anti-eqMCP-1 and developed with ECL.....	184
Figure 4.7: Alignment of the nine novel proteinase candidates in granzymeDB identified by Mascot database search.....	185

Figure 4.8: Alignment of the nine sequences in the granzymeDB. The sequences were grouped according to the residue at 226. Results are compared to the sequences for MCP1 <i>Ovis Aries</i> , GZMB <i>Mus Muscularis</i> and GZMB <i>Homo Sapiens</i> with known specificity.....	187
Figure 4.9: Alignment of the four selected sequences, TLP1, CLP1, GZMBL and GZM(BGH)L with MCP1 <i>ovis aries</i> , GZMB <i>Mus Muscularis</i> and GZMB <i>Homo Sapiens</i> for comparison and highlighted residues and important bases.....	190
Figure 4.10: N terminal aa sequence of the 9 proteins in the granzymeDB database	192
Figure 4.11: N terminal aa sequences from TLP1 compared with the sequences from human tryptase- β , ovine tryptase-1 and bovine tryptase.....	192
Figure 4.12: N terminal aa sequences from EQMCP-1, CLP1 and predicted sequences for GZMBL and GZM(BGH)L compared with the sequences human granzyme H, sheep mast cell proteinase-1 and bovine duodenase	192
Figure 4.13: Agarose gel image showing the PCR products using the four primer sets generated from cDNA from horses DV11 and DV12.....	193
Figure 4.14: A-D: Agarose gel image showing the PCR products from caecal tissue from horse DV3, DV5, DV6, DV10, DV12 and DV11	194
Figure 4.15: Alignment of nucleotide sequence of TLP1 amplicons from DV3 Caecum, DV6 Caecum, DV10 Caecum, DV11 Caecum and DV12 RVC.	196
Figure 4.16: Alignment of predicted protein sequence of TLP1 amplicons from DV3 Caecum, DV6 Caecum, DV10 Caecum, DV11 Caecum and DV12 RVC using reading frame 2 direct	196
Figure 4.17: Alignment of nucleotide sequence of GZMBL amplicons from DV3 Caecum, DV6 Caecum, DV10 Caecum, DV11 Caecum and DV12 RVC	196
Figure 4.18: Alignment of predicted protein sequence of GZMBL amplicons from DV3 Caecum, DV6 Caecum, DV10 Caecum, DV11 Caecum and DV12 RVC using reading frame 3 direct.....	197

Figure 4.19: Alignment of nucleotide sequence of CLP1 amplicons from DV3 Caecum, DV6 Caecum, DV10 Caecum, DV11 Caecum and DV12 RVC	197
Figure 4.20: Alignment of predicted protein sequence of CLP1 amplicons from DV3 Caecum, DV6 Caecum, DV10 Caecum, DV11 Caecum and DV12 RVC using reading frame 2 direct	197
Figure 4.21: Alignment of nucleotide sequence of GZM(BGH)L amplicons from DV3 Caecum, DV6 Caecum, DV10 Caecum, DV11 Caecum and DV12 RVC	198
Figure 4.22: Alignment of predicted protein sequence of GZM(BGH)L amplicons from DV3 Caecum, DV6 Caecum, DV10 Caecum, DV11 Caecum and DV12 RVC using reading frame 1 direct	198
Figure 4.23: Alignment of GZMB(L), GZM(BGH)L and human and rat granzyme H	199
Figure 4.24: Graph of average expression stability of reference target genes	200
Figure 4.25: Bar chart to determine optimal number of reference targets	201
Figure 4.26: Plasmid standard curves from qPCR for each of the four genes of interest	203
Figure 4.27: Bar charts of the normalised number of copies per μ l of TLP1, GZMBL, CLP1, GZM(BGH)L in A: Caecum. B: RVC. C: RB.....	205
Figure 4.28. Box plots of individual proteinase transcript levels divided by organ	206
Figure 4.29: Matrix scatter plot of caecal transcript levels of TLP1, GZMBL, CLP1 and GZM(BGH)L.....	207
Figure 4.30: Matrix scatter plot of RVC transcript levels of TLP1, GZMBL, CLP1 and GZM(BGH)L.....	209
Figure 4.31: Matrix scatter plot of RB transcript levels of TLP1, GZMBL, CLP1 and GZM(BGH)L	210
Figure 4.32. Relationship between $\log_{10}+1$ transformed Caecal TMB and: A: Caecal TLP1. B: Caecal GZMBL. C: Caecal CLP1. D: Caecal GZM(BGH)L.....	211

Figure 4.33. Relationship between log ₁₀ +1 transformed RVC TMB and: B: RVC TLP1. B: RVC GZMBL. C: RVC CLP1. D: RVC GZM(BGH)L.....	212
Figure 4.34: A: Relationship between log ₁₀ +1 transformed CTMB and A: Rectal TLP1. B: Rectal GZMBL. C: Rectal CLP1. D: Rectal GZM(GBH)L.....	213
Figure 4.35: Matrix scatter plot of log ₁₀ +1 transformed counts for caecal mast cell counts and caecal transcript levels	214
Figure 4.36: Matrix scatter plot of log ₁₀ +1 transformed counts for RVC mast cell counts and RVC transcript levels	215
Figure 4.37: Matrix scatter plot of log ₁₀ +1 transformed counts for RB mast cell counts and RB transcript levels.....	216
Figure 4.38: Matrix scatter plot of log ₁₀ +1 transformed data for the amount of caecal eqMCP-1 and eqTRYP from Tissue ELISA and caecal transcript levels.....	217
Figure 4.39: Matrix scatter plot of log ₁₀ +1 transformed data for the amount of RVC eqMCP-1 and eqTRYP from Tissue ELISA and RVC transcript levels	218
Figure 4.40: Matrix scatter plot of log ₁₀ +1 transformed data for the amount of RB eqMCP-1 and eqTRYP from Tissue ELISA and RB transcript levels	219
Figure 4.41: Matrix scatter plot of log ₁₀ +1 transformed data for the amount of caecal eqMCP-1 and eqTRYP from -20°C serum ELISA and caecal transcript levels	221
Figure 4.42: Matrix scatter plot of log ₁₀ +1 transformed data for the amount of RVC eqMCP-1 and eqTRYP from -20°C serum ELISA and RVC transcript levels.	222
Figure 4.43: Matrix scatter plot of log ₁₀ +1 transformed data for the amount of rectal eqMCP-1 and eqTRYP from -20 °C serum ELISA and RB transcript levels .	223
Figure 7.1: Barchart of mean eqMCP-1 tissue concentrations from ELISA.	277
Figure 7.2: Barchart of mean eqTRYP tissue concentrations from ELISA.....	278

Tables

Table 1.1: Table of human, mouse and horse mast cell subclasses	15
Table 2.1: Results of non-mucosal cyathostomin enumerations and tapeworm observations from abattoir horses, AB1-16	37
Table 2.2: Results of mucosal cyathostomin enumerations from abattoir horses.....	38
Table 2.3: Data collected from R(D)SVS horses including sample date, age, gender and reason for euthanasia	39
Table 2.4: Results of non-mucosal cyathostomin enumerations and tapeworm observations from R(D)SVS horses	40
Table 2.5: Results of mucosal cyathostomin enumerations from R(D)SVS horses ..	41
Table 2.6: Table of p-values and rho values for correlations between FEC and cyathostomin burdens.....	48
Table 2.7: Table of p-values and rho values for correlations between caecal and RVC TMB's and parasitology data	56
Table 2.8: Table of p values and rho values for correlation matrix of cyathostomin count data	59
Table 2.9: Results of mucosal and submucosal mast cell counts from the rectal sections and rectal biopsies of abattoir horses, AB1-16	60
Table 2.10: Median and range of mucosal and submucosal mast cell counts from the caecum, RVC and rectum of all horses, AB1-16 and DV1-12	62
Table 2.11: Correlations between caecal, RVC and RB mucosal mast cells	66
Table 2.12: Correlations between caecal, RVC and RB submucosal mast cells	66
Table 2.13: Correlations between caecal, RVC and RB mucosal and submucosal mast cells	67
Table 2.14: Median and range of mucosal and submucosal eosinophil counts from the caecum, RVC and rectum of horses DV6-12	69

Table 2.15: Median and range of MMC and SMMC from the caecum, RVC and rectum of all cyathostomin-negative horses.....	71
Table 3.1: Table of eqMCP-1 mast cell counts from horses DV 1, DV2, DV3 and DV 8.....	98
Table 3.2: Table of eqTRYP mast cell counts from horses AB16 and DV 9	99
Table 3.3: Inter- and Intra-assay Coefficients of Variation for the eqMCP-1 and eqTRYP serum and tissue ELISAs	106
Table 3.4: Median and range of MMC and SMMC eqMCP-1-labelled cells from the caecum, RVC and rectum of all horses, AB1-16 and DV1-12	112
Table 3.5: Median and range of MMC and SMMC eqTRYP-labelled cells from the caecum, RVC and rectum of all horses, AB1-16 and DV1-12	112
Table 3.6: Correlation matrix of p values and rho values for Toluidine blue, eqMCP-1 and eqTRYP-labelled mast cell count data	118
Table 3.7: Table of p-values for the significance of co-infection with <i>A. perfoliata</i> on TB, eqMCP-1 and eqTRYP-labelled MMC and SMMC in the caecum, RVC and rectum.....	122
Table 3.8: Table of p-values and r^2 values for the relationships between log ₁₀ +1 transformed MMC and SMMC Toluidine blue, eqMCP-1 and eqTRYP-labelled mast cell counts and log ₁₀ +1 transformed CTMB or CTLB.....	124
Table 3.9: Table of p and rho values for correlations of local serum ELISA eqMCP-1 and eqTRYP concentrations with mast cell counts.....	133
Table 3.10: Table of p and rho values for correlations of peripheral serum ELISA eqMCP-1 and eqTRYP concentrations with mast cell counts	134
Table 3.11: Median and range of eqMCP-1 tissue concentrations from the caecum, RVC and rectum of all horses, AB1-16 and DV1-12	138
Table 3.12: Table of p and rho values for correlations of tissue homogenate eqMCP-1 concentration between organs	139

Table 3.13: Table of p and rho values for correlations of eqMCP-1 concentrations from the caecum, RVC and rectum of all horses, AB1-16 and DV1-12	140
Table 3.14: Median and range eqTRYP tissue concentration from the caecum, RVC and rectum of all horses, AB1-16 and DV1-12.....	141
Table 3.15: Table of p and rho values for correlations of tissue homogenate eqTRYP concentrations between organs	141
Table 3.16: Table of p and rho values for correlations of eqTRYP tissue concentration from the caecum, RVC and rectum of all horses (AB1-16 and DV1-12) with TB, eqMCP-1- and eqTRYP- labelled cell counts	143
Table 3.17: Table of p and rho values for correlations of tissue homogenate eqMCP-1 concentration with eqTRYP concentration	144
Table 3.18: Table of p and rho values for correlations of tissue homogenate concentration of eqTRYP with local serum concentrations of eqTRYP and eqMCP-1	147
Table 3.19: Table of p and rho values for correlations of tissue homogenate concentration of eqMCP-1 with local serum concentrations of eqTRYP and eqMCP-1	147
Table 3.20: Table of p and r^2 values for linear regression analysis of the tissue proteinase concentration of eqMCP-1 and eqTRYP in the caecum, RVC and RB and the CTMB or CTLB	151
Table 4.1: Primer sequences and product length for each of the four amplicons of interest	172
Table 4.2: Table of results from a BLASTn search against the NCBI equine genome database using the PCR products for each gene of interest as the query sequence	173
Table 4.3: Table of the 15 samples of equine tissue selected at random for geNorm analysis.....	175
Table 4.4: Table of probe sequences and related information for each of the four genes of interest.....	177

Table 4.5: Table of the nine GranzymeDB sequences grouped according to their aa at residue 226	188
Table 4.6: Table of Ct values from Primer/Probe combinations	202
Table 4.7: Table of the range of efficiencies for each qPCR reaction	203
Table 4.8: Median and range of Caecal TLP1, GZMBL, CLP1 and GZM(BGH)L transcript levels	207
Table 4.9: Table of rho values and p values for correlations between genes of interest in the caecum.....	208
Table 4.10: Median and range of RVC TLP1, GZMBL, CLP1 and GZM(BGH)L transcript levels	208
Table 4.11: Table of rho values and p values for correlations between genes of interest in the RVC.....	209
Table 4.12: Median and range of rectal TLP1, GZMBL, CLP1 and GZM(BGH)L transcript levels	210
Table 4.13: Table of rho values and p values for correlations between genes of interest in the rectum from rectal biopsy	210
Table 4.14: Table of rho values and p values for correlations between genes of interest in the caecum and caecal TB, eqMCP-1 and eqTRYP MMC and SMMC	214
Table 4.15: Table of rho values and p values for correlations between genes of interest in the RVC and RVC TB, eqMCP-1 and eqTRYP MMC and SMMC	216
Table 4.16: Table of rho values and p values for correlations between genes of interest in the rectum and rectal TB, eqMCP-1 and eqTRYP MMC and SMMC from rectal biopsy	217
Table 4.17: Table of rho values and p values for correlations between Caecal genes of interest and Caecal eqMCP-1 and eqTRYP Tissue ELISA results	218

Table 4.18: Table of rho values and p values for correlations between RVC genes of interest and RVC eqMCP-1 and eqTRYP tissue ELISA results.....	219
Table 4.19: Table of rho values and p values for correlations between RB genes of interest and RB eqMCP-1 and eqTRYP tissue ELISA results.....	220
Table 4.20: Table of rho values and p values for correlations between genes of interest from Caecal tissue and eqMCP-1 and eqTRYP serum ELISA results.	221
Table 4.21: Table of rho values and p values for correlations between genes of interest from RVC tissue and eqMCP-1 and eqTRYP serum ELISA results ..	222
Table 4.22: Table of rho values and p values for correlations between genes of interest from rectal biopsy and eqMCP-1 and eqTRYP -20°C serum ELISA results	223
Table 7.1: Results of mucosal and submucosal mast cell counts from the caecum, RVC and rectum of all horses, AB1-16 and DV1-12	269
Table 7.2: Results of mucosal and submucosal eosinophil cell counts from the caecum, RVC and rectum of R(D)SVS horses	270
Table 7.3: Table of eqMCP-1 labelled mast cells in the mucosa and submucosa in the caecum, RVC and rectum from all horses, AB1-16 and DV1-12.....	271
Table 7.4: Table of eqTRYP labelled mast cells in the mucosa and submucosa in the caecum, RVC and rectum from all horses, AB1-16 and DV1-12.....	272
Table 7.5: Table of mean serum eqMCP-1 ELISA concentration results from serum collected from a local or peripheral site and stored at -20 °C or -80 °C.....	273
Table 7.6: Table of mean serum eqTRYP ELISA concentration results from serum collected from a local or peripheral site and stored at -20 °C or -80 °C.....	274
Table 7.7: Table of mean eqMCP-1 ELISA results from caecal, RVC and RB tissue	275
Table 7.8: Table of mean eqTRYP ELISA results from caecal, RVC and RB tissue	276

List of Abbreviations

AA	– Amino acid
AB	– Abattoir
ACN	– Acetonitrile
ACT β	– Beta-actin
B2M	– Beta-2-microglobulin
BZ	– Benzimidazole
CHCA	– α -cyano-4-hydroxycinnamic acid
CLP1	– Chymase-like Proteinase-1
Ct	– Threshold cycle
CTMB	– Combined total mucosal burden
CTLB	– Combined total luminal burden
CTMC	– Connective tissue mast cell
Cy-GALA	– Cyathostomin gut-associated larval antigen
DIG	– Pepsin tissue Digest
DL	–Developing larvae
EL3	– Encysted third stage larvae
ELISA	– Enzyme linked immunosorbent assay
EPG	– Egg per gram
EqMCP-1	– Equine mast cell proteinase-1
EqTRYP	– Equine tryptase
ERP	– Egg reappearance period
FEC	– Faecal egg count
GABA	– Gamma-aminobutyric acid
GALT	– Gut associated lymphoid tissue
GAPDH	– Glyceraldehyde 3-phosphate dehydrogenase
GZM(BGH)L	– Granzyme(BGH)-like
GZMBL	– Granzyme B-like
H&E	– Haemotoxylin and eosin
HPLC	– High-performance liquid chromatography
HPRT	– Hypoxanthine phosphoribosyltransferase
IHC	– Immunohistochemistry

IPTG – Isopropyl β -D-1-Thiogalactopyranoside
LL3 – Late third stage larvae
L – Local
Lum – Luminal
MC – Mast cell
MLS – Macrocyclic lactones
MMC – Mucosal mast cell
mMCP – Mouse mast cell proteinase
MS/MS – Tandem mass spectrometry
NCBI – National Center for Biotechnology Information
P – Peripheral
PBS – Phosphate buffered saline
PI – Post infection
PM – Post mortem
qPCR – Quantitative polymerase chain reaction
R(D)SVS – Royal (Dick) School of Veterinary Studies
RB – Rectal biopsy
RIN – RNA integrity number
RN18SRS – 18s ribosomal RNA
RVC – Right ventral colon
SDHA – Succinate dehydrogenase complex, subunit A, flavoprotein
SMMC – Submucosal mast cell
SNP – Single nucleotide polymorphism
TB – Toluidine blue
TH2 – T helper 2
THPS – Tetrahydropyrimidines
TLP1 – Tryptase-like proteinase-1
TMB – Total mucosal burden
TMI – Transmural illumination
TNF- β – Tumour necrosis factor- β

1 General Introduction

1.1 Equine Gastrointestinal Parasites

Equine parasites have been recognised as a cause of clinical disease for many centuries (Kaplan and Nielsen 2010). The introduction of the anthelmintic interval dosing strategies in the 1960's (Kaplan and Nielsen 2010), designed to primarily target *Strongylus* species, combined with the availability of benzimidazole anthelmintics (McKellar and Jackson 2004), was successful in reducing large strongyle nematode populations. This strategy was so effective that by the 1980's small strongyles, cyathostomins, frequently accounted for virtually 100% of faecal egg counts (FECs) (Drudge and Lyons 1966; Herd, Miller et al. 1981; Herd and Gabel 1990; Kaplan 2002; Kaplan and Nielsen 2010). Despite the concern that strict interpretation of the selective therapy regimen, based on the anthelmintic treatment of horses with FECs above a pre-determined threshold (Duncan and Love 1991), could be associated with an increase in prevalence of *Strongylus vulgaris* (Nielsen, Vidyashankar et al. 2012), cyathostomins are still considered the principal parasitic pathogen of horses over the age of six months (Love, Murphy et al. 1999; Kaplan and Nielsen 2010; Kornas, Cabaret et al. 2010; Hinney, Wirtherle et al. 2011). *Anoplocephala perfoliata* is the most common equine cestode and is prevalent in populations worldwide (Gasser, Williamson et al. 2005). This tapeworm has been implicated in various types of colic, including caeco-caecal intussusception (Edwards 1986; Owen, Jagger et al. 1989), spasmodic colic (Proudman, French et al. 1998) and intestinal obstruction (Slocombe 1979); however, recent studies have questioned these findings by demonstrating no association between colic and *A. perfoliata* infection (Trotz-Williams, Physick-Sheard et al. 2008). In foals, the principal parasite is the small intestinal nematode, *Parascaris equorum*, which can cause weight loss and gastrointestinal disease (Reinemeyer 2009). However, patent infection is rare and of less importance in adult horses, as protective immunity to this parasite is thought to develop by the age of six months (Clayton and Duncan 1979; Laugier, Sevin et al. 2012).

1.2 *Cyathostominae*

Cyathostomins (family Strongylidae, subfamily Cyathostominae) pose a major threat to the health and welfare of equidae worldwide (Mfitilodze and Hutchinson 1990; Love, Murphy et al. 1999). Their prevalence and pathogenicity make them the most important equine nematodes (Love, Murphy et al. 1999). The vast majority of grazing horses will be exposed to cyathostomin infection to varying degrees throughout their lives, the control of which relies heavily on anthelmintic treatments (Matthews 2011). Of the fifty or so cyathostomin species described, over forty have been reported in horses (Lichtenfels, Gibbons et al. 2002); however, the majority of animals have burdens mainly comprised of ten common species (Torbert, Klei et al. 1986; Lyons, Tolliver et al. 1999). These species are reported by Ogbourne (1976) as; *Cylicostephanus longibursatus*, *Cyathostomum catinatum*, *Cylicostephanus goldi*, *Cylicocyclus nassatus*, *Cyathostomum coronatum*, *Cylicostephanus calicatus*, *Cylicostephanus minutus*, *Cylicocyclus leptostomus*, *Cyathostomum pateratum* and *Cylicocyclus insigne* (Ogbourne 1976). Similar species' prevalence have been reported by Reineymeyer et al. (Reinemeyer, Smith et al. 1984), Torbert et al. (Torbert, Klei et al. 1986) Lyons et al. (Lyons, Tolliver et al. 1996; Lyons, Tolliver et al. 1996) and, more recently, Traversa et al. (Traversa, Milillo et al. 2010). In a comparative study between populations in Germany, Italy and the UK, a reverse line blot (RLB) macroprobing assay (Traversa, Iorio et al. 2007) was performed to assess the distribution of 13 common cyathostomin species (Traversa, Milillo et al. 2010). These species were the ten listed above with the addition of *Coronocyclus labiatum*, *Coronocyclus labratum* and *Cylicocyclus ashworthi* (Traversa, Iorio et al. 2007). Of the three countries, Italy had the highest proportion of horses with a low number of species; 12% of yards had 2-3 cyathostomin species compared to 5% in the UK and none in Germany. Germany in comparison had the highest proportion of horses with the most diverse number of species; 40% of yards had 10-13 cyathostomin species compared to 25% in Italy and 27% in the UK (Traversa, Milillo et al. 2010). The differences between countries may be due to selection pressure imposed by differing anthelmintic treatment approaches; the clinical significance of this variation is not yet known (Traversa, Milillo et al. 2010).

1.2.1 Life cycle

Cyathostomins have a direct, non-migratory life cycle (Figure 1.1). After ingestion from pasture, third stage larvae (L3) penetrate the wall of the large intestine, predominantly the caecum and the right ventral colon (Ogbourne 1976). Within the intestinal wall, larvae go through a number of developmental stages, initially as L3 and then fourth stage larvae (L4). The L4 emerge from the intestinal mucosa and continue development in the gut lumen to L5 and subsequently adults, the female of which produce eggs after mating, which are passed into the environment in faeces. The eggs hatch and release first stage larvae (L1) and these develop in the faeces into second stage larvae and then the infective L3 (Matthews 2008). Cyathostomin development in faeces is dependent on temperature and moisture (Nielsen, Kaplan et al. 2007; Matthews 2010; dos Santos, de Souza et al. 2011).

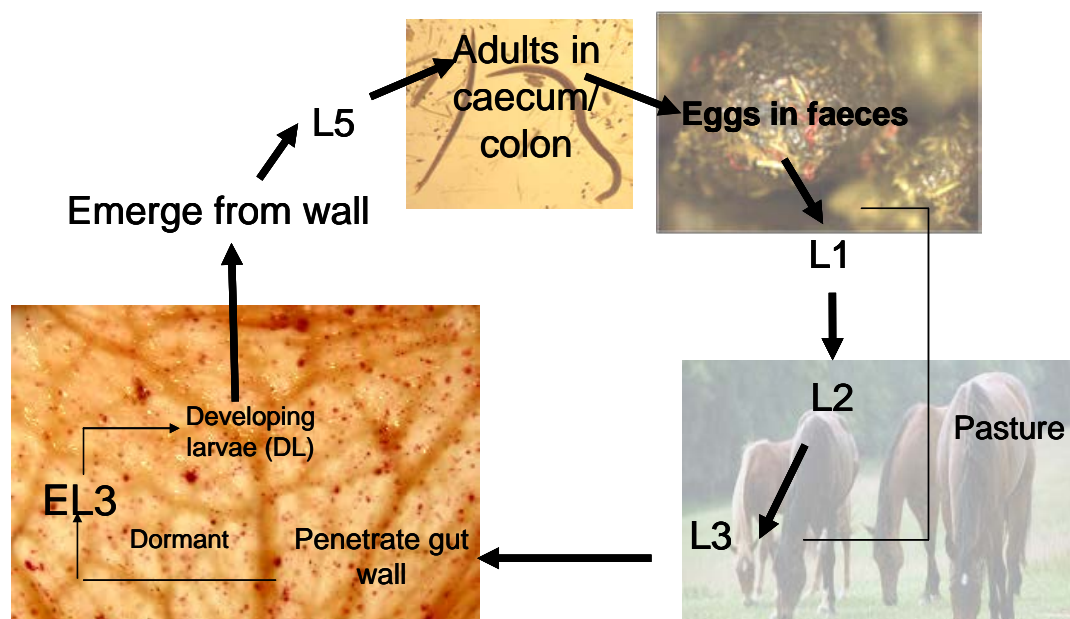


Figure 1.1: Cyathostomin life cycle. Developing larvae (DL) include late L3, early L4 and late L4 in the intestinal mucosa. (EL3: early third stage larvae).

1.2.2 Mucosal Larval Stages

The pre-patent period from ingestion of L3 to release of eggs in faeces has been stated as approximately 6-12 weeks (Love and Duncan 1992); however, L3 can encyst in the gut wall for a longer period of time (inhibited development) lasting from months to years (Gibson 1953; Murphy and Love 1997). A consequence of this is that larvae can potentially accumulate in the mucosa of the intestinal tract to the order of several million (Smets, Shaw et al. 1999; Dowdall, Matthews et al. 2002). These encysted larvae play an important role in the epidemiology and pathogenesis of cyathostominosis (Giles, Urquhart et al. 1985) as the natural period of larval maturation appears to coincide with clinical cases of larval cyathostominosis. The exact mechanisms controlling this inhibited state are poorly understood. Epidemiological risk factors associated with the diagnosis of cyathostminosis have been demonstrated through multivariate analysis of assigned parameters using logistic regression (Reid, Mair et al. 1995). It was highlighted that the disease is more probably a cause of chronic diarrhoea in horses younger than six yrs. Those animals that have received anthelmintic treatment within the previous two weeks have an increased likelihood of cyathstominosis diagnosis by three and a half times. Also, animals affected in the winter months are nearly five times more likely to have cyathostominosis than animals presenting with diarrhoea in the summer (Reid, Mair et al. 1995). In the UK and other temperate climates, larvae tend to encyst during the cooler winter months and may emerge en masse in the spring (Giles, Urquhart et al. 1985). In the case of tropical climate the reverse is seen, where larvae emerge in the autumn following inhibition during the hot summer period (Baudena, Chapman et al. 2000). It is also not clear as to what causes the encysted larvae to re-emerge. A reduction in the luminal cyathostomin population due to, for example, treatment with an anthelmintic may trigger mucosal emergence (Eysker, Boersema et al. 1997; Cobb and Boeckh 2009). Seasonal effects, host immunity, the magnitude and duration of challenge have all also been suggested (Murphy and Love 1997; Love, Murphy et al. 1999; Chapman, French et al. 2002; Matthews 2008).

1.2.3 Current Control Strategies

Anthelmintics are currently the main method of helminth control in horses (Stratford, McGorum et al. 2011). The anthelmintics currently available in the UK are divided into three classes; the benzimidazoles (BZs: fenbendazole, oxbendazole), tetrahydropyrimidines (THPS: pyrantel salts) and the macrocyclic lactones (MLs: ivermectin and moxidectin). The MLs approved for use in the horse are ivermectin and moxidectin, an avermectin and a milbemycin, respectively (Gokbulut, Nolan et al. 2001). These anthelmintics are thought to exert their effects by binding to gamma-aminobutyric acid (GABA) and glutamate-gated channels and paralyse parasites (Shoop, Mrozik et al. 1995; Cobb and Boeckh 2009). Both MLs have proven efficacy against adult worms (Xiao, Herd et al. 1994; Molento, Nielsen et al. 2012); however, there are reported differences in efficacies against inhibited third stage larvae. In some studies ivermectin has been reported to have little to no efficacy against inhibited third stage larvae (Eysker, Boersema et al. 1992; Klei, Chapman et al. 1993; Xiao, Herd et al. 1994). However, others have reported a significant reduction (>75%) in mucosal larvae following treatment with oral ivermectin paste compared to untreated controls (Love, Duncan et al. 1995). Reports for moxidectin vary in efficacies against encysted third stage cyathostomin larvae ranging from insignificant (Xiao, Herd et al. 1994; Monahan, Chapman et al. 1995) to greater than 90% (Bairden, Brown et al. 2001; Bairden, Davies et al. 2006). The discrepancies in observations for ivermectin and moxidectin efficacy may be related to experimental design (Love, Duncan et al. 1995). In particular, differences in the nature of experimental, compared to natural, infections may have an effect (Monahan, Chapman et al. 1996). Also in the case of moxidectin, which demonstrates persistent activity resulting in a long egg reappearance interval (Demeulenaere, Vercruysse et al. 1997; Vercruysse, Eysker et al. 1998), necropsies performed at different time points after treatment may lead to difficulty in interpretation of efficacy on various encysted stages (Eysker, Boersema et al. 1997; Bairden, Brown et al. 2001).

To date, specific targeted administration of anthelmintics based on encysted larval burdens has been hindered by a lack of knowledge of an individual's current infection status. FECs provide a rough estimate of adult luminal worms, but give no

indication of encysted larval burdens (Giles, Urquhart et al. 1985; Dowdall, Matthews et al. 2002). Mucosal larval stages, i.e. early L3, late L3 and developing L4, can constitute the major proportion of an individual's cyathostomin burden (Duncan, Bairden et al. 1998; Collobert-Laugier, Hoste et al. 2002; Dowdall, Matthews et al. 2002). Therefore, whilst FECs may be a good indicator of an individual's capacity to contaminate pasture and may also facilitate a reduction in selection pressure for anthelmintic resistance (Lester, Bartley et al. 2013), they do not give an accurate estimation of the encysted larval burden (Duncan, Bairden et al. 1998; Klei and Chapman 1999; Dowdall, Matthews et al. 2002). Due to the severity of the disease and the consequences of untreated infection, the use of regular blanket treatment against encysted cyathostomin larvae with moxidectin has been advocated (Bairden, Brown et al. 2001). Such non-targeted and frequent treatments are likely to be a significant risk factor for the development and spread of anthelmintic resistance (Matthews 2011).

1.2.4 Anthelmintic Resistance

A feature of growing concern with regards to equine cyathostomin infection is the development of anthelmintic resistance (Love and Mckeand 1997). Cyathostomins have demonstrated signs of resistance to all three available drug classes (Molento, Antunes et al. 2008; Traversa, von Samson-Himmelstjerna et al. 2009). A reversion to susceptibility does not seem to occur in parasitic nematodes in general (Jackson and Coop 2000; Slocombe, Cote et al. 2008) and the fact that resistance is essentially everlasting is a further incentive to encourage new, more sustainable, approaches to control (Sangster 1999; Kaplan 2004). As there are no new equine anthelmintics currently under development, it is important to preserve the efficacy of those presently available (Kaplan and Nielsen 2010; Lester, Spanton et al. 2013). Benzimidazole resistance in cyathostomins is well documented and widespread (Dorny, Meijer et al. 2000; Kaplan 2002; Matthews 2008) and resistance to the pyrantel salts has also been demonstrated (Kaplan, Klei et al. 2004; Slocombe and de Gannes 2006; Traversa, Castagna et al. 2012). The situation in Brazil is of great concern, where resistance to all three anthelmintic classes was reported after all

tested products failed to reduce FEC by 95% and gave inadequate cyathostomin control up to 28 days after treatment (Molento, Antunes et al. 2008; Molento, Nielsen et al. 2012). There is further evidence of multi-class resistance, as reduced efficacy of both fenbendazole and pyrantel have been reported (Kaplan 2004; Traversa, Klei et al. 2007; Traversa, Castagna et al. 2012; Relf, Lester et al. 2014).

The egg reappearance period (ERP), the time between administration and resumption of strongyle egg detection in faeces (Duncan 1985), is considered an early indicator of resistance (Sangster 1999). Evidence of a shortened ERP after ivermectin treatment has been reported in the Netherlands (Borgsteede, Boersma et al. 1993), and with moxidectin in Kentucky (Rossano, Smith et al. 2010) and the UK (Relf, Lester et al. 2014). The responsible use of moxidectin is of particular importance due to its reported efficacy against encysted larval, as well as adult stage cyathostomins (Vercruysse, Eysker et al. 1998; Bairden, Brown et al. 2001; Schumacher and Taintor 2008). Moxidectin's value in killing encysted larvae and its persistent activity resulting in a longer egg reappearance period are factors that differentiate it from other anthelmintics (Eysker, Boersema et al. 1992; Cobb and Boeckh 2009; Corning 2009). Should resistance to this drug continue to develop, there will be no efficacious treatment for control of encysted cyathostomin stages (Matthews 2008).

1.2.5 Clinical Significance

Although horses acquire an incomplete age-related resistance to cyathostomin re-infection (Klei and Chapman 1999), individual animals vary in their susceptibility to infection and this generally persists throughout an animal's life (Nielsen, Monrad et al. 2006). Cyathostomin populations are over-dispersed, with the majority of parasites often present in the minority of the host population (Matthews 2008). Although the vast majority of grazing horses are exposed to cyathostomin populations, most animals harbour sub-clinical infections that do not result in overt clinical signs (Matthews 2010). Cyathostomins are pathogenic at their luminal and mucosal stages and horses with high levels of infection can develop clinical signs. A large adult worm population within the intestinal lumen can cause weight loss and debilitation (Murphy and Love 1997; Corning 2009), but of main concern, is the

potential damage that can be caused by the larval stages. Mucosal damage can occur when larvae first enter the gut wall and encyst in the host tissue (Murphy and Love 1997). However, it is the mass emergence of encysted larvae, sometimes to the order of several million (Smets, Shaw et al. 1999; Dowdall, Matthews et al. 2002), that can cause significant intestinal damage. This life threatening inflammatory enteropathy is termed larval cyathostominosis (Giles, Urquhart et al. 1985; Bodecek, Jahn et al. 2010). Cases of clinical larval cyathostominosis have been reported most frequently in temperate climates in late winter and early spring (Giles, Urquhart et al. 1985) and susceptibility to cyathostomin infection or larval cyathostominosis is life long and varies between individuals (Hodgkinson, Lichtenfels et al. 2003). A number of clinical signs have been ascribed, including weight loss, anorexia, diarrhoea, colic, oedema and pyrexia (Love, Murphy et al. 1999; Smets, Shaw et al. 1999; Bodecek, Jahn et al. 2010). Experimental infection has been observed to disrupt normal intestinal motility (Bueno, Ruckebusch et al. 1979) and this could be associated, along with additional mechanisms such as intestinal mucosal oedema and stimulated local production of vasoconstrictive substances, with clinical signs of colic (Mair and Pearson 1995; Murphy, Keane et al. 1997). Most animals with larval cyathostominosis will develop a neutrophilia and hypoalbuminaemia (Giles, Urquhart et al. 1985; Murphy, Keane et al. 1997). However, in practice, disease related to cyathostomin infestation is challenging to diagnose because there are no pathognomonic haematological, biochemical or clinical features, and horses can present with a wide range of symptoms (Love, Murphy et al. 1999; Hodgkinson 2006; Bodecek, Jahn et al. 2010). In cases of larval cyathostominosis, aggressive therapy and additional supportive care, including fluid therapy, is necessary (Love and Mckeand 1997). In conjunction with oncotic and nutritional support the use of anti-inflammatory doses of corticosteroids is also recommended (Church, Kelly et al. 1986; Murphy, Keane et al. 1997; Peregrine, McEwen et al. 2006). Euthanasia may be advocated due to the poor prognosis of the condition (Giles, Urquhart et al. 1985; Bodecek, Jahn et al. 2010). In Europe, despite intensive treatment, approximately 50% of larval cyathostominosis cases do not survive (Giles, Urquhart et al. 1985; Murphy, Keane et al. 1997).

1.3 Mast cells in Gastrointestinal Parasitism

1.3.1 Mast Cell Overview

Mast cells are immune cells containing an abundance of lysosome-like secretory granules (Puri and Roche 2008) containing ‘mast cell mediators’ (Pejler, Ronnberg et al. 2010). These mediators can be classified into three broad categories; pre-formed secretory granule-associated mediators, lipid-derived mediators and cytokines (Metcalf, Baram et al. 1997). Mast cells are derived from haematopoietic bone marrow stem cells (Tertian, Yung et al. 1981) and normally circulate in an immature form (Urb and Sheppard 2012). The migration of mast cell progenitors to the intestine is constitutive and requires both adhesive interactions and directed migration (Gurish and Boyce 2006). In the mouse the recruitment of mucosal mast cells is controlled by the c-kit pathway and $\alpha 4\beta 7$ integrins (Gurish, Tao et al. 2001) which are expressed by mast cell progenitor cells (Gurish and Boyce 2006). The integrin, $\alpha 4\beta 7$, interacts with mucosal addressin cell adhesion molecule 1 and endothelial vascular cell adhesion molecule 1 for transendothelial migration (Abonia, Austen et al. 2005). Terminal differentiation and maturation, including development of mature granules, occurs locally once the precursors reach their destination (Nakano, Sonoda et al. 1985; Metz and Maurer 2007); this is governed by cytokines, including stem-cell factor, secreted by endothelial cells and fibroblasts (Urb and Sheppard 2012). Despite the fact that mast cells share many characteristics, they represent a heterogeneous population in the human, rodent and horse (Welle 1997; Pickles, Mair et al. 2010) comprised of specific subpopulations in different tissues (Befus, Pearce et al. 1982; Friend, Ghildyal et al. 1996; Scudamore, McMillan et al. 1997; Pemberton, McEuen et al. 2001). Mast cells have historically been classified as connective tissue mast cells (CTMC) or mucosal mast cells (MMC). These two populations are phenotypically different, as well as having differences in function and proteinase content (Metcalf, Baram et al. 1997). Mast cells have also been classified according to their proteinase content into mast cells that contain tryptase only, mast cells that contain chymase only and mast cells that contain both proteinases (Weidner and Austen 1993; Kube, Audigé et al. 1998; Küther, Audigé et al. 1998; Pejler, Ronnberg et al. 2010; Pickles, Mair et al. 2010).

Mast cells have a complex array of functions, they are widely regarded as key immune effector cells and are also involved in allergic responses. Mast cells play an important role in host defence (Urb and Sheppard 2012); however, mast cell mediated inflammation can be deleterious or protective (Caughey 2007). For example, in the human, mast cells in the lung display direct antimicrobial activity to *Streptococcus pneumoniae* (Cruse, Fernandes et al. 2010) and they are believed to have a protective role in acute septic peritonitis in the rodent (Echtenacher, Mannel et al. 1996; Malaviya, Ikeda et al. 1996). Also, in response to venom proteins in rodents, mast cells have the capability to detoxify harmful proteins via the action of their proteinases (Metz, Piliponsky et al. 2006). However, intestinal mast cells are implicated in ulcerative colitis (Tremaine, Brzezinski et al. 2002; Hamilton, Sinnamon et al. 2011) and the involvement of mast cell derived mediators in rodent inflammatory bowel disease is suggested due to the mucosal pathophysiological changes observed in these conditions (Scudamore, Jepson et al. 1998). Also, in response to venom proteins in rodents, mast cells have the capability to mediate a fatal anaphylactic reaction (N. K and K. G. A 1952; Dutta and Narayanan 1954; Caughey 2007). Human and murine mast cells are known for their well-established roles in innate or in T helper 2 (Th2) and IgE associated immune responses (Galli, Nakae et al. 2005) and can be activated in numerous ways (Urb and Sheppard 2012). The best documented of these in humans and rodents is activation through IgE bound to high affinity IgE receptor (FcRI) expressed on the mast cell surface (Kinet 1990). Other than crosslinking of IgE receptors, mast cells can also be stimulated by direct injury or by activated complement proteins (Erdei, Andrásfalvy et al. 2004), the constitutive expression of C3 and C5 on human skin mast cells has been demonstrated (Fukuoka, Hite et al. 2013). They can also be activated directly by pathogens through pattern recognition receptors (Urb and Sheppard 2012), such as the Toll-like receptor family (McCurdy, Lin et al. 2001). Non-FcRI dependent mast cell activation has been demonstrated in rats to occur through polybasic molecules such as Polymyxin B (Lagunoff and Benditt 1960; Kruger and Lagunoff 1981), lectins and dextrans (Lagunoff, Martin et al. 1983) and a number of peptides, including the neuropeptide substance P (Lorenz, Wiesner et al. 1998; Li, Guo et al.

2012). In addition, in humans, adenosine (Polosa, Rorke et al. 2002) and cell-to-cell contact with T-lymphocytes (Bhattacharyya, Drucker et al. 1998) have also been demonstrated to cause mast cell activation. Activated mast cells release preformed mediators, (for example histamine and serine proteinases), from granules by exocytosis (Blank 2011); a process dependent on cellular calcium regulation via calcium channels (Barnes 1983; Tshori and Razin 2010). The released mediators lead to a rapid inflammatory response and recruitment of leucocytes and additional mast cells (Brooks and Bailey 2010). Time-lapse photography has shown that mast cells can recover following activation and the repeated release of mediators post-recovery has been demonstrated (Xiang, Block et al. 2001). One of the consequences of mast cell activation is self-amplification and further recruitment of mast cells (He, Gaca et al. 1998). In humans, tryptase is a stimulus for histamine release from tonsillar mast cells (He, Gaca et al. 1998) and histamine has also been demonstrated to modulate tryptase release from large intestinal mast cells (He and Xie 2004). This self-amplification is of particular interest as stabilisation of mast cell populations, via histamine receptor antagonists, tryptase inhibitors and calcium channel antagonists, with the aim of preventing this self-amplification, is a potential therapeutic approach for conditions such as inflammatory bowel disease in humans (He, Xie et al. 2005) and laminitic horses (Owen 2009).

1.3.2 Mast Cells in Nematode infections

Mast cells are resident within tissues that interface with the external environment and play a sentinel role in host defence (Kumar and Sharma 2010) as well as regulating epithelial function (Scudamore, Jepson et al. 1998). The “common mucosal immune system” is based on observations that stimulation of one mucosal region can lead to activation of mucosal responses at sites distant to the initial region of exposure (van Ginkel, Nguyen et al. 2000), and is primarily mediated by the migration of mucosal immune cells from the site of stimulation to other distant mucosal sites. The mucosal immune system is the first line of defence against foreign antigens (Kiyono, Kweon et al. 2001). Organised sites of gut associated lymphoid tissue (GALT) in the intestine, such as the mesenteric lymph nodes and Peyer’s patches, comprise the

largest mass of lymphoid tissue in humans (Salminen, Bouley et al. 1998). One of the major mucosal effector sites is the lamina propria, where T cells and B cells are found in abundance alongside macrophages, eosinophils and mucosal mast cells (McGhee, Mestecky et al. 1992). With respect to the common mucosal system, mast cell numbers increase with proximity to the epidermis and increase with distance from the centre of the body, with mast cells in human skin displaying a proximal/distal and central/peripheral gradient (Weber, Knop et al. 2003). This supports the theory of their role as sentinel cells at these sites (Metz and Maurer 2007) and their ability to directly respond to pathogens and send signals to allow the modulation of both innate and adaptive host immune responses (Urb and Sheppard 2012).

Intestinal nematode infections have been associated with the development of IgE-mediated (Type-1) hypersensitivity responses in the gut (Jarrett and Miller 1982; King, Jia et al. 1997). Experiments using *Trichinella spiralis* and *Nippostrongylus brasiliensis* have demonstrated that the population of mucosal mast cells expands during T-cell dependent responses to these parasites (Mayrhofer and Fisher 1979 {Ruitenber, 1976 #483}). In rats, following infection with both *T. spiralis* and *N. brasiliensis*, mucosal mastocytosis was demonstrated to be maximal at day 12, with parasite expulsion by day 15 and 16, respectively (Woodbury, Miller et al. 1984). Mast cell infiltration in the large intestine of horses with cyathostomin infection has also been demonstrated (Pickles, Mair et al. 2010). Horses acquire immunity to cyathostomin infection, but this is incomplete and poorly understood (Klei and Chapman 1999; Chapman, French et al. 2002). Mature horses, kept under similar treatment and maintenance protocols as younger animals, have lower FECs (Lind, Höglund et al. 1999). In general, younger horses also demonstrate a shorter egg reappearance period (Klei and Chapman 1999). These differences are believed to be a consequence of the larger mucosal populations harboured by younger animals, which are less susceptible to anthelmintic treatment, compared to luminal parasites (Herd 1986; Herd and Gabel 1990; Klei and Chapman 1999). Following treatment, these mucosal stages may emerge from the mucosa, in greater numbers in younger animals (Klei and Chapman 1999). Along with a weaker immune response allowing

a higher level of re-infection, this greater mucosal population could explain the age-related differences (Klei and Chapman 1999). Variable worm burdens ranging from 18,700 to 825,900 have been demonstrated in horses of the same age group (one to two years) grazing together, suggesting that an aspect of the host immune status determines the magnitude of the total burden (Bairden, Brown et al. 2001). Studies performed over a three-year period demonstrated consistencies in individual FECs; with low shedders remaining low despite a lack of treatment and high FEC shedders remaining in this category despite selective therapy (Nielsen, Haaning et al. 2006).

Large intestinal mucosal mast cells (Pickles, Mair et al. 2010), CD4⁺ T helper cells, eosinophils (Collobert-Laugier, Hoste et al. 2002) and mucosal Th2 cytokines (Davidson, Hodgkinson et al. 2005) increase during cyathostomin infection. Th2 cytokines, such as interleukin-4 (IL-4) and IL-10, activate and stimulate mast cells during Th2-mediated inflammation, resulting in intestinal mast cell hyperplasia (Shelburne and Ryan 2001), though the direct/causal relationship in horses has not been demonstrated. These Th2 cell cytokines, IL-10 and IL-4, have been demonstrated to show significant correlation to cyathostomin burden (Davidson, Hodgkinson et al. 2005) and the phenomenon of a Th2 driven immune response correlates with results observed in nematode models in mice (Lawrence, Paterson et al. 1998; Schopf, Hoffmann et al. 2002). The development of the appropriate Th response by CD4⁺ T helper cells is critical to the successful resolution of infection with the caecal intestinal nematode *Trichuris muris* (Else, Finkelman et al. 1994). A dominant Th1 response, with the production of interferon-gamma, IL-2 and tumour necrosis factor-beta (TNF- β) (Romagnani 1999), is associated with susceptibility to the parasite; in contrast, a Th2 driven response, characterised by production of IL-4, IL-5, IL-6, IL-9, IL-10 and IL-13 (Romagnani 1999), is associated with host protection (Else and Grencis 1991; Else, Hültner et al. 1992; Else, Finkelman et al. 1994). Also, in support of this, mice deficient in IL-10 and IL-4 fail to expel *T. muris* (Schopf, Hoffmann et al. 2002). The findings in horses to date are supportive of a Th2 type immune response to cyathostomin challenge (du Toit, McGorum et al. 2007), however, the precise role of these cytokines in the horse has not been defined. Whilst it is hypothesised that they are protective in the host immune response to

parasites the factors driving these cytokines and their downstream mechanisms have yet to be thoroughly investigated (Davidson, Hodgkinson et al. 2005).

1.3.3 Mast Cell Serine Proteinases

The term “mast cell proteinase” is used to describe a proteinase that is transcribed in mast cells and stored in their secretory granules (Pejler, Ronnberg et al. 2010). The three main mast cell proteinase types are tryptase, chymase and carboxypeptidase-A. Each of these is diverse in form, activity and pattern of expression (Caughey 2007). These mast cell proteinases are expressed and stored at exceptionally high levels (Schwartz, Irani et al. 1987). Carboxypeptidase-A is a zinc-dependent metalloproteinase that hydrolyses C-terminal amino acid residues (Arolas, Vendrell et al. 2007; Pejler, Knight et al. 2009). Tryptase and chymase are classed as serine proteinases, because of the nucleophilic serine residue at the active site (Hedstrom 2002). Tryptases and chymases are found in both mammals and bacteria and despite the fact that these proteinases are often found together within in the same mast cell granules, they appear to share no established common ancestor or evolutionary association (Gallwitz and Hellman 2006; Gallwitz, Reimer et al. 2006; Trivedi, Tong et al. 2007; Trivedi and Caughey 2010). Serine proteinase specificity is conferred by the topology of the substrate specific binding site, which is adjacent to the catalytic triad (Hedstrom 2002). This catalytic triad, part of a wide hydrogen bonding network, consists of Histidine-57 and Aspartate-102 at one side of the active site cleft and Serine-195 on the other (Hedstrom 2002). Two different loci encode the mast-cell expressed enzymes in mammals (Reimer, Samollow et al. 2010). There are a range of mast cell granule serine proteinases and these have distinct specificities and vary among mast cell subsets and between mammalian species (Table 1.1).

Species	Mast Cell Subclass	Chymases	Tryptases*
Human	MC _T	h-chymase	α
			β (I, II, III)
	MC _{TC}		α
			β (I, II, III)
Mouse	MMC	mMCP-1	
		mMCP-2	
	CTMC	mMCP-4	mMCP-6
		mMCP-5	mMCP-7
		mMCP-9†	
Horse	MMC	eqMCP-1	eqTRYP
	CTMC	eqMCP-1	eqTRYP

Table 1.1: Table of human, mouse and horse mast cell subclasses (adapted from Pejler, Ronnberg et al. 2010). *Refers to tetrameric, secreted tryptases. †Preferentially expressed in uterine mast cells (Hunt, Friend et al. 1997). (MMC: mucosal mast cell; CTMC: connective tissue mast cell; h-chymase: human chymase; mMCP: mouse mast cell proteinase; CPA: carboxypeptidase A; eqMCP-1: equine Mast Cell Proteinase-1; eqTRYP: equine Tryptase).

Different mammals express varying numbers and types of tryptases and chymases (Caughey 2007). Multiple closely-related chymases are expressed by many mammalian species (McAleese, Pemberton et al. 1998; Miller and Pemberton 2002). Heterogeneous expression of mast cell proteinases was first described in rodents where antibodies specific to different mast cell proteinases demonstrated that the rat mucosal mast cell lacked the basic beta chymase (RMCP-I) but expressed the highly soluble beta chymase (RMCP-II) (Gibson and Miller 1986; Miller and Pemberton 2002). Two equine mast cell proteinases have been purified from equine mastocytoma tissue and identified as equine tryptase and equine mast cell proteinase-1 (eqMCP-1) (Pemberton, McEuen et al. 2001). The high salt mastocytoma extract was a highly concentrated source of mast cell serine proteinases and contained approximately 3% equine tryptase and 7% eqMCP-1 (Pemberton, McEuen et al. 2001). After purification and N-terminal amino acid sequencing, the tryptase was found to be very similar to the sequence for human tryptase- β (85% identity over 20 residues), had a similar subunit molecular size (34-36 kDa as demonstrated by SDS-

PAGE) and showed similar activity in substrate cleavage specificity (Dacre, McAleese et al. 2006). The 32 kDa chymotrypsin-like component, eqMCP-1, was found to be very similar to human granzyme H (95% over 19 residues) and immunolocalised to intestinal mucosal and submucosal mast cells (Pemberton, McEuen et al. 2001).

Mast cell proteinase expression also varies between tissues in horses. Tryptase-positive mast cells are abundant in equine lung and the predominant pulmonary mast cell type is tryptase-positive and chymase-negative (Pemberton, McEuen et al. 2001; Dacre 2005). In contrast, studies on equine intestinal cells demonstrated that the predominant mast cell type is chymase-positive and tryptase-negative (Pickles, Mair et al. 2010). Studies of the equine endometrium during the puerperal period identified two potential sub populations of mast cell, one that is chymase-negative and tryptase-positive and another that is hypothesised to be both chymase- and tryptase-negative (Welle, Audige et al. 1997).

1.3.3.1 Tryptase

Tryptases are trypsin-like serine proteinases that cleave peptide substrates on the carboxyl side of lysine and arginine residues (Little and Johnson 1995). The enzymatically active form is a tetramer of 120-140 kDa that consists of four tryptase monomer subunits of 31-34 kDa in a ring-like structure with a central pore (Pereira, Bergner et al. 1998). The active site is protected and largely inaccessible to endogenous mammalian proteinase inhibitors (Pejler, Ronnberg et al. 2010). The multigene tryptase locus encodes mast cell tryptases and also a number of tryptase-like proteinases that are active in other tissues but are not mast cell related (Reimer, Samollow et al. 2010). This locus is structurally similar in humans and mice and can be divided into two regions; one encoding Group 1 tryptases (membrane-bound tryptase-like proteinases) and the other encoding soluble mast cell-derived Group 2 tryptases (Wong, Yasuda et al. 2004). Analysis of data available from the dog, bovine, opossum and platypus genomes along with orthologs from bird, fish and frog species, has shown that this locus is well conserved with an indication that the

present genes within the multigene tryptase locus are mammalian specific (Reimer, Samolloy et al. 2010).

Tryptase is stored almost exclusively in mast cells (Walls, Jones et al. 1990) and is a widely used marker of systemic mast cell activation and mastocytosis (Schwartz, Metcalfe et al. 1987; Schwartz 2001; Akin, Soto et al. 2007). In the mouse, tryptase contributes to the immune response to *T. spiralis* through eosinophil recruitment (Shin, Watts et al. 2008). Tryptase also plays a role in self-amplification with its release inducing further mast cell activation and degranulation (He, Gaca et al. 1998). Cloning and sequencing of equine mastocytoma-derived tryptase has been performed (Dacre, McAleese et al. 2006). Observations made using the chymotrypsinogen numbering system, based on the alignment of amino acid sequences with chymotrypsinogen (Hartley and Neurath 1970; Hedstrom 2002), indicated that the sequence is the same length as (245 amino acid mature protein) and shares >70 % identity with other mammalian tryptases (Dacre, McAleese et al. 2006). Many features were found to be characteristic of trypsin-like proteinases including the characteristic aspartate residue at position 189 which governs substrate specificity (Perona, Hedstrom et al. 1995), the activation site region IVGG (residues 31-34) and cysteine residues at positions 191 and 220 (Czapinska and Otlewski 1999; Dacre, McAleese et al. 2006). Residue 216 is important in determining substrate specificity (Perona, Hedstrom et al. 1995) therefore it is interesting that equine tryptase has alanine at this position, instead of glycine. The biological significance of this difference is not known (Dacre, McAleese et al. 2006).

1.3.3.2 Chymase

Chymases, one of the major mast cell granule constituents, are monomeric and have chymotrypsin-like cleavage specificity and cleave substrates on the C-terminal side of aromatic amino acids (Andersson, Karlson et al. 2008). The chymase family can be subdivided into two groups, alpha and beta chymases, based on their phylogenetic analyses (Chandrasekharan, Sanker et al. 1996). This family has a range of substrate preferences and activity (Trivedi and Caughey 2010). The mast cell chymase locus has been mapped for a number of species and, in all cases, the locus contains a

minimum of one mast cell chymase alpha gene, two T and Natural Killer (NK) cell-expressed granzyme genes and one gene for neutrophil cathepsin G (Reimer, Samolow et al. 2010). In humans, chymase and cathepsin G belong to a family of serine proteinases which include factor D of the complement system, elastase, proteinase-3 and the lymphocyte and NK cell derived human granzymes A, B, H and M (Trivedi and Caughey 2010). Many placental mammals demonstrate dramatic expansion of this locus (Reimer, Samolow et al. 2010) but it is unknown why some mammals express more chymases than others (Trivedi and Caughey 2010). The large dimensions of the rodent chymase loci are partly due to gene families that have no homologues in the human (Gallwitz and Hellman 2006; Gallwitz, Enoksson et al. 2007). The genome of the rat contains 13 closely-related functional chymases (Gallwitz and Hellman 2006), compared to at least 14 in mice (Gallwitz and Hellman 2006) and four in humans (Caughey, Schaumberg et al. 1993; Gallwitz and Hellman 2006). Apart from ruminants, where two very similar alpha-chymase genes have been described (Gallwitz, Reimer et al. 2006), in all other species investigated a single alpha-chymase has been found (Andersson, Karlson et al. 2008). The mouse locus is almost three times larger than the human equivalent and also contains three times the number of functional genes (Gallwitz and Hellman 2006). Two subfamilies, beta chymases and mouse mast cell proteinase-8 (mMCP-8), have been found in the mouse but not in the human genome (Lützelschwab, Huang et al. 1998). The rat chymase locus has also undergone considerable expansion (Puente and López-Otín 2004) and despite a high number of pseudogenes, it has a similar number of functional genes to the mouse (Gallwitz and Hellman 2006). Rat mast cell proteinase I is a chymase that is primarily found in the connective tissue (Woodbury, Everitt et al. 1978; Rouleau, Garbarg et al. 1994). However, the chemically and antigenically distinct rat mast cell proteinase II, another chymase, is localized to respiratory and intestinal mucosal mast cells (Woodbury, Gruzinski et al. 1978). Rat MCP-II, has been demonstrated to be released systemically following *N. brasiliensis* challenge and has been measured using an enzyme linked immunosorbent assay (ELISA) (Miller, Woodbury et al. 1983). The translocation of this proteinase to the gut lumen in parasitised rats challenged with worm antigen has been demonstrated

(King and Miller 1984). *In vitro* studies have demonstrated that the action of this chymase increases epithelial permeability and alters the distribution of tight junction proteins (Scudamore, Jepson et al. 1998). The role of chymases in parasite infection has been investigated with the use of knockout strains of mice deficient in certain proteinases (Pejler, Ronnberg et al. 2010). The absence of mMCP-1 has been demonstrated to affect the kinetics of *N. brasiliensis* infection (Wastling, Knight et al. 1998). This knockout also had a negative effect on the clearance of *T. spiralis* (Knight, Wright et al. 2000) and the intestinal inflammation associated with this helminth was ameliorated suggesting that this chymase plays a significant role in this process (Lawrence, Paterson et al. 2004). *T. spiralis* infection is associated with an increased paracellular permeability of the jejunum, a phenomenon which is blocked in the absence of mMCP-1 and could potentially be a reason for the inability of the deficient mice to efficiently expel the parasites (McDermott, Bartram et al. 2003).

As with equine tryptase mentioned above, the cloning and sequencing of the equine mastocytoma derived eqMCP-1 has been previously investigated (Dacre 2005). When attempting to clone and sequence the chymase sequence from equine tissue the deduced amino acid (aa) sequence for the putative equine mast cell proteinase-1 (referred to in this thesis as Chymase-like Proteinase -1, CLP1) had an N-terminal aa sequence that differed from the mastocytoma derived eqMCP-1 by two aa. Also, peptide masses predicted by trypsin digestion of the cloned putative aa sequence corresponded poorly with the fingerprint of mastocytoma derived eqMCP-1 (Dacre 2005). Due to these differences it was hypothesised that a similar but novel proteinase was cloned and sequenced.

Both CLP1 and eqMCP-1 sequences shared similar identities with the lymphocyte derived human granzyme H (Dacre 2005). Granzymes are members of a chymotrypsin related family of serine proteinases produced by cytotoxic T-cells and NK cells (Trapani 2001). Granzymes can be grouped according to their specificity; their subfamilies have tryptase-like, chymotrypsin-like and elastase-like properties. Eight granzymes have been identified in the mouse (granzyme A-G and granzyme M) compared to five in the human (granzyme A, B, H, M and granzyme 3) (Trapani 2001). The subfamily with chymotrypsin-like specificity is grouped on the chymase

locus and includes mouse granzyme B, C, D, E, F and G and granzyme B and H in the human (Trapani 2001).

1.3.4 Mast Cell Serine Proteinases in Nematode Infections

There is evidence of local mast cell activation at the site of parasite infection (Metcalf, Baram et al. 1997) and mast cells and their associated proteinases have been implicated in the protective host immune response against nematode infection in mammals (Miller 1996; Wastling, Scudamore et al. 1997; McDermott, Bartram et al. 2003). Mast cells can reversibly alter their proteinase phenotypes depending on host disease state (Ghildyal, Friend et al. 1993; Friend, Ghildyal et al. 1996). Activation of innate immune responses relies on the recognition of pathogen-associated products (Marshall and Jawdat 2004) and mast cells have been implicated in this process (Heib, Becker et al. 2008).

In rodents, the mast cell serine proteinases, tryptase and chymase, contribute to innate immunity and tissue remodelling, through proteolysis of matrix proteins, to aid nematode expulsion (Miller and Pemberton 2002). In the rat, mucosal mast cells have a functional role in immune elimination of the intestinal *T. spiralis* and *N. brasiliensis* with systemic secretion of rat MCP-II maximal at the time of parasite expulsion (Woodbury, Miller et al. 1984). Murine mast cell serine proteinase expression has been shown to be reversibly modified through infection with *T. spiralis* (Friend, Ghildyal et al. 1996; Friend, Ghildyal et al. 1998). Furthermore in the mouse, ablation of the murine chymase mouse mMCP-1 compromises expulsion of *T. spiralis* (Knight, Wright et al. 2000; McDermott, Bartram et al. 2003). Differential mast cell proteinase expression has been demonstrated during the inflammatory response to nematode infection as the cells migrate towards the mucosa (Friend, Ghildyal et al. 1996; Friend, Ghildyal et al. 1998). In one four-week study of mice infected with *T. spiralis*, jejunal mast cells in the submucosa, lamina propria and epithelium were shown to exhibit sequential changes in their granule ultrastructure and chymase phenotype. At 2-3 weeks post infection (pi), the mucosal mast cell population increased more than 25-fold relative to non-infected mice (Friend, Ghildyal et al. 1996). These cells expressed the chymase mouse mast cell

proteinase 2 (mMCP-2), ceased expressing mMCP-5 and finally expressed mMCP-1, as the cells progressed respectively through the tissues. In the recovery phase, four weeks post infection (pi), as the cells reached the tips of the villi, the base of the villi and the submucosa, they ceased expressing mMCP-1, expressed mMCP-5 and finally ceased expressing mMCP-2, respectively (Friend, Ghildyal et al. 1996).

In the equine case the two neutral serine proteinases previously extracted from equine mastocytoma tissue, eqTRYP and eqMCP-1 (Pemberton, McEuen et al. 2001) have been used to investigate the intestinal immune response to cyathostomin infection (Pickles, Mair et al. 2010). Polyclonal antibodies against these proteinases were raised in rabbits (Pemberton, McEuen et al. 2001) and these antibodies were subsequently purified and their specificity validated (Dacre, McGorum et al. 2007). Immunohistochemical labelling of equine formalin-fixed large intestinal sections using these reagents identified increased numbers of tryptase-positive mast cells in cyathostomin infected horses despite the use of a tissue fixative that is not ideal for immunohistochemical staining (du Toit, McGorum et al. 2007). More recent studies using Carnoy's fixed tissue (Pickles, Mair et al. 2010) demonstrated a strong positive linear relationship between cyathostomin burden and the presence of equine tryptase and eqMCP-1 within the caecal wall of naturally infected horses. The majority of mast cells labelled for eqMCP-1 however, the strongest relationship with cyathostomin burden was with tryptase-labelled mast cells. Total cyathostomin burden was estimated to account for 57 % of the variation in tryptase-labelled mast cells counts in the caecal mucosa in this study (Pickles, Mair et al. 2010).

1.4 Diagnostic Approach to Cyathostomin Infection

The development of a minimally invasive diagnostic test to provide information on an individual's encysted larval cyathostomin burden has the potential to improve horse welfare and health. Knowledge of an individual's encysted larval burden would be beneficial to inform strategic and targeted treatments, especially in young horses that are more susceptible to clinical disease (Traversa, Milillo et al. 2010). Serum is relatively easy to obtain, hence it is an attractive potential sample for diagnostic testing. Previous work has identified two antigen complexes (20 and 25

kDa) in somatic antigen preparations of larval cyathostomins that may have diagnostic potential (Dowdall, Matthews et al. 2002; Dowdall, Proudman et al. 2003; Dowdall, Proudman et al. 2004). The majority of work to date has concentrated on a protein present in a 25 kDa antigen complex specifically detected in the encysted larval stages. This antigen is known as cyathostomin gut associated larval antigen (Cy-GALA) (McWilliam, Nisbet et al. 2010). A diagnostic IgG(T) ELISA using recombinant versions of this protein generated from a number of common cyathostomin species is currently being assessed (Matthews 2011). The serum half-life of circulating IgG(T) antibodies has been measured as 21 days in horses (Sheoran, Timoney et al. 2000) and the dynamics of antigen specific IgG(T) responses, particularly following treatment, are a concern when considering the utility of a diagnostic assay, as levels of parasite-specific IgG(T) may persist following clearance of active infections. Concurrent measurement of a biomarker indicating active mucosal infection would be a useful and complimentary diagnostic tool (McWilliam, Nisbet et al. 2010).

Mast cell tryptase, is frequently used as a biomarker for mast cell activation and mastocytosis (Schwartz, Metcalfe et al. 1987; Schwartz 2001; Akin, Soto et al. 2007). ELISAs have been used with success to measure the systemic release of mast cell proteinases into blood in rats (Miller, Woodbury et al. 1983; Woodbury, Miller et al. 1984), mice (Huntley, Gooden et al. 1990) and sheep (Huntley, Gibson et al. 1987) with nematode infections. An increase in caecal mast cells expressing proteinases has been demonstrated during cyathostomin infection (du Toit, McGorum et al. 2007; Pickles, Mair et al. 2010) and measurement of these enzymes in serum has diagnostic potential as a biomarker of active infection. An optimised mast cell proteinase ELISA has potential to identify active cyathostomin infections, which would be of significant benefit to veterinary practitioners as larval cyathostominosis can present with a wide range of clinical signs which, as previously stated, are not pathognomonic for the disease (Love, Murphy et al. 1999). Also, a further potential benefit of a serum diagnostic would be to assess the level of encysted burden to inform strategic targeted anthelmintic treatments.

Biopsies of rectal mucosa are taken routinely by veterinarians in practice as a diagnostic aid for evaluation of intestinal disease, in particular inflammatory bowel disorders (Lindberg, Nygren et al. 1996). They are relatively non-invasive, cheap and easy to perform. The presence of cyathostomins in rectal tissue taken from rectal biopsy has been documented (Church, Kelly et al. 1986; Ricketts 1996), but this finding is rare. As indicated above, the common mucosal immune system has the potential to evoke mucosal immune responses throughout the gut, including the rectum (Lycke 2012). Mast cells are commonly found at interfaces to the external environment such as the rectum (Knight, Wright et al. 2000; Heib, Becker et al. 2008), leading to the hypothesis that mast cells could be recruited throughout the large intestine and rectum in numbers positively associated with cyathostomin burden, such that rectal biopsy may have diagnostic potential for prediction of total cyathostomin burden.

1.5 Thesis aims

The work presented here aims to examine three complementary hypotheses.

There is a positive association between mast cell numbers and cyathostomin burden throughout the large intestine such that rectal biopsy may have a diagnostic potential for estimation of total cyathostomin burden.

Serum and large intestinal tissue mast cell proteinase concentrations are positively associated with mast cell number and proteinase expression, and with cyathostomin burden, such that they have diagnostic potential for prediction of total cyathostomin burden.

There are novel equine mast cell proteinases that have not yet been identified. The release of these novel proteinases may be more closely related to worm burden.

Research in these areas will improve the understanding of the role of mast cells and their proteinases in cyathostomin infection. This thesis will further investigate the involvement of these cells in naturally infected horses. The primary aim is to evaluate the potential for mast cell proteinase assays or rectal biopsy methods to be used in minimally invasive diagnostic tests to assist in estimating the total (i.e. including mural stages) cyathostomin burden. A secondary aim is to explore the potential for novel equine mast cell proteinases.

2 Investigation of Recruitment of Large Intestinal Mast Cells in Response to Cyathostomin Infection

2.1 Introduction

A central element of the cyathostomin lifecycle is the arrested period during which encysted larvae are believed to inhibit development in the equine gut wall. Cyathostomin mucosal larval populations can persist at high levels (over 3 million larvae have been enumerated in some individuals (Dowdall, Matthews et al. 2002), which are thought to put the individual at risk of life-threatening intestinal damage (Matthews, Hodgkinson et al. 2004). Equine larval cyathostominosis, in which there is mass emergence of encysted cyathostomin larvae from the intestinal wall, results in severe diarrhoea, weight loss and ventral oedema, and has up to a 50% mortality rate (Love, Murphy et al. 1999). The biological factors underlying cyathostomin inhibition are not well understood and it is not known what makes certain individuals more susceptible to high numbers of encysted larvae. Factors associated with the emergence of these larvae are also not well described. It has been hypothesised that season, feedback from luminal mature worms, host immunity and the magnitude of challenge may all play a role in development of larval cyathostominosis (Love, Murphy et al. 1999; Chapman, French et al. 2002; Matthews 2008). There are currently no specific diagnostic tests for the assessment of an individual's mucosal cyathostomin burden. Virtually all grazing equids will be exposed to cyathostomins and are therefore at risk (Matthews 2011). Whilst most horses have low level infections (Matthews 2008; Traversa, von Samson-Himmelstjerna et al. 2009), current recommendations are for the annual administration of anthelmintics effective against cyathostomin mucosal stages to prevent the accumulation of large encysted larval populations (Lester, Spanton et al. 2013). As there are no new anthelmintic classes currently in development, the responsible and targeted use of those that are available is of paramount importance. There is also a requirement for the development of robust diagnostic assays that will enable identification of horses at risk of severe parasitic disease, in conjunction with informing strategic anthelmintic targeting protocols.

Mast cells are commonly found in large numbers at mucosal interfaces (Kumar and Sharma 2010). The role of the mast cell as a key element to the pathogenesis of immediate-type hypersensitivity reactions including urticaria, bronchial asthma and allergic rhinitis is well established (Welle 1997). Pronounced hyperplasia, differentiation, and activation of mucosal mast cells occurs in the intestine during nematode infections (Woodbury, Miller et al. 1984; Miller 1996) and it is proposed that equine mast cells play a key role in the immune response to equine cyathostomin infection. A previous study reported a positive relationship between total adult cyathostomin burden and mucosal mast cell counts in the caecum and dorsal colon and between the percentage of encysted L3 and mucosal mast cell counts in the ventral colon of aged horses, i.e. those older than 10 years (Collobert-Laugier, Hoste et al. 2002). A further study has shown a significant positive linear relationship between total larval cyathostomin burden and the number of Toluidine Blue (TB) stained mast cells in the mucosa and submucosa of the caecum of naturally infected horses (Pickles, Mair et al. 2010). The investigation into the role of mast cells in cyathostomin infection is continued in this chapter through the characterisation of parasite burden and mast cell enumeration in 28 naturally infected horses.

The aim of the work presented here was to examine the first hypothesis:

There is a positive association between mast cell numbers and cyathostomin burden throughout the large intestine such that rectal biopsy may have diagnostic potential for estimation of total cyathostomin burden.

Specifically, an optimised protocol for cyathostomin larval enumeration was developed and the resultant larval burdens compared with the mast cell numbers in individual horses from a population comprising of 28 horses. The relationship between mast cell populations in the mucosa and submucosa in the intestine at the level of the caecum, right ventral colon (RVC) and rectum were also compared.

2.2 Materials and Methods

2.2.1 Sampling Protocol

Samples were collected for parasite enumeration, histological evaluation, mast cell enumeration and proteinase expression between November 2010 and September 2012. The protocol was optimised for the sampling sites, the equine abattoir (Cheshire Equine Services, Nantwich, UK) and the Royal (Dick) School of Veterinary Studies (R(D)SVS, Edinburgh, UK).

2.2.2 Abattoir Sampling Protocol

Samples were collected and processed in the gut room of the abattoir (Figure 2.1). Following slaughter, the equine gastrointestinal organs were passed through to the gut room for disposal. Large intestinal tracts were selected at random following confirmation that the full tract, including the rectum, was present to ensure that all necessary samples could be collected. The abattoir processes equine tissue for human consumption. Regulations require that horses slaughtered for human consumption should not have been treated with anthelmintics for at least 35 (ivermectin) or 64 (moxidectin) days prior to slaughter. If these regulations have been met this cohort should not have been treated close to sampling, however, due to the nature of the slaughter process it was not possible to access reliable clinical history, age of horse or recent anthelmintic administration for individual animals.

2.2.3 R(D)SVS Sampling Protocol

Samples were collected and processed in the post mortem suite at the R(D)SVS (Figure 2.1). Apart from individual DV3, a clinical case of larval cyathostominosis, only horses with no known gastrointestinal pathology were selected. Horses from the R(D)SVS were sampled immediately (within 30 min) following euthanasia. The clinical histories, ages and prior anthelmintic administration for horses from R(D)SVS were recorded where possible.

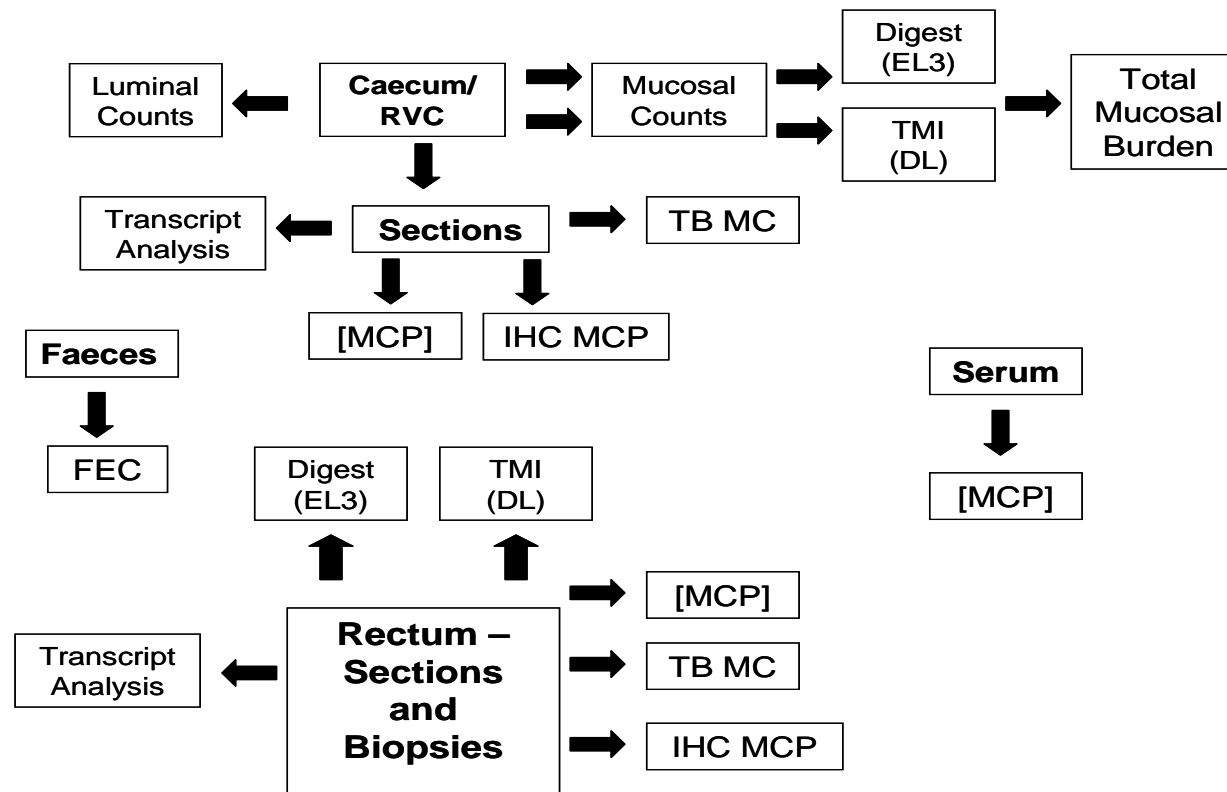


Figure 2.1: Schematic of protocol for processing of samples including tissue, serum and faeces collected from the R(D)SVS and equine abattoir. (FEC: Faecal Egg Count; RVC: Right ventral colon; DL: Developing larvae; EL3: Encysted third stage larvae; TMI: Transmural Illumination; TB: Toluidine Blue; MC: Mast Cell; IHC: Immunohistochemistry; MCP: Mast Cell Proteinase; TMB: Total Mucosal Burden; CTMB: Combined Total Mucosal Burden).

2.2.4 Serum Samples

Left or right colonic vein blood samples were collected post mortem as a source of local serum draining the site of interest. Blood was collected by syringe and needle aspiration and left to clot overnight at 4 °C. Serum was collected after centrifugation at 1,730 x g for 10 min at 4 °C and stored in aliquots at -20 °C and -80 °C. A peripheral blood sample was also collected from either the jugular vein or lower limb vessels from horses sampled at the R(D)SVS. Due to the nature of the slaughter line process it was not feasible to collect peripheral blood samples from the horses sampled at the abattoir.

2.2.5 Faecal Samples

Approximately 50 g of faecal matter was taken from the rectum and placed in a grip seal bag. Air was removed from the bag which was then placed in a chill box for transport. Once transferred to the laboratory, faecal samples were stored at 4 °C for a maximum of two days until a faecal egg count (FEC) was performed. Smaller faecal samples of approximately 3 g were also sampled and snap frozen and transported on dry ice. Samples were then transferred to -80 °C.

2.2.6 Rectal Samples

Rectal biopsies (8 per horse) were taken using endometrial biopsy forceps (Equivet uterine biopsy forceps, Kruuse). The rectum was orientated anatomically such that biopsies could be taken in a similar manner and position to those taken for diagnostic purposes in the live animal. Biopsies were taken 20 cm cranial to the anus, which corresponds to the level described previously for collecting equine rectal mucosal biopsies to aid differential diagnoses (Traver and Thacker 1979). A gloved hand was introduced through the anal sphincter and a fold of mucosa palpated. The biopsy instrument was advanced and the jaws of the forceps closed onto the mucosa to obtain a biopsy sample. The biopsies were taken avoiding the 12 o'clock position to avoid the dorsal vasculature. Two biopsies were placed in glass bijoux of Carnoy's fixative for subsequent immunohistochemistry. After ≥ 24 h in Carnoy's fixative,

these samples were transferred to 70 % ethanol until further processing into paraffin blocks and sectioning. Two more biopsies were placed in a plastic bag and snap frozen on dry ice for transfer to -80 °C and storage for ELISA experiments. Two biopsies were placed in a plastic bijoux containing RNAlater (Sigma-Aldrich). These samples were stored overnight at 4 °C and then the tissue transferred to -80 °C storage. The final two biopsies were put in a plastic bag and stored in a cool box until transferred to storage at -20 °C for pepsin digestion and larval enumeration. Rectum from horses from the equine abattoir was incised and a large sample of rectal mucosa (approx 15 cm²) dissected. These sections were stored at -20 °C for pepsin digestion and larval enumeration. Two rectal sections (approx 1 cm²) were harvested from horses from the abattoir (horses AB1-AB16) using dissecting scissors and placed in glass bijoux of Carnoy's fixative, as previously described. Taking rectal biopsies requires the use of biopsy forceps which use a pincer motion to extract a sample. There is potential to damage the tissue through crushing and cutting and therefore may not produce a representative sample. To examine this effect, rectal sections were taken from all the abattoir cases (horses AB1-AB16) and processed in the same manner as the biopsy sections for comparison. Microscopy was performed without knowledge of the sampling technique, horse sampled or cyathostomin burden. These sections were taken to compare the biopsies with tissue sections to ensure that the biopsy method did not damage the tissue.

2.2.7 Luminal Contents for Parasite Enumeration

The caecum was identified and isolated by tying off the distal ileum and caecocolic junction with lengths of string. The RVC was isolated by identifying the pelvic flexure and placing a string tie halfway between the caecocolic junction and the pelvic flexure to separate right and left ventral colons. The caecum and RVC were separated from the rest of the gastrointestinal tract using a dissecting knife and placed into separate buckets. The organ was opened along a taenial band and the contents emptied into a measuring bucket. Any gross pathology was noted. The caecum was examined for evidence of *Anoplocephala perfoliata*, paying particular attention to the caecal wall, caecal base and ileocaecal valve (Fogarty, del Piero et al.

1994; Williamson, Gasser et al. 1997). The caecal mucosa was washed with 1 L tap water twice to remove any attached luminal parasites. The total volume of contents, including washings, was recorded. The contents were stirred thoroughly and a 100 ml sample collected. The sample was stored in a cool box and preserved with an equal volume of 10 % neutral buffered formalin. This process was repeated for the RVC.

2.2.8 Tissue Samples for Parasite and Mast Cell Enumeration and Mast Cell Proteinase Quantitation

The opened organs were examined visually and any attached parasites or gross pathology noted. The caecum was placed in an empty bucket on top of a set of wash down scales (Digital Retail Scale WBZ 6, Adam Equipment Co. Ltd) and the mass recorded. Using scissors, a 5 % by mass longitudinal sample from base to apex was harvested for transmural illumination (TMI), avoiding taenial bands. This section was stored in a cool box and transferred to -20°C until further processing. A further 5 % by mass sample was taken and stored in the same manner for pepsin digestion. Six adjacent approximately 1 cm^2 sections were obtained using dissection scissors. Two sections were put in a plastic bag on dry ice to be stored at -80°C for ELISA experiments. Two sections were placed in glass bijoux of Carnoy's fixative as described for mast cell enumeration and immunolabelling. The final two sections were placed in RNAlater solution (Invitrogen). This process was repeated for the RVC. All equipment was cleaned thoroughly between horses to avoid contamination.

2.2.9 Faecal Egg Count

Faeces collected from the rectum post mortem were stored at 4°C for a maximum of two days. A FEC was performed in duplicate using a salt floatation method modified by Bartley et al. (2006) originally described by Christie and Jackson (1982) and accurate down to one egg per gram (EPG).

2.2.10 Luminal Cyathostomin Enumeration

The 100 ml caecal and RVC samples were stored in 100 ml of 10 % neutral buffered formalin at 4 °C until enumerated. To aid enumeration, iodine was added to the luminal contents (15 ml per 100 ml). The stained contents were washed over a 53 µm aperture sieve (Fisher) to remove formalin and excess iodine and re-suspended in water. The samples were screened using scored Petri dishes and a stereomicroscope (Leica S8 APO, Leica Microsystems) at x 10 magnification. All stages of larvae enumerated were classed as luminal cyathostomins.

2.2.11 Transmural Illumination to Detect Mural Cyathostomins

Developing mucosal larvae, late L3 (LL3) and developing L4 (DL4), were enumerated using TMI following a method similar to that described by Reinemeyer and Herd (1986). The frozen samples were re-weighed and then defrosted in tepid water. Once thawed, the mucosa was stripped from the serosa and the serosa discarded. The mucosa was cut using dissecting scissors into sections of approximately 5 cm². Each small section was enumerated individually on a scored Petri dish illuminated from below using a dissecting microscope (Leica S8 APO, Leica Microsystems). The mucosa was stretched out across the surface of the Petri dish, serosa side down, using a small amount of water to aid stretching. The developing larvae were identified according to Lichtenfels (1975) and enumerated at x 12.5 magnification with the aid of a grid.

2.2.12 Peptic Digestion

2.2.12.1 Peptic Digestion Method and Larval Enumeration

Caecal, RVC and rectal biopsy samples were digested using a modification of techniques described by Duncan, Bairden et al. (1998) and Dowdall, Matthews et al. (2002). Five percent, by weight, frozen samples were re-weighed and then defrosted in tepid water. Once thawed, the mucosa was manually stripped from the serosa and the serosa discarded. The tissue was digested in a solution of 1 % (w/v) 1:10,000 pepsin/1.5 % (v/v) concentrated hydrochloric acid (Fisher Scientific) in warm tap

water with up to 25 g of tissue per 100 ml digest solution. The digest was performed at 37 °C using a magnetic stirrer to constantly agitate the mixture of tissue and solution. Every 45 to 60 min, a ‘milking’ procedure was performed, as described by Murphy and Love (1997). The digest solution and mucosa was passed through a 2 mm aperture sieve (Cole-Palmer Instrument co. Ltd) and undigested material was returned to the same conditions in 200 ml of fresh digest solution. To stop the digestion process, the solution containing digested material was centrifuged at $450 \times g$ for 2 min in 50 ml Falcon tubes and the pellet recovered and made up to a volume 50 ml of 7 % (v/v) formal saline. This process was performed a total of 2-3 times, every 45-60 min. Digestion was continued until no host tissue remained in the sieve. The entire pellet was recovered and made up to a volume 50 ml of 7 % (v/v) formal saline. Two, 0.5 ml aliquots of the re-suspended pellet (above) were examined at x 80 magnification (Leica S8 APO, Leica Microsystems) to count inhibited third stage larvae (EL3) (Dowdall, Matthews et al. 2002). These were extremely small and uniform in size and morphology as described by Duncan et al. (1998). Larval counts were aided by the addition of 0.5 ml iodine. The total organ count was calculated from the percentage by weight of the sample and multiplied to allow for dilution of the pellet after centrifugation. Developing larvae (DL) were identified according to Lichtenfels (1975) and also counted in the aliquots. This was done to compare the digest method with the TMI method for enumeration of DL.

2.2.13 Mast Cell Staining

Tissue samples were fixed in Carnoy’s fixative. The samples were kept in solution at room temperature for 24 h prior to being transferred to 70 % ethanol before paraffin embedding. Slides were prepared in duplicate for each organ, one from each of two separate tissue samples taken adjacently. Tissue sections were cut to 8 µm thick and mounted onto Superfrost Plus slides (Fisher Scientific). Sections were de-waxed with xylene, rehydrated through graded alcohols and water and then immersed in 0.5 % Toluidine Blue (VWR International) in 0.5M HCl, pH 0.5. Slides were left in this solution overnight. Sections were then briefly washed with tap water and counter

stained by immersion in 1 % eosin (VWR International) in 70 % ethanol for 3 sec. Slides were again washed with tap water and then dehydrated and mounted.

2.2.14 Mast Cell Enumeration

All histological counts were performed without knowledge of cyathostomin burden. Sections were observed using an Olympus BX50 microscope and photographed using an Olympus U-CMAD digital camera and AnalySIS Five software (Soft Imaging System GmbH, Münster, Germany). Positively-stained cells were identified and enumerated using a calibrated graticule over five mucosal and submucosal fields of view per slide (giving a total of 10 per field for each organ) under x 400 magnification. Total area per graticule field at this magnification was 0.0625 mm². Mast cells were expressed as MC per mm².

2.2.15 Haematoxylin and Eosin Staining

Caecal, RVC and rectal tissue samples from horses DV6-DV12 inclusive were collected for haematoxylin and eosin (H&E) staining and eosinophil enumeration. Tissues samples of approximately 1 cm² were taken adjacent to those samples stored in Carnoy's and preserved in 10% neutral buffered formalin before paraffin embedding. Tissue sections were cut to 8 µm thick, mounted onto Superfrost Plus slides and dewaxed in xylene and rehydrated to water. The tissue was then stained with Eosin followed by Haematoxylin Z (both Cellpath) and washed with tap water. Unfortunately, background staining was too high in Carnoy's fixed tissue.

2.2.16 Carbol Chromotrope Staining

Tissue sections from the caecum, RVC and rectum were fixed in either 10% formal saline or Carnoy's fixative. The tissue samples in Carnoy's were kept in solution at room temperature for 24 hs and then transferred to 70% ethanol. Sections were dewaxed in xylene and rehydrated with water. The tissue was then stained with Haematoxylin Z (Cellpath) and washed with tap water. Following this, sections were destained in acid/alcohol, washed in Scott's tap water substitute and washed again in

tap water. Sections were stained overnight at room temperature in Carbol Chromotrope stain (0.5% Chromatropene (Sigma) in 1% Phenol). The following day sections were washed in tap water, dehydrated and mounted.

2.2.17 DAB Staining for Eosinophils

Tissue samples from the caecum, RVC and rectum were fixed in 10% Formal Saline or Carnoy's fixative. Sections were de-waxed with xylene and rehydrated through graded alcohols and water. Slides were then transferred to Sequenza slide carriers (Thermo Shandon) and washed through with phosphate buffered saline (PBS). Following washing, 100 µl of 3,3'-diaminobenzidine (DAB) (Envision kit, Dako Ltd) were added to each section for 8 min to visualise the eosinophils through peroxidase staining reaction (Kingston and Pearson 1981). Slides were washed with distilled water, counterstained with Haematoxylin Z (Cellpath) and then dehydrated and mounted.

2.2.18 Enumeration of Eosinophils

All histological counts were performed without knowledge of cyathostomin burden. Positively-staining cells, which were pink with H&E and Carbol Chromotrope and brown with DAB (Kingston and Pearson 1981), were identified and counted as per mast cell enumeration. Eosinophils were expressed as eosinophil cells (EC) per mm².

2.2.19 Data Analysis

As data were not normally distributed, non-parametric tests were selected. For optimal graphical representation log transformed (log10+1) data is sometimes presented. Statistical analyses and graphical displays were performed using the statistical computer package R Studio (V 0.97.551), Minitab 15 statistical software and GraphPad Prism5. For investigating parasitological relationships, correlations were assessed using the Spearman rank test in R. Correlations were also investigated between mast cell counts, using the same test also in R. For comparison of paired data the Wilcoxon Signed rank test was selected and for unpaired, the Mann-Whitney

Mast Cell Recruitment and Activation as Measures of Cyathostomin Burden

test using GraphPad Prism5. Standard linear regression analysis was used to explore the relationships between log₁₀+1 transformed mucosal and submucosal mast cell counts and log₁₀+1 transformed combined total mucosal burdens using Minitab 15. The presence of *A. perfoliata* was added as a confounding variable. Results were considered statistically significant at $p < 0.05$.

2.3 Results

2.3.1 Sample Cohort

Samples were collected for parasite enumeration, histological evaluation, mast cell enumeration and proteinase expression from the equine abattoir and the R(D)SVS.

2.3.1.1 Equine Abattoir

Sixteen horses were sampled from the equine abattoir. On post mortem there was evidence of *A. perfoliata* infection from gross examination in 6 of the 16 horses (37.5%) (Table 2.1). Luminal cyathostomins were found in 75% and 88% of the horses in the caecum and the RVC, respectively (Table 2.1).

Horse	Av FEC (EPG)	Tapeworm on FEC	Tapeworm on PM	Tapeworm Status	Total Luminal count in Caecum	Total Luminal count in RVC
AB 1	21	Y	N	Y	0	1,800
AB 2	7	N	Y	Y	263	0
AB 3	0	N	N	N	0	0
AB 4	16	N	Y	Y	975	3,375
AB 5	0	N	N	N	0	138
AB 6	13	Y	N	Y	1,750	27,750
AB 7	10	N	N	N	4,020	46,340
AB 8	39	N	N	N	0	1,320
AB 9	29	N	N	N	2,520	400
AB 10	17	N	Y	Y	70	5,120
AB 11	290	N	Y	Y	8,600	81,300
AB 12	141	N	Y	Y	9,780	16,600
AB 13	315	N	N	N	1,260	19,590
AB 14	186	N	N	N	100	2,700
AB 15	36	N	N	N	540	760
AB 16	16	N	Y	Y	115	1,200

Table 2.1: Results of non-mucosal cyathostomin enumerations and tapeworm observations from abattoir horses, AB1-16. (Av FEC: Average Faecal Egg Count; EPG: Eggs Per Gram; PM: Post Mortem; RVC: Right ventral colon).

Mast Cell Recruitment and Activation as Measures of Cyathostomin Burden

Developing larvae enumerated by TMI were found in 14 of the 16 (88%), and 15 of the 16 (94%) horses in the caecum and RVC, respectively (Table 2.2). This finding was consistent with the enumerations performed by peptic digestion. Of all the 16 abattoir horses only one, AB3, had no detectable parasites.

Horse	Total TMI count in Caecum	Total TMI count in RVC	Total DIG count in Caecum	Total DIG count in RVC	TMB count in Caecum	TMB count in RVC
AB 1	2,536	14,000	143,746	312,653	146,281	326,653
AB 2	21,002	41,804	32,085	77,878	53,087	119,683
AB 3	0	0	0	0	0	0
AB 4	1,075	670	3,880	664	4,954	1,334
AB 5	21	20	2,079	1,015	2,100	1,035
AB 6	29,198	88,919	102,807	80,684	132,004	169,603
AB 7	3,665	3,818	216,994	226,746	220,659	230,564
AB 8	3,670	5,849	3,266	9,333	6,935	15,183
AB 9	199	393	20,670	23,794	20,869	24,187
AB 10	2,452	8,554	94,623	109,315	97,075	117,870
AB 11	8,043	17,085	46,246	86,360	54,289	103,445
AB 12	4,240	7,326	31,799	71,712	36,039	79,038
AB 13	18,911	14,166	95,589	55,714	114,499	69,880
AB 14	1,098	1,934	19,238	25,483	20,335	27,417
AB 15	4,786	1,209	12,733	4,491	17,519	5,700
AB 16	0	446	0	7,910	0	8,355

Table 2.2: Results of mucosal cyathostomin enumerations from abattoir horses AB1-16. (RVC: Right ventral colon; DIG: Digest; TMI: Transmural Illumination; TMB: Total Mucosal Burden).

2.3.1.2 R(D)SVS

Twelve horses were sampled at the R(D)SVS over the period 28/01/11 to 05/09/2012. Where possible, gender, age and the reason for euthanasia for each case were reported, as detailed in Table 2.3.

Horses	Sample Date	Age (year)	Gender	Reason for Euthanasia
DV 1	28/01/2011	15	Male	Poor performance
DV 2	09/02/2011	22	Female	Elective
DV 3	05/04/2011	3	Female	Larval cyathostominosis
DV 4	11/05/2011	14	Male	Lame
DV 5	18/05/2011	>15	Female	Laminitis
DV 6	13/12/2011	4	Female	Elective
DV 7	31/05/2012	4	Male	Elective
DV 8	07/06/2012	>15	Male	Elective
DV 9	04/07/2012	5-15	Male	Elective
DV 10	09/07/2012	5-15	Male	Elective
DV 11	11/07/2012	25	Female	Hyperadrenocorticism
DV 12	05/09/2012	1	Male	Elective

Table 2.3: Data collected from R(D)SVS horses DV1-12 including sample date, age, gender and reason for euthanasia.

On post mortem there was evidence of *A. perfoliata* from gross examination in 1 of the 16 cases (Table 2.4). No horses had evidence of tapeworm on FEC, though this methodology is not validated for these worms. Luminal cyathostomins were found in 50% of the cases, in both the caecum and the RVC (Table 2.4).

Mast Cell Recruitment and Activation as Measures of Cyathostomin Burden

Horses	Av FEC (EPG)	Tapeworm on FEC	Tapeworm on PM	Tapeworm Status	Total Luminal count in Caecum	Total Luminal count in RVC
DV 1	0	N	N	N	0	0
DV 2	89	N	Y	Y	500	188
DV 3	0	N	N	N	400	570
DV 4	16	N	N	N	120	1,200
DV 5	0	N	N	N	0	0
DV 6	0	N	N	N	0	0
DV 7	7	N	N	N	0	120
DV 8	396	N	N	N	230	19,000
DV 9	155	N	N	N	600	11,160
DV 10	1	N	N	N	0	0
DV 11	1	N	N	N	0	0
DV 12	26	N	N	N	90	0

Table 2.4: Results of non-mucosal cyathostomin enumerations and tapeworm observations from R(D)SVS horses, DV1-12. (Av FEC: Average Faecal Egg Count; EPG: Eggs Per Gram; PM: Post Mortem; RVC: Right ventral colon).

Developing larvae were enumerated by TMI and found in 5 of the 12 (42%) and 8 of the 12 (67%) horses in the caecum and RVC, respectively. In the case of encysted larvae, EL3 were found in 4 of the 12 (33 %) and 7 of the 12 (58%) horses in the caecum and RVC, respectively. Three of the R(D)SVS cases (25%), DV1, DV5 and DV6, were found to be strongyle free. Horse DV3 had a markedly higher cyathostomin burden with more than 1.7 million larvae in the caecum and more than 2 million larvae in the RVC (Table 2.5).

Horses	Total TMI count in Caecum	Total TMI count in RVC	Total DIG count in Caecum	Total DIG count in RVC	TMB count in Caecum	TMB count in RVC
DV 1	0	0	0	0	0	0
DV 2	187	87	0	1,947	187	2,035
DV 3	96,928	51,124	1,676,119	2,002,927	1,773,046	2,054,051
DV 4	0	19	0	643	0	662
DV 5	0	0	0	0	0	0
DV 6	0	0	0	0	0	0
DV 7	0	75	0	0	0	75
DV 8	40	334	0	656	40	990
DV 9	2,323	6,380	23,853	109,791	26,177	116,171
DV 10	0	0	0	656	0	656
DV 11	0	39	640	0	640	39
DV 12	699	1320	665	656	1364	1976

Table 2.5: Results of mucosal cyathostomin enumerations from R(D)SVS horses, DV1-12. (RVC: Right ventral colon; DIG: Digest; TMI: Transmural Illumination; TMB: Total Mucosal Burden).

2.3.2 Comparison of Location of Sample Collection

The two different sampling sites, the R(D)SVS and the abattoir, represent two distinct cohorts. Individual value plots (Figures 2.2 and 2.3) are presented of the luminal and total mucosal burden. The two cohorts were different in their luminal ($p=0.007$) and total mucosal ($p=0.005$) burdens with the abattoir cohort having significantly greater burdens than the R(D)SVS population.

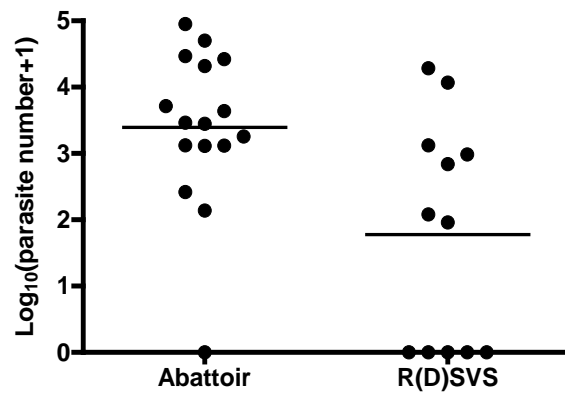


Figure 2.2: Individual value plot of $(\log_{10}+1)$ transformed total luminal cyathostomin counts from abattoir and R(D)SVS horses for comparison of sample location. Luminal counts for the abattoir horses were significantly higher than the horses sampled from the R(D)SVS, $p=0.007$ (Test: Mann-Whitney). The non-axis horizontal line indicates the median.

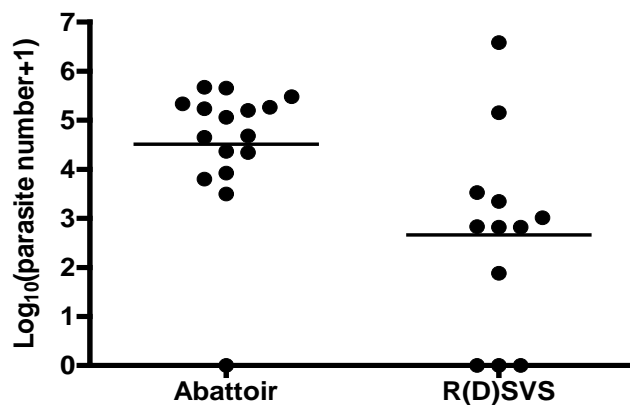


Figure 2.3: Individual value plot of $(\log_{10}+1)$ transformed CTMB counts from Abattoir and R(D)SVS horses for comparison of sample location. CTMB counts for the abattoir horses were significantly higher than the horses sampled from the R(D)SVS, $p=0.005$ (Test: Mann-Whitney). The non-axis horizontal line indicates the median.

2.3.3 Cyathostomin Recovery

2.3.3.1 Larval Recovery Techniques

The peptic tissue digest method was optimised for enumeration of EL3 (Figure 2.4: black arrow). Developing larvae were also observed in the digested matter (Figure 2.4). These larvae displayed evidence of morphological damage which increased with digest time (Figure 2.5: black arrow).

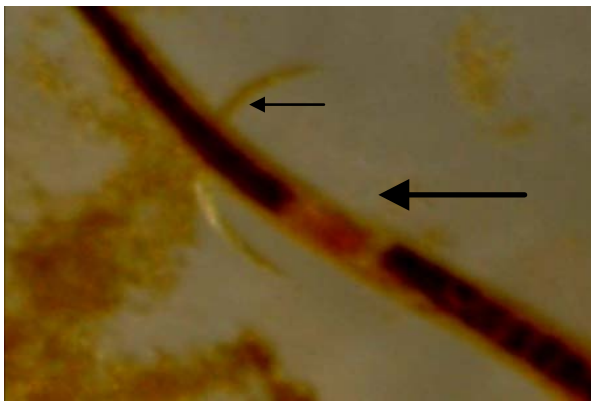
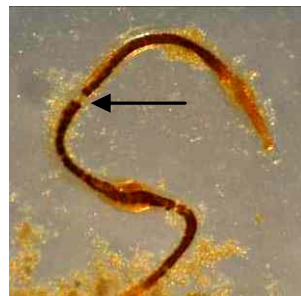


Figure 2.4: Image of large developing larvae (large black arrow) and encysted third stage larvae below it (small, eye lash shaped – small black arrow) following tissue digest for comparison of difference in size at developmental stages.



A



B

Figure 2.5: Images of larvae released from tissue. A: Image of encysted third stage larvae released from caecal tissue and stained with iodine, following peptic digestion. B: Image of developing larvae released from mucosa following tissue digest and displaying evidence of morphological damage (black arrow).

2.3.3.2 Evidence of Empty Cysts on Transmural Illumination

In a number of cases, evidence of previous larval damage was observed (Figure 2.6). Areas suggestive of the recent presence of larvae were noted on TMI in 10 out of the 28 horses (36%). These areas of fibrous capsules surrounding a more translucent empty cyst-like structure have previously been documented as potential areas of larval damage (Steinbach, Bauer et al. 2006; Pickles, Mair et al. 2010; Stancampiano, Gras et al. 2010). Horse AB3 was negative for cyathostomins on TMI but had a large number of areas suggestive of previous larval cysts.

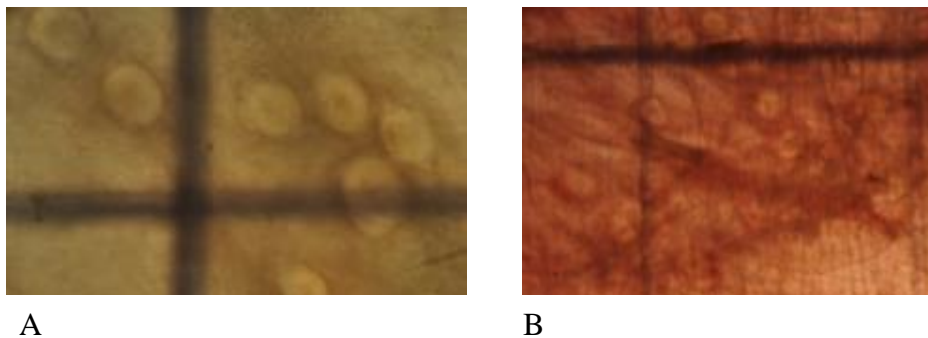


Figure 2.6: Image from Transmural Illumination of areas suggestive of empty cysts. A: AB16 Caecum. B: AB3 Right ventral colon.

2.3.3.3 Evidence of Encysted Larvae in Rectal Mucosa

Two rectal biopsies were taken from each of the 28 horses and examined by TMI for the presence of developing larvae. The mean mass of the combined biopsies was 0.5g +/- 0.2g. The tissue was subsequently digested and this digest examined for EL3. Of the 28 horses, encysted L3 were seen in one case (4%) (AB2) and DL in two (7%) (AB6 and DV3) (Figure 2.7).

2.3.3.4 Case of Larval Cyathostominosis



Figure 2.9: Image of a clinical case of larval cyathostominosis, horse DV3, at post mortem. This horse was sampled at the R(D)SVS.

Horse DV3 was confirmed at post mortem to have larval cyathostominosis. The horse was in poor body condition (Figure 2.9) and there was evidence of numerous adult cyathostomin larvae around the rectum and in the faeces. The intestinal tissue was inflamed, hyperaemic and oedematous (Figure 2.10). The FEC for this animal was negative. The luminal count was positive, with burdens of 800 and 1,140 larvae in the caecum and RVC respectively. On TMI assessment, numerous larvae were seen at various stages of development. Tissue digest revealed EL3 burdens of approximately 1.7 million and over 2 million in the caecum and RVC, respectively. Evidence of DL was seen on TMI of biopsied rectal tissue.



Figure 2.10: Image of inflamed, hyperaemic and oedematous tissue from the right ventral colon of Horse DV3, a case of larval cyathostominosis.

2.3.4 Parasitology

2.3.4.1 Faecal Egg Counts

A negative FEC was observed in six cases (21 %) (AB3, AB5, DV1, DV3, DV5 and DV6). The median FEC was 16 EPG (range 0 - 396 EPG). Three horses (AB11, AB13 and DV8) had FEC greater than 200 EPG (Figure 2.11). Table 2.6 shows the p values for correlation between FEC and the cyathostomin counts using a Spearman rank correlation test for non-parametric data. The FEC significantly positively correlated with the luminal count in the caecum and RVC but not the EL3 and TMB in the caecum (Table 2.6).

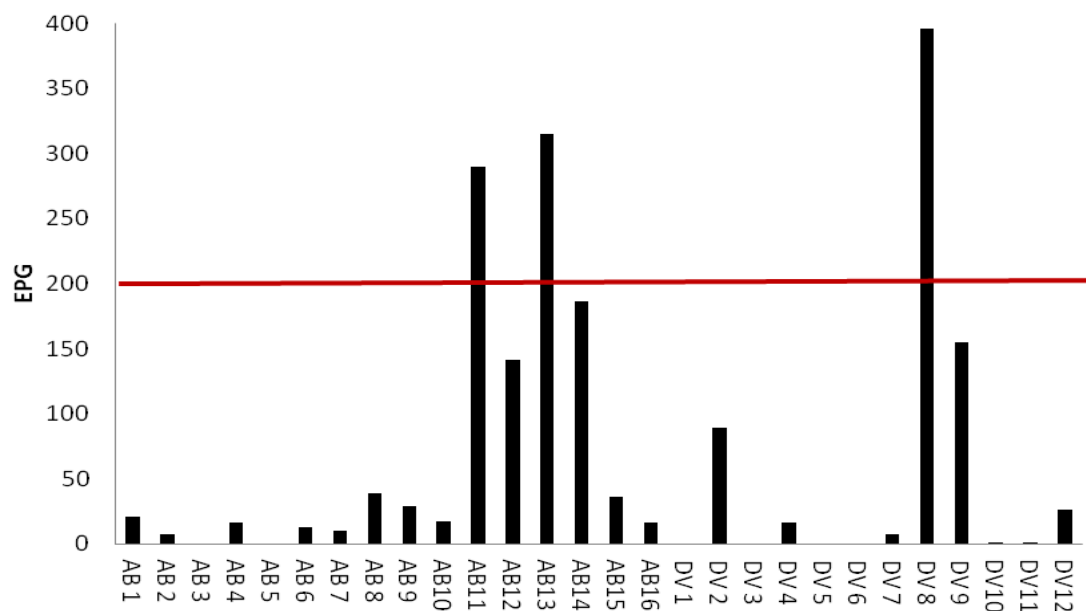


Figure 2.11: Barchart of average faecal egg count (FEC) of all horses sampled (AB1-16 and DV1-12). Red line indicates a FEC of 200 egg per gram (EPG).

	FEC	
	p-value	rho
Luminal Caecum	0.002	0.566
Luminal RVC	<0.001	0.675
DL Caecum	0.018	0.442
DL RVC	0.011	0.474
EL3 Caecum	<i>0.149</i>	0.280
EL3 RVC	0.031	0.409
TMB Caecum	<i>0.062</i>	0.358
TMB RVC	0.031	0.407

Table 2.6: Table of *p-values* (italic) and rho values (bold) for correlations between FEC and cyathostomin burdens. Correlations performed using Spearman rank analysis. Significant correlations ($p < 0.05$) are highlighted. (FEC: Faecal egg count; RVC: Right ventral colon; DL: Developing larvae; EL3: Encysted third stage larvae; TMB: Total Mucosal Burden).

2.3.4.2 Luminal Counts

Luminal counts were performed on the caecal and RVC contents. The visualisation of cyathostomin was greatly improved with the addition of iodine. Male and female cyathostomins were observed (Figure 2.12). Six horses (21%) had no evidence of luminal burdens (AB3, DV1, DV5, DV6, DV10 and DV11). Horses AB1, AB5, AB8 and DV7 were negative in the caecum but had RVC luminal burdens. Conversely, horses AB2 and DV12 had burdens in their caecum only.



Figure 2.12: Image of male (left) and female (right) luminal cyathostomins stained with iodine.

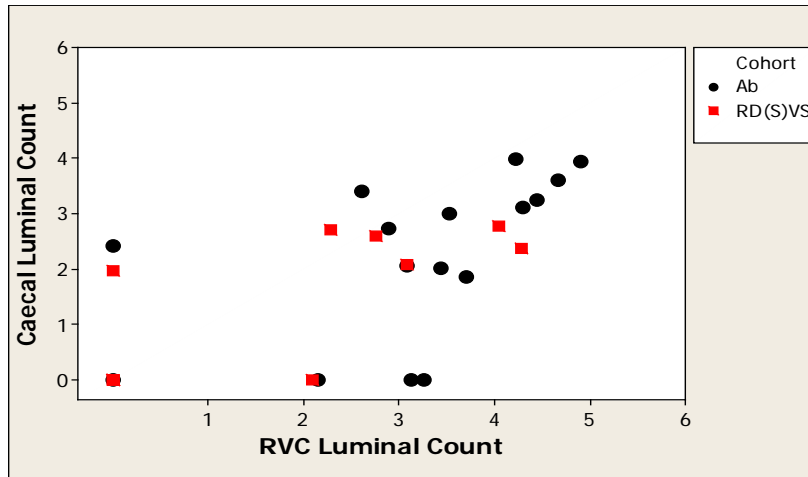


Figure 2.13: Scatterplot of log₁₀+1 transformed RVC luminal (y-axis) versus caecal luminal (x-axis) counts coloured according to sample location (Abattoir (ab): black; R(D)SVS: red). $p < 0.001$, $\rho = 0.695$. (Test: Spearman rank). (RVC: Right ventral colon).

Luminal counts ranged from 0 to 9,780 (AB 12) in the caecum (median 118) and 0 to 81,300 (AB 11) in the RVC (median 980). There was a strong correlation between the counts in the two organs, $p < 0.001$ (Figure 2.13). In the majority of cases (86%) the luminal burden was greater in the RVC than the caecum and this was statistically significant, $p = 0.001$ (Figure 2.14).

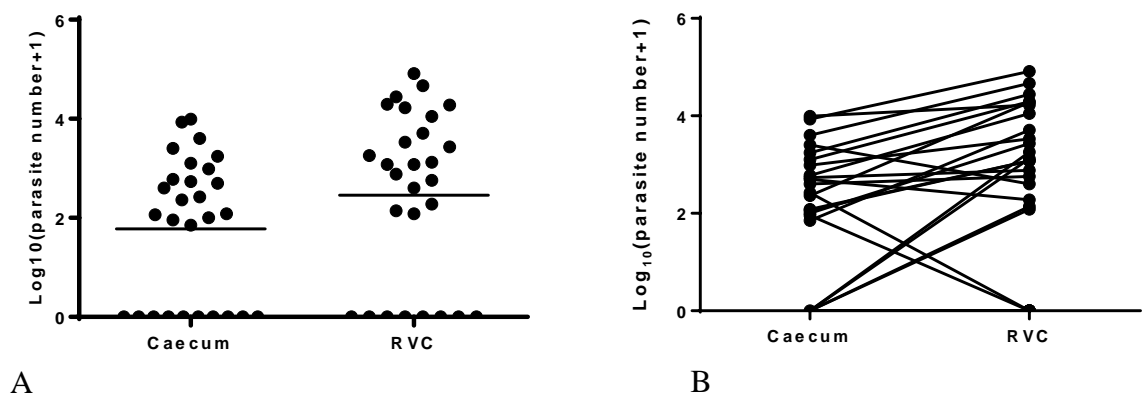


Figure 2.14: A: Individual log₁₀+1 transformed value plot of caecal and RVC luminal counts. The luminal count in the RVC was significantly greater than in the caecum, $p = 0.001$ (Test: Wilcoxon signed rank test). The non-axis horizontal line indicates the median. B: Graph of individual values of log₁₀+1 caecal and RVC luminal counts with lines connecting the values for each horse. (RVC: Right ventral colon).

2.3.4.3 Mucosal Counts

2.3.4.3.1 *Developing larvae*

Developing larvae were enumerated using the TMI method (Figure 2.15). Five horses were negative on TMI (AB3, DV1, DV5, DV6 and DV10). A further four horses were DL-negative in the caecum, but positive for these stages in the RVC (AB16, DV4, DV7 and DV11). There were no horses that were positive for DL in the caecum yet negative for these stages in the RVC.

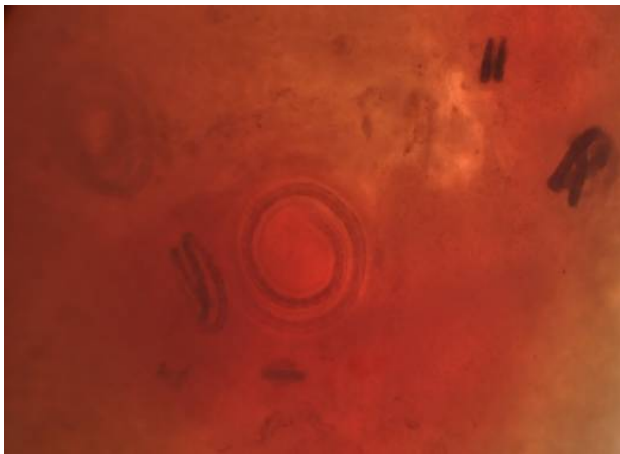


Figure 2.15: Image of evidence of developing larvae (DL) at various stages on Transmural Illumination (TMI) from the caecum of horse AB6.

DL counts ranged from 0 to 96,928 (DV3) in the caecum (median 887) and 0 to 88,919 (AB6) in the RVC (median 939). There was a strong correlation between the counts in the two organs, $p < 0.001$ (Figure 2.16). In the majority of cases the DL burden was greater in the RVC than in the caecum and this difference was statistically significant, $p = 0.037$ (Figure 2.17).

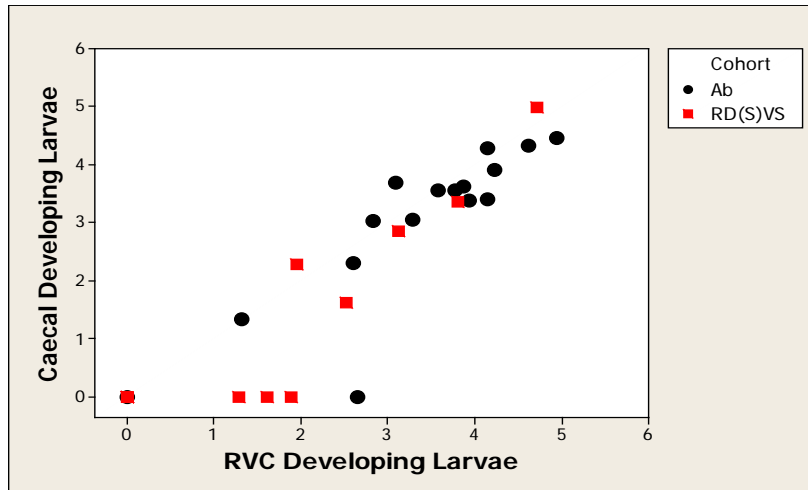


Figure 2.16: Scatterplot of $\log_{10}+1$ transformed RVC DL (x-axis) versus caecal DL (y-axis) counts coloured according to sample location (Abattoir (ab): black, R(D)SVS: red). $p < 0.001$, $\rho = 0.931$. (Test: Spearman rank). (DL: Developing larvae; RVC: Right ventral colon).

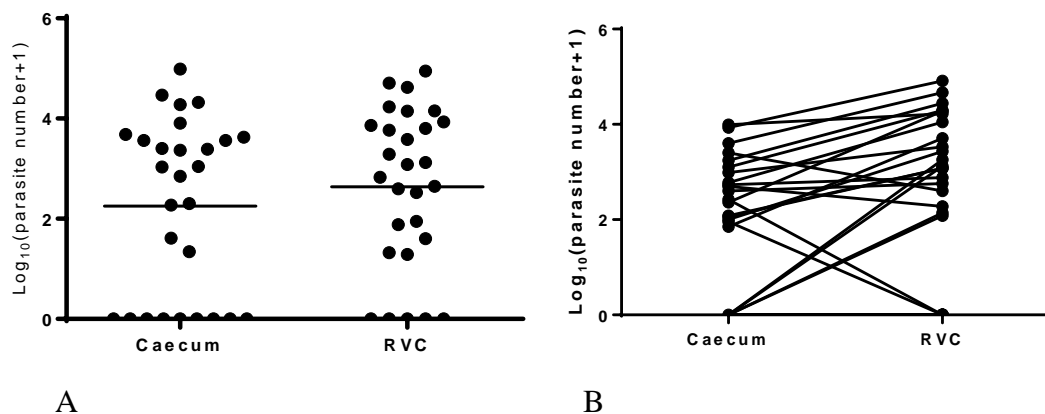


Figure 2.17: A: Individual value plot of $\log_{10}+1$ transformed caecal and RVC DL counts. The DL count in the RVC was significantly greater than that in the caecum, $p = 0.037$ (Test: Wilcoxon signed rank test). The non-axis horizontal line indicates the median. B: Graph of individual values of $\log_{10}+1$ caecal and RVC DL counts with lines connecting the values for each horse. (RVC: Right ventral colon).

2.3.4.3.2 EL3 Count

Early L3 were enumerated from tissue digest (Figure 2.18). Five horses had no evidence of EL3 burdens (AB3, DV1, DV5, DV6 and DV7). Horses AB16, DV2, DV4, DV8 and DV10 were negative in the caecum, but had evidence of EL3 in the RVC. Horse DV11 had evidence of EL3 in the RVC and not the caecum.



Figure 2.18: Image of encysted third stage larvae (EL3) released from tissue through pepsin digest and stained with iodine.

EL3 counts ranged from 0 to 1,676,119 (DV3) in the caecum (median 6,200) and 0 to 2,002,927 (DV3) in the RVC (median 10,254). There was a strong correlation between EL3 counts in the two organs, $p < 0.001$ (Figure 2.19). In the majority of cases, the EL3 burden was greater in the RVC than in the caecum and this difference was statistically significant, $p = 0.025$ (Figure 2.20).

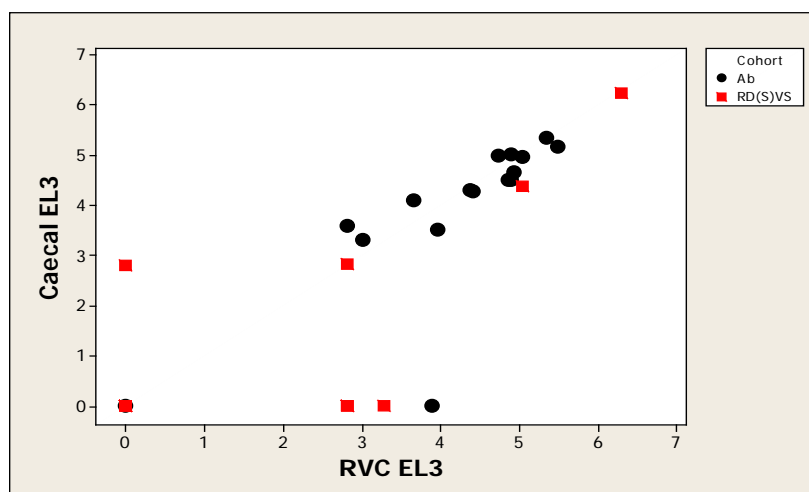


Figure 2.19: Scatterplot of log₁₀+1 transformed caecal EL3 (x-axis) versus RVC EL3 (y-axis) counts coloured according to sample location (Abattoir (ab): black, R(D)SVS: red). $p < 0.001$, $\rho = 0.897$. (Test: Spearman rank). (EL3: Encysted third stage larvae; RVC: Right ventral colon).

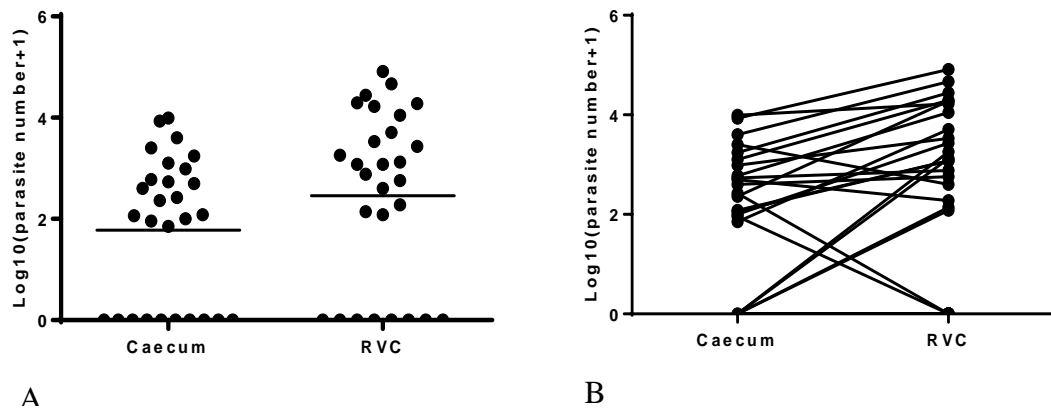


Figure 2.20: A: Individual value plot of log₁₀+1 transformed caecal and RVC EL3 counts. The EL3 count in the RVC was significantly greater than that in the caecum, $p=0.025$ (Test: Wilcoxon signed rank test). The non-axis horizontal line indicates the median. B: Graph of individual values of log₁₀+1 caecal and RVC EL3 counts with lines connecting the values for each horse. (RVC: Right ventral colon).

2.3.4.4 Comparison of Larval Recovery Techniques

Caecal and RVC DL were enumerated in two ways: from TMI assessment and tissue digest analysis (DIG). In both organs, the two methods produced counts that were significantly correlated, $p<0.001$ (Figure 2.21). In the caecum, there was no significant difference between the two counting techniques, $p=0.507$ (Figure 2.22). However, in the RVC the TMI count was significantly different to those estimated by DIG, $p=0.040$ (Figure 2.23). Therefore, for all developing larval (DL) comparisons TMI counts were used.

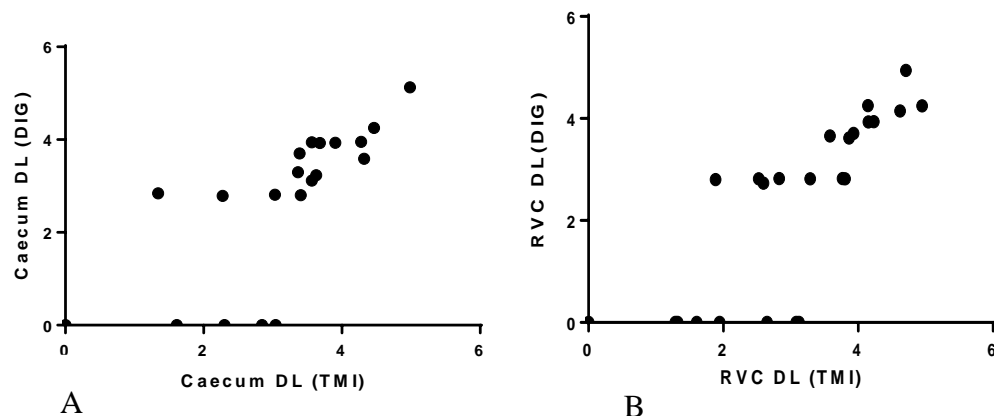


Figure 2.21: A: Scatterplot of log₁₀+1 transformed caecal DL from TMI (x-axis) versus caecal DL from DIG (y-axis) counts, $p < 0.001$, $\rho = 0.889$. (Test: Spearman rank). B: Scatterplot of log₁₀+1 transformed counts of RVC DL from TMI (x-axis) versus RVC DL from DIG (y-axis). $p < 0.001$, $\rho = 0.888$. (RVC: Right ventral colon; DL: Developing larvae; EL3: Encysted third stage larvae; TMI: Transmural Illumination; Dig: Digest).

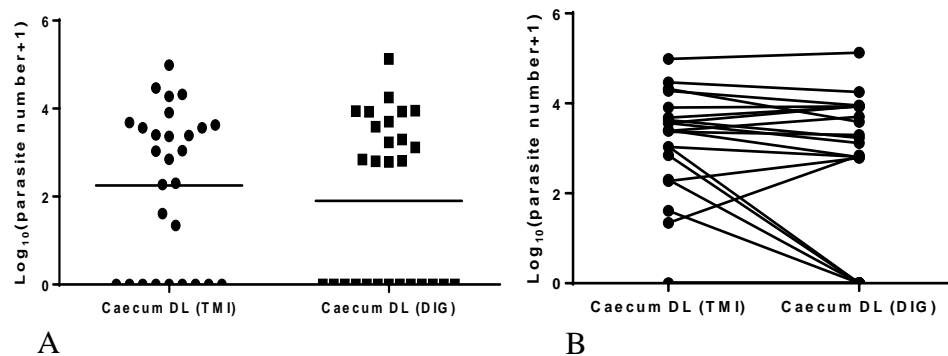


Figure 2.22: A: Individual log₁₀+1 transformed value plot of caecal DL from TMI and caecal DL from DIG counts. There was no significant difference between the caecal DL count from TMI or DIG, $p = 0.507$ (Test: Wilcoxon signed rank test). The non-axis horizontal line indicates the median. B: Graph of individual values of log₁₀+1 caecal DL from TMI and caecal DL from DIG counts with lines connecting the values for each horse. (DL: Developing larvae; TMI: Transmural Illumination; Dig: Digest).

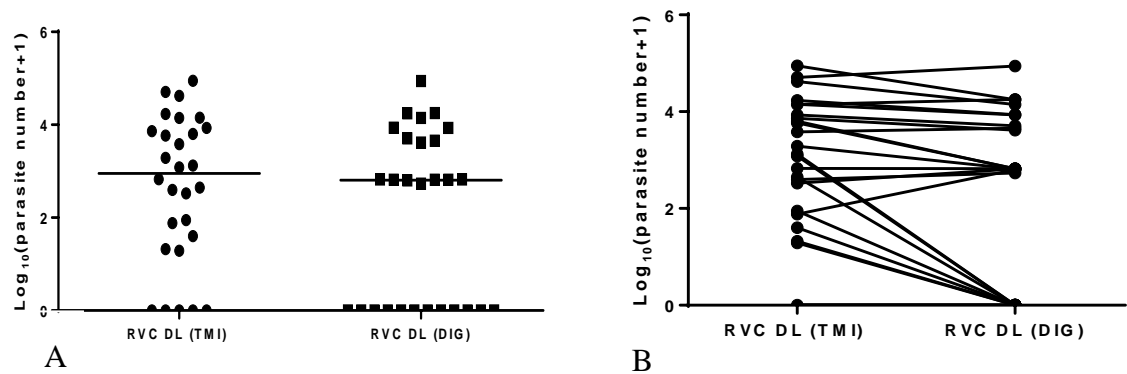


Figure 2.23: A: Individual log₁₀+1 transformed value plot of RVC DL from TMI and RVC DL from DIG counts. There were significantly more DL counted from TMI than from DIG, $p=0.040$ (Test: Wilcoxon signed rank test). The non-axis horizontal line indicates the median. B: Graph of individual values of log₁₀+1 RVC DL from TMI and RVC DL from DIG counts with lines connecting the values for each horse. (RVC: Right ventral colon; DL: Developing larvae; TMI: Transmural Illumination; Dig: Digest).

2.3.4.5 Total Mucosal Burdens

The TMB for each organ was calculated from the combination of DL from TMI and EL3 populations from tissue digest. The TMB of the caecum ranged from 0–1,773,047 encysted larvae with a median of 5,945. The RVC had a greater TMB range of 0–2,054,051 and a median of 7,028. The RVC had a significantly greater total population, $p=0.006$ (Figure 2.24). Using a Spearman rank correlation test for non-parametric data, Table 2.7 shows the p values for correlation between cyathostomin TMB in the caecum or RVC and the various cyathostomin developmental stages. The only non-significant correlation was between the FEC and the caecal TMB ($p=0.062$, $\rho=0.358$).

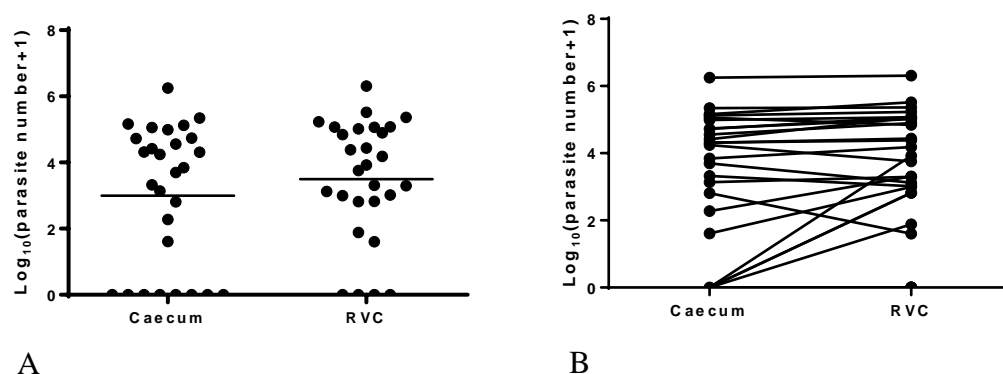


Figure 2.24: A: Individual log₁₀+1 transformed value plot of caecal TMB and RVC TMB. The RVC had a significantly greater TMB than the caecum, $p=0.006$ (Test: Wilcoxon signed rank test) The non-axis horizontal line indicates the median. B: Graph of individual values of log₁₀+1 caecum and RVC TMB with lines connecting the values for each horse. (RVC: Right ventral colon).

	TMB Caecum		TMB RVC	
	<i>p-value</i>	rho	<i>p-value</i>	rho
FEC	0.062	0.358	0.031	0.407
Luminal C	0.001	0.594	0.001	0.601
Luminal RVC	<0.001	0.636	<0.001	0.649
Total Luminal	<0.001	0.693	<0.001	0.711
DL Caecum	<0.001	0.905	<0.001	0.862
DL RVC	<0.001	0.900	<0.001	0.927
Total DL	<0.001	0.909	<0.001	0.925
EL3 Caecum	<0.001	0.988	<0.001	0.910
EL3 RVC	<0.001	0.910	<0.001	0.980
Total EL3	<0.001	0.949	<0.001	0.979
TMB Caecum	NA	NA	<0.001	0.927
TMB RVC	<0.001	0.927	NA	NA
CTMB	<0.001	0.962	<0.001	0.984

Table 2.7: Table of p-value (italic) and rho values (bold) for correlations between caecal and RVC TMB's and parasitology data. Significant p values (<0.05) are highlighted. (Test: Spearman rank). (FEC: Faecal egg count; RVC: Right ventral colon; DL: Developing larvae; EL3: Encysted third stage larvae; TMB: Total Mucosal Burden; CTMB: Combined Total Mucosal Burden).

Of the cyathostomin-positive horses, in all but three cases (DV4, DV7 and DV8), the mucosal burden made up more than 50% of the total cyathostomin count. Mural counts were significantly higher than luminal counts in both the caecum and RVC ($p<0.001$). Similarly, in all but two horses (DV6 and DV12) the EL3 population made up more than 50% of the TMB and EL3 counts were significantly higher than DL counts in both organs ($p<0.001$). The matrix plot (Figure 2.25) graphically demonstrates the relationships between the combined (caecum and RVC) luminal, total DL, total EL3, combined total mucosal burden (CTMB) and average FEC. The corresponding p values can be found in Appendix Table 2.8. The CTMB displayed a strong correlation with the total EL3 ($p<0.001$, $\rho=0.990$). The only non-significant correlations were between the average FEC and the EL3 count and TMB of the caecum (Table 2.8).

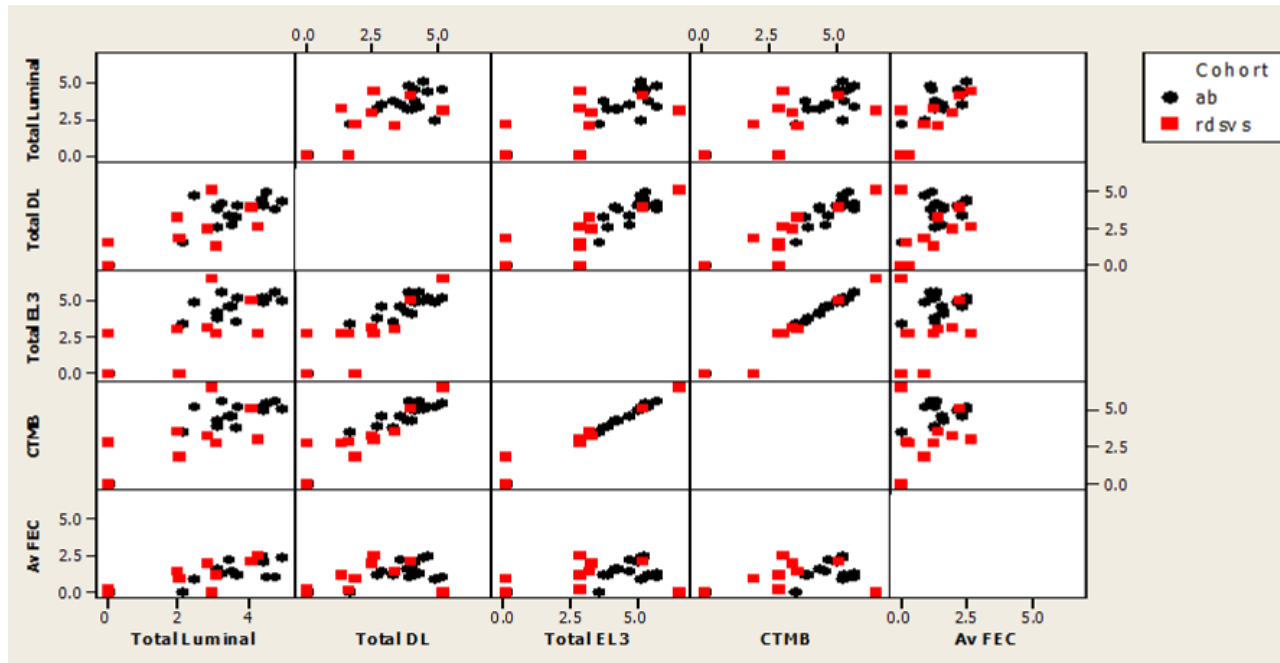


Figure 2.25: Matrix scatterplot of log10+1 transformed data for total (caecum and RVC combined) luminal, total DL, total EL3, CTMB and average FEC grouped according to sample location (Abattoir: black, R(D)SVS: red). (FEC: Faecal Egg Count; DL: Developing larvae; EL3: Encysted third stage larvae; CTMB: Combined Total Mucosal Burden).

Mast Cell Recruitment and Activation as Measures of Cyathostomin Burden

	FEC	Lum. Caecum	Lum. RVC	Total Lum	DL Caecum	DL RVC	Total DL	EL3 Caecum	EL3 RVC	Total EL3	TMB Caecum	TMB RVC	CTMB
FEC		0.566	0.675	0.707	0.442	0.474	0.472	0.280	0.409	0.401	0.358	0.407	0.405
Luminal C	<i>0.002</i>		0.695	0.795	0.643	0.597	0.607	0.564	0.586	0.595	0.594	0.601	0.602
Luminal RVC	<i><0.001</i>	<i><0.001</i>		0.970	0.600	0.649	0.642	0.604	0.673	0.680	0.636	0.649	0.672
Total Luminal	<i><0.001</i>	<i><0.001</i>	<i><0.001</i>		0.656	0.703	0.698	0.661	0.718	0.723	0.693	0.711	0.724
DL Caecum	<i>0.018</i>	<i><0.001</i>	<i>0.001</i>	<i><0.001</i>		0.931	0.953	0.883	0.827	0.860	0.905	0.862	0.881
DL RVC	<i>0.011</i>	<i>0.001</i>	<i><0.001</i>	<i><0.001</i>	<i><0.001</i>		0.995	0.885	0.875	0.901	0.900	0.927	0.934
Total DL	<i>0.011</i>	<i>0.001</i>	<i><0.001</i>	<i><0.001</i>	<i><0.001</i>	<i><0.001</i>		0.893	0.876	0.904	0.909	0.925	0.936
EL3 Caecum	<i>0.149</i>	<i>0.002</i>	<i>0.001</i>	<i><0.001</i>	<i><0.001</i>	<i><0.001</i>	<i><0.001</i>		0.895	0.941	0.988	0.910	0.952
EL3 RVC	<i>0.031</i>	<i>0.001</i>	<i><0.001</i>	<i><0.001</i>	<i><0.001</i>	<i><0.001</i>	<i><0.001</i>	<i><0.001</i>		0.983	0.910	0.980	0.963
Total EL3	<i>0.034</i>	<i>0.001</i>	<i><0.001</i>	<i><0.001</i>	<i><0.001</i>	<i><0.001</i>	<i><0.001</i>	<i><0.001</i>	<i><0.001</i>		0.949	0.979	0.990
TMB Caecum	<i>0.062</i>	<i>0.001</i>	<i><0.001</i>	<i><0.001</i>	<i><0.001</i>	<i><0.001</i>	<i><0.001</i>	<i><0.001</i>	<i><0.001</i>	<i><0.001</i>		0.927	0.962
TMB RVC	<i>0.031</i>	<i>0.001</i>	<i><0.001</i>	<i><0.001</i>	<i><0.001</i>	<i><0.001</i>	<i><0.001</i>	<i><0.001</i>	<i><0.001</i>	<i><0.001</i>	<i><0.001</i>		0.984
CTMB	<i>0.033</i>	<i>0.001</i>	<i><0.001</i>	<i><0.001</i>	<i><0.001</i>	<i><0.001</i>	<i><0.001</i>	<i><0.001</i>	<i><0.001</i>	<i><0.001</i>	<i><0.001</i>	<i><0.001</i>	

Table 2.8: Table of p values (italics) and rho values (bold) for correlation matrix of parasite count data. Significant p values (<0.05) are highlighted. (FEC: Faecal Egg Count; RVC: Right ventral colon; DL: Developing larvae; EL3: Encysted third stage larvae; TMB: Total Mucosal Burden; CTMB: Combined Total Mucosal Burden).

2.3.5 Mast Cell Response

2.3.5.1 Validation of Rectal Biopsy Technique

To verify that rectal biopsies were representative of rectal tissue, cell counts of rectal tissue sections and rectal biopsy pilot data were compared as average cell count per field. Mucosal and submucosal mast cells were enumerated and the results are shown in Table 2.9. The mast cell counts from the rectal biopsy and tissue sections were significantly correlated in the case of the mucosa and the submucosa, $p < 0.001$ (Figure 2.26). There was no significant difference between the two methods of tissue sampling for mast cell counts in either the mucosa, $p = 0.128$ (Figure 2.27), or submucosa, $p = 0.171$ (Figure 2.28).

	RS	RB	RS	RB
	MMC	MMC	SMMC	SMMC
	(av cell count/field)	(av cell count/field)	(av cell count/field)	(av cell count/field)
AB1	12	6	10	17
AB2	28	26	18	15
AB3	9	6	5	4
AB4	34	29	18	14
AB5	7	6	7	6
AB6	26	20	12	13
AB7	4	3	9	10
AB8	26	18	11	20
AB9	11	20	9	14
AB10	33	26	12	15
AB11	28	19	14	18
AB12	31	34	19	21
AB13	13	22	10	10
AB14	11	9	12	13
AB15	10	8	10	11
AB16	12	13	9	8

Table 2.9: Results of mucosal (MMC) and submucosal (SMMC) mast cell counts from the rectal sections (RS) and rectal biopsies (RB) of abattoir horses (AB1-16). Cells expressed as average cell count per field.

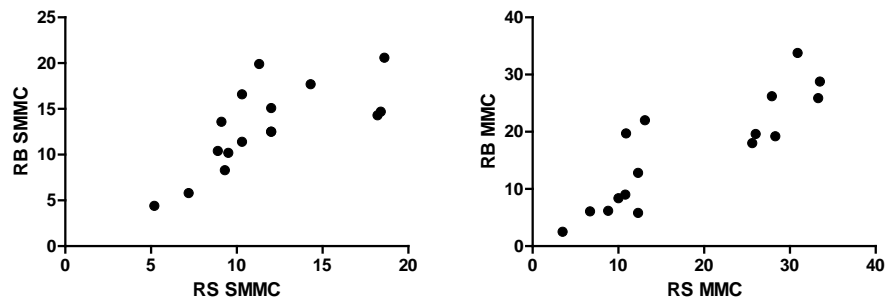


Figure 2.26: Scatterplot of average cell count per field of MMC from rectal sections (x-axis) versus rectal biopsies (y-axis), $p < 0.001$, $\rho = 0.850$. (Test: Spearman rank). Scatterplot of average cell count per field of SMMC from rectal sections (x-axis) versus rectal biopsies (y-axis), $p < 0.001$, $\rho = 0.758$. Note different y-axis scales. (Test: Spearman rank). (MMC: Mucosal mast cell; SMMC: Submucosal mast cell; RS: Rectal Section; RB: Rectal biopsy).

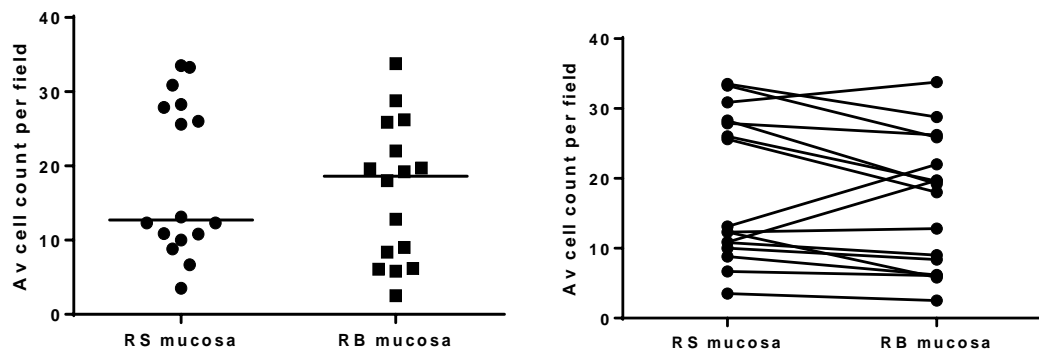


Figure 2.27: A: Individual value plot of average cell count per field of RS and RB mucosal mast cell (MMC) counts. There was no significant difference between RS and RB MMC counts, $p = 0.128$ (Test: Wilcoxon signed rank test). The non-axis horizontal line indicates the median. B: Graph of individual values of RS and RB mucosal mast cell (MMC) counts with lines connecting the values for each horse. (RS: Rectal Section; RB: Rectal biopsy).

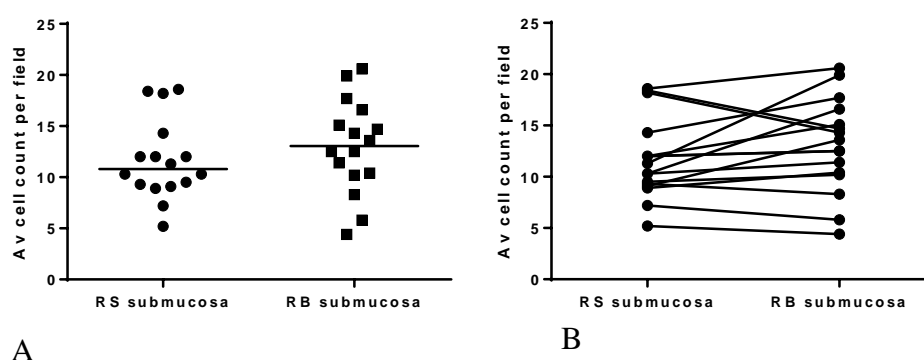


Figure 2.28: A: Individual value plot of average cell count per field of RS and RB submucosal mast cell counts. There was no significant difference between RS and RB SMMC counts, $p=0.171$ (Test: Wilcoxon signed rank test). The non-axis horizontal line indicates the median. B: Graph of individual values of RS and RB submucosal mast cell (SMMC) counts with lines connecting the values for each horse. (RS: Rectal Section; RB: Rectal biopsy).

2.3.5.2 Mast Cell Counts

Using Toluidine Blue mast cells stained blue (Figure 2.29). Mast cells in the submucosa had a greater staining intensity compared with the mucosal populations. Mast cells in the submucosa were also more distinct in their cell outline. The median and range of the mucosal and submucosal mast cell counts for the caecum, RVC and RB for all the horses (AB1-AB16 and DV1-DV12) are shown in Table 2.10. The mucosal and submucosal mast cell counts for the caecum, RVC and RB are shown in Table 7.1 of the appendix for the abattoir and R(D)SVS horses.

	MMC Caecum (MC/mm ²)	SMMC Caecum (MC/mm ²)	MMC RVC (MC/mm ²)	SMMC RVC (MC/mm ²)	MMC RB (MC/mm ²)	SMMC RB (MC/mm ²)
Median	444	261	428	322	190	192
Range	22-1,062	110-437	34-1,470	110-445	19-541	70-383

Table 2.10: Median and range of MMC and SMMC from the caecum, RVC and rectum of all horses (AB1-16 and DV1-12). Cells expressed as MC per mm². (MMC: Mucosal mast cell; SMMC: Submucosal mast cell; RVC: Right ventral colon; RB: Rectal biopsy).

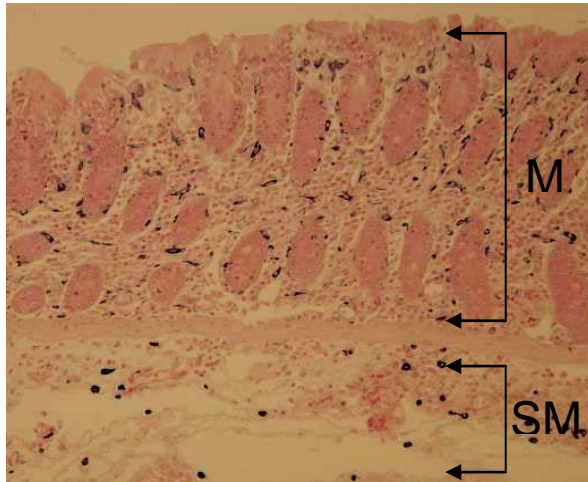


Figure 2.29: Image of caecal tissue section from horse AB9 stained with Toluidine Blue. Mast cells in the mucosa and submucosa are stained blue. (M: Mucosa; SM: Submucosa).

2.3.5.3 Histopathology of a Case of Larval Cyathostomniosis

Tissue sections from Horse DV3 fixed in Carnoy's and stained with Toluidine Blue can be seen in Figures 2.30 and 2.31. The submucosa was markedly expanded by increased clear space, consistent with oedema. Muscle bundles within the *tunica muscularis* are also separated by increased clear space. Multifocal to coalescing zones of the *lamina propria* and superficial submucosa were expanded and effaced by increased numbers of lymphocytes, plasma cells, eosinophils, macrophages and giant cells. Mucosal and submucosal larvae were present in the tissue surrounded by dense sheets of epithelioid macrophages, giant cells and outer halos of lymphocytes and fibroblasts (mature granulomas) (Pers Comm: Ms Helena Ferreira).



Figure 2.30: Image of caecal tissue section from horse DV3 stained with Toluidine Blue. Mast cells in the mucosa and submucosa are stained blue. The arrows show larvae present in the centre of submucosal granulomas. (M: Mucosa; SM: Submucosa).



Figure 2.31: Image of right ventral colon mucosal tissue from horse DV3 stained with Toluidine Blue. Mast cells are stained blue. The arrows show encysted larvae present in the centre of mucosal granulomas.

2.3.6 Correlations between Mast Cell Counts at Different Mucosal Sites

The mucosal and submucosal mast cells populations correlated significantly with one another in the caecum (Figure 2.32: $p < 0.001$, $\rho = 0.719$) the RVC (Figure 2.33: $p < 0.001$, $\rho = 0.648$) and the rectum (Figure 2.34: $p < 0.027$, $\rho = 0.417$). All correlations are presented in Table 2.13. The mucosal mast cells counts were significantly correlated between organs (Table 2.11: $p < 0.001$), and this can be seen graphically in the matrix plot (Figure 2.35). The matrix plot in Figure 2.36 demonstrates graphically that the submucosal mast cells counts were also significantly correlated between organs (Table 2.12: $p < 0.001$).

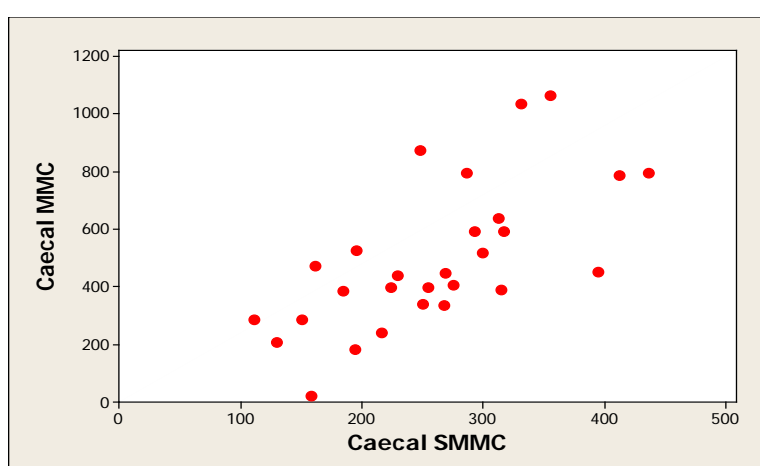


Figure 2.32: Scatterplot of caecal MMC (x-axis) versus caecal SMMC (y-axis). Cells expressed as MC per mm², $p < 0.001$, $\rho = 0.719$. (Test: Spearman rank). (MMC: Mucosal mast cell; SMMC: Submucosal mast cell).

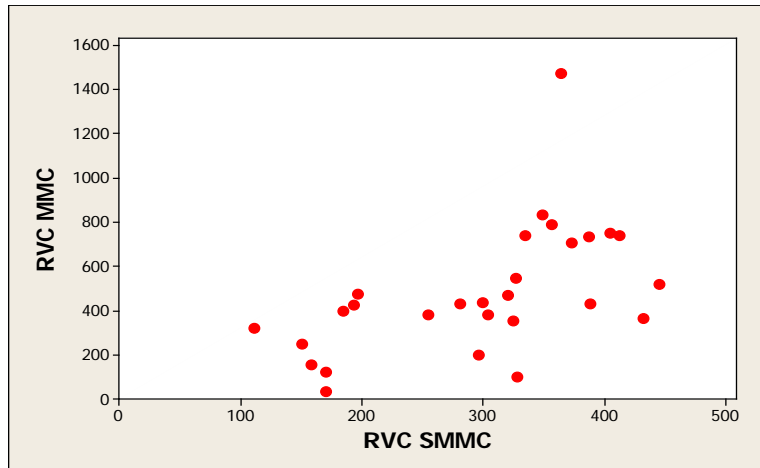


Figure 2.33: Scatterplot of RVC SMMC (x-axis) versus RVC MMC (y-axis). Cells expressed as MC per mm^2 , $p < 0.001$, $\rho = 0.648$. (Test: Spearman rank). (MMC: Mucosal mast cell; SMMC: Submucosal mast cell; RVC: Right ventral colon).

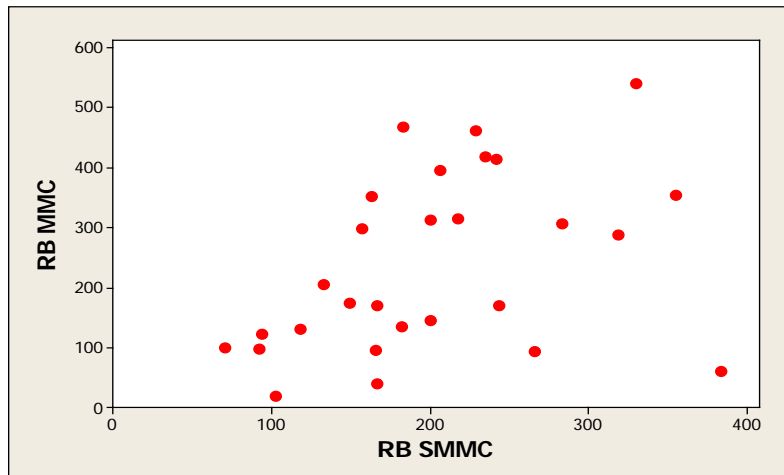


Figure 2.34: Scatterplot of RB SMMC (x-axis) versus RB MMC (y-axis). Cells expressed as MC per mm^2 , $p = 0.027$, $\rho = 0.417$. (Test: Spearman rank). (MMC: Mucosal mast cell; SMMC: Submucosal mast cell; RB: Rectal biopsy).

Mast Cell Recruitment and Activation as Measures of Cyathostomin Burden

	Caecum MMC	RVC MMC	RB MMC
Caecum MMC	-	0.933	0.630
RVC MMC	<0.001	-	0.638
RB MMC	<0.001	<0.001	-

Table 2.11: Correlations between caecal, RVC and RB mucosal mast cells (Test: Spearman rank). p values in italics, rho values in bold. Significant p values (<0.05) are highlighted. (MMC: Mucosal mast cell; RVC: Right ventral colon; RB: Rectal biopsy).

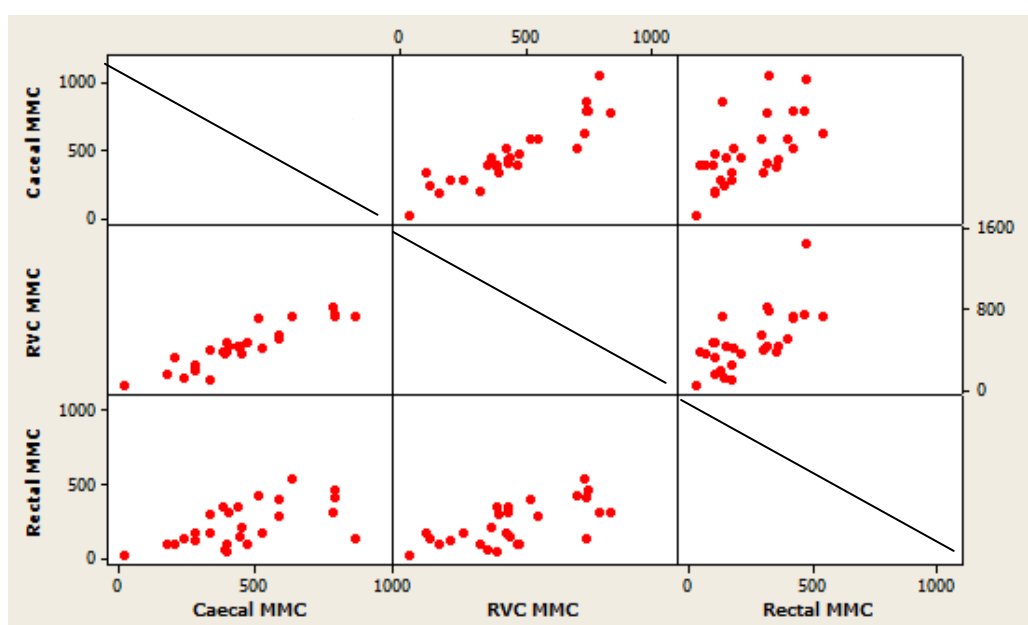


Figure 2.35: Matrix scatterplot of counts for caecal, RVC and RB MMC. Cells expressed as MC per mm^2 . (MMC: Mucosal mast cell; SMMC: Submucosal mast cell; RVC: Right ventral colon).

	Caecum SMMC	RVC SMMC	RB SMMC
Caecum SMMC	-	0.811	0.646
RVC SMMC	<0.001	-	0.488
RB SMMC	<0.001	0.008	-

Table 2.12: Correlations between caecal, RVC and RB submucosal mast cells. (Test: Spearman rank). p values in italics, rho values in bold. Significant p values (<0.05) are highlighted. (SMMC: Submucosal mast cell; RVC: Right ventral colon; RB: Rectal biopsy).

	MMC Caecum	SMMC Caecum	MMC RVC	SMMC RVC	MMC Rectum	SMMC Rectum
MMC Caecum		0.719	0.933	0.732	0.630	0.422
SMMC Caecum	<i><0.001</i>		0.664	0.811	0.563	0.646
MMC RVC	<i><0.001</i>	<i><0.001</i>		0.648	0.638	0.447
SMMC RVC	<i><0.001</i>	<i><0.001</i>	<i><0.001</i>		0.655	0.488
MMC Rectum	<i><0.001</i>	<i>0.002</i>	<i><0.001</i>	<i><0.001</i>		0.417
SMMC Rectum	<i>0.025</i>	<i><0.001</i>	<i>0.017</i>	<i>0.008</i>	<i>0.027</i>	

Table 2.13: Correlations between caecal, RVC and RB mucosal and submucosal mast cells. (Test: Spearman rank). p values in italics, rho values in bold. Significant p values (<0.05) are highlighted. (MMC: Mucosal mast cell; SMMC: Submucosal mast cell; RVC: Right ventral colon).

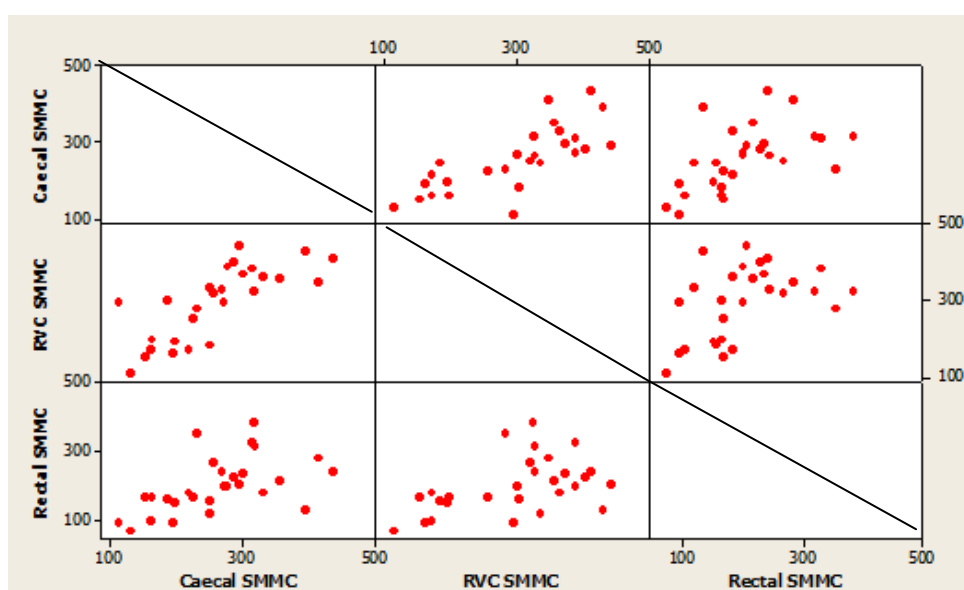


Figure 2.36: Matrix scatterplot of counts for caecal, RVC and RB SMMC. Cells expressed as MC per mm^2 . (SMMC: Submucosal mast cell; RVC: Right ventral colon).

2.3.7 Eosinophil Populations

2.3.7.1 Effect of Tissue Fixation on Eosinophil Enumeration

To enumerate mucosal eosinophil populations, Carnoy's or formalin fixed tissue was stained with H&E. It was not possible to reliably count eosinophils on H&E stained Carnoy's fixed tissue because it proved difficult to delineate individual eosinophils due to the high background pink staining and low eosinophil specific staining (Figure 2.37A). In contrast, H&E staining of formalin fixed tissue sections stained eosinophils bright pink, and resulted in less background pink staining, allowing the accurate identification of eosinophils (Black arrow: Figure 2.37B). As Carnoy's fixative was used for all tissue samples, but formalin was only used in a subset of samples, other methods of visualization of eosinophils on Carnoy's fixed sections were attempted, such as examining sections for autofluorescence, DAB staining and carbol chromatrope staining; however none of these methods were sufficient to allow for reliable counts. Therefore formalin fixed tissue was used to enumerate eosinophils.

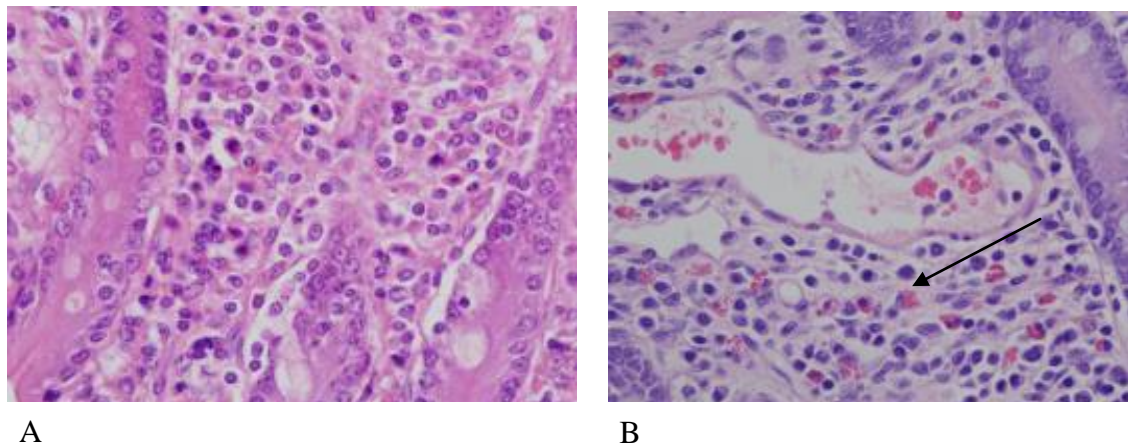


Figure 2.37: A: Image of a caecal tissue section fixed in Carnoy's and stained with H&E. B: Image of a caecal tissue section fixed in formalin and stained with H&E. The arrow points to an eosinophil. (H&E: Haemotoxylin and eosin)

2.3.7.2 Eosinophil Mucosal and Submucosal Counts

Formalin fixed tissue from Horses DV6-DV12 were used to ascertain eosinophil counts (Table 7.2). Median and range of mucosal and submucosal eosinophil counts

from the caecum, RVC and rectum are shown in Table 2.14. Tissue stored in formalin was available for seven of the 28 horses and eosinophil counts were performed on this tissue (Table 2.14). However, this was deemed an insufficient sample size for further analysis.

	Mucosa Caecum (EC/mm ²)	Submucosa Caecum (EC/mm ²)	Mucosa RVC (EC/mm ²)	Submucosa RVC (EC/mm ²)	Mucosa RB (EC/mm ²)	Submucosa RB (EC/mm ²)
Median	376	419	403	315	19	174
Range	218-1,178	80-734	166-875	106-605	6-94	42-778

Table 2.14: Median and range of mucosal and submucosal eosinophil counts from the caecum, RVC and rectum of horses DV6-12. Cells expressed as eosinophil count per mm² (EC/mm²). (RVC: Right ventral colon).

2.3.7.3 Tapeworm Status

The presence of tapeworm was confirmed in nine of the 28 horses (32%) either on PM or from FEC; eight of which were from the abattoir and one from the R(D)SVS. Co-infection with *A. perfoliata* is associated with significantly higher TB mast cells in the caecal mucosa and submucosa ($p=0.039$ and $p=0.004$) (Figure 2.38), RVC mucosa and submucosa ($p=0.019$ and $p<0.001$) (Figure 2.39) and RB mucosa and submucosa ($p=0.012$ and $p=0.046$) (Figure 2.40). Due to this, ‘co-infection with *A. perfoliata*’ was added as a confounding variable for all analyses involving Toluidine Blue mast cell counts within this Chapter and Chapters 3 and 4.

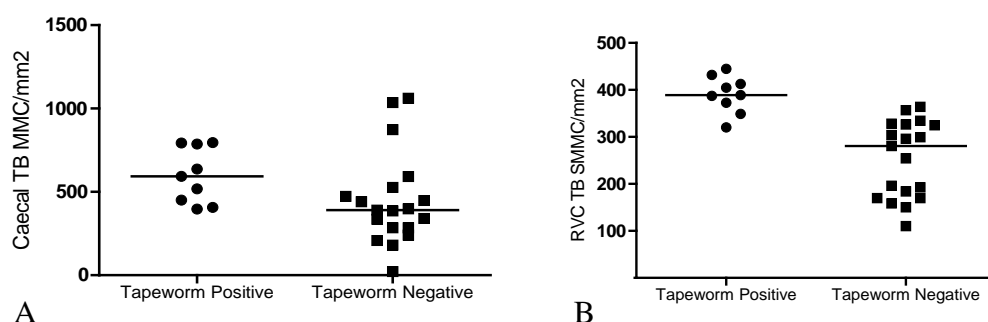


Figure 2.38: Individual Value Plot of A: caecal MMC and B: caecal SMMC. Cells expressed as Toluidine Blue Mucosal mast cell per mm² (TB MMC/mm²) and grouped according to presence or absence of Tapeworm, A: $p=0.039$ and B: $p=0.004$. (Test: Mann Whitney). Note different y-axis scales. The non-axis horizontal line indicates the median.

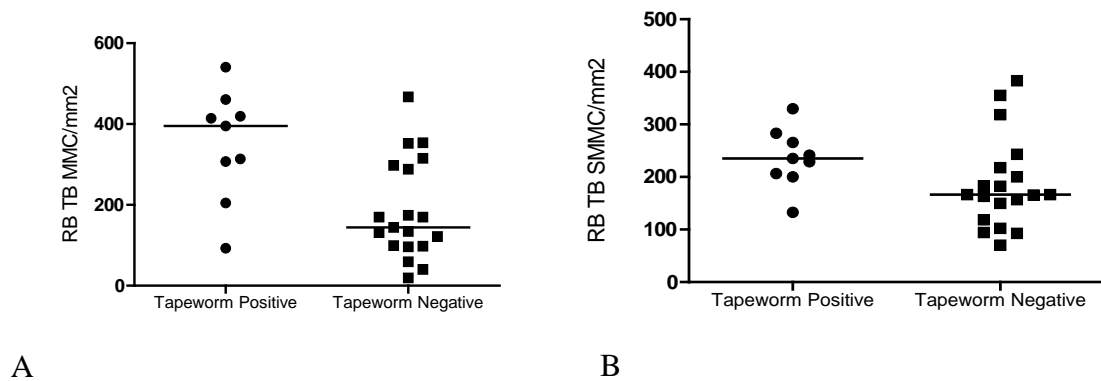


Figure 2.39: Individual Value Plot of A: RVC MMC and B: RVC SMMC Cells expressed as Toluidine Blue Mucosal mast cell per mm² (TB MMC/mm²) or Toluidine Blue Submucosal mast cell per mm² (TB SMMC/mm²) and grouped according to presence or absence of Tapeworm, A: $p=0.019$ and B: $p<0.001$. (Test: Mann Whitney). Note different y-axis scales. The non-axis horizontal line indicates the median. (RVC: Right ventral colon).

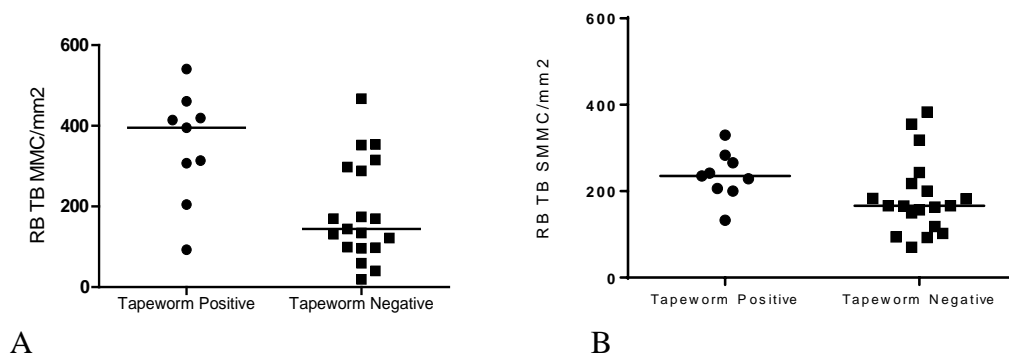


Figure 2.40: Individual Value Plot of A: RB MMC and B: RB SMMC Cells expressed as Toluidine Blue Mucosal mast cell per mm² (TB MMC/mm²) or Toluidine Blue Submucosal mast cell per mm² (TB SMMC/mm²) and grouped according to presence or absence of Tapeworm, A: $p=0.012$ and B: $p=0.046$ (Test: Mann Whitney). The non-axis horizontal line indicates the median. (RB: Rectal biopsy).

2.3.8 Mast Cells and Cyathostomin Burdens

Four horses, AB3, DV1, DV5 and DV6 were negative for cyathostomins on FEC, luminal content count, caecal and RVC TMI and caecal, RVC and rectal tissue digest. These horses were deemed cyathostomin-negative. The MMC and SMMC ranges and medians for these horses are shown in Table 2.15.

Mast Cell Recruitment and Activation as Measures of Cyathostomin Burden

	MMC Caecum (MC/mm ²)	SMMC Caecum (MC/mm ²)	MMC RVC (MC/mm ²)	SMMC RVC (MC/mm ²)	MMC RB (MC/mm ²)	SMMC RB (MC/mm ²)
Median	246	154	283	160	134	130
Range	22-341	130-250	34-394	110-184	19-298	70-166

Table 2.15: Median and range of MMC and SMMC from the caecum, RVC and rectum of all cyathostomin-negative horses (AB3, DV1, DV5 and DV6). Cells expressed as mast cell (MC) per mm². (MMC: Mucosal mast cell; SMMC: Submucosal mast cell; RVC: Right ventral colon; RB: Rectal biopsy).

To investigate whether age had an effect on MMC and SMMC and CTMB the R(D)SVS horses (DV1-DV12) were divided into two groups. Group 1 were those horses less than 15 years old (DV3, DV4, DV6, DV7, DV9, DV10, DV12) and Group 2 were those horses older than 15 years (DV1, DV2, DV5, DV8, DV11). There was no significant difference between the two groups with respect to CTMB or caecal, RVC and rectal MMC and SMMC ($p>0.5$).

All horses were grouped into four groups according to their combined total mucosal burdens. Group 1 (n=4) were cyathostomin-negative, Group 2 (n=8) had a range of encysted burdens of 75 to 3,340, Group 3 (n=6) ranged from 6,289 to 47,753 and Group 4 (n=10) had a range of 115,077 to 3,827,097 (Figure 2.41). Boxplots of caecal TB MMC (Figure 2.42A), caecal TB SMMC (Figure 2.42B), RVC TB MMC (Figure 2.43A), RVC TB SMMC (Figure 2.43B), RB TB MMC (Figure 2.44A) and RB TB SMMC (Figure 2.44B) divided by these groups are shown below. Kruskal-Wallis analysis revealed the only significant difference between groups to be in the case of RVC TB SMMC (Figure 2.43B: $p=0.028$).

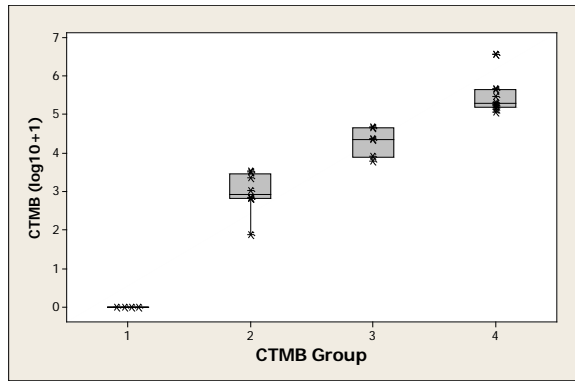


Figure 2.41: Boxplot of the 28 horses divided into 4 groups according to combined Total Mucosal Burden (CTMB).

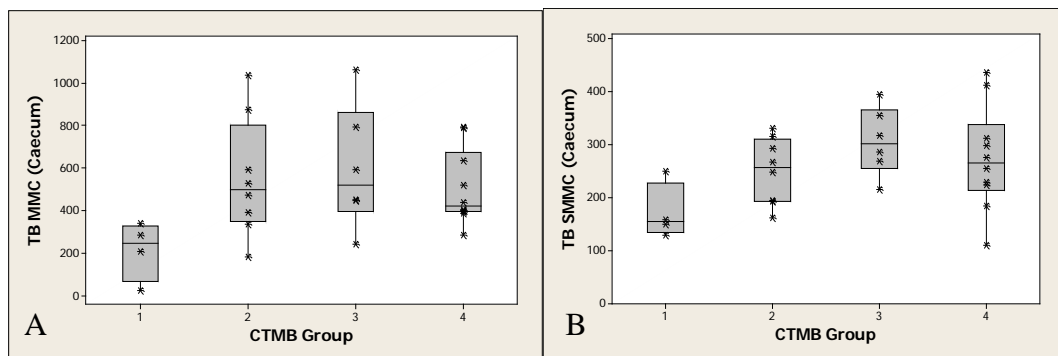


Figure 2.42: Boxplots: A: Caecal TB MMC counts (MC/mm²). Kruskal-Wallis analysis revealed no significant difference in Caecal TB MMC between groups ($p=0.059$). B: Caecal TB SMMC counts. Kruskal-Wallis analysis revealed no significant difference in Caecal TB SMMC between groups ($p=0.066$). (TB MMC: Toluidine Blue Mucosal mast cell; TB SMMC: Toluidine Blue Submucosal mast cell; CTMB: Combined Total Mucosal Burden).

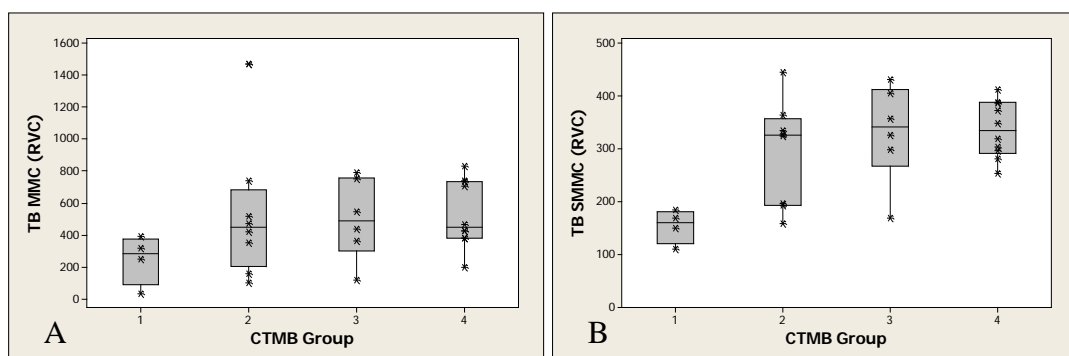


Figure 2.43: Boxplots: A: RVC TB MMC counts (MC/mm²). Kruskal-Wallis analysis revealed no significant difference in RVC TB MMC between groups ($p=0.190$). B: RVC TB SMMC counts. Kruskal-Wallis analysis revealed a significant difference in RVC TB SMMC between groups ($p=0.028$). (TB MMC: Toluidine Blue Mucosal mast cell; TB SMMC: Toluidine Blue Submucosal mast cell; CTMB: Combined Total Mucosal Burden; RVC: Right ventral colon).

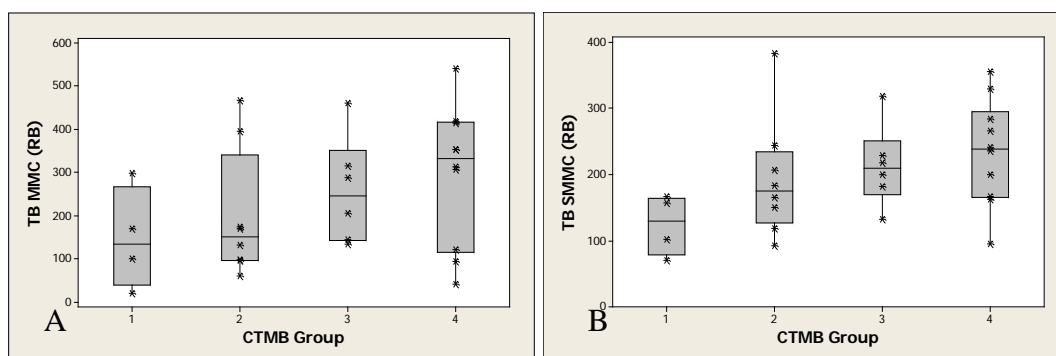


Figure 2.44: Boxplots: A: RB TB MMC counts (MC/mm^2). Kruskal-Wallis analysis revealed no significant difference in RB TB MMC between groups ($p=0.340$). B: RB TB SMMC counts. Kruskal-Wallis analysis revealed no significant difference in RB TB SMMC between groups ($p=0.093$). (TB MMC: Toluidine Blue Mucosal mast cell; TB SMMC: Toluidine Blue Submucosal mast cell; CTMB: Combined Total Mucosal Burden; RB: Rectal biopsy).

Linear regression analysis of $\log_{10}+1$ transformed data, with *A. perfoliata* as a confounding variable showed a significant positive relationship between the CTMB and the caecal MMC (Figure 2.45: $p=0.048$, $r^2=16.9\%$). The caecal SMMC and CTMB relationship was not significant (Figure 2.46: $p=0.507$, $r^2=26.9\%$).

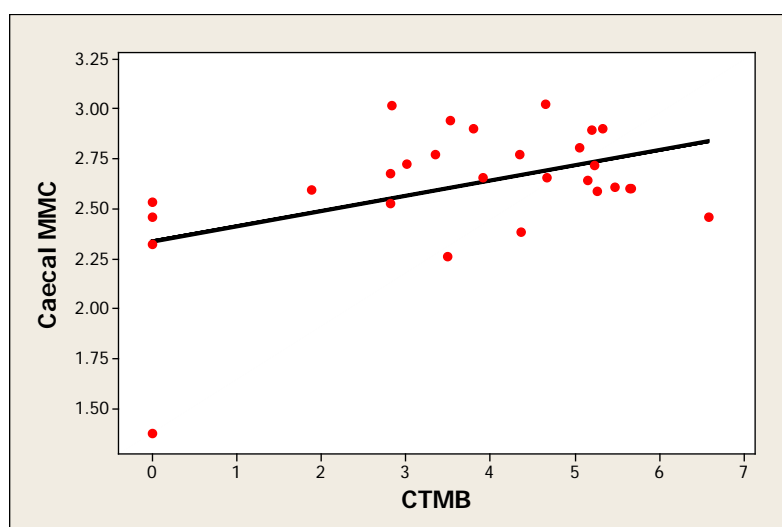


Figure 2.45: Relationship between $\log_{10}+1$ transformed CTMB (x-axis) and Caecal MMC (MC/mm^2) (y-axis), $p=0.048$, $r^2=16.9\%$ (MMC: Mucosal mast cell; CTMB: Combined Total Mucosal Burden).

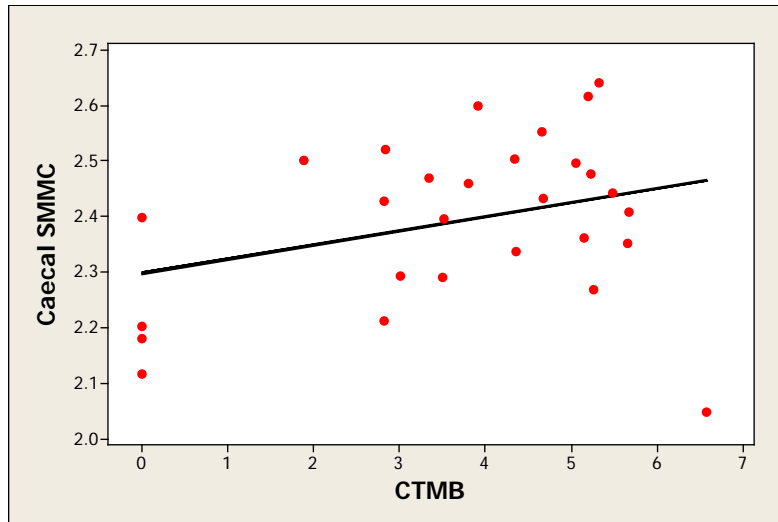


Figure 2.46: Relationship between log10+1 transformed CTMB (x-axis) and Caecal SMMC (MC/mm²) (y-axis), $p=0.507$, $r^2=26.9\%$. (SMMC: Submucosal mast cell; CTMB: Combined Total Mucosal Burden).

Linear regression analysis of log10+1 transformed data, with *A. perfoliata* as a confounding variable showed a significant relationship between the CTMB and the RVC SMMC (Figure 2.48: $p=0.005$, $r^2=51.4\%$). The RVC MMC and CTMB relationship was not significant (Figure 2.47: $p=0.211$, $r^2=13.8\%$).

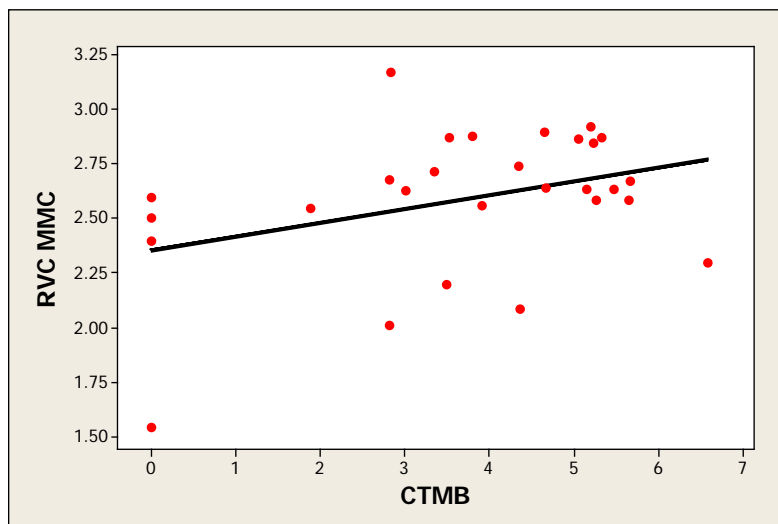


Figure 2.47: Relationship between log10+1 transformed CTMB (x-axis) and RVC MMC (MC/mm²) (y-axis), $p=0.211$, $r^2=13.8\%$. (MMC: Mucosal mast cell; CTMB: Combined Total Mucosal Burden; RVC: Right ventral colon).

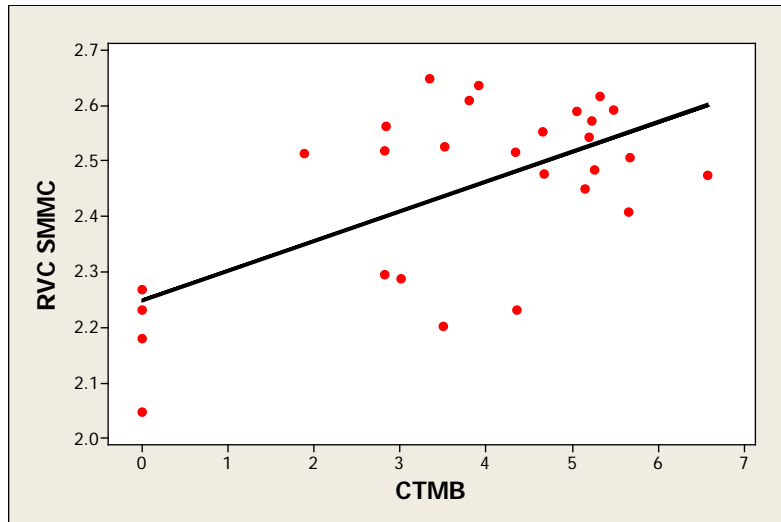


Figure 2.48: Relationship between log10+1 transformed CTMB (x-axis) and RVC SMMC (MC/mm²) (y-axis), $p=0.005$, $r^2=51.4\%$. (SMMC: Submucosal mast cell; CTMB: Combined Total Mucosal Burden; RVC: Right ventral colon).

Linear regression analysis of log10+1 transformed data, with *A. perfoliata* as a confounding variable showed no significant relationship between the CTMB and the RB MMC (Figure 2.49: $p=0.366$, $r^2=17.8\%$) or RB SMMC (Figure 2.50: $p=0.188$, $r^2=11.5\%$).

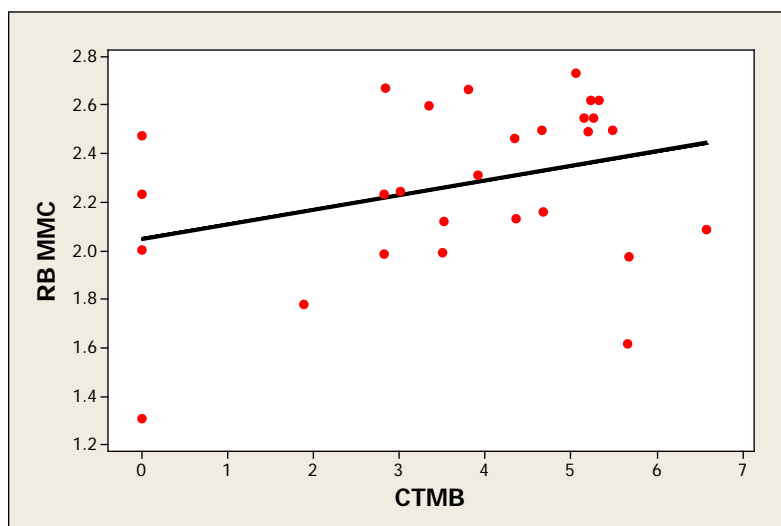


Figure 2.49: Relationship between log10+1 transformed CTMB (x-axis) and RB MMC (MC/mm²) (y-axis), $p=0.366$, $r^2=17.8\%$. (MMC: Mucosal mast cell; CTMB: Combined Total Mucosal Burden; RB: Rectal biopsy).

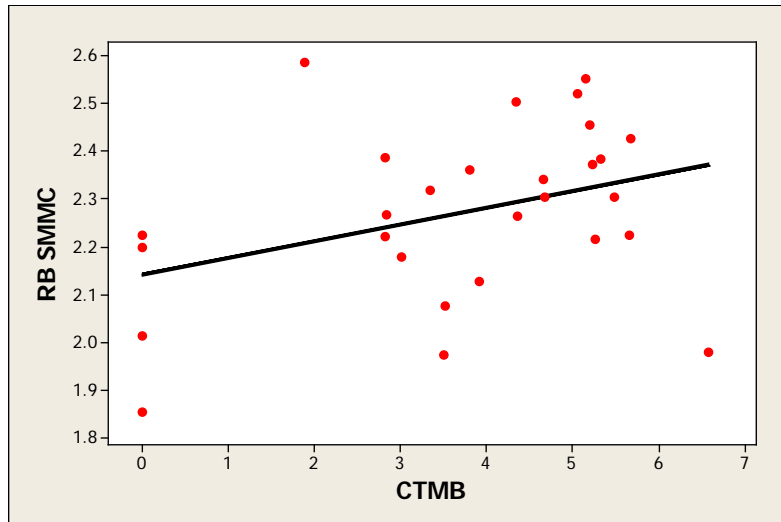


Figure 2.50: Relationship between $\log_{10}+1$ transformed CTMB (x-axis) and RB SMMC (MC/mm^2) (y-axis), $p=0.188$, $r^2=11.5\%$. (SMMC: Submucosal mast cell; CTMB: Combined Total Mucosal Burden; RB: Rectal biopsy).

2.4 Discussion

The aim here was to explore the relationship between mast cell numbers and cyathostomin burden throughout the large intestine to allow investigation of the potential for rectal biopsies as a diagnostic predictor of total cyathostomin burden. Of the 28 horses sampled, four were found to be cyathostomin-negative. The remaining 24 (86%) had natural patent infections of varying severity with a combined mucosal total burden (CTMB), calculated from the caecum and RVC total burdens (EL3+DL), ranging from 75 to 3,827,097 larvae. Mucosal burdens to the order of several million have previously been reported (Dowdall, Matthews et al. 2002) and the horse with the greatest burden, DV3, was confirmed to be a case of larval cyathostominosis here. Those horses sampled from the abattoir had higher luminal and mucosal burdens than those sampled at the referral hospital. Although the clinical history of the abattoir horses was not available some of these horses were known to be feral and sourced from the New Forest, therefore they may never have been treated with anthelmintics. This may partially explain the higher parasite burdens seen in this population.

To calculate the total mucosal cyathostomin burden, populations of EL3 and DL must be enumerated. Following the recommendations of Eysker and Klei (1999) TMI and tissue digest were used to determine the encysted larval count. TMI alone is of no use in enumerating EL3 because this larval stage is too small to visualise in tissue (Eysker, Boersema et al. 1997): using this method larvae cannot be classified by stage and hence must all be grouped as developing larvae (Eysker and Klei 1999). In contrast tissue digest allows enumeration of EL3 and also allows easier differentiation of encysted larval stages (Chapman, Kearney et al. 1999). However, there are disadvantages to this method in that there is concern about the damaging effects of digestion on larger developing larvae (LL3 and DL4) (Reinemeyer and Herd 1986). Preliminary studies using the digestion method here support this (Figure 2.5). Significant structural damage to developing larvae was observed using the tissue digest method and this increased with digest time, similar to findings of Reinemeyer and Herd (1986). To limit potential damage to all cyathostomin stages, a 'milking' process, first described by Murphy and Love (1997), was performed to

remove digested tissue and halt digestion of any larvae already released from tissue, which are thought to be more susceptible to damage. The RVC DL count from the tissue digest was significantly less than the TMI counts from the equivalent samples, supporting the need for both methods of enumeration. Therefore, in this study the total mucosal burden (TMB) for each organ was estimated from the EL3 count using the results from the tissue digest and the DL count using the results from TMI method. The combined TMB (CTMB) was calculated from the addition of the caecal and RVC TMBs.

In this study larvae were found in the rectal wall of eight horses. This has been previously reported (Ricketts 1996) and it has been suggested that examination of rectal biopsies for encysted cyathostomins may be of diagnostic value (Church, Kelly et al. 1986). It was more common for larvae to be observed in the rectum when burdens were high: those horses with evidence of rectal larvae had a significantly higher CTMB. Four horses (14%) had CTMB (range 184,380 – 472,935) that were within the range of those with a positive rectal biopsy but were larval-negative at the rectum. This test has high specificity, with few false positive results i.e. positive rectal biopsy but low cyathostomin burden. However, the considerable number of false negative cases, negative rectal biopsies from horses with high cyathostomin burdens, demonstrates that cyathostomin identification from rectal biopsy alone is not a reliable indicator of cyathostomin mucosal burden.

Here, in most cases (86%), luminal burdens were greater in the RVC than the caecum. Previous studies have found the greater part of the adult cyathostomin population concentrated in the ventral colon when compared to the caecum (Ogbourne 1976; Gawor 1995; Collobert-Laugier, Hoste et al. 2002). A similar finding was observed with respect to the distribution of larvae, both from the TMI and digest enumerations. Over 50 cyathostomin species have been described, 10 of which are highly represented (Reinemeyer, Smith et al. 1984; Lyons, Tolliver et al. 1999). There is evidence (Ogbourne 1976; Gawor 1995; Collobert-Laugier, Hoste et al. 2002) to support the suggestion that cyathostomin species have preferential sites of infection. In a French study of 42 naturally infected horses, where 20 cyathostomin species were identified, 12 of these species demonstrated a site

preference of the ventral colon compared to only one, *Cyathostomum coronatum*, in the caecum (Collobert-Laugier, Hoste et al. 2002). This supports the predominance of cyathostomin populations in the RVC demonstrated in this chapter, although species identification was out with the project scope.

The phenomenon of over dispersion in strongyle FEC has been well demonstrated (Sangster 2003; Kaplan and Nielsen 2010; Lester, Bartley et al. 2013; Lester, Spanton et al. 2013) and is supported here: only three horses (AB11, AB13 and DV8) had FEC greater than 200 EPG. It has been demonstrated that using this threshold for anthelmintic treatment can reduce pasture contamination (Eysker, Bakker et al. 2008); however FEC does not correlate with mucosal encysted larvae levels (McWilliam, Nisbet et al. 2010). This is demonstrated most clearly here in the case of DV3, as this horse had a negative FEC but had the highest developing larval burden. The luminal count for DV3 was positive, with burdens of 800 and 1140 larvae in the caecum and RVC, respectively. These luminal burdens, although positive, were lower than counts in over 50% of the samples collected. It is likely that this case was treated with an anthelmintic in the weeks prior to euthanasia. This would have eliminated anthelmintic sensitive nematodes, in particular adult stage worms in the lumen and would have had a significant impact on this horse's FEC. The effect on the encysted larval population would depend on the anthelmintic used. Pyrantel salts are relatively ineffective against inhibited cyathostomin stages (Corning 2009) and ivermectin has been shown to have limited efficacy against encysted or developing larvae (Xiao, Herd et al. 1994). Benzimidazoles have a licensed efficacy against encysted cyathostomin larvae when administered as a 5 day course at 7.5 mg/kg (Duncan, Bairden et al. 1998) although efficacy of this product against cyathostomins in the UK and abroad is questionable due to anthelmintic resistance (Matthews 2008; Stratford, McGorum et al. 2011). In some cases, moxidectin has been demonstrated to be efficacious against encysted larvae (Bairden, Brown et al. 2001; Bairden, Davies et al. 2006) and is licensed for this use. On TMI of material from horse DV3 there was evidence of larval stages emerging from the mucosa and it is possible that the luminal larval population mainly comprised late L4. This case highlights the necessity for a diagnostic test that provides information

on the quantity of mucosal stages as FECs do not correlate with encysted burden (Table 2.6).

Significant correlations were observed between mucosal mast cells and submucosal mast cells within the caecum, RVC and rectal biopsy (RB) tissue. Encouragingly, there was no significant difference in rectal mast cell counts in either rectal mucosal tissue sections or rectal biopsies for either the mucosa or the submucosa of the rectum, indicating the reliability of the rectal biopsy technique used here to enumerate mast cells. In the mouse it has been demonstrated that mast cells migrate through intestinal tissue from the submucosa to the tips of the villi, therefore the submucosal population are contributing to that of the mucosa (Friend, Ghildyal et al. 1996; Friend, Ghildyal et al. 1998). Also, in the mouse, it has been demonstrated that intestinal infection with schistosomiasis causes the expansion of both mucosal and submucosal mast cell populations (De Jonge, Van Nassauw et al. 2002). These processes previously described in rodents could be responsible for the correlations seen in these results in the horse. Significant correlations were also observed between mucosal mast cells across intestinal sites within individual horses. This supports the theory of the common mucosal system which is based on observations that stimulation of one mucosal region can lead to activation of mucosal immune responses at sites distant to the initial region of exposure (van Ginkel, Nguyen et al. 2000). In the lamina propria, mast cells act to identify the presence of antigen through IgE bound to high affinity IgE receptor (FcRI) expressed on the mast cell surface, and initiate a defensive inflammatory response (Wallace and Granger 1996). Mast cell mediators can be differentially released depending on the stimulus applied (Theoharides, Patra et al. 2000). Mast cells are ideally situated at interfaces to the external environment and are hypothesised to have a key function in surveillance with a role in initiating the host immune response (Welle 1997; Knight, Wright et al. 2000).

Pronounced hyperplasia, differentiation, and activation of mucosal mast cells occurs in the intestine during nematode infections in rodents (Woodbury, Miller et al. 1984; Miller 1996). Linear regression analysis of log₁₀+1 transformed data showed a significant relationship between the CTMB and the caecal mucosal mast cell (MMC)

($p=0.048$, $r^2=16.9\%$), although the relationship between CTMB and caecal submucosal mast cells (SMMC) was not significant. Conversely, there was a significant relationship between the CTMB and the RVC SMMC ($p=0.005$, $r^2=51.4\%$). The relationship between the CTMB and RVC MMC was not significant ($p=0.211$, $r^2=13.8\%$). A difference in correlations at various sites of the large intestine has been demonstrated previously with an association described between the percentage of EL3 with MMC and SMMC counts in the ventral colon, but not the caecum or dorsal colon in a study in 42 horses (Collobert-Laugier, Hoste et al. 2002). The study by Collobert-Laugier et al. (2002) found no significant variations according to breed but horses over 10 years-old had significantly more mucosal mast cells in their caecum, dorsal and ventral colon. Conversely age was not found to affect MC counts or cyathostomin burden in Pickles et al. (2010). It was not feasible to record the ages of the horses sampled from the abattoir (AB1-16) here so the findings cannot be compared with this population in the current study. When R(D)SVS horses were divided into two age categories (Group 1 <15 years, Group 2 >15 years), no significant differences in caecal, RVC or rectal MMC and SMMC were identified between the two age categories. There was also no significant difference in CTMB or FEC between the age groups. Although in the French study 64% of horses were co-infected with *A. perfoliata*, the relevance of this was not investigated (C. Collobert-Laugier et al. 2002). From here, significantly higher levels of Toluidine Blue-stained mast cells were associated, both in the mucosa and submucosa in the caecum, RVC and RB, when there was co-infection with *A. perfoliata*. This result is corroborated by previous studies that have shown *A. perfoliata* to be a confounding variable for Toluidine Blue-stained mast cell numbers (Pickles, Mair et al. 2010).

The relationship between CTMB and MC in the caecum here was not as strong as that seen in a previous study by Pickles et al. (2010). In their study, a statistically significant positive linear relationship was observed between cyathostomin burden and both mucosal and submucosal log₁₀ transformed caecal Toluidine Blue-stained MC counts (Pickles et al. 2010). This previous work was performed using caecal material only. These horses (Thoroughbred horses, n=25) displayed a lower range in

their caecal luminal (0–2,400) and their caecal encysted (200–2,690) larval burdens. All horses were positive for cyathostomin infection and the sampling frame was relatively short (four months). In comparison, the samples obtained here over 23 months represent a more diverse population from horses of different breeds, husbandry and from diverse environments, with caecal luminal burdens of 0–9,780 and caecal encysted burdens of 0–1,773,047. It is possible that the horses here sampled over a longer time frame had a more complex relationship between mast cell populations and cyathostomin burden as the immune response may vary depending on the stage of infection (Monahan, Chapman et al. 1998). This could contribute to the weaker relationships observed here when compared to those in Pickles et al. (2010). Also, the presence of cyathostomin larval-negative horses with evidence of recent anthelmintic treatment or larval expulsion in the current study, may have an effect on mast cell count data, as recruited mast cells may still remain in the tissue after worm death (du Toit, McGorum et al. 2007). Methods for mast cell staining and enumeration and tissue sample collection were similar among these studies but there were some differences in sample processing. Here, EL3 cyathostomins comprised the majority of the mucosal population and, as previously reported by Pickles et al. (2010) and Collobert-Laughier et al. (2002), the mucosal population was significantly greater than in the lumen, however Pickles et al. 2010 did not describe a separate method for enumerating DL, such as TMI. DL enumerated were released following tissue digestion and there was no ‘milking’ process to preserve later stage mucosal larvae in the digestion fluid. This is similar in the methodologies described by Collobert-Laugier et al. (2002) and the previously described technique on which this method was based (Monahan, Chapman et al. 1998). This could affect integrity of a proportion of the larvae, in particular the L4 and late L3. These factors may contribute to an underestimation of mucosal burden which could affect the relationship between cyathostomin burdens and mast cell numbers.

No significant relationship between the CTMB and RB MMC or RB SMMC was observed. Similar observations were reported by Collobert-Laughier et al. (2002), who found that total worm burdens and total larval counts did not correlate with mast cell densities in any of the intestinal sites assessed. Although every effort was made

to produce as representative a count as possible, there will always be some error due to the nature of tissue cell count methods. Although 10 fields were chosen at random, as in previous studies (Collobert-Laugier, Hoste et al. 2002; du Toit, McGorum et al. 2007; Pickles, Mair et al. 2010) this may not provide an accurate representation of the whole organ. Other mast cell studies have also assessed this number of fields (Strobel, Miller et al. 1981; Sarin, Malhotra et al. 1987; Sonti 2012). However, for more accuracy, some studies have used as many as 1,000–1,800 fields to describe the mast cell distribution in camels (Al-Zghoul, Al-Rukibat et al. 2009), bovines (Küther, Audigé et al. 1998), canines (Kube, Audigé et al. 1998) and in the equine endometrium (Welle, Audige et al. 1997). Also, due to the limitations of these equine-based investigations with a lack of experimentally controlled infections, interpretations of the results is rendered more difficult as only one time point is studied. Future rectal biopsy studies, including a greater number of examined fields, would be an obvious way of examining the dynamics of this response.

The superiority of Carnoy's fixed tissue for mast cell staining and identification has been well described (Strobel, Miller et al. 1981; Irani, Schechter et al. 1986; Küther, Audigé et al. 1998; Al-Zghoul, Al-Rukibat et al. 2009). The recommended standard technique for processing human biopsies of the intestine, specifically to ensure the preservation of mucosal mast cell information is fixation in Carnoy's or basic lead acetate (BLA) and the use of Toluidine Blue or astra-blue/safranin as a subsequent stain (Strobel, Miller et al. 1981). For equine mast cell preservation and staining/labelling Carnoy's fixed tissues are superior to formalin fixed tissue, even with antigen retrieval techniques, (K. Dacre 2005). The fixing of tissue in Carnoy's is optimal for mast cell enumeration (with Toluidine Blue staining); however it is suboptimal for eosinophil enumeration (with H&E staining) when compared to formalin fixed, H&E stained tissue, as was demonstrated in Figures 2.37 A and B. Because of this, it was not possible to enumerate mast cells and eosinophils within the same sample to directly compare these two cell populations in the tissues collected. Associations have been demonstrated between eosinophil numbers and cyathostomin burdens in the caecum and colon of naturally infected horses (Collobert-Laugier, Hoste et al. 2002); however, as formalin fixed tissue was only

available for seven of the 28 horses this relationship could not be investigated further here due to inadequate sample size.

Toluidine Blue stains the metachromatic granules of mast cells (Strobel, Miller et al. 1981): this method requires that these granules are present. Once degranulated, mast cells are difficult to stain (Sonti 2012) due to the loss of their staining granules. Also, immature mast cells may not contain these granules rendering them unidentifiable using this stain (Khatri, Desai et al. 2013). Mast cells have been demonstrated to be immature at the time of maximal enzyme release (Woodbury, Miller et al. 1984). These immature mast cells may not have been well stained or enumerated by the staining method used here. For these reasons, exploration of mast cell proteinase production and expression will provide a more accurate picture of this complex relationship (see Chapters 3 and 4). Those horses in Group 4, with the highest CTMB range (115,077 and 3,827,097), are more likely to be demonstrating an active mast cell response and hence have a greater proportion of immature or degranulated mast cells which are difficult to stain. This could contribute to the lower mast cell numbers for this group than might be expected. In 10 out of the 28 horses studied here, evidence of previous larval damage was observed on TMI as areas suggestive of empty cysts. AB3 is of particular interest as this horse was negative for cyathostomins on TMI yet had numerous fibrous capsules observed in the mucosa: it is thought that these might represent previous larval encystment sites (Davidson et al. 2005). Such horses, whilst having a low or negative cyathostomin mucosal burden, may have relatively high residual mast cell counts. Previous studies have also demonstrated mast cell populations in equine cyathostomin larval-negative sections which were suggested to relate to prior helminth exposure (du Toit, McGorum et al. 2007). In the rodent, there are negligible mast cell numbers in helminth free individuals (du Toit, McGorum et al. 2007; Xing, Austen et al. 2011). As the majority of grazing horses are exposed to cyathostomins (Matthews 2008), it is likely that those classified as cyathostomin-negative at the time of death may have been previously infected. This is supported by the fact that although the mast cell populations enumerated in Group 1, the cyathostomin-negative horses, were lower

than in Groups 2, 3 and 4 they still demonstrated significant mast cell populations, particularly in the rectum (Figures 2.44 A and B).

In summary, these results demonstrate a positive relationship between mast cells numbers throughout the intestine. However, a complex relationship between mast cells and cyathostomin burdens exists and this is affected by a number of variables. Some of these were measureable here, such as the presence or absence of *A. perfoliata*. Differences in horse management existed, for example some of the horses in this study from the abattoir were sourced from the New Forest where they are kept extensively and are unlikely to have ever been treated with anthelmintics. This is vastly different to the majority of privately owned horses sampled from the referral hospital. The phase of immune response may also be a factor. Cyathostomin larvae are pathogenic on their entry into the mucosa (Murphy and Love 1997) and their development is associated with a fibroblastic response and a marked inflammatory cellular reaction (Giles, Urquhart et al. 1985; Church, Kelly et al. 1986; Love, Murphy et al. 1999). Therefore, the level of mast cell involvement and the dynamics of the response may be affected by the stage of infection and also, the number of larvae at each stage within the mucosal wall. The results may also have been confounded by age, particularly as older horses have demonstrated an acquired immune response (Love and Duncan 1992) which during its maturation targets increasing numbers of parasite stages (Monahan, Chapman et al. 1998). Variations in levels of pasture contamination, frequency of anthelmintic treatment and nutrition, travelling or concurrent diseases may also act as confounding factors (Collobert-Laugier, Hoste et al. 2002). For mucosal mast cells and their proteinases to be considered for use as a diagnostic there is a requirement that they are associated with cyathostomin burden regardless of season, age, breed and common history. As this is such a complex picture the relationships will be further explored in Chapter 3 in conjunction with the immunolabelling of mast cells for proteinase expression and the use of immunoassays to measure mast cell serine proteinase concentration in the tissue and serum.

3 Characterisation of Large Intestinal Mast Cell Activation in Response to Cyathostomin Infection

3.1 Introduction

Mast cells comprise a heterogeneous population that is species and tissue specific and this heterogeneity can be expressed as differences in functional, biochemical and histochemical characteristics (Welle 1997). Like humans (Irani and Schwartz 1994), rats (Le Trong, Neurath et al. 1987) and mice (Miller and Pemberton 2002), horses have mast cell subpopulations that differ in neutral proteinase content (Pickles, Mair et al. 2010). These proteinases have been demonstrated to play an important role in the host response to helminth infection in other species (Friend, Ghildyal et al. 1996; Miller 1996; Scudamore, McMillan et al. 1997; Wastling, Scudamore et al. 1997; Knight, Wright et al. 2000; McDermott, Bartram et al. 2003).

Mast cells contain many potent mediators including serine proteinases, biological amines, prostaglandins, leukotrienes and cytokines (Metcalf, Baram et al. 1997). Mast cell subsets have been described in the rat (Gibson, Mackeller et al. 1987), mouse (Friend, Ghildyal et al. 1996; Tchougounova, Pejler et al. 2003), human (Caughey, Raymond et al. 2000), sheep (Sture, Huntley et al. 1995), cow (Küther, Audigé et al. 1998) and camel (Al-Zghoul, Al-Rukibat et al. 2009). Mucosal mast cells (MMC) in the gastrointestinal tract are distinct from mast cells in other tissues in their biochemical and functional properties and also in their neutral granule serine proteinases content (Miller, Huntley et al. 1988; Stevens, Friend et al. 1994; Knight, Wright et al. 2000). During gastrointestinal nematode challenge MMCs undergo a pronounced T-cell dependent hyperplasia, differentiation, and activation (Woodbury, Miller et al. 1984; Miller 1996). In the sheep, mouse and rat this is associated with the systemic release of mucosal mast cell granule chymases (chymotrypsin-like serine proteinases) at the time of worm expulsion (Miller 1996). The detection of tryptase released from mast cells is recognised as the most reliable indicator of mast cell activation (Hogan and Schwartz 1997). In the human, mast cells expressing tryptase are the predominant cell type in the intestinal mucosa (Irani, Schechter et al. 1986). Two serine proteinases, one tryptase-like referred to as equine Tryptase (eqTRYP) and the second, chymotrypsin-like (chymase), referred to as equine Mast

Cell Proteinase-1 (eqMCP-1), have previously been isolated from equine mastocytoma tissue (Pemberton, McEuen et al. 2001). Polyclonal antibodies raised in rabbits to both proteinases (Pemberton, McEuen et al. 2001) have been purified and validated to investigate the role of mast cells and their proteinases in equine heaves. (Dacre, McAleese et al. 2006). The eqTRYP antibody has also been used to investigate mast cell degranulation and tryptase release into the airways of horses following organic dust exposure (Dacre, McGorum et al. 2007). Both antibodies have been used to establish an immunohistochemical technique to demonstrate the involvement of mast cell proteinases in the large intestinal response to cyathostomin infection (du Toit, McGorum et al. 2007). These antibodies were also used to demonstrate a strong positive linear relationship between cyathostomin burden and the production of mast cell proteinases in the caecal wall of naturally infected horses (Pickles, Mair et al. 2010).

In the equine caecum there appears to be a predominance of chymase-positive mast cells (eqMCP-1) compared to tryptase-labelled mast cells in the mucosa and submucosa (Pickles, Mair et al. 2010). A strong relationship has been observed between total cyathostomin burden and mucosal mast cells labelled with tryptase (eqTRYP) (Pickles, Mair et al. 2010) such that total cyathostomin burden accounted for 57% of the variation in eqTRYP-labelled mast cells. Immunohistochemical studies of Carnoys-fixed tissues (Pickles, Mair et al. 2010) demonstrated strong positive linear relationships between total or mucosal cyathostomin burden and the production of both eqTRYP and eqMCP-1 in the caecal wall of naturally infected horses. There were also significant positive linear relationships between total larval cyathostomin population, and individual mural and luminal counts, and the number of Toluidine Blue (TB) stained mast cells in the mucosa and submucosa of the caecum (Pickles, Mair et al. 2010). This association supports the basis of the second hypothesis of this thesis, that mast cell proteinase concentrations may have diagnostic potential for prediction of cyathostomin burden.

Mast cells and their associated proteinases have been implicated in the protective host immune response against nematode infection in mammals (Friend, Ghildyal et al. 1996; Miller 1996; Scudamore, McMillan et al. 1997; Wastling, Scudamore et al.

1997; Knight, Wright et al. 2000; McDermott, Bartram et al. 2003). Chymase appears critical to *Trichinella spiralis* expulsion in mice: deletion of the murine mast cell proteinase-1 (mMCP-1) gene results in delayed nematode expulsion and increased deposition of larvae in the muscle (Knight, Wright et al. 2000). Mouse intestinal MCP-1 is expressed constitutively in mucosal tissue, but levels increase in the bloodstream and intestinal lumen of parasitised mice and are maximal at the time of worm expulsion (Huntley, Gooden et al. 1990). Sheep mast cell proteinase-1 (SMCP-1) is expressed in abundance in gastrointestinal cells (Pemberton, McAleese et al. 2000) and demonstrates both chymase- and tryptase-like specificity (Pemberton, Huntley et al. 1997). There is a pronounced mucosal mastocytosis in response to *Haemonchus contortus* infection in sheep (Huntley, Newlands et al. 1992) and ELISAs have demonstrated elevated serum concentrations of SMCP-1 following infection with *Trichostrongylus colubrifformis* (Douch, Green et al. 1996). As sheep, mouse and rat mast cell proteinases are released both systemically and into the gut lumen (Huntley, Gooden et al. 1990; Scudamore, Thornton et al. 1995; Miller 1996) in response to intestinal nematode infections, it is hypothesised that they participate in the effector response (Knight, Wright et al. 2000). This Chapter aimed to investigate this response in the horse and focussed on examining the hypothesis that serum and tissue mast cell proteinase concentrations are positively associated with mast cell number and proteinase expression, and with cyathostomin burden, such that they have diagnostic potential for prediction of total cyathostomin burden. This chapter therefore explored the mast cell proteinases (MCPs), eqTRYP and eqMCP-1, in two different ways.

1. Immunolabelling of large intestinal tissue sections to enumerate proteinase-labelled mucosal mast cells (MMC) and submucosal mast cells (SMMC) in tissue sections. This allowed the relationship between Toluidine Blue (TB) stained mast cells (Chapter 2) and proteinase-labelled mast cells to be explored. Mast cell heterogeneity in the horse will be described further. The relationship between proteinase-labelled mast cells and cyathostomin burden will also be investigated.

2. An optimised ELISA, using the antibodies previously raised in rabbits against the two proteinases of interest, to measure the amount of each proteinase in large intestinal tissue homogenate and serum. This allowed the relationship between proteinase concentration and cyathostomin burden to be explored.

3.2 Materials and Methods

3.2.1 Purified Proteinase Verification and Validation

To examine the integrity of the available, previously purified MCPs (Pemberton, McEuen et al. 2001), a sodium dodecyl sulphate polyacrylamide gel electrophoresis (SDS-PAGE), using NuPage Novex Bis-Tris Mini gels (Invitrogen), was performed as per the manufacturer's instructions. Four μ l of each reduced proteinase (denatured by heating with a reducing agent) were loaded per well. This was equivalent to 0.56 μ g eqMCP-1 and 1 μ g eqTRYP. The concentration of eqMCP-1 had been determined previously by Dr K. Pickles (Dacre 2005). To quantify the concentration of eqTRYP in the samples available a Bicinchoninic Acid Protein assay (BCA) was performed using a Pierce Micro BCATM protein assay kit according to manufacturer's instructions (Thermo Scientific). The gel was stained with Simply BlueTM Safe Stain (Invitrogen) for 1 h and destained overnight in ddH₂O.

3.2.2 IgG Purification from Rabbit Sera

Rabbit antisera to eqMCP-1 and eqTRYP previously generated by Dr A. Pemberton was supplied by Dr K. Pickles. The rabbit antisera was raised by inoculating 50 μ g protein/rabbit in Freund's complete adjuvant, followed by two boosts of 50 μ g protein/rabbit in Freud's incomplete adjuvant and the rabbits bled 10 days after the final boost (Pemberton, McEuen et al. 2001). To purify rabbit IgG the antisera was diluted 1:5 in binding buffer (20 mM sodium phosphate, pH 7.0). A Protein G column for IgG purification (GE Healthcare) was washed with deionised H₂O for five min and then equilibrated with binding buffer for 10 min. The rabbit antiserum was then circulated through the column for 30 min followed by binding buffer for 10 min to wash the column. Elution buffer (0.1 M glycine-HCL, pH 2.7) was circulated and samples collected in 1 ml aliquots in tubes containing 40 μ l of Tris-HCL, pH 9. Collected samples were stored at -20 °C. SDS-PAGE was performed to ascertain the purity of the antibody eluted. A Western blot was performed to validate the specificity of the purified anti-eqMCP-1 and anti-eqTRYP rabbit IgG.

Previous work had shown that the eqMCP-1 preparation used to immunise rabbits in Section 3.2.2 also contained serum albumin and that as a result, the rabbit antisera was likely to contain anti-equine albumin IgG. Contamination of purified rabbit anti eqMCP-1 IgG generated in Section 3.2.2 with anti-equine albumin IgG was verified by Western blot using the antibody preparation (1 µg/ml) and equine albumin (Europa Bioproducts Ltd) at 0.5 µg and 1 µg per lane and purified eqMCP-1 at 1 µg per lane. To remove contaminating anti-equine albumin IgG, the purified rabbit anti-eqMCP-1 IgG was cross-absorbed against equine albumin by circulating the antibody preparation through a previously validated column (HiTrap NHS-activated, 1 ml, Pharmacia) (Pemberton, McEuen et al. 2001) to which 10 mg equine albumin had been conjugated, according to manufacturer's instructions. The concentration of IgG in the unbound fraction was quantified using a BCA assay. To ensure the successful removal of anti-equine albumin IgG the Western blot was repeated with equine albumin and purified eqMCP-1 as described above.

3.2.3 Biotinylation of anti eqMCP-1 Rabbit IgG

For dual immunolabelling rabbit anti- eqMCP-1 IgG was biotinylated using the Lightning-LinkTM Biotin Conjugation Kit (Innova Biosciences) as per the manufacturer's instructions. Rabbit IgG (Sigma-Aldrich) was biotinylated for use as a negative control.

3.2.4 Tissue Samples for Parasite and Mast Cell Enumeration and Mast Cell Proteinase Quantitation

The caecum and right ventral colon (RVC) were processed as described in Chapter 2.2.8 and two 5 % by weight longitudinal samples harvested for transmural illumination (TMI) and pepsin digestion. Adjacent to this area, tissue samples (approximately 1 cm²) were taken in duplicate and placed in glass bijoux of Carnoy's fixative for mast cell enumeration and immunolabelling. The tissue sections were kept in Carnoy's solution at room temperature for 24 h prior to being transferred to 70 % ethanol. Serial 8 µm sections were cut and processed for immunolabelling on Superfrost plus slides (Thermo Shandon).

3.2.5 Immunohistochemistry

3.2.5.1 Single Immunofluorescent Labelling

Tissue sections were stored at 4 °C and brought to room temperature for processing before dewaxing in xylene. The sections were rehydrated from xylene to water through graded alcohols. Sections were then placed in constantly stirred 3 % hydrogen peroxide in methanol for 20 min. The slides were washed and loaded into Sequenza chambers (Thermo Shandon) using phosphate buffered saline (PBS). The slides were incubated with 100 µl of 25 % normal goat serum in PBS for 30 min at room temperature. One hundred µl of diluted antibody (5 µg/ml in PBS of biotinylated rabbit IgG, biotinylated anti eqMCP-1 rabbit IgG, rabbit IgG (Sigma) or anti eqTRYP rabbit IgG) were applied directly and incubated overnight at 4 °C. The following day slides were washed three times in PBS. For rabbit IgG or anti-eqTRYP rabbit IgG slides 100 µl of goat anti-rabbit IgG conjugated to Alexa Fluor® 488 (Invitrogen) at 2 µg/ml were added per slide and incubated for 2 h at 4 °C. Biotinylated rabbit IgG and biotinylated anti-eqMCP-1 rabbit IgG slides were processed using the TSA™ Kit #24, with Horse Radish Peroxidase (HRP) conjugated Streptavidin and Alexa Fluor® 568 Tyramide (Invitrogen) as per the manufacturer's instructions. After incubating with 100 µl HRP-streptavidin (Invitrogen) (1:100 in 1 % blocking solution) for 30 min the slides were incubated for 10 min with tyramide working solution (1:100). After this incubation all slides were washed three times in PBS and mounted with Mowiol mounting medium (Calbiochem–Novabiochem; San Diego, CA). Slides were viewed using an Axiovert 200M inverted fluorescence microscope (Carl Zeiss Ltd., Welwyn Garden City, UK) at x 400 magnification.

3.2.5.2 Dual-Immunofluorescent Labelling

To visualise mast cells expressing both eqTRYP and eqMCP-1 a dual-immunofluorescent labelling protocol was performed. Slides were prepared as above for single immunofluorescent labelling and incubated overnight at 4 °C with either rabbit IgG (5 µg/ml in PBS) or 100 µl of diluted anti-eqTRYP rabbit IgG (5 µg/ml in PBS). The following day, slides were washed three times in PBS and 100 µl

of goat anti-rabbit IgG conjugated to Alexa Fluor® 488 at 2 µg/ml at 2 µg/ml were added per slide and incubated for 2 h at 4 °C. The slides were washed three times in PBS and incubated with 100 µl of 25 % normal rabbit serum in PBS. Slides were incubated at 4 °C in the dark for 4 h. Slides were then incubated with 100 µl diluted antibody (5 µg/ml in PBS) of biotinylated rabbit IgG or biotinylated anti-eqMCP-1 rabbit IgG and stored at 4 °C in the dark overnight. On the third day, slides were processed using the TSA™ Kit #24, with HRP-Streptavidin and Alexa Fluor® 568 Tyramide (Invitrogen) as per the manufacturer's instructions. After incubation, all slides were washed three times in PBS and mounted with Mowiol® 4-88 mounting medium (Sigma-Aldrich). Slides were viewed using an Axiovert 200M inverted fluorescence microscope at x 400 magnification. Due to high background labelling, control experiments were performed with the addition of 100 µl Diaminobenzidine (DAB) (Envision kit, Dako Ltd) for 5 min to quench any endogenous peroxidase activity (Kingston and Pearson 1981) and 100 µl of biotin solution (Vector laboratories) for 15 min to block endogenous biotin.

3.2.6 Single Immunohistochemistry using DAB Substrate

Tissue sections were brought to room temperature and placed in xylene to dewax. The sections were rehydrated through graded alcohols, washed in water, and then placed in constantly-stirred 3% hydrogen peroxide in methanol for 20 min. The slides were washed and loaded into Sequenza chambers (Thermo Scientific) using PBS before incubation with 100 µl of 25 % normal goat serum in PBS for 30 min at room temperature. Slides were then incubated with 100 µl of primary antibody (anti-eqMCP-1 rabbit IgG or anti-eqTRYP rabbit IgG) at 0.2 µg/ml in PBS and the slides incubated overnight at 4 °C. In each Sequenza rack one slide was incubated with rabbit IgG at 0.2 µg/ml as a negative control. The next day, slides were washed three times with PBS before incubating with 100 µl of goat anti-rabbit HRP (Envision) for 30 min at room temperature. After a further three washes in PBS, the slides were incubated with DAB for 8 min at room temperature. The slides were washed in tap water then placed in an automated stainer (Thermo Scientific) where cell nuclei were stained with haematoxylin (Haematoxylin Z, Cellpath). Slides were dehydrated to

xylene through graded alcohols and mounted with Consul-mount (Shandon) using an automated coverslipper (Consul model, Shandon).

3.2.6.1 Optimal Antibody Concentrations for Immunohistochemistry

Pilot studies were performed to optimise the antibody concentrations for immunohistochemistry. Two tissue sections were chosen, AB9 caecum (high TB mast cell count; 1062 MMC/mm²) and AB5 caecum (low TB mast cell count; 181 MMC/mm²). Serial sections were taken and four dilutions of each antibody were compared: 0.1 µg/ml, 0.2 µg/ml, 0.5 µg/ml and 1 µg/ml.

3.2.6.2 Enumeration of Proteinase-Labelled Mast Cells

All histological counts were performed without knowledge of cyathostomin burden or labelling antibody. Sections were observed using an Olympus BX50 microscope and photographed using an Olympus U-CMAD digital camera and AnalySIS Five software (Soft Imaging System GmbH, Münster, Germany). Positively-labelled cells were identified and enumerated using a calibrated graticule over 10 mucosal and submucosal fields of view per slide under x 400 magnification. The total area per graticule field at this magnification was 0.0625 mm². Mast cells were expressed as mast cell (MC) per mm².

3.2.7 Serum Collection and Storage for ELISA

Left or right colonic vein blood samples were collected post mortem as a source of local (L) serum draining the site of interest. Approximately 2 ml of blood was collected using a needle and syringe and left to clot overnight at 4 °C. Serum was harvested by centrifugation at 1730 x g for 10 min at 4 °C and stored in aliquots at -20 °C or -80 °C. Peripheral (P) blood samples were also collected from horses at the R(D)SVS. Due to the nature of the slaughter line process it was not logistically feasible to collect peripheral blood samples from the horses at the abattoir. A BCA assay was performed using a Pierce Micro BCA™ protein assay kit (Thermo Scientific) to estimate the concentration of protein in each serum sample.

3.2.7.1 Cyathostomin-Negative Serum

Serum was pooled from four ponies from a previous study (Murphy and Love 1997). These ponies were reared indoors with their dams, weaned at 4 months of age and maintained on a high-fibre pelleted ration and bedded on wood shavings. The ponies were considered to be helminth-naïve at the time of sampling.

3.2.8 Tissue Preparation for ELISA

3.2.8.1 Tissue Homogenisation and Protein Content Analysis

Tissue was stored at -80 °C. Samples of 20-30 mg were weighed into Precellys CK28 tubes (Peglab) and 500 µl of PBS containing 1M NaCl, 0.05% Tween 20 (Sigma-Aldrich) and proteinase inhibitors (Complete Mini Proteinase inhibitor Cocktail [Roche]). The tissue was homogenised for five, 23-second cycles using a Precellys 24 tissue homogeniser (Precellys) at 6200 rpm, with 2 min on ice between cycles. Homogenised tissue was centrifuged at 5000 rpm for 5 min and the supernatant collected and stored at -80 °C. A BCA assay was performed to estimate the concentration of protein in each homogenate sample.

3.2.9 Optimisation of Serum and Tissue ELISAs for eqTRYP and eqMCP-1

3.2.9.1 Proteins for ELISA Standard Curves

Previously-purified proteinases derived from equine mastocytoma tissue (Pemberton, McEuen et al. 2001) were available at concentrations of 0.14 mg/ml (eqMCP-1) and 0.25 mg/ml (eqTRYP). These proteinases were aliquoted and stored at -80 °C prior to use. The integrity of these proteinases had been previously verified by SDS-PAGE and Simply Blue™ staining (Section 3.2.1). A standard curve using the appropriate proteinase (eqTRYP or eqMCP-1) diluted in PBS 0.05 % Tween20 was prepared from a new aliquot for each individual ELISA plate.

3.2.9.2 General ELISA Protocol

High binding 96-well ELISA plates (Immulon 96W, Dynatech M 129B, Thermo Life Sciences) were coated with 50 µl polyclonal rabbit anti proteinase (anti-eqTRYP or anti-eqMCP-1) at an optimal concentration (µg/ml) in carbonate buffer (pH 9.6). Plates were sealed and incubated at 4 °C overnight. Plates were washed six times with ELISA wash buffer, PBS 0.05 % Tween20 (PBST20) and then incubated with blocking buffer (4 % BSA PBST20, 200 µl/well) for 2 hs at 37 °C. Plates were washed again six times with 4 % BSA PBST20 and 50 µl of test sample (diluted in blocking buffer where necessary) were added to each well. Plates were incubated for 1 h at 37 °C. Samples were tested in duplicate. Following a further six washes, plates were incubated with 50 µl/well biotinylated rabbit polyclonal antibody at an optimal concentration (µg/ml) for 1 h at 37 °C. Plates were washed a final six times and then incubated for 30 min at 23 °C with 50 µl/well streptavidin-HRP conjugate (Sigma, 1:1000). To each well, 50 µl Sure Blue TMB substrate (Insight Biotechnology Ltd) were added and plates incubated for 5-10 min. Reactions were stopped with the addition of 50 µl/well 0.18M H₂SO₄. The reaction was read within 10 min using an ELISA plate reader (Tecan Sunrise) at 450 nm.

3.2.9.3 Optimal Concentrations of Capture and Detection Antibodies for eqMCP-1 ELISA

A pilot ELISA was performed to determine the optimal antibody concentrations, using rabbit anti- eqMCP-1 as the capture antibody (C) and biotinylated rabbit anti-eqMCP-1 as the detection antibody (D). These antibodies have previously been used in a sandwich ELISA (Dacre 2005). Combinations of capture and detection antibody at concentrations of 1, 2 and 5 µg/ml were tested. The combination of capture antibody at 5 µg/ml and detection antibody at 5 µg/ml were selected as this gave the greatest range of OD (0.079 to 1.180) over the standard protein dilutions.

3.2.9.4 Optimal Concentrations of Capture and Detection Antibodies for eqTRYP ELISA

As in Section 3.2.11.1, an ELISA was performed to determine the optimal concentrations of capture and detection antibodies. Rabbit anti-eqTRYP IgG was used as the capture antibody and biotinylated rabbit anti-eqTRYP as the detection antibody. The secondary antibody had previously been used in a sandwich ELISA (Dacre 2005). Standard curves of purified eqTRYP at a range of 2.5 - 40 ng/ml were prepared in duplicate to test combinations of capture and detection antibodies at concentrations 1, 2 and 5 µg/ml however the OD values with these concentrations were low (<0.55) resulting in a lack of sensitivity. Further optimisation was therefore required. The top eqTRYP standard was increased to 20 ng/ml. The combinations of concentrations of capture and detection antibody at 5 µg/ml and 10 µg/ml were assessed. Serum over a range of dilutions from 1:8 to 1:64 from horse DV2 was also tested on each combination of antibodies. The combination of capture antibody at 5 µg/ml and detection antibody at 10 µg/ml was selected. This gave a satisfactory range of OD over the standard protein dilutions (0.030 to 1.079). There was minimal difference between the serum ODs when the capture antibody was used at either 5 µg/ml or 10 µg/ml so to preserve the reagents the lower concentration of 5 µg/ml was selected.

3.2.9.5 Optimal Serum Concentrations for eqMCP-1 ELISA

Serum was selected from four horses (DV1, DV2, DV3 and DV8) with a range of eqMCP-1 mast cell burdens ascertained from immunohistochemistry counts (Table 3.1) in order to assess the optimal serum concentration for the eqMCP-1 ELISA. Four serial dilutions (4 % BSA in PBST20) of each sample were prepared ranging from 1:2 to 1:16. The dilution curves were compared against an eight-point standard curve of purified eqMCP-1 which ranged from 0.04 to 5 ng/ml. The ELISA was performed as in Section 3.2.8.1 using a capture antibody at 5 µg/ml and a detection antibody at 5 µg/ml.

Horse ID	eqMCP-1 MMC Caecum (MC/mm ²)	eqMCP-1 SMMC Caecum (MC/mm ²)	eqMCP-1 MMC RVC (MC/mm ²)	eqMCP-1 SMMC RVC (MC/mm ²)	eqMCP-1 MMC RB (MC/mm ²)	eqMCP-1 SMMC RB (MC/mm ²)
DV 1	56	64	56	50	3	8
DV 2	301	98	272	213	85	19
DV 3	70	69	19	38	59	58
DV 8	408	131	509	218	309	226

Table 3.1: Table of eqMCP-1 mast cell counts from horses DV 1, DV2, DV3 and DV 8. Cells expressed as MC per mm². (eqMCP-1: equine Mast Cell Proteinase-1; MMC: Mucosal mast cell; SMMC: Submucosal mast cell; RVC: Right ventral colon; RB: Rectal biopsy).

ELISA determination of eqMCP-1 values in the four serial dilutions of equine peripheral serum (P) from these horses are shown in Figure 3.1. A dilution factor of 1:2 (Figure 3.1: circled) was selected as it gave the greatest discrimination between samples.

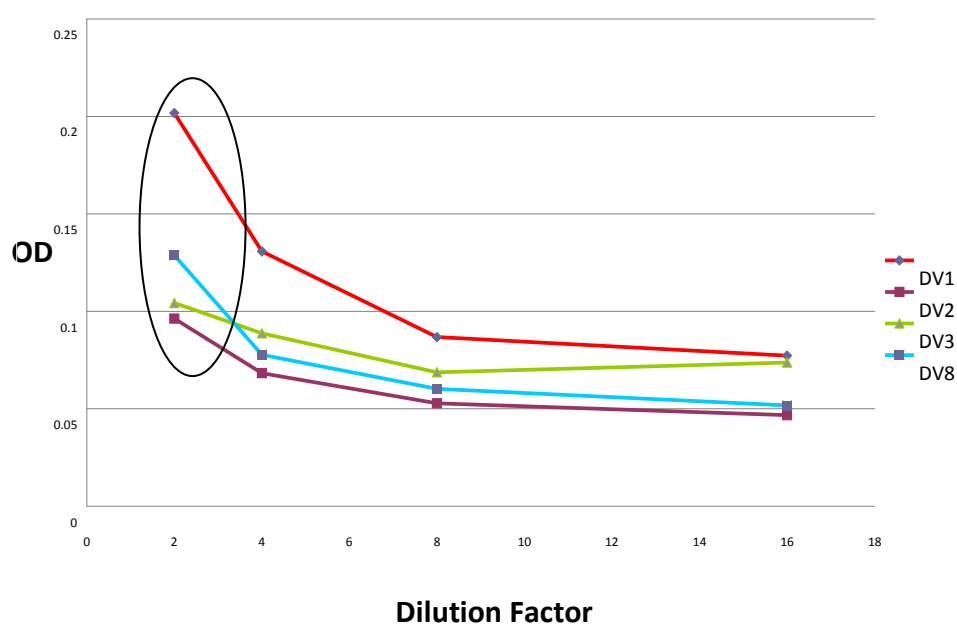


Figure 3.1: EqMCP-1 serum ELISA: Graph of serum dilution curves of four horses (DV1, DV2, DV3 and DV8). The circle area represents the selected dilution factor, 2 (eqMCP-1: equine Mast Cell Proteinase-1; OD: Optical Density).

3.2.9.6 Optimal Serum Concentrations for eqTRYP ELISA

Serum was selected from two local serum samples, DV9 and AB16 in order to assess the optimal serum concentration for the eqTRYP ELISA. This serum had demonstrated consistently high optical density (OD) in the eqMCP-1 serum ELISA. These horses, AB16 and DV9, had also demonstrated low and high eqTRYP mucosal MMC and SMMC burdens respectively (Table 3.2). Five serial dilutions (4 % BSA in PBST20) of each sample and the cyathostomin-negative serum were prepared ranging from 1:16 to 1:256. The dilution curves were compared against an eight - point standard curve of purified eqTRYP which ranged from 0.04 to 20 ng/ml. The ELISA was performed as in Section 3.2.8.1 using a capture antibody at 5 µg/ml and a detection antibody at 10 µg/ml.

Horse ID	eqTRYP MMC Caecum (MC/mm ²)	eqTRYP SMMC Caecum (MC/mm ²)	eqTRYP MMC RVC (MC/mm ²)	eqTRYP SMMC RVC (MC/mm ²)	eqTRYP MMC RB (MC/mm ²)	eqTRYP SMMC RB (MC/mm ²)
AB 16	11	6	46	40	24	21
DV 9	149	66	117	190	174	181

Table 3.2: Table of eqTRYP mast cell counts from horses AB16 and DV 9. Cells expressed as MC per mm². (eqTRYP: equine Tryptase; MMC: Mucosal mast cell; SMMC: Submucosal mast cell; RVC: Right ventral colon; RB: Rectal biopsy).

The five serial dilutions (PBST20) prepared ranging from 1:16 to 1:256 of the local serum sample from horses, DV9 and AB16 and the pooled cyathostomin-negative serum are shown in Figure 3.2. The ELISA was performed using the chosen concentrations of capture antibody at 5 µg/ml and detection antibody at 10 µg/ml. A dilution factor of 1:128, circled on Figure 3.2, was selected which gave a range of ODs from 0.775 (DV9 Local) to 0.105 (NEG: cyathostomin-negative serum). This dilution factor was selected as it gave good separation between the samples. The cyathostomin-negative serum (Figure 3.6: green line) had a markedly lower OD than the infected samples.

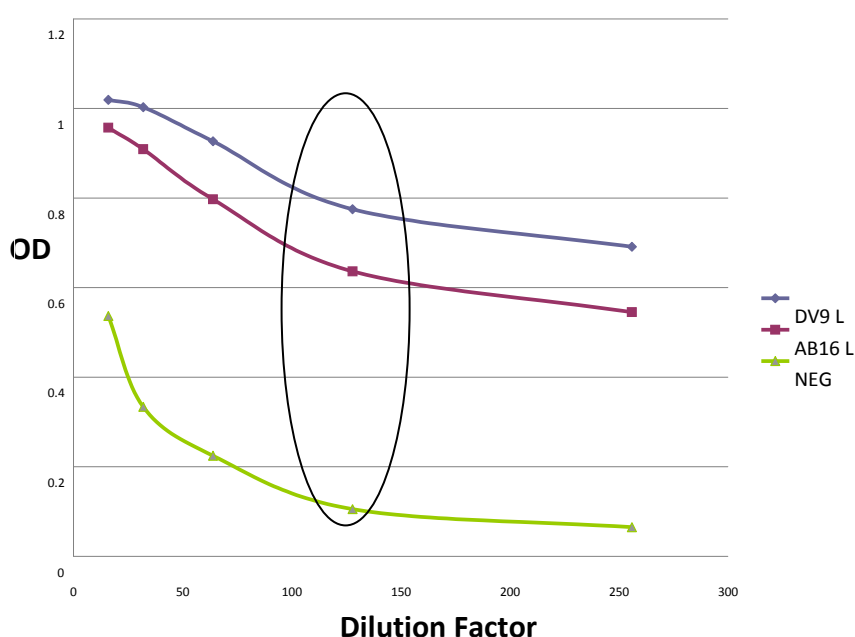


Figure 3.2: EqtRYP serum ELISA: Graph of serum dilution curves from two horses (DV9 and AB16) and the pooled serum of cyathostomin-negative horses (NEG). (eqTRYF: equine Tryptase; L: Local; OD: Optical Density).

3.2.9.7 Optimal Tissue Sample Concentrations for eqMCP-1 and eqTRYP ELISA

Caecal tissue homogenates from three horses DV2, AB1 and DV9 were used to optimise homogenate dilution for ELISA assays. Serial dilutions of tissue homogenate (4 % BSA in PBST20) were performed ranging from 1:64 to 1:512. The capture and detection antibody concentrations for the eqMCP-1 ELISA were both 5 $\mu\text{g/ml}$. The capture and detection antibody concentrations were 5 $\mu\text{g/ml}$ and 10 $\mu\text{g/ml}$ respectively for the eqTRYP ELISA. The dilution factor of 1:256 and 1:512 was chosen for the eqTRYP and eqMCP-1 tissue ELISAs respectively, circled on Figures 3.3 and 3.4, as these dilutions gave the best separation between the tissue homogenate samples.

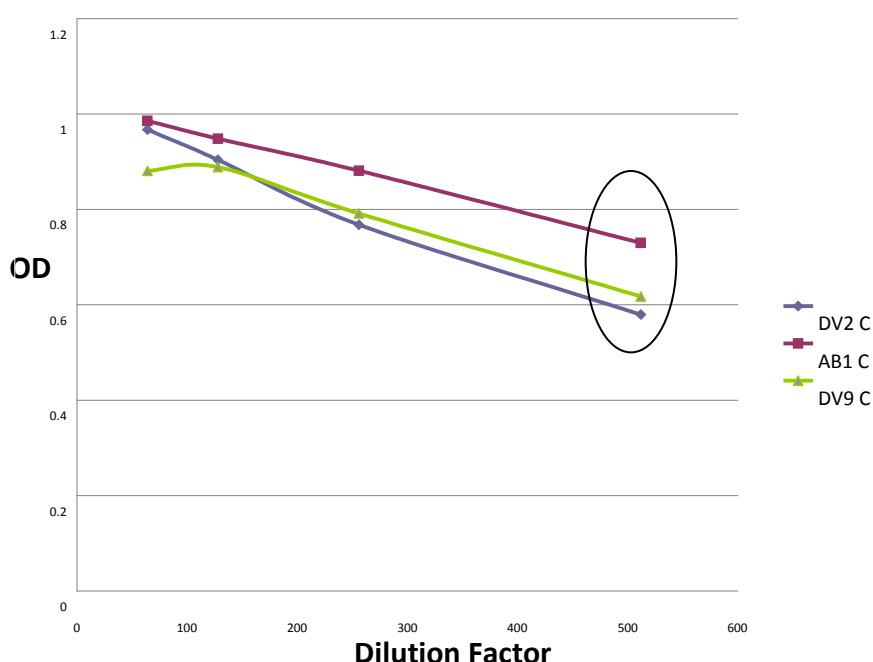


Figure 3.3: EqMCP-1 caecal tissue ELISA: Graph of tissue homogenate dilution curves from three horses (DV2, AB1 and DV9). The circle represents the selected dilution factor, 512. (eqMCP-1: equine Mast Cell Proteinase-1; C: Caecal tissue homogenate; OD: Optical Density).

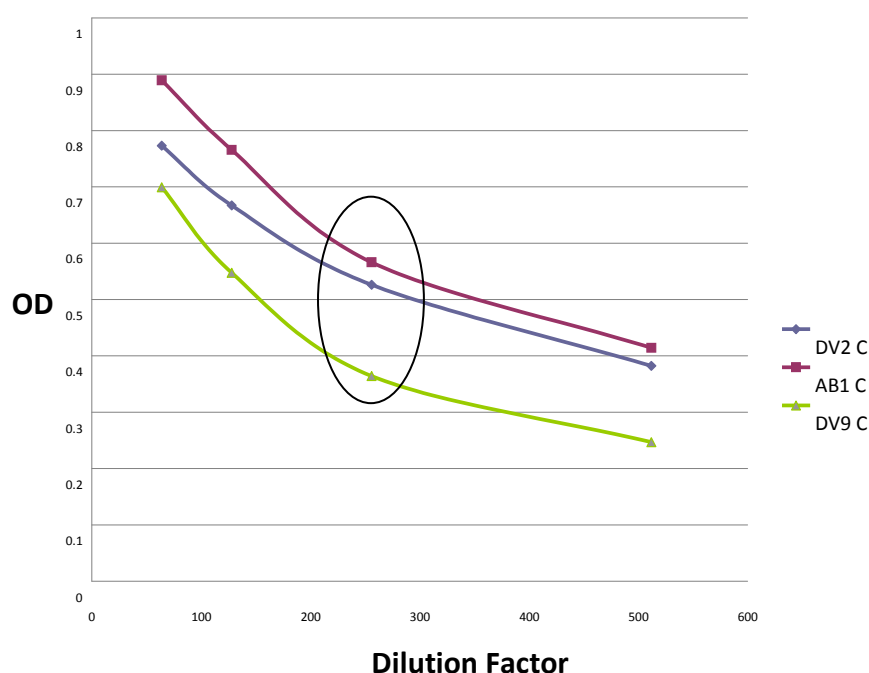


Figure 3.4: EqTRYP tissue homogenate ELISA: Graph of caecal tissue homogenate dilution curves from three horses (DV2, AB1 and DV9). (eqTRYP: equine Tryptase; C: Caecal tissue homogenate; OD: Optical Density).

3.2.9.8 Further Optimisation of eqTRYP ELISA

As the capture antibody for the eqTRYP ELISA (rabbit anti-eqTRYP IgG) had not been previously validated, further experiments were performed to optimise this assay.

3.2.9.8.1 Capture Antibody for eqTRYP ELISA

To validate that the signal from the capture antibody rabbit anti-eqTRYP IgG was specific and not due to non-specific effects of rabbit IgG an experiment was performed using normal rabbit IgG at 5 µg/ml as the capture antibody. Tissue homogenate from four horses and serum from six horses with a range of OD from pilot studies were used to conduct further studies to ensure the capture antibody was specific. There was a significant difference between the ODs of each sample with the two capture antibodies, Figure 3.5 ($p=0.004$); the rabbit IgG capture antibody gave significantly lower OD values (generally <0.1) compared to the rabbit anti eqTRYP IgG capture antibody. This suggested that the OD signal from the capture anti-eqTRYP IgG was specific for eqTRYP.

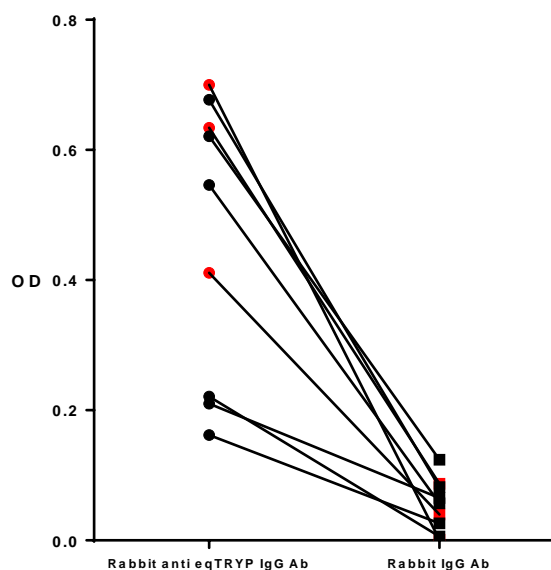


Figure 3.5: Graph of OD readings at 492nm for serum and tissue samples for eqTRYP ELISA with two different capture antibodies, rabbit anti eqTRYP IgG and rabbit IgG. The red symbols represent tissue samples and the black symbols represent serum samples. The ODs observed with rabbit anti eqTRYP IgG were significantly greater than those with rabbit IgG, $p=0.004$. (eqTRYP: equine Tryptase; OD: Optical Density; Ab: Antibody).

3.2.9.8.2 Optimal Block for eqTRYP ELISA

A pilot study was performed to ascertain the optimal blocking solution. An ELISA was performed using three different blocks for comparison, 4 % BSA in PBST20, 10 % normal rabbit serum (NRS) in PBST20 and 10 % NRS in 4 % BSA PBST20. A positive control of eqTRYP (80 ng/ml), tissue from the equine mastocytoma (diluted 1:40), tissue from DV3 RVC (diluted 1:40) and serum from DV7 P and DV9 L (diluted 1:64) were used to compare the effects of the blocking solution. These results are displayed in Figure 3.6. There was no significant difference between the blocking solutions.

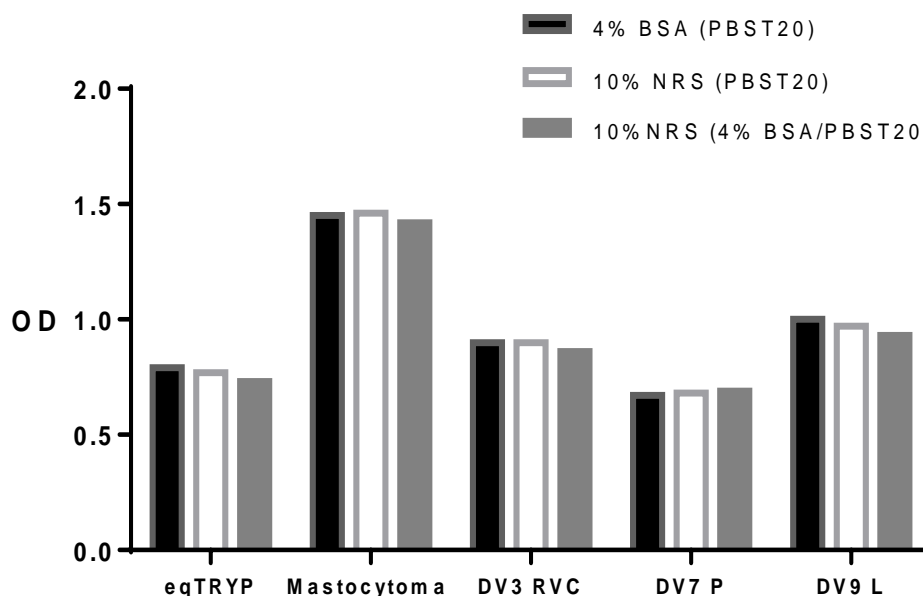


Figure 3.6: Barchart of samples for eqTRYP ELISA with three different blocking solutions. There was no significant difference between the ODs observed (Test: Friedman Test) ($p=0.271$). (eqMCP-1: equine Mast Cell Proteinase-1; eqTRYP: equine Tryptase; L: Local; P: Peripheral; OD: Optical Density; RVC: Right ventral colon; BSA: Bovine Serum Albumin. NRS: Normal Rabbit Serum. PBST20: Phosphate Buffered Saline Tween 20).

3.2.9.9 Serum Storage Conditions

The serum storage conditions did not have a consistent effect on the proteinase concentration measured in the sample. The -20°C stored serum concentrations of eqMCP-1 were significantly higher than the concentration in the -80°C stored serum in the local, ($p<0.001$), and peripheral, ($p=0.016$), samples. However, the -20°C stored serum samples containing significantly lower eqTRYP concentrations than the -80°C stored local serum, ($p=0.021$) whereas there was no significant difference in eqTRYP concentrations between the two storage temperatures for the peripheral serum samples ($p=0.424$). The -20°C and -80°C serum results significantly correlated for the eqMCP-1 local and peripheral samples and also the eqTRYP local and peripheral samples. As these results demonstrated no consistent advantage for storage at -80°C , further analysis was performed on the -20°C stored serum values.

3.2.9.10 Final ELISA Protocols

3.2.9.10.1 Final eqMCP-1 ELISA Protocol

All serum and tissue samples were run in the optimised ELISA protocol in duplicate, on three separate occasions, using 5 µg/ml capture and detection antibodies. Serum samples were diluted 1:2 in 4 % BSA in PBST20. There was insufficient peripheral serum from horse DV4 stored at -20 °C to obtain an eqMCP-1 concentration. Tissue samples were diluted to 1:512 in 4 % BSA in PBST20.

3.2.9.10.2 Final eqTRYP ELISA Protocol

All serum and tissue samples were run in the optimised ELISA protocol in duplicate, on three separate occasions, with concentrations of capture and detection antibodies at 5 and 10 µg/ml, respectively. Serum samples were diluted 1:128 in 4 % BSA in PBST20. There was insufficient peripheral serum from horse DV4 stored at -20 °C and -80 °C to obtain an eqTRYP concentration. Tissue samples were diluted to 1:256 in 4 % BSA in PBST20.

3.2.9.11 Intra- and Inter- assay Coefficients of Variation (CV) for ELISAs

To determine intra-assay variability the proteinase concentration was measured in duplicate for each ELISA (eqMCP-1 serum, n=28), (eqMCP-1 tissue, n=36), (eqTRYP serum, n=35), (eqTRYP tissue, n=35). The coefficients of variation (CVs) were determined by expressing the standard deviation as a percentage of the mean for each group of values. Inter-assay variability was determined by running the same sample on different ELISA plates on three separate occasions. For this CV one sample from a horse with a high proteinase concentration and one from a horse with a low proteinase concentration measured by ELISA was selected for both the serum and tissue ELISAs. The inter- and intra-assay CVs are shown in Table 3.3. The serum assays and the tissue eqMCP-1 assay had intra-assay CVs less than 10% and that of the tissue eqTRYP was 11.2%. The inter-assay CVs for all four ELISAs were

greater than 25%. Wherever possible samples were run on the same day, to minimise the effect of the high inter-assay variation.

		Inter-assay CV (%)	Intra-assay CV (%)
eqMCP-1	Serum	34.0	8.4
	Tissue	25.5	7.9
eqTRYP	Serum	32.9	8.0
	Tissue	32.9	11.2

Table 3.3: Inter- and Intra-assay Coefficients of Variation (CV) for the eqMCP-1 and eqTRYP serum and tissue ELISAs. (eqMCP-1: equine Mast Cell Proteinase-1; eqTRYP: equine Tryptase).

3.2.10 Data Analysis

As data were not normally distributed, non-parametric tests were selected. For optimal graphical representation, log transformed ($\log_{10}+1$) data is sometimes presented. Statistical analyses and graphical displays were performed using the statistical computer package R Studio (V 0.97.551), Minitab 15 statistical software and GraphPad Prism5. For investigating the relationships between mast cell measures, including TB-stained mast cell counts, eqMCP-1- and eqTRYP-labelled mast cell counts, ELISA serum and tissue values correlations were assessed using the Spearman rank test. For comparison of paired data the Wilcoxon Signed rank test was selected and for unpaired, the Mann-Whitney test using GraphPad Prism5. Standard linear regression analyses were used to explore the relationships between $\log_{10}+1$ transformed mast cell measures and $\log_{10}+1$ transformed combined total mucosal burdens. Bland-Altman analysis was used to assess agreement between the local and peripheral serum proteinase levels. The presence of *A. perfoliata* was investigated and added as a confounding variable. Results were considered statistically significant at $p < 0.05$.

3.3 Results

3.3.1 Validation of eqTRYP and eqMCP-1

SDS-PAGE of eqMCP-1 and eqTRYP followed by Simply Blue staining was performed to validate the integrity of the proteinases. EqMCP-1 gave a single band of approximately 32 kDa (Figure 3.7: lane 1, green arrow). EqTRYP gave a triple band complex at approximately 33-36 kDa (Figure 3.7: lane 2, three black arrows). These results are characteristic of these proteinases (Pemberton, McEuen et al. 2001).

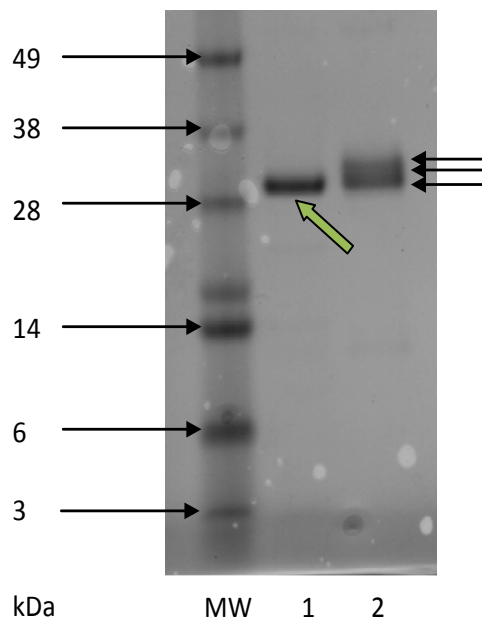


Figure 3.7: Validation of equine mast cell proteinases. Scanned image of a Simply Blue stained SDS-PAGE gel. MW: broad range molecular weight markers; 1: eqMCP-1; 2: eqTRYP. (eqMCP-1: equine Mast Cell Proteinase-1; eqTRYP: equine Trypsin).

3.3.1.1 Validation of rabbit anti eqTRYP IgG and Rabbit Anti eqMCP-1 IgG from Rabbit Sera

A Western blot was performed to confirm that the rabbit anti-eqTRYP IgG and rabbit anti-eqMCP-1 IgG purified from rabbit sera bound to eqTRYP and eqMCP-1, respectively. Probing eqMCP-1 with anti-eqMCP-1 IgG resulted in a single band of reactivity at approximately 32 kDa (Figure 3.8: lane 2). Probing eqTRYP with anti-eqTRYP IgG gave a triple band of reactivity at approximately 33-36 kDa (Figure 3.8: lane 4). These results are consistent with Figure 3.7 and characteristic of these

proteinases (Pemberton, McEuen et al. 2001). No reactivity was observed when the eqTRYP or eqMCP-1 blots were probed with control rabbit IgG (Figure 3.8: lanes 1 and 3).

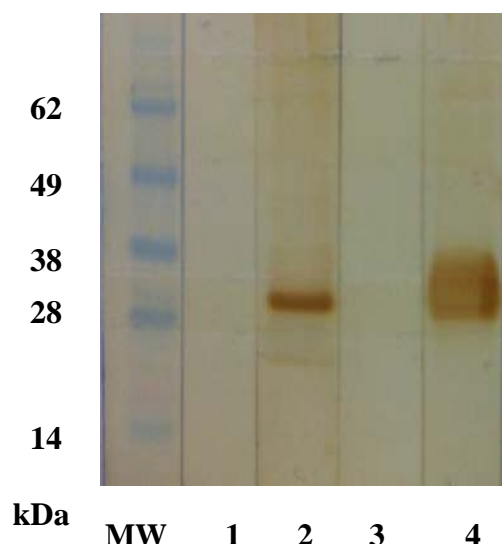


Figure 3.8: Validation of equine mast cell proteinases. Scanned image of a Western blot. Lane 1 and 2 contained 0.5 μ g of eqMCP-1 and lanes 3 and 4 contained 1 μ g of eqTRYP. Lanes 1 and 3 were treated with rabbit IgG (1 μ g/ml), lane 2 treated with rabbit IgG anti eqMCP-1 (1 μ g/ml) and lane 4 treated with rabbit IgG anti eqTRYP (1 μ g/ml). MW: broad range molecular weight markers. (eqMCP-1: equine Mast Cell Proteinase-1; eqTRYP: equine Tryptase).

3.3.1.2 Removal of Anti-Equine Albumin from Rabbit IgG Anti eqMCP-1 Sera

The purified rabbit IgG anti-eqMCP-1 antisera was suspected by Dr A. Pemberton to be contaminated with anti-equine albumin antibodies (Pemberton, McEuen et al. 2001). This contamination was verified by Western blot performed using equine serum albumin and purified eqMCP-1 (Figure 3.9). A band was observed in lane 2 and 3 at approximately 67 kDa which is consistent with the size of equine albumin (Fjeldsgaard and Paulsen 1993). The purified rabbit IgG anti eqMCP-1 was therefore cross-absorbed against equine albumin by passing through a previously generated column (Pemberton, McEuen et al. 2001) to which 10 mg equine albumin had been conjugated. The Western blot was repeated and confirmed the successful removal of anti-equine albumin IgG as the band at approximately 67 kDa was no longer present (Figure. 3.9: Lanes 5 and 6).

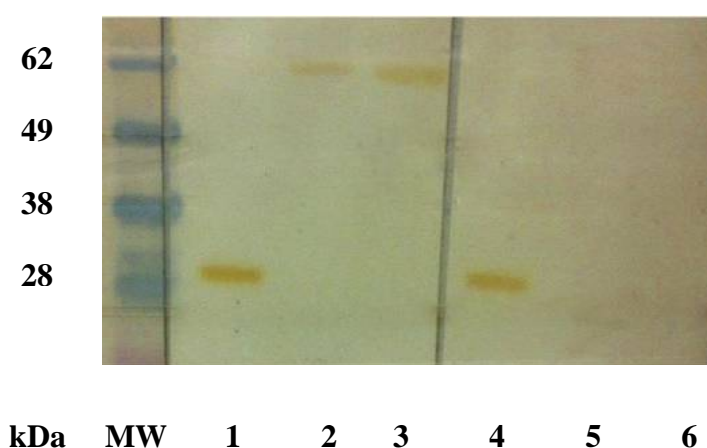


Figure 3.9: Validation of anti-equine albumin removal from anti eqMCP-1 antiserum. Scanned image of Western blots. Lanes 1 and 4 contained purified eqMCP-1 (1 μ g), lanes 2, 3, 5 and 6 contained equine serum albumin (0.5 μ g in lanes 2 and 5, 1 μ g in lanes 3 and 6). Lanes 1, 2 and 3 were treated with rabbit IgG anti-eqMCP-1 before cross-absorption with albumin. Lanes 4, 5 and 6 were treated with rabbit IgG anti-eqMCP-1 IgG after cross-absorption with albumin. (MW: broad range molecular weight markers; eqMCP-1: equine Mast Cell Proteinase-1; eqTRYP: equine Tryptase).

3.3.2 Dual-Immunofluorescence

Dual-labelled immunofluorescence was performed on caecal material from horse AB9 with a high TB mast cell count (1062 MMC/mm²) to optimise the procedure. Figure 3.10 shows a slide that has been dual-labelled with immunofluorescent polyclonal rabbit antibodies, with eqTRYP-labelled green (AlexaFluor® 488, Figure 3.10A) and eqMCP-1-labelled red (AlexaFluor® 568, Figure 3.10B). Pilot studies showed that there was significant background signal with biotinylated rabbit IgG which acted as the negative control for eqMCP-1 (Figure 3.11). A control experiment was performed using slides incubated omitting primary antibody, streptavidin-HRP and tyramide separately. Significant background signal was still apparent with tyramide only in the absence of HRP. Further control experiments were performed using a biotin blocking step prior to addition of the primary antibody, HRP-streptavidin and Alexa Fluor® 568 Tyramide but this did not have a significant effect on the background signal. These results suggested that the background was due to endogenous peroxidase activity reacting with the Alexa Fluor® 568 Tyramide and therefore an additional control experiment was performed using Diaminobenzidine

(DAB) to quench any endogenous eosinophil peroxidase activity. However, significant background was still observed and it was concluded that eqMCP-1 positive cells could not be counted reliably using dual-labelled immunofluorescence.

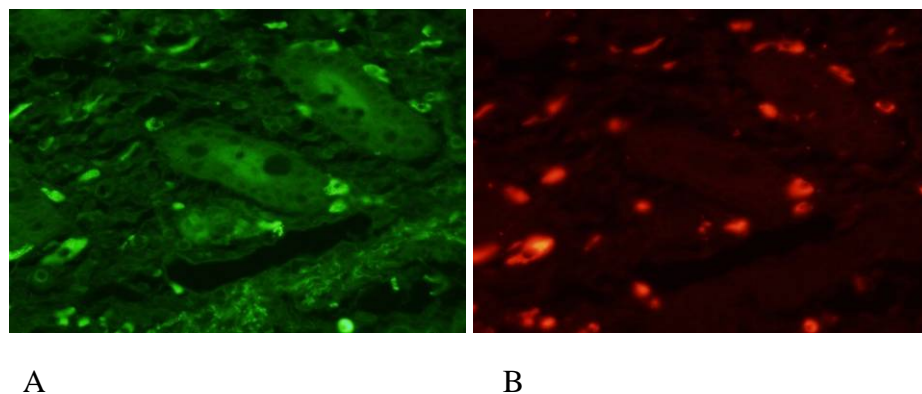


Figure 3.10: Image of caecal mucosa demonstrating immunolabelled cells. A: eqTRYP at 2µg/ml (green) and B: eqMCP-1 at 2µg/ml (red). (eqMCP-1: equine Mast Cell Proteinase-1; eqTRYP: equine Tryptase).

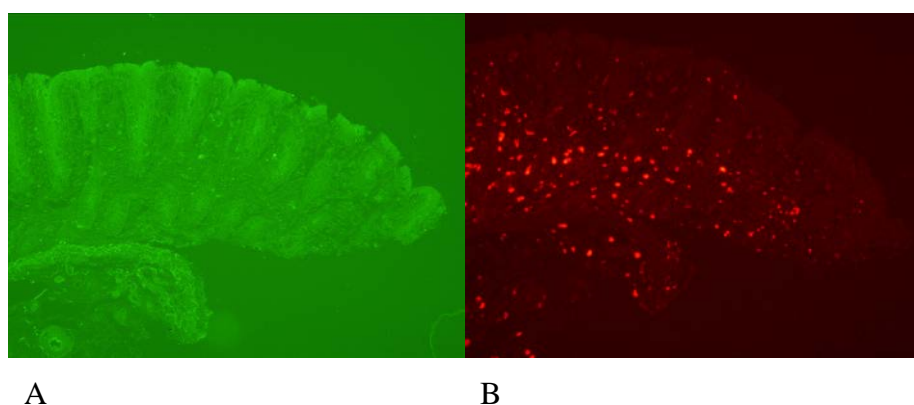


Figure 3.11: Image of caecal tissue dual-immunolabelled with negative control antibodies. A: Rabbit IgG at 2µg/ml labelled with goat anti -rabbit IgG-alexafluor 488. B: biotinylated rabbit IgG at 2µg/ml labelled with HRP-Streptavidin and Alexa Fluor® 568 Tyramide.

3.3.3 Immunohistochemistry

A single immunohistochemistry protocol was optimised.

3.3.3.1 Optimal Antibody Concentrations for Immunohistochemistry

Antibody concentrations of 0.5 $\mu\text{g/ml}$ and 1 $\mu\text{g/ml}$ produced too much background staining to reliably count labelled mast cells. This was particularly apparent in sections from horse AB9. These sections had a high MMC count from TB staining (1062 MMC/ mm^2). The optimal concentration was 0.2 $\mu\text{g/ml}$ for both rabbit anti-eqMCP-1 IgG (Figure 3.12) and rabbit anti-eqTRYP IgG (Figure 3.13). The staining was more intense with eqMCP-1. Some mast cells appear to be degranulating in the tissue sections from this horse (Figure 3.12: black arrow).

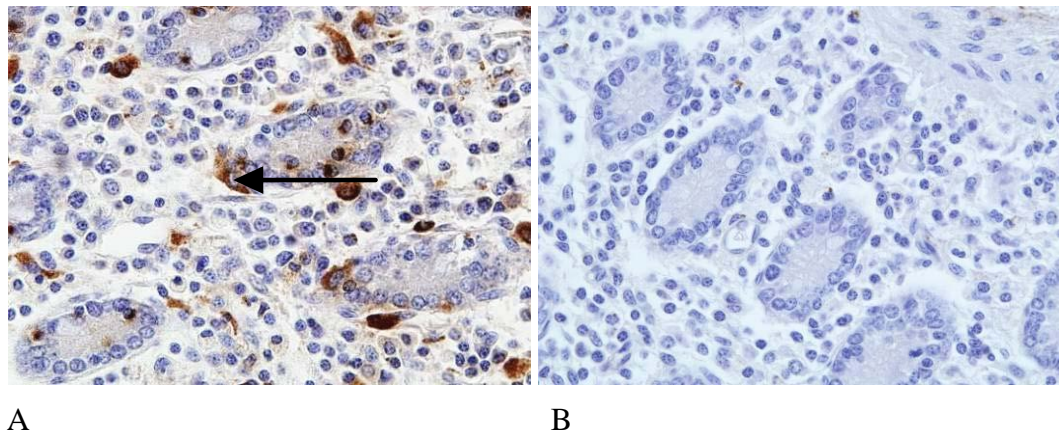


Figure 3.12: Image of a section of caecal tissue from horse AB9 at x 400 magnification labelled with A: rabbit anti eqMCP-1 IgG at 0.2 $\mu\text{g/ml}$. Positive cells are labelled brown. Some labelled cells appear to be in the process of degranulating (black arrow). B: rabbit IgG at 0.2 $\mu\text{g/ml}$. (eqMCP-1: equine Mast Cell Proteinase-1).

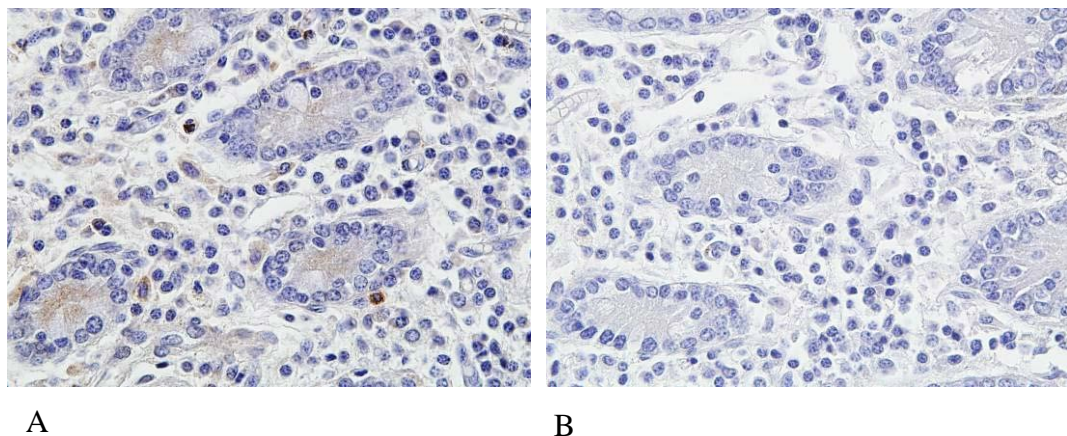


Figure 3.13: Image of a section of caecal tissue from horse AB9 at x 400 magnification labelled with A: rabbit anti eqTRYP IgG at 0.2 $\mu\text{g/ml}$. B: rabbit IgG at 0.2 $\mu\text{g/ml}$. Positive cells are labelled brown. (eqTRYP: equine Tryptase).

3.3.3.2 Proteinase-Labelled Mast Cell Counts

The median and range of the eqMCP-1- and eqTRYP-labelled MMC and SMMC counts for the caecum, RVC and RB for all horses (AB1-AB16 and DV1-DV12) are shown in Table 3.4 and 3.5, respectively. The widest range of eqMCP-1 MMC was in the RVC (19 – 1323 MC/mm²) and the widest range of eqTRYP MMC was observed in the caecum (6 – 432 MC/mm²). MMC and SMMC counts for the caecum, RVC and RB of the abattoir (AB) and R(D)SVS (DV) horses are shown in Table 7.3 for eqMCP-1 and Table 7.4 for eqTRYP.

	EqMCP-1 MMC Caecum (MC/mm ²)	EqMCP-1 SMMC Caecum (MC/mm ²)	EqMCP-1 MMC RVC (MC/mm ²)	EqMCP-1 SMMC RVC (MC/mm ²)	EqMCP-1 MMC RB (MC/mm ²)	EqMCP-1 SMMC RB (MC/mm ²)
Median	374	146	363	172	111	50
Range	54-1027	14-230	19-1323	38-288	3-613	0-258

Table 3.4: Median and range of MMC and SMMC eqMCP-1-labelled cells from the caecum, RVC and rectum of all horses (AB1-16 and DV1-12). Cells expressed as MC per mm². (eqMCP-1: equine Mast Cell Proteinase-1; MMC: Mucosal mast cell; SMMC: Submucosal mast cell; RVC: Right ventral colon; RB: Rectal biopsy).

	EqTRYP MMC Caecum (MC/mm ²)	EqTRYP SMMC Caecum (MC/mm ²)	EqTRYP MMC RVC (MC/mm ²)	EqTRYP SMMC RVC (MC/mm ²)	EqTRYP MMC RB (MC/mm ²)	EqTRYP SMMC RB (MC/mm ²)
Median	98	44	72	51	32	17
Range	6-432	2-214	8-261	6-245	2-174	0-181

Table 3.5: Median and range of MMC and SMMC eqTRYP-labelled cells from the caecum, RVC and rectum of all horses (AB1-16 and DV1-12). Cells expressed as MC per mm². (eqTRYP: equine Tryptase; MMC: Mucosal mast cell; SMMC: Submucosal mast cell; RVC: Right ventral colon; RB: Rectal biopsy).

3.3.3.3 Comparison of Proteinase-Labelled Mast Cell Counts

There were significantly more eqMCP-1-labelled MMC and SMMC than eqTRYP-labelled MMC and SMMC in the caecum (Figure 3.14) (MMC: $p < 0.0001$. SMMC: $p < 0.0001$), RVC (Figure 3.15) (MMC: $p < 0.0001$. SMMC: $p < 0.0001$) and rectum (Figure 3.16) (MMC: $p < 0.0001$. SMMC: $p < 0.001$).

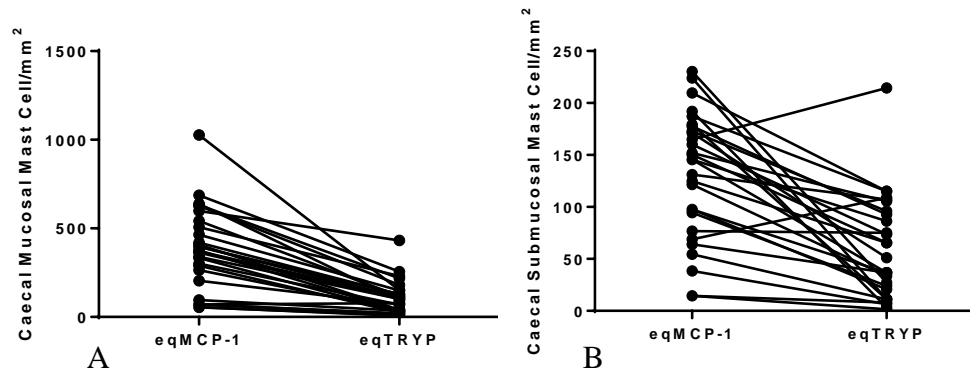


Figure 3.14: A: Graph of individual values of caecal mucosal eqMCP-1- counts and eqTRYP-labelled mast cell counts with lines connecting the values for each horse. There were significantly more eqMCP-1+ caecal MMC, than eqTRYP⁺ caecal MMC $p < 0.0001$. B: Graph of individual values of caecal submucosal eqMCP-1 counts and eqTRYP-labelled mast cell counts with lines connecting the values for each horse. There were significantly more eqMCP-1+ caecal SMMC, than eqTRYP⁺ caecal SMMC $p < 0.0001$. Note different y-axis scales. (eqMCP-1: equine Mast Cell Proteinase-1; eqTRYP: equine Tryptase; MMC: Mucosal mast cell; SMMC: Submucosal mast cell).

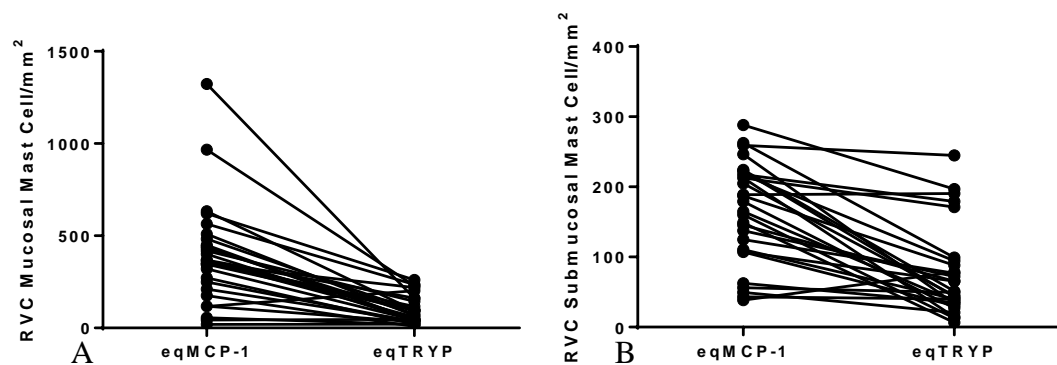


Figure 3.15: A: Graph of individual values of RVC mucosal eqMCP-1- and eqTRYP-labelled mast cell counts with lines connecting the values for each horse. There were significantly more eqMCP-1 RVC MMC, than eqTRYP⁺ RVC MMC $p < 0.0001$. B: Graph of individual values of RVC submucosal eqMCP-1+ and eqTRYP-labelled mast cell counts with lines connecting the values for each horse. There were significantly more eqMCP-1+ RVC SMMC, than eqTRYP⁺ RVC SMMC $p < 0.0001$. Note different y-axis scales. (eqMCP-1: equine Mast Cell Proteinase-1; eqTRYP: equine Tryptase; MMC: Mucosal mast cell; SMMC: Submucosal mast cell; RVC: Right ventral colon).

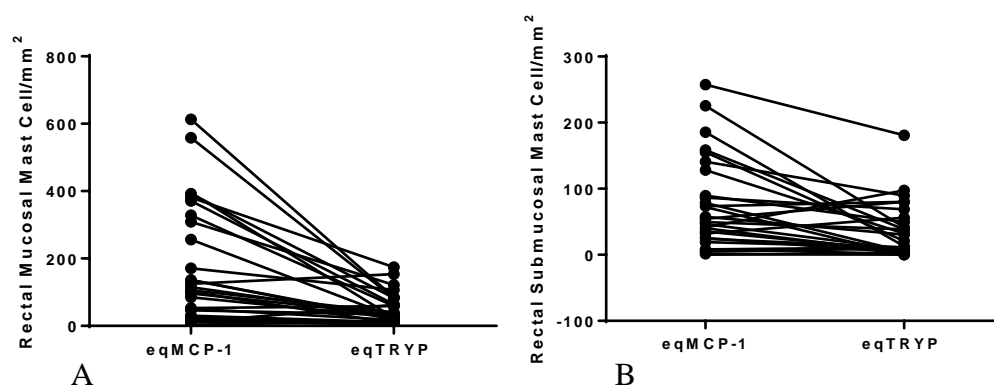


Figure 3.16: A: Graph of individual values of rectal mucosal eqMCP-1- and eqTRYP-labelled mast cell counts with lines connecting the values for each horse. There were significantly more eqMCP-1+ rectal MMC, than eqTRYP⁺ rectal SMMC $p<0.0001$. B: Graph of individual values of rectal submucosal eqMCP-1- and eqTRYP-labelled mast cell counts with lines connecting the values for each horse. There were significantly more eqMCP-1+ rectal SMMC, than eqTRYP⁺ rectal SMMC $p<0.001$. Note different y-axis scales. (eqMCP-1: equine Mast Cell Proteinase-1; eqTRYP: equine Trypsin; MMC: Mucosal mast cell; SMMC: Submucosal mast cell).

3.3.3.4 Comparison of Proteinase-Labelled Mast Cell Counts with TB Mast Cell Counts

The proteinase-labelled mast cell and TB mast cell counts were compared to ensure that the staining methods used here produced comparable results and to provide confidence in the enumeration of the labelled cells. In the caecum and RVC there were significantly more TB MMC than eqMCP-1-labelled MMC (Figure 3.17A, $p=0.0024$ [caecum] and Figure 3.18A, $p=0.030$ [RVC]) and also significantly more TB stained SMMC than eqMCP-1-labelled SMMC mast cells (Figure 3.17B, $p<0.0001$ [caecum] and Figure 3.18B, $p<0.0001$ [RVC]). In the case of the rectum there was no significant difference between TB and eqMCP-1-labelled MMC numbers counted (Figure 3.19A: $p=0.085$); however there were significantly more TB stained SMMC than eqMCP-1-labelled SMMC (Figure 3.19B: $p<0.0001$).

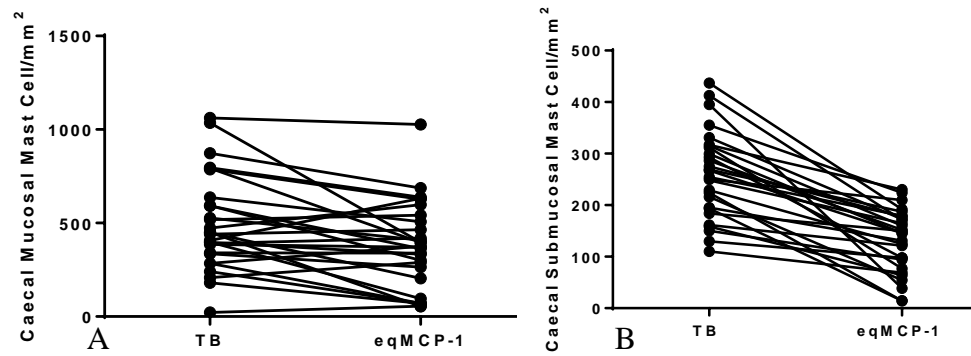


Figure 3.17: A: Graph of individual values from caecal mucosal TB counts and eqMCP-1 counts with lines connecting the values for each horse. There were significantly more TB caecal MMC, than eqMCP-1⁺ caecal MMC $p=0.0024$. B: Graph of individual values from caecal submucosal TB counts and eqMCP-1 counts with lines connecting the values for each horse. There were significantly more TB caecal SMMC, than eqMCP-1⁺ caecal SMMC $p<0.0001$. Note different y-axis scales. (eqMCP-1: equine Mast Cell Proteinase-1; eqTRYP: equine Tryptase; MMC: Mucosal mast cell; SMMC: Submucosal mast cell).

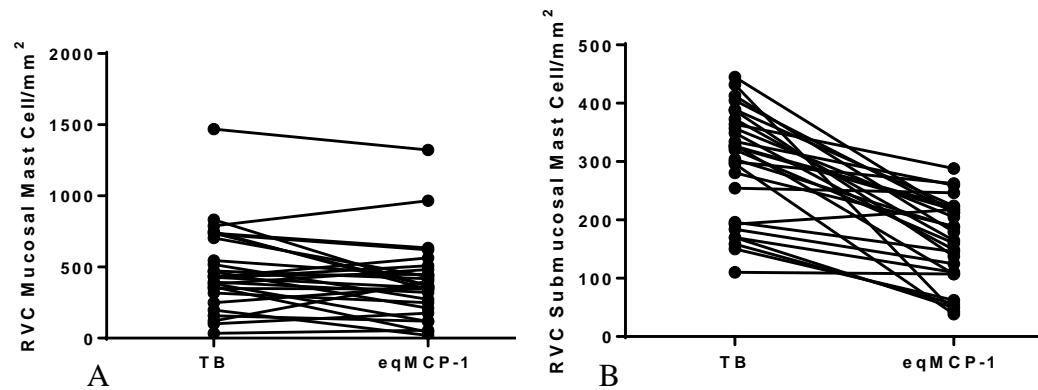


Figure 3.18: A: Graph of individual values from RVC mucosal TB counts and eqMCP-1 counts with lines connecting the values for each horse. There were significantly more TB RVC MMC, than eqMCP-1⁺ RVC MMC $p=0.030$. B: Graph of individual values from RVC submucosal TB counts and eqMCP-1 counts with lines connecting the values for each horse. There were significantly more TB RVC SMMC, than eqMCP-1⁺ RVC SMMC $p<0.0001$. Note different y-axis scales. (eqMCP-1: equine Mast Cell Proteinase-1; eqTRYP: equine Tryptase; RVC: Right ventral colon; MMC: Mucosal mast cell; SMMC: Submucosal mast cell).

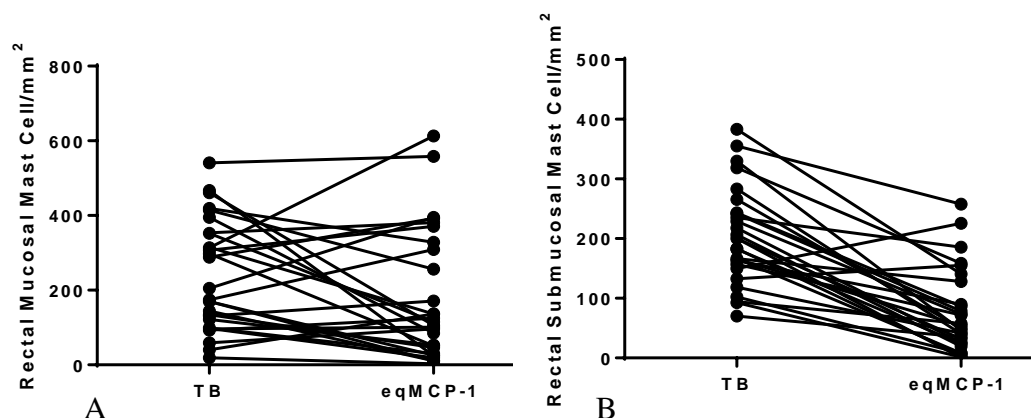


Figure 3.19: A: Graph of individual values from rectal mucosal TB counts and eqMCP-1 counts with lines connecting the values for each horse. There was no significant difference between TB and eqMCP-1 rectal MMC counts, $p=0.085$. B: Graph of individual values from rectal submucosal TB counts and eqMCP-1 counts with lines connecting the values for each horse. There were significantly more TB rectal SMMC, than eqMCP-1⁺ rectal SMMC $p<0.0001$. Note different y-axis scales. (eqMCP-1: equine Mast Cell Proteinase-1; eqTRYF: equine Tryptase; MMC: Mucosal mast cell; SMMC: Submucosal mast cell).

3.3.3.5 Relationship between Mast Cell Counts

A correlation matrix of the counts of TB stained, eqTRYF-labelled and eqMCP-1-labelled MMC and SMMC of the caecum, RVC and rectum is shown in Table 3.6. Individual scatter plot matrices of the $\log_{10}+1$ data for each organ are shown in Figures 3.20 (caecum), 3.21 (RVC) and 3.22 (rectum). Caecal eqMCP-1-labelled MMC counts were positively correlated with caecal TB and with eqTRYF MMC counts ($p<0.001$ and $p<0.001$, respectively). In the case of the RVC, similar positive correlations were observed between eqMCP-1-labelled and TB populations ($p<0.001$) and also eqMCP-1- and eqTRYF-labelled MMC populations ($p=0.001$). The relationships were also similar between these cell populations in the rectum with positive correlations between eqMCP-1-labelled and TB populations ($p=0.026$) and eqMCP-1- and eqTRYF-labelled MMC populations ($p<0.001$). The relationships between submucosal populations were less clear. Caecal eqMCP-1-labelled SMMC levels correlated with the caecal TB SMMC counts ($p=0.004$) but not with the caecal eqTRYF SMMC counts ($p=0.719$). In the case of the RVC and rectum, no significant correlations were found between the eqMCP-1-labelled SMMC counts and the TB-stained SMMC counts or with the local eqTRYF SMMC counts.

MMC and SMMC eqMCP-1-labelled cell counts correlated positively in the caecum ($p=0.002$), RVC ($p<0.001$) and rectum ($p=0.002$). These correlations were of a similar magnitude to those observed between MMC and SMMC eqTRYP-labelled counts in the same organs ($p=0.014$), ($p=0.034$) and ($p=0.001$), respectively. Across different sites caecal eqMCP-1-labelled MMC counts correlated with RVC eqMCP-1- MMC ($p<0.001$) and with the rectal eqMCP-1-labelled MMC counts ($p=0.004$). Similarly caecal eqTRYP-labelled MMC counts correlated with the RVC eqTRYP-labelled MMC counts ($p<0.001$) but the correlation was not significant when the caecal eqTRYP-labelled MMC was compared with the rectal eqTRYP MMC counts ($p=0.068$). Caecal eqMCP-1-labelled SMMC counts correlated with the RVC eqMCP-1-labelled SMMC counts ($p=0.003$), but not with the rectal eqMCP-1-labelled SMMC ($p=0.762$). Similarly, caecal eqTRYP-labelled SMMC counts correlated with the RVC eqTRYP-labelled MMC counts ($p<0.001$) but again the correlation was not significant when caecal eqTRYP-labelled SMMC counts were compared with those obtained in the rectal samples ($p=0.184$).

The rectal proteinase-labelled mast cell populations were further examined. The RB eqMCP-1-labelled MMC correlated significantly with 11 of the possible 17 cell count measures (Table 3.6): caecal TB MMC ($p=0.004$), caecal TB SMMC ($p=0.011$), caecal eqMCP-1 MMC ($p=0.004$), caecal eqTRYP MMC ($p=0.008$), RVC TB MMC ($p=0.008$), RVC TB SMMC ($p=0.004$), RVC eqTRYP MMC ($p=0.001$), RB TB MMC ($p=0.026$), RB TB SMMC ($p=0.036$), RB eqMCP-1 SMMC ($p=0.002$) and RB eqTRYP MMC ($p<0.001$). In contrast, RB counts of eqTRYP-labelled MMC correlated significantly with only four of the 17 possible cell count measures (Table 3.6): RB TB SMMC ($p=0.010$), RB eqMCP-1 MMC ($p<0.001$), RB eqMCP-1 SMMC ($p=0.002$) and RB eqTRYP SMMC ($p=0.001$).

Mast Cell Recruitment and Activation as Measures of Cyathostomin Burden

	Caecum TB MMC	Caecum TB SMMC	Caecum eqMCP-1 MMC	Caecum eqMCP-1 SMMC	Caecum eqTRYP MMC	Caecum eqTRYP SMMC	RVC TB MMC	RVC TB SMMC	RVC eqMCP-1 MMC	RVC eqMCP-1 SMMC	RVC eqTRYP MMC	RVC eqTRYP SMMC	RB TB MMC	RB TB SMMC	RB eqMCP-1 MMC	RB eqMCP-1 SMMC	RB eqTRYP MMC	RB eqTRYP SMMC
Caecal TB MMC	-	0.719	0.684	0.508	0.636	0.171	0.933	0.732	0.641	0.606	0.639	0.191	0.630	0.422	0.532	0.130	0.258	0.126
Caecal TB SMMC	<i><0.001</i>	-	0.412	0.523	0.343	-0.071	0.664	0.811	0.447	0.380	0.367	-0.063	0.563	0.646	0.474	0.148	0.194	-0.096
Caecal eqMCP-1 MMC	<i><0.001</i>	<i>0.029</i>	-	0.565	0.846	0.201	0.726	0.399	0.635	0.463	0.765	0.212	0.469	0.443	0.533	0.155	0.357	0.261
Caecal eqMCP-1 SMMC	<i>0.006</i>	<i>0.004</i>	<i>0.002</i>	-	0.481	0.314	0.609	0.347	0.418	0.539	0.315	0.181	0.341	0.450	0.196	0.060	0.226	0.014
Caecal eqTRYP MMC	<i><0.001</i>	<i>0.074</i>	<i><0.001</i>	<i>0.010</i>	-	0.459	0.694	0.426	0.480	0.468	0.790	0.461	0.460	0.429	0.489	0.161	0.350	0.365
Caecal eqTRYP SMMC	<i>0.384</i>	<i>0.719</i>	<i>0.305</i>	<i>0.104</i>	<i>0.014</i>	-	0.170	0.096	0.053	0.347	0.185	0.700	0.209	0.010	-0.067	0.034	0.285	0.259
RVC TB MMC	<i><0.001</i>	<i><0.001</i>	<i><0.001</i>	<i>0.001</i>	<i><0.001</i>	<i>0.387</i>	-	0.648	0.621	0.588	0.653	0.111	0.638	0.447	0.490	0.019	0.221	0.023
RVC TB SMMC	<i><0.001</i>	<i><0.001</i>	<i>0.035</i>	<i>0.071</i>	<i>0.024</i>	<i>0.627</i>	<i><0.001</i>	-	0.268	0.351	0.417	0.016	0.655	0.488	0.525	0.173	0.329	0.172
RVC eqMCP-1 MMC	<i><0.001</i>	<i>0.018</i>	<i><0.001</i>	<i>0.027</i>	<i>0.010</i>	<i>0.788</i>	<i><0.001</i>	<i>0.169</i>	-	0.644	0.598	0.138	0.399	0.374	0.362	-0.050	0.065	-0.057
RVC eqMCP-1 SMMC	<i><0.001</i>	<i>0.046</i>	<i>0.013</i>	<i>0.003</i>	<i>0.012</i>	<i>0.071</i>	<i>0.001</i>	<i>0.068</i>	<i><0.001</i>	-	0.510	0.399	0.255	0.350	0.264	0.080	0.201	0.318
RVC eqTRYP MMC	<i><0.001</i>	<i>0.055</i>	<i><0.001</i>	<i>0.102</i>	<i><0.001</i>	<i>0.346</i>	<i><0.001</i>	<i>0.027</i>	<i>0.001</i>	<i>0.006</i>	-	0.402	0.506	0.315	0.593	0.155	0.226	0.313
RVC eqTRYP SMMC	<i>0.331</i>	<i>0.751</i>	<i>0.279</i>	<i>0.358</i>	<i>0.014</i>	<i><0.001</i>	<i>0.572</i>	<i>0.936</i>	<i>0.485</i>	<i>0.035</i>	<i>0.034</i>	-	0.179	-0.005	-0.027	0.177	0.130	0.441
RB TB MMC	<i><0.001</i>	<i>0.002</i>	<i>0.012</i>	<i>0.076</i>	<i>0.014</i>	<i>0.286</i>	<i><0.001</i>	<i><0.001</i>	<i>0.035</i>	<i>0.191</i>	<i>0.006</i>	<i>0.363</i>	-	0.417	0.419	0.130	0.212	-0.044
RB TB SMMC	<i>0.025</i>	<i><0.001</i>	<i>0.018</i>	<i>0.016</i>	<i>0.023</i>	<i>0.961</i>	<i>0.017</i>	<i>0.008</i>	<i>0.050</i>	<i>0.068</i>	<i>0.102</i>	<i>0.980</i>	<i>0.027</i>	-	0.399	0.301	0.477	0.253
RB eqMCP-1 MMC	<i>0.004</i>	<i>0.011</i>	<i>0.004</i>	<i>0.317</i>	<i>0.008</i>	<i>0.734</i>	<i>0.008</i>	<i>0.004</i>	<i>0.058</i>	<i>0.175</i>	<i>0.001</i>	<i>0.891</i>	<i>0.026</i>	<i>0.036</i>	-	0.567	0.660	0.350
RB eqMCP-1 SMMC	<i>0.508</i>	<i>0.454</i>	<i>0.432</i>	<i>0.762</i>	<i>0.413</i>	<i>0.865</i>	<i>0.925</i>	<i>0.379</i>	<i>0.800</i>	<i>0.686</i>	<i>0.432</i>	<i>0.366</i>	<i>0.511</i>	<i>0.120</i>	<i>0.002</i>	-	0.555	0.583
RB eqTRYP MMC	<i>0.185</i>	<i>0.323</i>	<i>0.063</i>	<i>0.247</i>	<i>0.068</i>	<i>0.141</i>	<i>0.258</i>	<i>0.087</i>	<i>0.742</i>	<i>0.305</i>	<i>0.249</i>	<i>0.509</i>	<i>0.279</i>	<i>0.010</i>	<i><0.001</i>	<i>0.002</i>	-	0.582
RB eqTRYP SMMC	<i>0.524</i>	<i>0.627</i>	<i>0.181</i>	<i>0.943</i>	<i>0.057</i>	<i>0.184</i>	<i>0.910</i>	<i>0.382</i>	<i>0.772</i>	<i>0.099</i>	<i>0.104</i>	<i>0.019</i>	<i>0.826</i>	<i>0.194</i>	<i>0.068</i>	<i>0.001</i>	<i>0.001</i>	-

Table 3.6: Correlation matrix of p values (italic) and rho values (bold) for Toluidine blue (TB), eqMCP-1 and eqTRYP-labelled mast cell count data. Significant correlations are highlighted in yellow. (eqMCP-1: equine Mast Cell Proteinase-1; eqTRYP: equine Tryptase; MMC: Mucosal mast cell; SMMC: Submucosal mast cell; RVC: Right ventral colon; RB: Rectal biopsy)

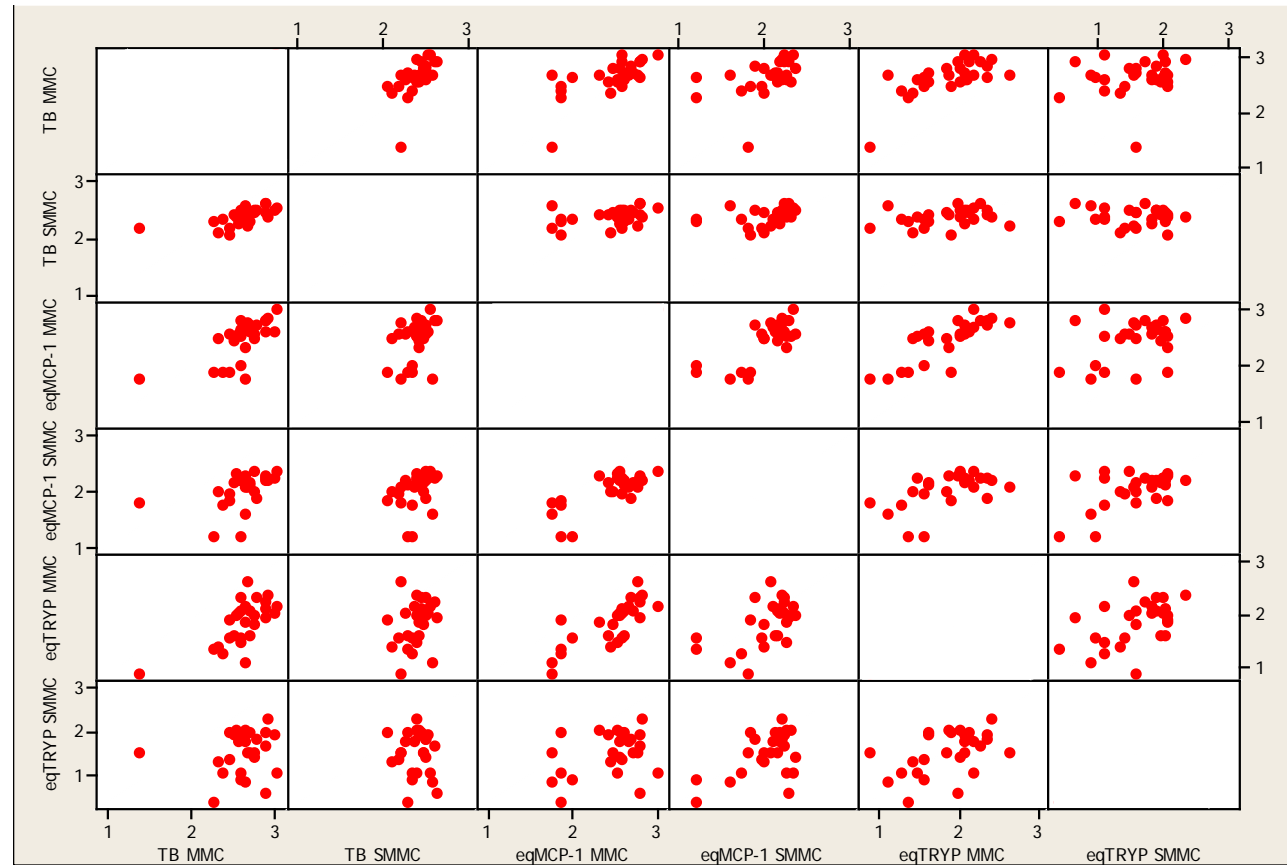


Figure 3.20: Matrix scatterplot of $\log_{10} + 1$ transformed counts for caecal Toluidine blue (TB), eqMCP-1 and eqTRYP MMC and SMMC. Cells expressed as MC per mm^2 . (eqMCP-1: equine Mast Cell Proteinase-1; eqTRYP: equine Tryptase; MMC: Mucosal mast cell; SMMC: Submucosal mast cell).

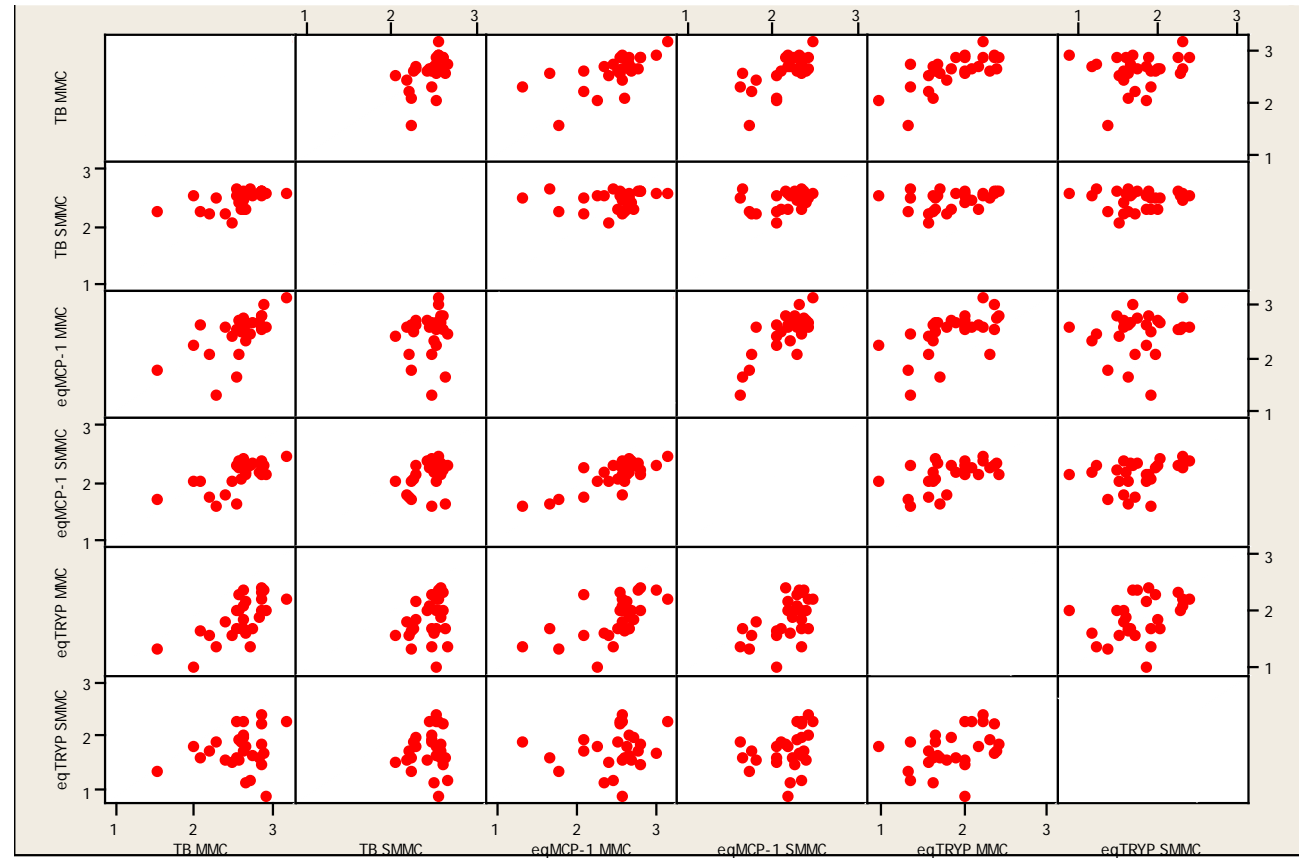


Figure 3.21: Matrix scatterplot of $\log_{10} + 1$ transformed counts for RVC Toluidine blue (TB), eqMCP-1 and eqTRYP MMC and SMMC. Cells expressed as MC per mm^2 . (eqMCP-1: equine Mast Cell Proteinase-1; eqTRYP: equine Tryptase; MMC: Mucosal mast cell; SMMC: Submucosal mast cell; RVC: Right ventral colon).

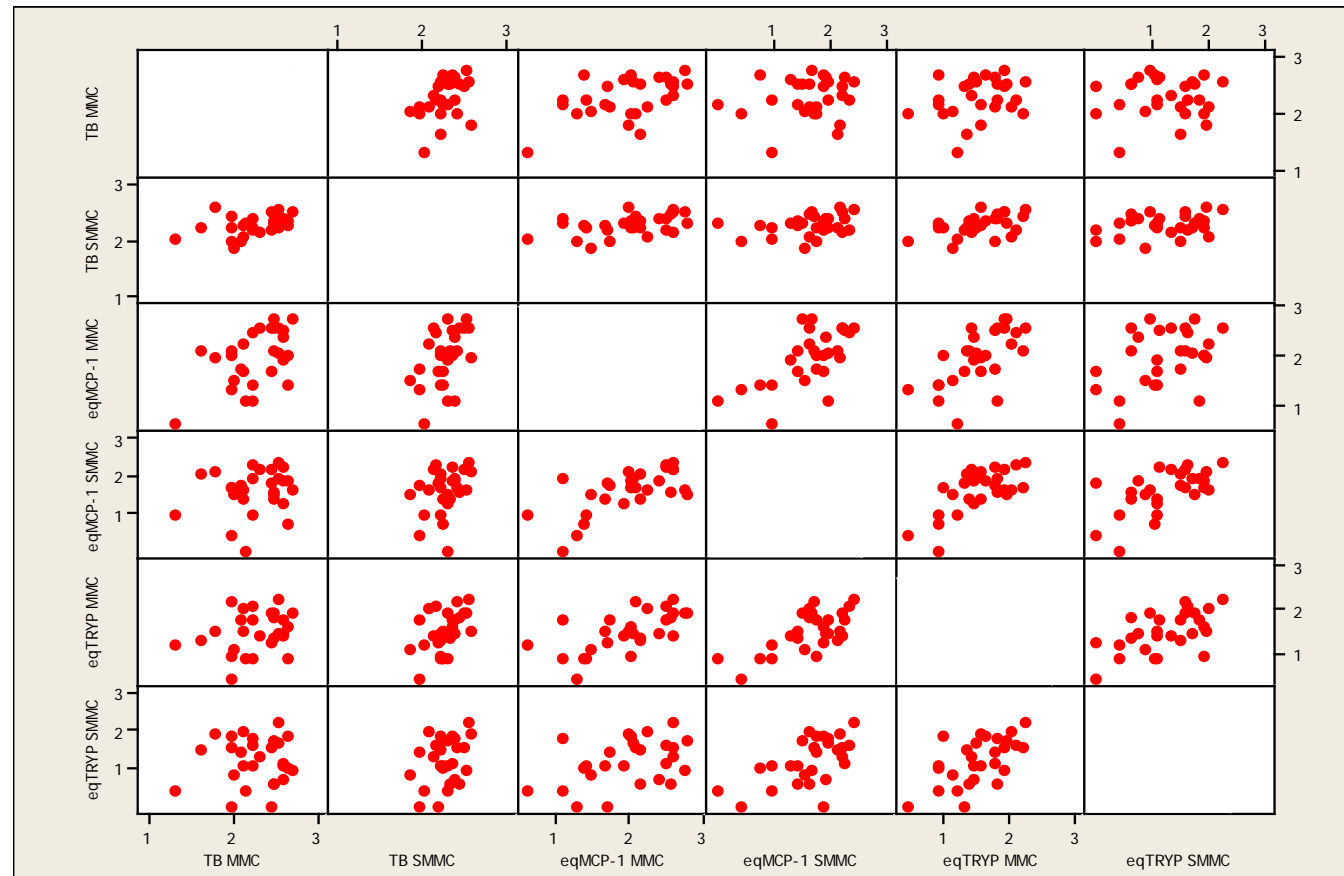


Figure 3.22: Matrix scatterplot of $\log_{10} + 1$ transformed counts for Rectal Toluidine blue (TB), eqMCP-1 and eqTRYP MMC and SMMC. Cells expressed as MC per mm^2 . (eqMCP-1: equine Mast Cell Proteinase-1; eqTRYP: equine Tryptase; MMC: Mucosal mast cell; SMMC: Submucosal mast cell).

3.3.3.6 Co-infection with *Anoplocephala perfoliata*

The presence of tapeworm was confirmed in nine of the 28 horses (32 %) either on post mortem by gross examination, paying particular attention to the caecal base and ileocaecal valve, or from FEC analysis. As evaluated in Chapter 2 and shown in Table 3.7, co-infection with *A. perfoliata* was associated with significantly higher TB mast cell counts in both the caecal mucosa and submucosa ($p=0.039$ and $p=0.004$), RVC mucosa and submucosa ($p=0.019$ and $p<0.001$) and RB mucosa and submucosa ($p=0.012$ and $p=0.046$). The presence or absence of *A. perfoliata* also had a significant effect on eqTRYP-labelled SMMC in the RVC ($p=0.037$) and eqMCP-1-labelled MMC in the rectum ($p=0.006$). Due to this, co-infection with *A. perfoliata* was added as a confounding variable for all analyses involving mast cell counts.

Mast Cell Population	Caecum (p-value)	RVC (p-value)	Rectum (p-value)
TB MMC	0.039	0.019	0.012
TB SMMC	0.004	<0.001	0.046
EqMCP-1 MMC	0.219	0.731	0.006
EqMCP-1 SMMC	0.623	0.961	0.658
EqTRYP MMC	0.403	0.268	0.085
EqTRYP SMMC	0.460	0.037	0.902

Table 3.7: Table of p-values for the significance of co-infection with *A. perfoliata* on TB, eqMCP-1 and eqTRYP-labelled MMC and SMMC in the caecum, RVC and rectum. Significant p-values are highlighted in yellow. (eqMCP-1: equine Mast Cell Proteinase-1; eqTRYP: equine Tryptase; TB: Toluidine Blue; MMC: Mucosal mast cell; SMMC: Submucosal mast cell; RVC: Right ventral colon).

3.3.3.7 Relationship between Mast Cell Counts and Cyathostomin Burden

Standard linear regression analyses were performed to investigate the relationship between $\log_{10}+1$ transformed mucosal and submucosal eqMCP-1- and eqTRYP-labelled mast cell counts and $\log_{10}+1$ transformed combined total mucosal burden (CTMB). Linear regression was also performed on the mast cell populations and $\log_{10}+1$ transformed combined total luminal burden (CTLB). There were no significant relationships between the CTMB and the caecal or RVC eqMCP-1- or eqTRYP-labelled mast cell counts (Table 3.8). There was however, a significant positive linear relationship between the eqMCP-1-labelled MMC in the rectal biopsy tissue and CTMB (Figure 3.23: $p=0.018$, $r^2=38.5\%$). There was also a significant positive linear relationship between the eqTRYP-labelled MMC in the rectal biopsies and CTMB (Figure 3.24: $p=0.048$, $r^2=18.4\%$). Similar significant positive relationships were seen in the rectal MMC with CTLB (eqMCP-1: $p=0.009$, $r^2=41.5$; eqTRYP: $p=0.007$, $r^2=28.9\%$). The relationships between CTMB or CTLB and proteinase-labelled MC populations in the Rectal biopsy submucosa were not statistically significant (Table 3.8).

Mast Cell Recruitment and Activation as Measures of Cyathostomin Burden

	Mast Cell Population	CTMB		CTLB	
		p-value	r ² (%)	p-value	r ² (%)
Caecum	eqMCP-1 MMC	0.972	0.0	0.910	0.0
	eqMCP-1 SMMC	0.718	0.0	0.703	0.0
	eqTRYP MMC	0.135	3.4	0.477	0.0
	eqTRYP SMMC	0.803	0.0	0.884	0.0
RVC	eqMCP-1 MMC	0.972	0.0	0.749	0.0
	eqMCP-1 SMMC	0.204	0.0	0.109	3.2
	eqTRYP MMC	0.211	2.8	0.305	0.7
	eqTRYP SMMC	0.485	13.7	0.630	12.8
RB	eqMCP-1 MMC	0.018	38.5	0.009	41.5
	eqMCP-1 SMMC	0.403	0.0	0.137	4.7
	eqTRYP MMC	0.048	18.4	0.007	28.9
	eqTRYP SMMC	0.119	2.2	0.125	1.9

Table 3.8: Table of p-values and r² values for the relationships between log10+1 transformed MMC and SMMC Toluidine blue (TB), eqMCP-1 and eqTRYP-labelled mast cell counts and log10+1 transformed combined total mucosal burden (CTMB) or combined total luminal burden (CTLB). Significant p-values are highlighted in yellow. (eqMCP-1: equine Mast Cell Proteinase-1; eqTRYP: equine Tryptase; MMC: Mucosal mast cell; SMMC: Submucosal mast cell; RVC: Right ventral colon. RB: Rectal biopsy).

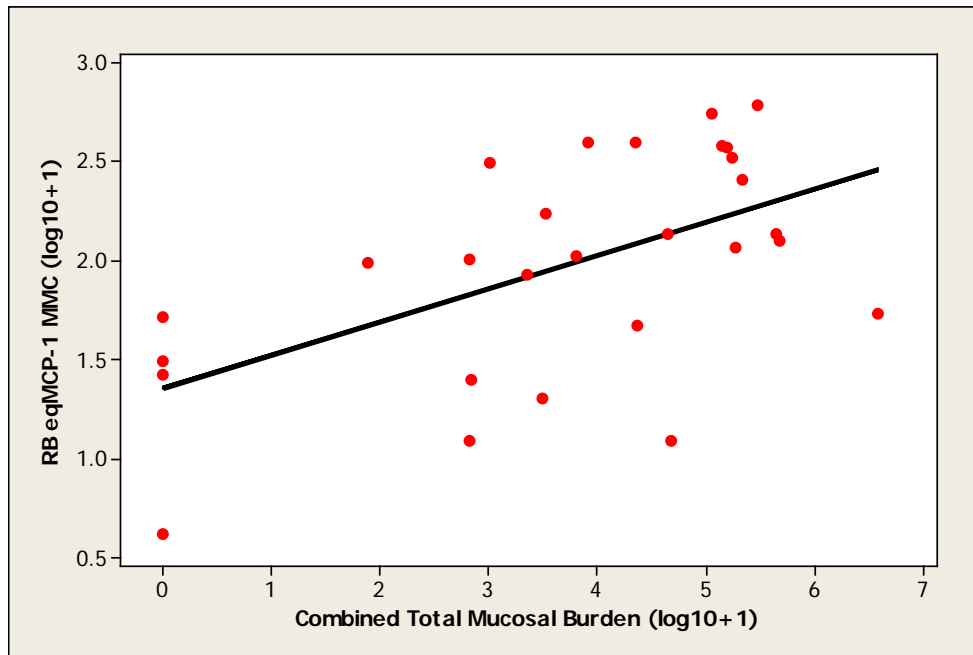


Figure 3.23: Relationship between log10+1 transformed CTMB (x-axis) and RB eqMCP-1 MMC (MC/mm²) (y-axis), $p=0.018$, $r^2=38.5\%$. (eqMCP-1: equine Mast Cell Proteinase-1; MMC: Mucosal mast cell; CTMB: Combined Total Mucosal Burden; RB: Rectal biopsy).

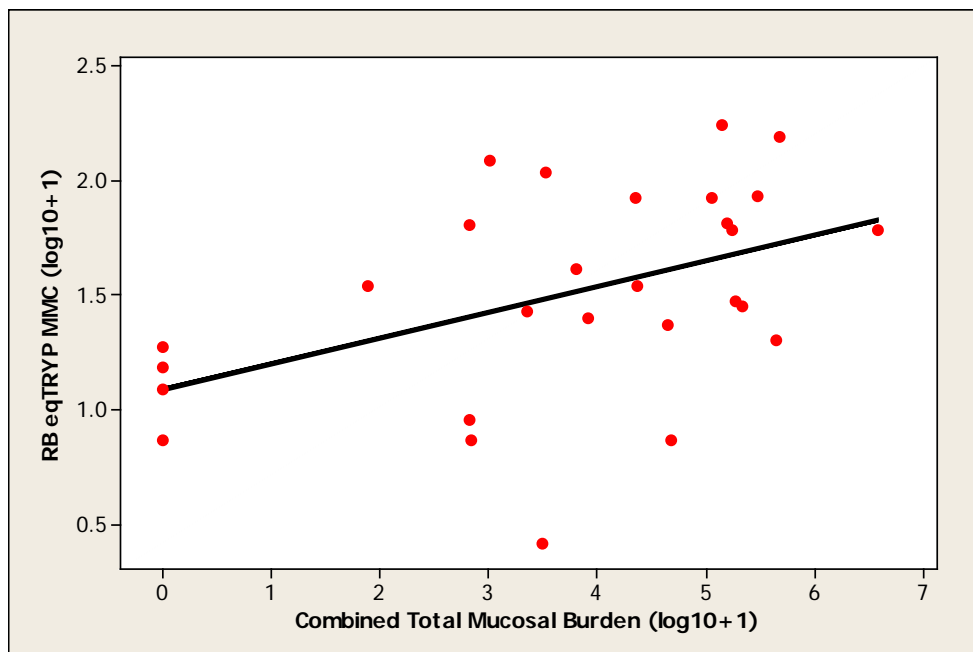


Figure 3.24: Relationship between log10+1 transformed CTMB (x-axis) and RB eqTRYF MMC (MC/mm²) (y-axis), $p=0.048$, $r^2=18.4\%$. (eqTRYF: equine Tryptase; MMC: Mucosal mast cell; CTMB: Combined Total Mucosal Burden; RB: Rectal biopsy).

3.3.3.8 Serum eqMCP-1 ELISA results

The mean results for the serum eqMCP-1 ELISA from the two different collection sites (Local [L] or Peripheral [P]), where available, and the two different storage conditions (-20 °C and -80 °C) are shown in Table 7.5 along with the standard error of the mean (SEM). Where possible samples were run on the same day, with the aim of minimising the effect of the high inter-assay variation. ELISA results for the different storage conditions were compared to assess stability of the proteinases and determine optimal storage conditions. Peripheral and local serum results were compared to determine whether peripherally sourced serum was representative of the proteinase concentrations from serum obtained from a vascular site local to cyathostomin infection i.e. the colonic vein. The serum eqMCP-1 values are displayed graphically in the barchart, Figure 3.25. .

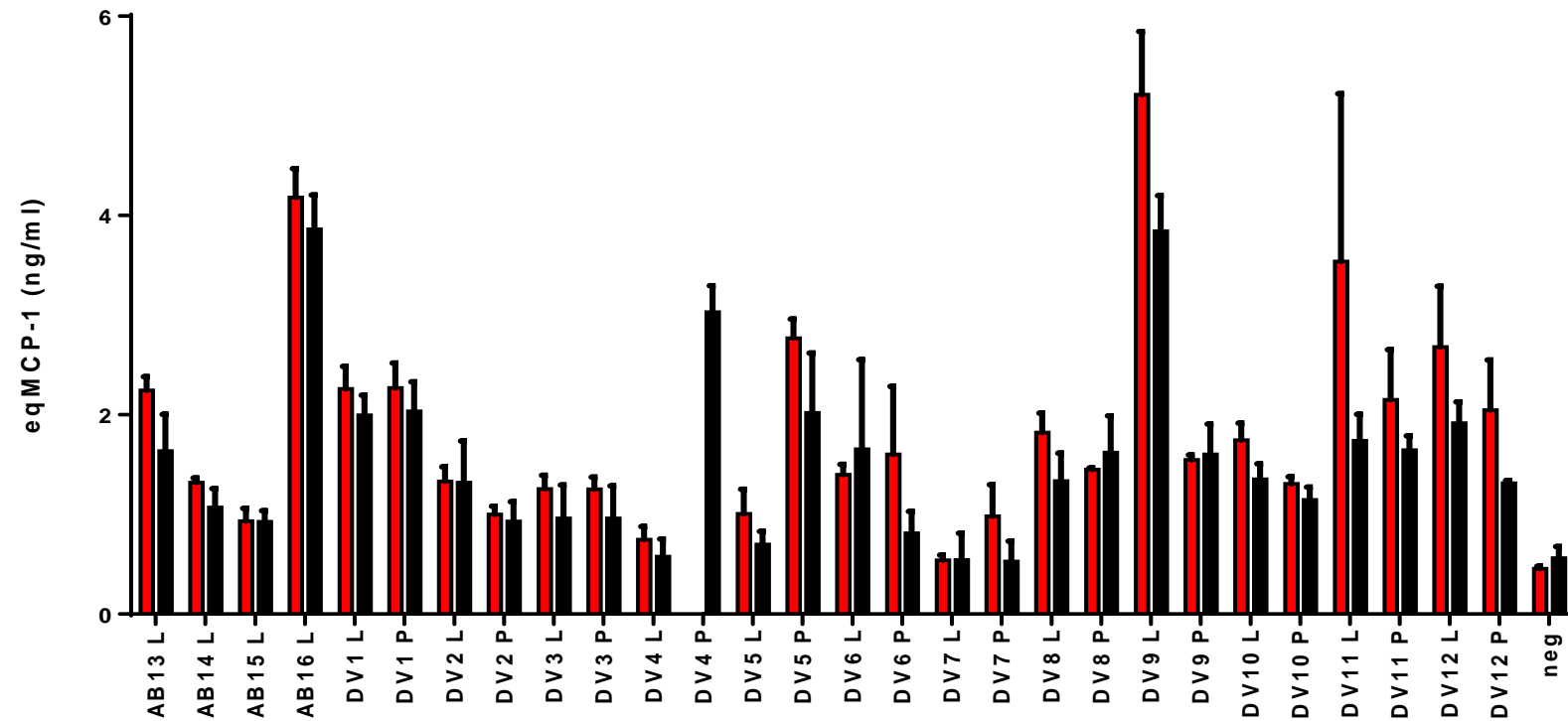


Figure 3.25: Barchart of eqMCP-1 concentrations of serum samples stored at -20 °C (red) and -80 °C (black). Error bars show standard error of the mean. (eqMCP-1: equine Mast Cell Proteinase-1; neg: serum from cyathostomin-negative ponies).

The median eqMCP-1 concentrations for local and peripheral serum samples were 1.75 ng/ml and 1.55 ng/ml, respectively, and these were not significantly different from one another (Figure 3.27A: $p=0.288$). However, no significant correlation was observed between the eqMCP-1 levels in the serum collected from the local or peripheral sites (Figure 3.26A: $p=0.203$, $\rho=0.418$), indicating that within each individual animal concentrations of eqMCP-1 in one site were not associated with concentrations in the other site (Figure 3.27B). In addition, considering the relatively small range of eqMCP-1 concentration in the samples from both sites (0.5 - 5.21 ng/ml), the limits of the agreement between sample sites (limits of agreement: 0.402 ± 1.33), are clinically significant.

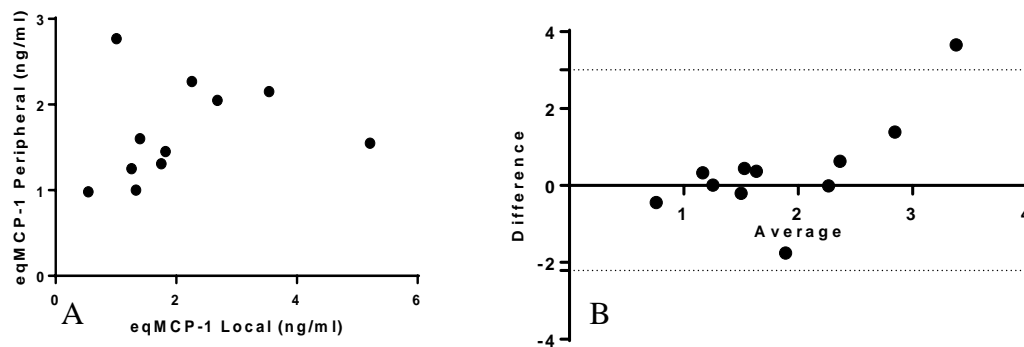


Figure 3.26: A: Scatterplot of eqMCP-1 concentrations from local (x-axis) and peripheral (y-axis) serum ($p=0.203$, $\rho=0.418$). B: Bland-Altman plot of the average of the local and peripheral serum eqMCP-1 measures (x-axis) vs. the difference of the local and peripheral serum eqMCP-1 measures (y-axis), bias= 0.402 , sd of bias= 1.33 . Upper and lower 95% limits of agreement are indicated by the dotted lines. (eqMCP-1: equine Mast Cell Proteinase-1).

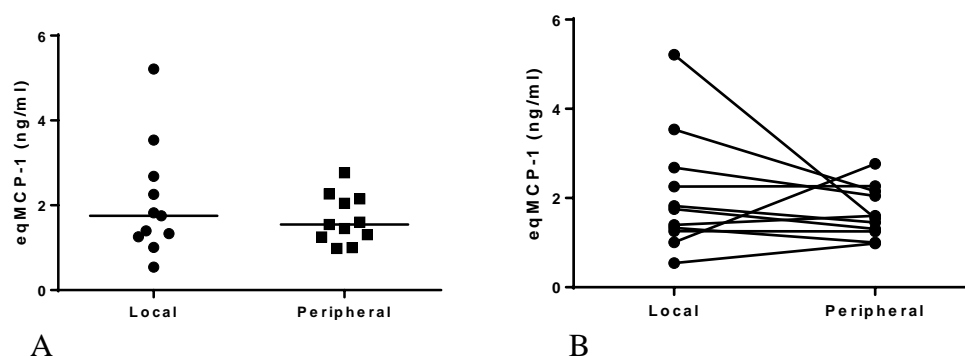


Figure 3.27: A: Individual value plot of eqMCP-1 serum concentrations (ng/ml) from local and peripheral sites, $p=0.288$ (Test: Wilcoxon signed rank test). The non-axis horizontal line indicates the median. (Test: Wilcoxon signed rank test) B: Graph of individual values of eqMCP-1 serum concentrations (ng/ml) from local and peripheral sources with lines connecting the values for each horse. (eqMCP-1: equine Mast Cell Proteinase-1).

3.3.3.9 Serum eqTRYP ELISA

3.3.3.9.1 ELISA results

The mean results for the serum eqTRYP ELISA from the different sites where available (Local, L or Peripheral, P) and the two different storage conditions (-20° C and -80 °C) are shown in Table 7.6 along with the standard error of the mean (SEM). Samples were run on the same day where possible. The serum eqTRYP concentrations are displayed graphically in the barchart, Figure 3.28.

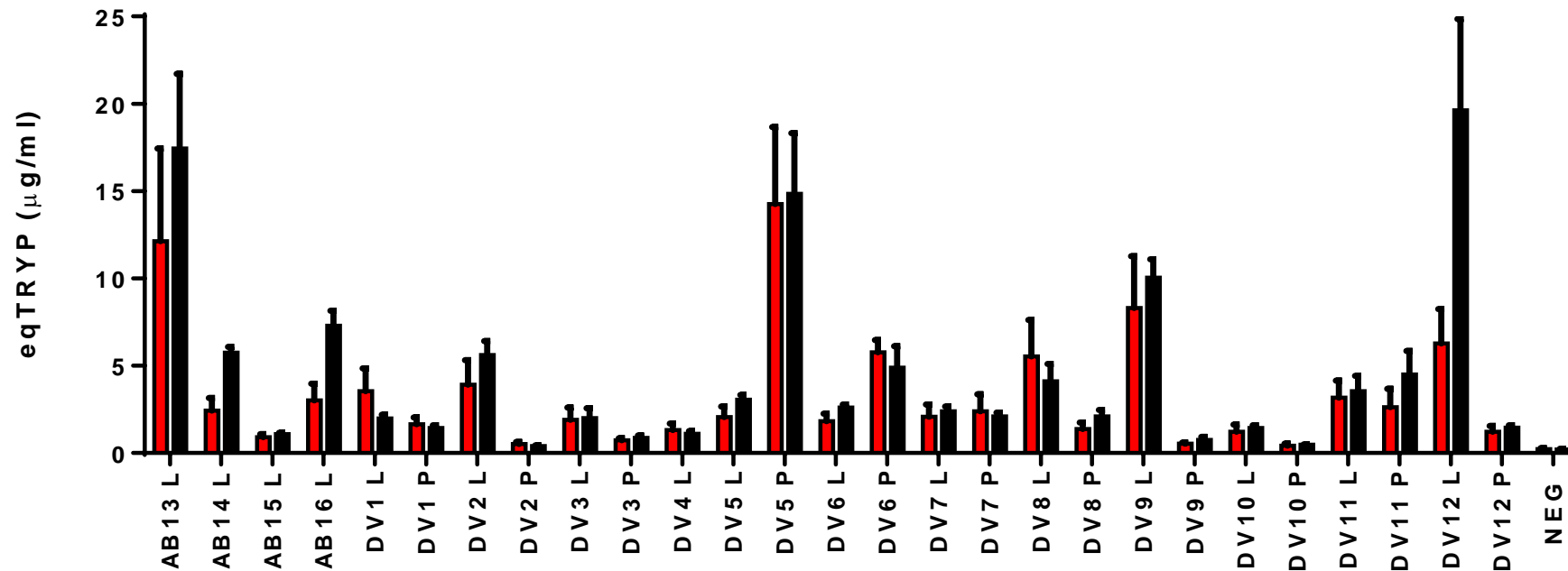


Figure 3.28: Barchart of eqTRY P concentrations of serum samples stored at -20 °C (red) and -80 °C (black). Error bars show standard error of the mean. (eqTRY P: equine Tryptase; P: Peripheral; L: Local; NEG: serum from cyathostomin-negative ponies).

As was observed with the eqMCP-1 ELISA, there was no significant correlation between the eqTRYP levels the-serum from the local or peripheral sampling sites, Figure 3.29A ($p=0.539$, $\rho=-0.210$). In addition, the limits of agreement are clinically significant (-0.759 ± 5.282) and the variability is inconsistent; as the average increases the magnitude of the differences between the methods tends to increase and the scatter around the bias line is greater (Figure 3.29B). In a similar finding to the eqMCP-1 ELISA, there was no significant difference in eqTRYP concentrations between the sampling sites. Neither site demonstrated significantly greater eqTRYP concentrations, Figure 3.30 ($p=0.240$). The median eqTRYP concentration for the local serum samples was $3.16 \mu\text{g/ml}$ and $1.37 \mu\text{g/ml}$ for the peripheral serum samples.

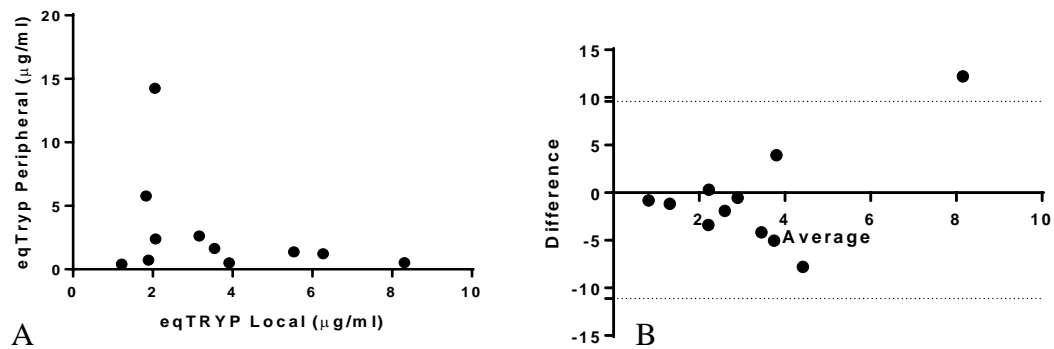


Figure 3.29: A: Scatterplot of eqTRYP concentrations from local (x-axis) and peripheral (y-axis) serum ($p=0.539$, $\rho=-0.210$). B: Bland-Altman plot of the average of the local and peripheral serum eqTRYP measures (x-axis) vs. the difference of the local and peripheral serum eqTRYP measures (y-axis), bias= -0.759 , sd of bias= 5.282 . Upper and lower 95% limits of agreement are indicated by the dotted lines. (eqTRYP: equine Tryptase).

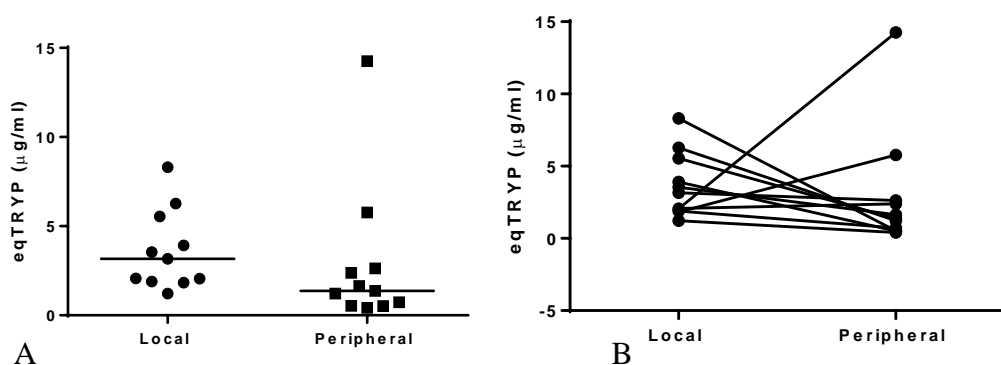


Figure 3.30: A: Individual value plot eqTRYP serum concentration ($\mu\text{g/ml}$) from local and peripheral sites, $p=0.240$. The non-axis horizontal line indicates the median (Test: Wilcoxon signed rank test) B: Graph of individual values of eqTRYP serum concentrations ($\mu\text{g/ml}$) from local and peripheral sources with lines connecting the values for each horse. (eqTRYP: equine Tryptase).

3.3.3.10 Serum Concentrations of eqMCP-1 and eqTRYP

The concentrations of eqMCP-1 and eqTRYP in local serum samples were significantly positively correlated, Figure 3.31A ($p=0.006$, $\rho=0.665$). In contrast, concentrations of eqMCP-1 and eqTRYP in peripheral serum did not significantly correlate, Figure 3.31B ($p=0.076$, $\rho=0.564$).

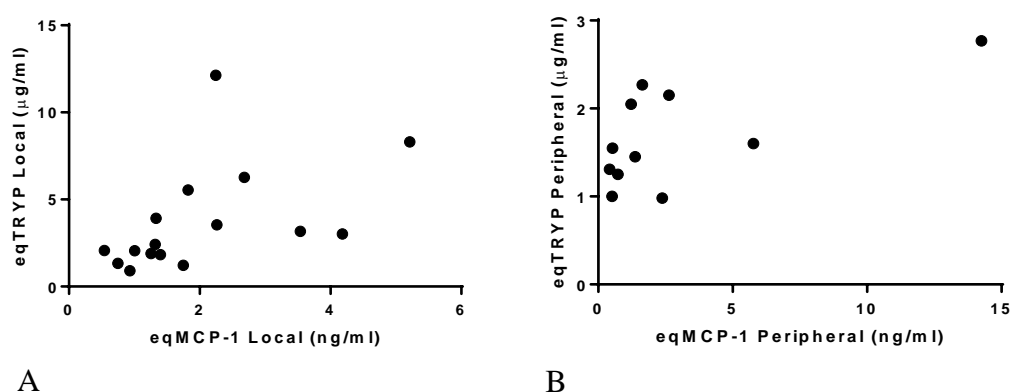


Figure 3.31 A: Scatterplot of local serum results eqMCP-1 (ng/ml) (x-axis) and eqTRYP (μg/ml) (y-axis) serum ($p=0.006$, $\rho=0.665$) (eqMCP-1: equine Mast Cell Proteinase-1; eqTRYP: equine Tryptase). B: Scatterplot of peripheral serum results eqMCP-1 (ng/ml) (x-axis) and eqTRYP (μg/ml) (y-axis) serum ($p=0.076$, $\rho=0.564$) (eqMCP-1: equine Mast Cell Proteinase-1; eqTRYP: equine Tryptase).

3.3.3.10.1 Relationship Serum Concentration of eqMCP-1 and eqTRYP with Mast Cell Counts

The Spearman rank test was used to calculate p and ρ values for the correlations between the MMC and SMMC in the caecum, RVC and RB with the local (Table 3.9) and peripheral (Table 3.10) serum eqMCP-1 and eqTRYP concentrations. There were no significant correlations between the MMC and SMMC in the caecum, RVC and RB with local serum eqMCP-1 or eqTRYP levels (Table 3.9). Similarly, there were no significant correlations between the MMC and SMMC in the caecum, RVC and RB with peripheral serum eqMCP-1 or eqTRYP levels (Table 3.10).

Mast Cell Recruitment and Activation as Measures of Cyathostomin Burden

	Local eqMCP-1 conc	Local eqMCP-1 conc	Local eqTRYP conc	Local eqTRYP conc
Caecal TB MMC	0.065	0.472	0.093	0.434
Caecal TB SMMC	0.673	0.115	0.746	0.088
Caecal eqMCP-1 MMC	0.520	0.174	0.294	0.280
Caecal eqMCP-1 SMMC	1.000	0.000	0.534	0.168
Caecal eqTRYP MMC	0.456	0.200	0.477	0.191
Caecal eqTRYP SMMC	0.991	-0.003	0.498	0.183
RVC TB MMC	0.064	0.477	0.120	0.406
RVC TB SMMC	0.415	0.219	0.212	0.330
RVC eqMCP-1 MMC	0.891	0.038	0.908	-0.032
RVC eqMCP-1 SMMC	0.538	0.166	0.110	0.415
RVC eqTRYP MMC	0.064	0.474	0.072	0.461
RVC eqTRYP SMMC	0.291	0.281	0.162	0.367
RB TB MMC	0.119	0.406	0.117	0.408
RB TB SMMC	0.204	-0.335	0.755	-0.085
RB eqMCP-1 MMC	0.068	0.468	0.083	0.446
RB eqMCP-1 SMMC	0.527	0.171	0.421	0.216
RB eqTRYP MMC	0.896	0.035	0.288	0.283
RB eqTRYP SMMC	0.753	0.086	0.363	0.244

Table 3.9: Table of p and rho values for correlations of local serum ELISA eqMCP-1 and eqTRYP concentrations with mast cell counts. (Test: Spearman rank) (eqMCP-1: equine Mast Cell Proteinase-1; eqTRYP: equine Tryptase; L: Local; MMC: Mucosal mast cell; SMMC: Submucosal mast cell; RVC: Right ventral colon; RB: Rectal biopsy).

	Peripheral eqMCP-1 conc	Peripheral eqMCP-1 conc	Peripheral eqTRYP conc	Peripheral eqTRYP conc
Caecal TB MMC	0.649	-0.155	0.392	-0.287
Caecal TB SMMC	0.503	-0.227	0.694	0.136
Caecal eqMCP-1 MMC	0.755	-0.109	0.451	-0.255
Caecal eqMCP-1 SMMC	0.989	-0.009	0.356	0.309
Caecal eqTRYP MMC	0.341	-0.318	0.203	-0.418
Caecal eqTRYP SMMC	0.769	-0.100	0.719	0.123
RVC TB MMC	0.860	-0.064	0.356	-0.309
RVC TB SMMC	0.121	-0.500	0.214	-0.409
RVC eqMCP-1 MMC	0.451	0.255	0.776	0.100
RVC eqMCP-1 SMMC	0.749	-0.109	1.000	0.000
RVC eqTRYP MMC	0.821	0.077	0.811	-0.082
RVC eqTRYP SMMC	0.946	0.027	0.818	0.082
RB TB MMC	0.797	0.091	0.903	0.046
RB TB SMMC	0.386	-0.291	0.968	0.018
RB eqMCP-1 MMC	0.137	-0.482	0.066	-0.582
RB eqMCP-1 SMMC	0.079	-0.551	0.416	-0.273
RB eqTRYP MMC	0.179	-0.437	0.189	-0.428
RB eqTRYP SMMC	0.228	-0.396	0.098	-0.524

Table 3.10: Table of p and rho values for correlations of peripheral serum ELISA eqMCP-1 and eqTRYP concentrations with mast cell counts. (Test: Spearman rank) (eqMCP-1: equine Mast Cell Proteinase-1; eqTRYP: equine Tryptase; P: Peripheral; MMC: Mucosal mast cell; SMMC: Submucosal mast cell; RVC: Right ventral colon; RB: Rectal biopsy).

3.3.3.10.2 Serum Concentrations of eqMCP-1 and eqTRYP and Cyathostomin Burden

To investigate the relationship between cyathostomin burden and serum proteinase concentrations, linear regression analysis of log₁₀+1 transformed data, with *A. perfoliata* as a confounding variable, was explored. There was no significant positive relationship observed between local serum eqMCP-1 concentrations and the combined total mucosal burden (CTMB) (Figure 3.32A: $p=0.414$, $r^2=0.0\%$). Similarly, there was no significant positive relationship between local serum eqTRYP concentrations and the CTMB (Figure 3.32B: $p=0.321$, $r^2=0.0\%$). There was no significant positive relationship between CTMB and local serum eqMCP-1

(Figure 3.33A: $p=0.875$, $r^2=0.0\%$) or eqTRYP (Figure 3.33B: $p=0.113$, $r^2=6.0\%$) concentrations. In the case of peripheral serum proteinase (eqMCP-1 and eqTRYP) concentrations, all relationships with CTMB and CTLB were negative, only one of which was statistically significant. This statistically significant negative relationship was between peripheral serum eqMCP-1 concentrations and the combined total mucosal burden (CTMB) (Figure 3.34A: $p=0.019$, $r^2=44.5\%$). The relationship with eqTRYP and CTMB was not significant (Figure 3.34B: $p=0.150$, $r^2=19.6\%$). There was no significant relationship between CTLB and peripheral serum eqMCP-1 (Figure 3.35A: $p=0.137$, $r^2=14.7\%$) or eqTRYP (Figure 3.35B: $p=0.154$, $r^2=22.1\%$) concentrations.

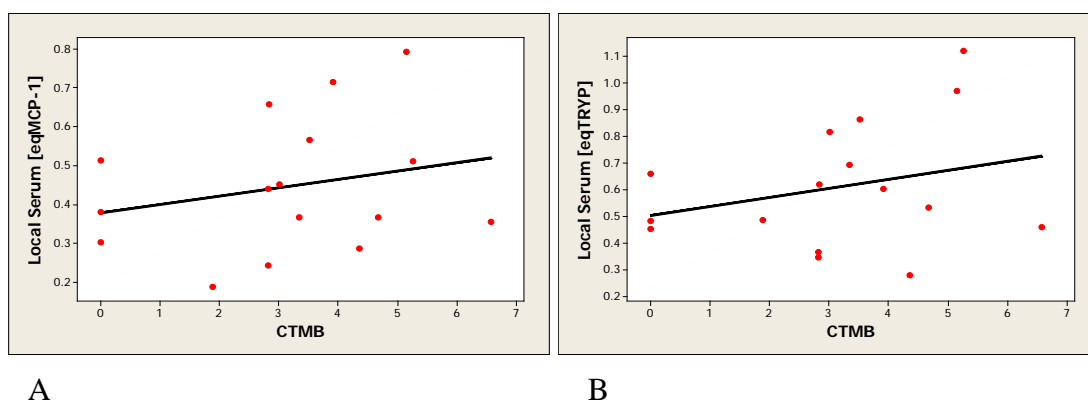


Figure 3.32: A: Relationship between log10+1 transformed CTMB (x-axis) and local serum eqMCP-1 concentrations (ng/ml) (y-axis), $p=0.414$, $r^2=0.0\%$. B: Relationship between log10+1 transformed CTMB (x-axis) and local serum eqTRYP concentrations ($\mu\text{g/ml}$) (y-axis), $p=0.321$, $r^2=0.0\%$ (eqMCP-1: equine Mast Cell Proteinase-1; CTMB: Combined Total Mucosal Burden)

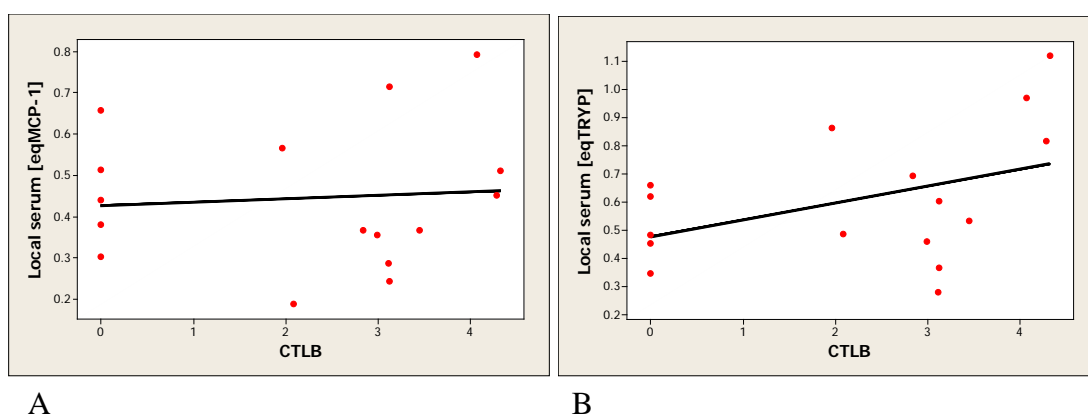


Figure 3.33: A: Relationship between log10+1 transformed CTLB (x-axis) and local serum eqMCP-1 concentrations (ng/ml) (y-axis), $p=0.875$, $r^2=0.0\%$. B: Relationship between log10+1 transformed CTLB (x-axis) and local serum eqTRYP concentrations ($\mu\text{g/ml}$) (y-axis), $p=0.113$, $r^2=6.0\%$ (eqMCP-1: equine Mast Cell Proteinase-1; CTLB: Combined Total Luminal Burden).

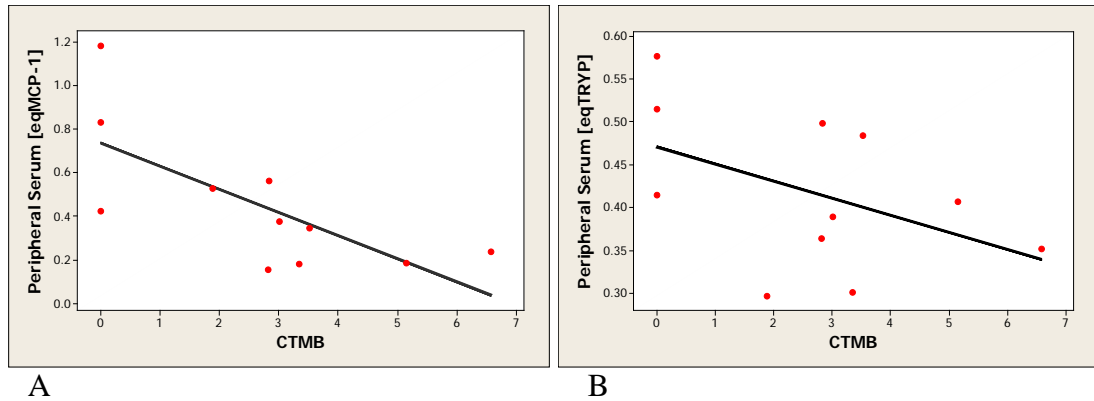


Figure 3.34: A: Relationship between $\log_{10}+1$ transformed CTMB (x-axis) and peripheral serum eqMCP-1 concentrations (ng/ml) (y-axis), $p=0.019$, $r^2=44.5\%$. B: Relationship between $\log_{10}+1$ transformed CTMB (x-axis) and peripheral serum eqTRYP concentrations (μg/ml) (y-axis), $p=0.150$, $r^2=19.6\%$ (eqMCP-1: equine Mast Cell Proteinase-1; CTMB: Combined Total Mucosal Burden).

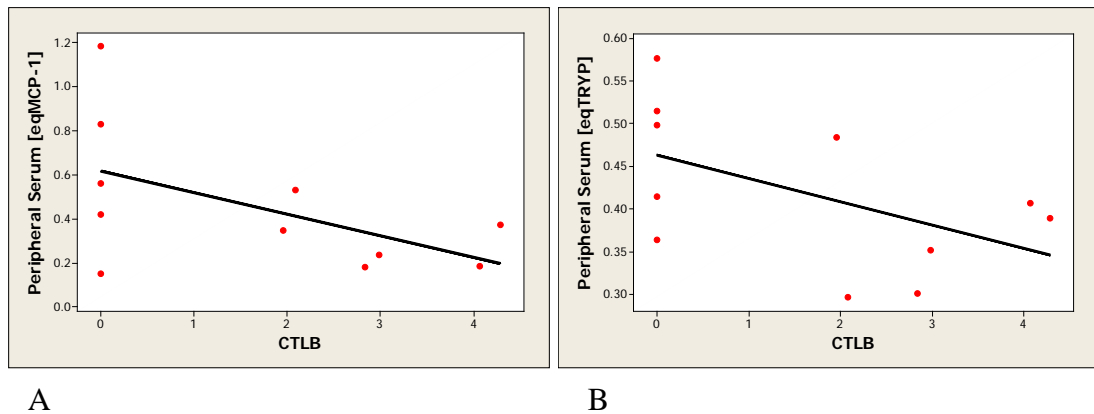


Figure 3.35: A: Relationship between $\log_{10}+1$ transformed CTLB (x-axis) and peripheral eqMCP-1 concentrations (ng/ml) (y-axis), $p=0.137$, $r^2=14.7\%$. B: Relationship between $\log_{10}+1$ transformed CTLB (x-axis) and peripheral serum eqTRYP concentrations (μg/ml) (y-axis), $p=0.154$, $r^2=22.1\%$ (eqMCP-1: equine Mast Cell Proteinase-1; CTLB: Combined Total Luminal Burden).

To investigate whether there was a significant difference in local serum eqTRYP and eqMCP-1 concentrations between horses with low and high cyathostomin burdens, all horses for which there were local serum samples (AB13, AB14, AB15, AB16 and DV1-DV12) were grouped according to their CTMB (Figure 3.36). These groupings were different to those described in Chapter 2 as there were no local serum values available for horses AB1-AB12. Group 1 (n=3) were cyathostomin-negative, Group 2 (n=4) had a range of encysted burdens of 75-680, Group 3 (n=4) ranged from 1,029-8,355 and Group 4 (n=5) had a range of 23,219 to 3,827,097 (Figure 3.36).

Boxplots of eqMCP-1 serum concentrations (Figure 3.37), and eqTRYP serum concentrations (Figure 3.38) separated by these groupings are shown below. Kruskal-Wallis analysis revealed no significant difference among groups in the case of either eqMCP-1 ($p=0.553$) or eqTRYP ($p=0.251$) concentrations measured in locally derived serum.

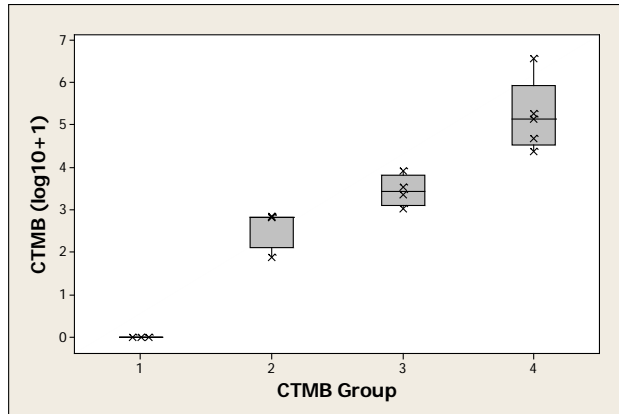


Figure 3.36: Boxplot of the 16 horses with serum samples divided into four groups according to combined total mucosal burden (CTMB). Group 1 (n=3) were cyathostomin-negative, Group 2 (n=4) mucosal burden range of 75- 680, Group 3 (n=4) ranged from 1,029 to 8,355 and Group 4 (n=5) had a range of 23,219 to 3,827,097.

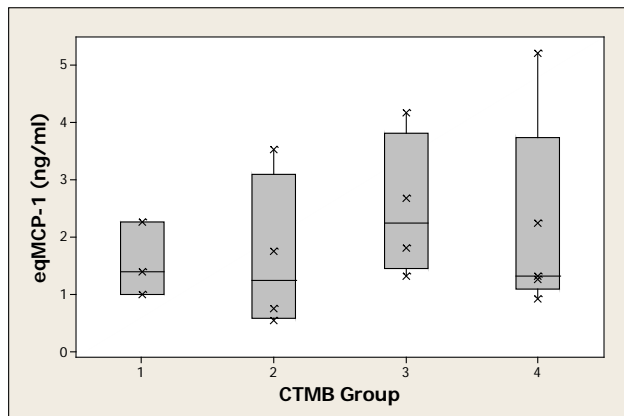


Figure 3.37: Local eqMCP-1 serum concentrations (ng/ml) of the 16 horses with serum samples divided into four groups according to combined total mucosal burden (CTMB). Kruskal-Wallis analysis revealed no significant difference in local serum eqMCP-1 concentration between groups ($p=0.553$). (eqMCP-1: equine Mast Cell Proteinase-1).

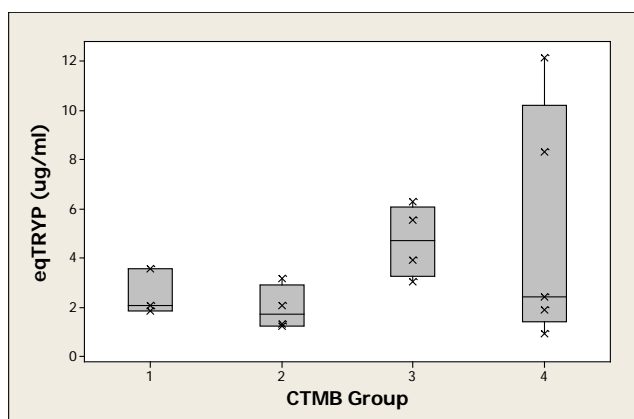


Figure 3.38: Local eqTRYP serum concentrations ($\mu\text{g/ml}$) of the 16 horses with serum samples divided into four groups according to combined total mucosal burden (CTMB). Kruskal-Wallis analysis revealed no significant difference in local serum eqTRYP concentration between groups ($p=0.251$). (eqTRYP: equine Tryptase).

3.3.3.11 Tissue Homogenate eqMCP-1 ELISA Analysis

The tissue homogenate ELISA was performed in duplicate for each sample and repeated on at least three occasions. Where possible samples were run on the same day. The eqMCP-1 concentration for each organ is shown in Table 7.7 with the standard error of the mean (SEM) and as a barchart in Figure 7.1. The median and range for each organ are shown in Table 3.11. The RVC had the highest median ($56.35 \mu\text{g/g}$) and the greatest range ($3.96 - 404.90 \mu\text{g/g}$).

	EqMCP-1 Caecum	EqMCP-1 RVC	EqMCP-1 RB
Median	35.78	56.35	26.51
Range	2.74 - 386.30	3.96 - 404.90	2.54 - 209.50

Table 3.11: Median and range eqMCP-1 tissue concentrations ($\mu\text{g/g}$) from the caecum, RVC and rectum of all the horses (AB1-16 and DV1-12). (eqMCP-1: equine Mast Cell Proteinase-1; RVC: Right ventral colon; RB: Rectal biopsy).

Table 3.12 shows the p and rho values for the correlations using the Spearman rank test in eqMCP-1 concentration between organs. There was a significant positive correlation between the eqMCP-1 concentrations in the three organs examined (caecum and RVC, $p<0.001$, $\rho=0.812$), (caecum and RB, $p=0.003$, $\rho=0.544$) (RVC and RB, $p<0.001$, $\rho=0.706$).

	Caecum eqMCP-1 ($\mu\text{g/g}$) p-value	Caecum eqMCP-1 ($\mu\text{g/g}$) Rho value	RVC eqMCP-1 ($\mu\text{g/g}$) p-value	RVC eqMCP-1 ($\mu\text{g/g}$) Rho value	RB eqMCP-1 ($\mu\text{g/g}$) p-value	RB eqMCP-1 ($\mu\text{g/g}$) Rho value
Caecum eqMCP1 ($\mu\text{g/g}$)	NA	NA	<0.001	0.812	0.003	0.544
RVC eqMCP1 ($\mu\text{g/g}$)	<0.001	0.812	NA	NA	<0.001	0.706
RB eqMCP1 ($\mu\text{g/g}$)	0.003	0.544	<0.001	0.706	NA	NA

Table 3.12: Table of p and rho values for correlations of tissue homogenate eqMCP-1 concentration ($\mu\text{g/g}$) between organs. Significant p-values are highlighted in yellow. (Test: Spearman rank) (eqMCP-1: equine Mast Cell Proteinase-1; RVC: Right ventral colon; RB: Rectal biopsy).

Table 3.13 shows correlations of eqMCP-1 tissue concentrations from the caecum, RVC and rectum of all horses (AB1-16 and DV1-12) with TB, eqMCP-1- and eqTRYP-labelled cell counts. Caecal eqMCP-1 concentrations were significantly positively correlated with the caecal TB MMC ($p=0.008$, $\rho=0.489$) and SMMC numbers ($p=0.008$, $\rho=0.496$). There were no significant correlations between the caecal eqMCP-1- or caecal eqTRYP-labelled mast cell populations and the caecal eqMCP-1 tissue concentrations. In the case of the RVC, tissue eqMCP-1 concentrations positively correlated significantly with the RVC TB MMC ($p=0.003$, $\rho=0.549$), RVC TB SMMC numbers ($p<0.001$, $\rho=0.702$) and the RVC eqTRYP-labelled MMC count ($p=0.014$, $\rho=0.459$) but not with the eqMCP-1-labelled counts. As opposed to the observations made with the caecal and RVC material, RB tissue eqMCP-1 ELISA concentrations did not correlate with the RB TB MMC and SMMC counts. However, there were significant positive correlations between the RB tissue eqMCP-1 concentrations and RB eqMCP-1 MMC ($p=0.002$, $\rho=0.564$) and

RB eqTRYP-labelled MMC ($p=0.011$, $\rho=0.471$) counts. The RB eqMCP-1 concentration also significantly positively correlated with the caecal eqMCP-1-labelled MMC ($p=0.016$, $\rho=0.450$) and eqTRYP-labelled MMC ($p=0.012$, $\rho=0.467$) counts, as well as the eqTRYP-labelled MMC counts in the RVC ($p=0.006$, $\rho=0.507$).

	Caecum eqMCP-1 ($\mu\text{g/g}$) p-value	Caecum eqMCP-1 ($\mu\text{g/g}$) Rho value	RVC eqMCP-1 ($\mu\text{g/g}$) p-value	RVC eqMCP-1 ($\mu\text{g/g}$) Rho value	RB eqMCP-1 ($\mu\text{g/g}$) p-value	RB eqMCP-1 ($\mu\text{g/g}$) Rho value
Caecal TB MMC	0.008	0.489	0.001	0.573	0.137	0.288
Caecal TB SMMC	0.008	0.496	0.011	0.476	0.347	0.184
Caecal eqMCP-1 MMC	0.087	0.330	0.081	0.336	0.016	0.450
Caecal eqMCP-1 SMMC	0.461	0.145	0.680	0.082	0.902	0.024
Caecal eqTRYP MMC	0.185	0.258	0.016	0.453	0.012	0.467
Caecal eqTRYP SMMC	0.845	0.039	0.453	0.148	1.00	0.000
RVC TB MMC	0.012	0.467	0.003	0.549	0.119	0.301
RVC TB SMMC	<0.001	0.677	<0.001	0.702	0.118	0.302
RVC eqMCP-1 MMC	0.421	0.158	0.386	0.170	0.438	0.152
RVC eqMCP-1 SMMC	0.320	0.195	0.318	0.196	0.791	-0.053
RVC eqTRYP MMC	0.058	0.362	0.014	0.459	0.006	0.507
RVC eqTRYP SMMC	0.250	-0.225	0.931	-0.017	0.979	-0.005
RB TB MMC	0.029	0.412	0.023	0.428	0.230	0.234
RB TB SMMC	0.150	0.280	0.094	0.323	0.095	0.322
RB eqMCP-1 MMC	0.002	0.567	<0.001	0.640	0.002	0.564
RB eqMCP-1 SMMC	0.517	0.128	0.295	0.205	0.082	0.334
RB eqTRYP MMC	0.036	0.398	0.008	0.494	0.011	0.471
RB eqTRYP SMMC	0.781	0.055	0.240	0.230	0.032	0.407

Table 3.13: Table of p and rho values for correlations of eqMCP-1 concentrations ($\mu\text{g/g}$) from the caecum, RVC and rectum of all horses (AB1-16 and DV1-12) with TB, eqMCP-1 and eqTRYP cell counts. Significant p-values are highlighted in yellow. (eqMCP-1: equine Mast Cell Proteinase-1; eqTRYP: equine Tryptase; TB: Toluidine Blue; MMC: Mucosal mast cell; SMMC: Submucosal mast cell; RVC: Right ventral colon; RB: Rectal biopsy).

3.3.3.12 Tissue Homogenate eqTRYP ELISA Analysis

The eqTRYP concentrations measured in tissue homogenate for each organ are shown in Table 7.8 with the SEM and as a barchart in Figure 7.2. The median and range of eqTRYP concentrations for each organ are shown in table 3.14. As was observed with the levels of eqMCP-1, the RVC had the highest median (56.87 µg/g) and the greatest range (9.08 - 371.40 µg/g) of eqTRYP concentrations.

	EqTRYP Caecum (µg/g)	EqTRYP RVC (µg/g)	EqTRYP RB (µg/g)
Median	46.47	56.87	30.56
Range	5.00 - 306.20	9.08 - 371.40	3.59 - 209.60

Table 3.14: Median and range eqTRYP tissue concentration (µg/g) from the caecum, RVC and rectum of all horses (AB1-16 and DV1-12). (eqTRYP: equine Tryptase; RVC: Right ventral colon; RB: Rectal biopsy).

	Caecum eqTRYP (µg/g) p-value	Caecum eqTRYP (µg/g) Rho value	RVC eqTRYP (µg/g) p-value	RVC eqTRYP (g/g) Rho value	RB eqTRYP (µg/g) p-value	RB eqTRYP (µg/g) Rho value
Caecum eqTRYP (µg/g)	NA	NA	0.003	0.553	0.011	0.480
RVC eqTRYP (µg/g)	0.003	0.553	NA	NA	0.001	0.616
RB eqTRYP (µg/g)	0.011	0.480	0.001	0.616	NA	NA

Table 3.15: Table of p and rho values for correlations of tissue homogenate eqTRYP concentrations (µg/g) between organs. Significant p-values are highlighted in yellow (eqTRYP: equine Tryptase; RVC: Right ventral colon; RB: Rectal biopsy).

There was a significant positive correlation between the eqTRYP concentrations measured in the three organs examined (caecum and RVC, $p=0.003$, $\rho=0.553$), (caecum and RB, $p=0.011$, $\rho=0.480$) (RVC and RB, $p=0.001$, $\rho=0.616$) (Table 3.15). Caecal tissue eqTRYP concentrations measured positively correlated with the

caecal TB MMC ($p=0.016$, $\rho=0.451$) and SMMC population ($p=0.005$, $\rho=0.522$) counts (Table 3.16). There was also a significant positive correlation observed between the caecal eqMCP-1-labelled mast cell population counts and the caecal eqTRYP tissue concentration ($p=0.013$, $\rho=0.464$). In the case of the RVC, tissue eqMCP-1 concentrations measured positively correlated with the TB MMC ($p<0.001$, $\rho=0.697$) and SMMC populations ($p<0.001$, $\rho=0.682$). There was also a significant positive correlation with the RVC eqMCP-1-labelled SMMC ($p=0.050$, $\rho=0.374$) and the RVC eqTRYP-labelled MMC counts ($p<0.001$, $\rho=0.731$). Unlike in the caecum and RVC, RB tissue eqTRYP concentrations measured did not correlate with the RB TB MMC counts. However, there were significant positive correlations observed (Table 3.16) between the RB eqTRYP concentrations measured and all other rectal mast cell count parameters (RB TB MMC, RB TB SMMC, RB eqMCP-1 MMC, RB eqMCP-1 SMMC, RB eqTRYP MMC and RB eqTRYP SMMC). The RB eqTRYP concentration measured also significantly positively correlated with the caecum and RVC TB MMC ($p=0.044$, $\rho=0.384$: $p=0.017$, $\rho=0.448$ respectively), the caecum eqMCP-1-labelled MMC ($p<0.001$, $\rho=0.631$) and eqTRYP MMC ($p=0.002$, $\rho=0.581$) counts and the eqTRYP-labelled MMC counts in the RVC ($p=0.002$, $\rho=0.573$).

Mast Cell Recruitment and Activation as Measures of Cyathostomin Burden

	Caecum eqTRYP (µg/g) p-value	Caecum eqTRYP (µg/g) Rho value	RVC eqTRYP (µg/g) p-value	RVC eqTRYP (µg/g) Rho value	RB eqTRYP (µg/g) p-value	RB eqTRYP (µg/g) Rho value
Caecal TB MMC	0.016	0.451	<0.001	0.654	0.044	0.384
Caecal TB SMMC	0.005	0.522	<0.001	0.639	0.018	0.448
Caecal eqMCP-1 MMC	0.013	0.464	0.001	0.596	<0.001	0.631
Caecal eqMCP-1 SMMC	0.124	0.298	0.020	0.438	0.013	0.462
Caecal eqTRYP MMC	0.066	0.353	<0.001	0.640	0.001	0.581
Caecal eqTRYP SMMC	0.932	-0.017	0.636	0.094	0.865	-0.034
RVC TB MMC	0.014	0.459	<0.001	0.697	0.017	0.448
RVC TB SMMC	0.017	0.449	<0.001	0.682	0.050	0.374
RVC eqMCP-1 MMC	0.088	0.329	0.175	0.263	0.108	0.310
RVC eqMCP-1 SMMC	0.083	0.334	0.050	0.374	0.148	0.281
RVC eqTRYP MMC	0.034	0.401	<0.001	0.627	0.002	0.573
RVC eqTRYP SMMC	0.702	-0.076	0.632	0.095	0.986	0.004
RB TB MMC	0.264	0.219	0.013	0.464	0.409	0.163
RB TB SMMC	0.088	0.329	0.009	0.483	<0.001	0.650
RB eqMCP-1 MMC	0.008	0.492	<0.001	0.731	<0.001	0.620
RB eqMCP-1 SMMC	0.703	0.075	0.075	0.342	0.041	0.388
RB eqTRYP MMC	0.283	0.210	0.005	0.517	0.012	0.467
RB eqTRYP SMMC	0.849	0.038	0.172	0.266	0.010	0.478

Table 3.16: Table of p and rho values for correlations of eqTRYP tissue concentration (µg/g) from the caecum, RVC and rectum of horses (AB1-16 and DV1-12) with TB, eqMCP-1 and eqTRYP cell counts. Significant p-values are highlighted in yellow (eqMCP-1: equine Mast Cell Proteinase-1; eqTRYP: equine Trypsin; TB: Toluidine Blue; MMC: Mucosal mast cell; SMMC: Submucosal mast cell; RVC: Right ventral colon; RB: Rectal biopsy).

3.3.4 Analysis of Equine Tissue eqMCP-1 and eqTRYP Concentrations Measured by ELISA

3.3.4.1 Comparison of eqMCP-1 and eqTRYP Concentrations between each Organ

Within each organ, the eqMCP-1 and eqTRYP concentrations measured significantly positively correlated (caecum; $p=0.002$, $\rho=0.563$. RVC; $p<0.001$, $\rho=0.790$. RB; $p=0.002$, $\rho=0.577$) (Table 3.17). Figure 3.39A demonstrates the relationship in the caecum ($p=0.002$, $\rho=0.563$), Figure 3.39B shows the RVC ($p<0.001$, $\rho=0.790$) and Figure 3.39C shows the rectum (RB, $p=0.002$, $\rho=0.577$). There was no significant difference between the levels of the two proteinase concentrations measured in the caecum (Figure 3.40A, $p=0.800$), the RVC (Figure 3.40B, $p=0.255$) or in the rectum (Figure 3.40C, $p=0.157$). The RVC eqTRYP concentrations measured correlated significantly with the caecal eqMCP-1 concentrations ($p<0.001$, $\rho=0.651$) and the RB eqMCP-1 concentrations ($p=0.002$, $\rho=0.577$) (Table 3.17).

	Caecum eqMCP-1 ($\mu\text{g/g}$) p-value	Caecum eqMCP-1 ($\mu\text{g/g}$) Rho value	RVC eqMCP-1 ($\mu\text{g/g}$) p-value	RVC eqMCP-1 ($\mu\text{g/g}$) Rho value	RB eqMCP-1 ($\mu\text{g/g}$) p-value	RB eqMCP-1 ($\mu\text{g/g}$) Rho value
Caecum eqTRYP ($\mu\text{g/g}$)	0.002	0.563	0.102	0.316	0.609	0.101
RVC eqTRYP ($\mu\text{g/g}$)	<0.001	0.651	<0.001	0.790	0.003	0.555
RB eqTRYP ($\mu\text{g/g}$)	0.145	0.284	0.066	0.354	0.002	0.577

Table 3.17: Table of p and rho values for correlations of tissue homogenate eqMCP-1 concentration ($\mu\text{g/g}$) with eqTRYP concentration ($\mu\text{g/g}$). Significant p-values are highlighted in yellow. (eqMCP-1: equine Mast Cell Proteinase-1; eqTRYP: equine Tryptase; RVC: Right ventral colon; RB: Rectal biopsy).

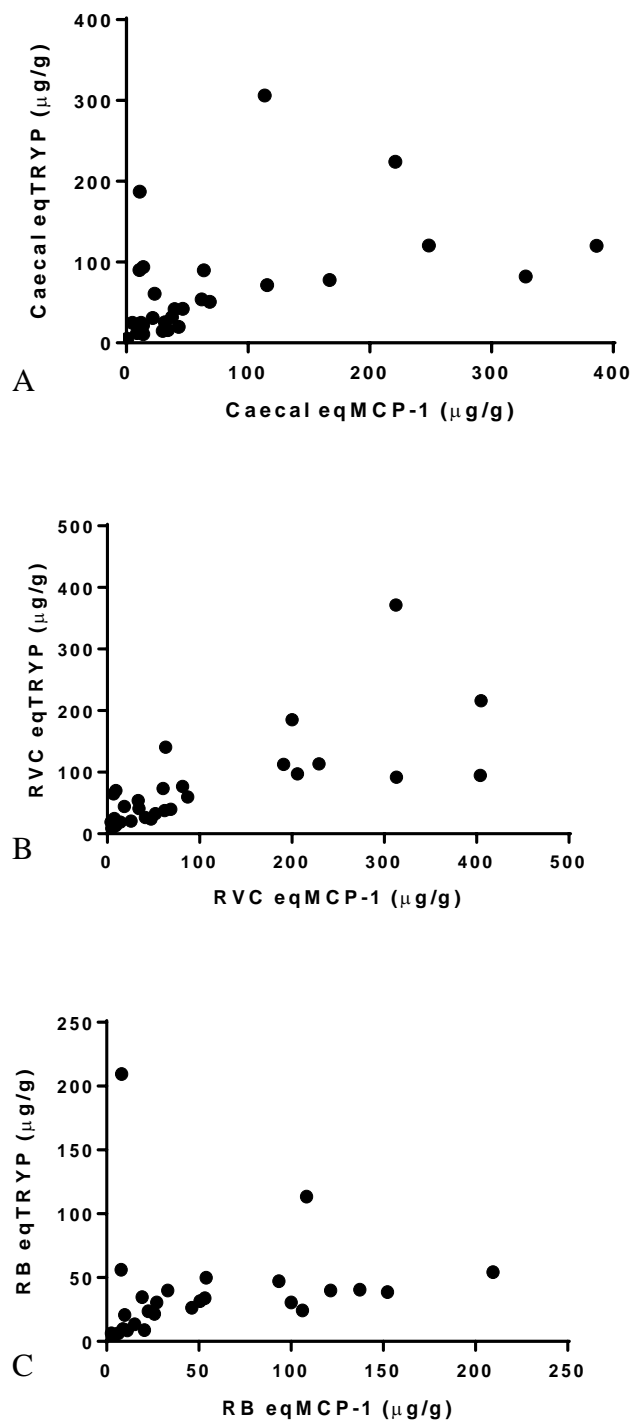


Figure 3.39: Scatterplot of eqMCP-1(x-axis) and eqTRYP (y-axis) tissue concentration ($\mu\text{g/g}$). There was a significant positive correlation between eqMCP-1 and eqTRYP concentrations in the; Caecum: ($p=0.002$, $\rho=0.563$); B: RVC: ($p<0.001$, $\rho=0.790$); C: Rectum: ($p=0.001$, $\rho=0.577$). Note different y-axis scales. (eqMCP-1: equine Mast Cell Proteinase-1; eqTRYP: equine Tryptase; RVC: Right ventral colon; RB: Rectal biopsy).

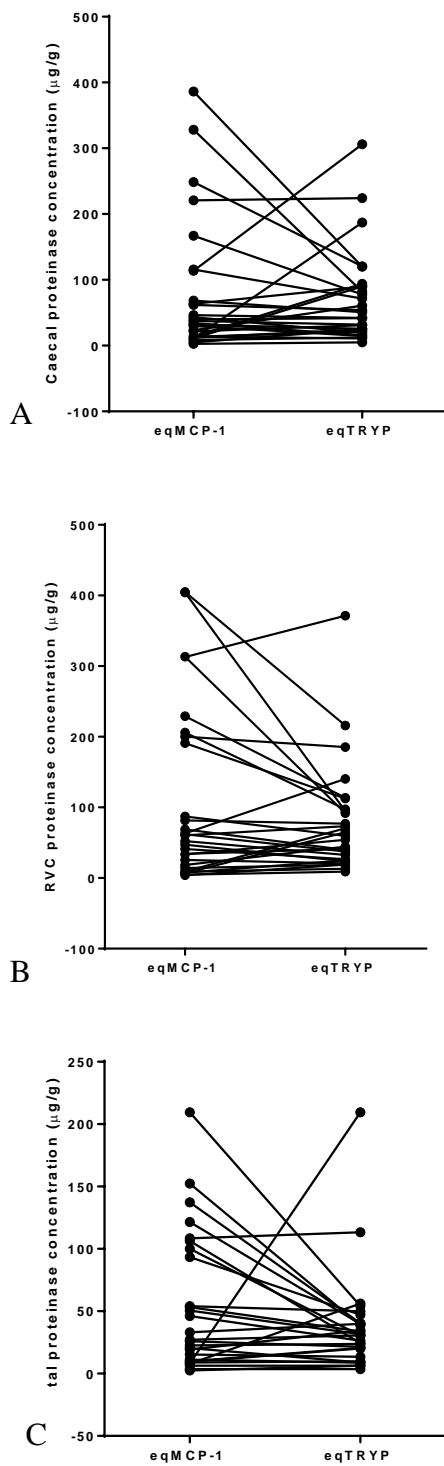


Figure 3.40: Graphs of individual horse eqMCP-1 and eqTRYP tissue concentrations ($\mu\text{g/g}$) with lines connecting the values for each horse. There was no significant difference between proteinase concentrations in the; A: Caecum: $p=0.800$; B: RVC: $p=0.255$; C: Rectum: $p=0.157$. Note different y-axis scales. (Test: Wilcoxon signed rank test). (eqMCP-1: equine Mast Cell Proteinase-1; eqTRYP: equine Trypsin; RVC: Right ventral colon).

3.3.4.2 The Relationship of eqMCP-1 and eqTRYP Concentrations Measured in Tissue with those Measured in Serum

The relationship between concentrations of eqTRYP and eqMCP-1 measured in caecal, RVC and rectal tissue and eqMCP-1 and eqTRYP levels measured in local serum are shown in Table 3.18 and 3.19. There was a significant positive relationship between the eqTRYP levels measured in serum and the eqMCP-1 measured in the caecal tissue ($p=0.009$, $\rho=0.641$).

Tissue	Caecum eqTRYP ($\mu\text{g/g}$) p-value	Caecum eqTRYP ($\mu\text{g/g}$) Rho value	RVC eqTRYP ($\mu\text{g/g}$) p-value	RVC eqTRYP ($\mu\text{g/g}$) Rho value	RB eqTRYP ($\mu\text{g/g}$) p-value	RB eqTRYP ($\mu\text{g/g}$) Rho value
Local serum						
eqMCP-1 (ng/ml)	0.822	0.062	0.080	0.453	0.822	0.062
eqTRYP ($\mu\text{g/ml}$)	0.165	0.365	0.094	0.435	0.900	-0.035

Table 3.18: Table of p and rho values for correlations of tissue homogenate concentration ($\mu\text{g/g}$) of eqTRYP with local serum concentrations of eqTRYP ($\mu\text{g/ml}$) and eqMCP-1 (ng/ml). Significant p-values are highlighted in yellow (eqMCP-1: equine Mast Cell Proteinase-1; eqTRYP: equine Trypsin; RVC: Right ventral colon; RB: Rectal biopsy).

Tissue	Caecum eqMCP-1 ($\mu\text{g/g}$) p-value	Caecum eqMCP-1 ($\mu\text{g/g}$) Rho value	RVC eqMCP-1 ($\mu\text{g/g}$) p-value	RVC eqMCP-1 ($\mu\text{g/g}$) Rho value	RB eqMCP-1 ($\mu\text{g/g}$) p-value	RB eqMCP-1 ($\mu\text{g/g}$) Rho value
Local serum						
eqMCP-1 (ng/ml)	0.096	0.432	0.089	0.441	0.310	0.271
eqTRYP ($\mu\text{g/ml}$)	0.009	0.641	0.361	0.244	0.839	-0.056

Table 3.19: Table of p and rho values for correlations of tissue homogenate concentration ($\mu\text{g/g}$) of eqMCP-1 with local serum concentrations of eqTRYP ($\mu\text{g/ml}$) and eqMCP-1 (ng/ml). Significant p-values are highlighted in yellow (eqMCP-1: equine Mast Cell Proteinase-1; eqTRYP: equine Trypsin; RVC: Right ventral colon; RB: Rectal biopsy).

3.3.4.3 Comparison of eqMCP-1 and eqTRYP Tissue Concentration According to Cyathostomin Burden

All horses were grouped into four groups according to their CTMB as in Chapter 2 Section 2.4.8. Boxplots showing the caecal eqMCP-1 tissue concentration (Figure 3.41), caecal eqTRYP tissue concentration (Figure 3.42), RVC eqMCP-1 tissue concentration (Figure 3.43), RVC eqTRYP tissue concentration (Figure 3.44), RB eqMCP-1 tissue concentration (Figure 3.45) and RB eqTRYP tissue concentration (Figure 3.46) in these four groups are shown. There was a general trend of the group medians increasing across all three organs in relation to CTMB. The RVC was the only organ where eqMCP-1 and eqTRYP concentrations were observed to be significantly different among the different groups ($p=0.009$, $p=0.019$ respectively) with Groups 3 and 4 having the highest median proteinase concentrations and Group 1 the lowest (Figures 3.43 and 3.44).

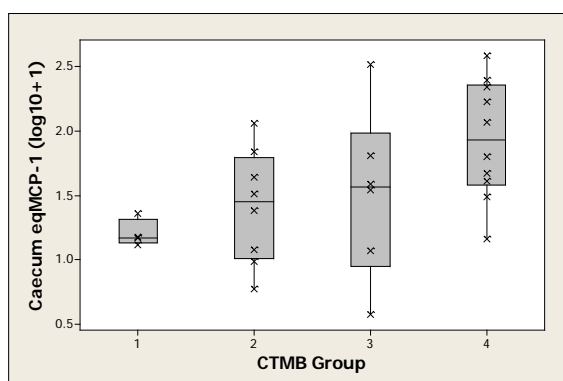


Figure 3.41: Caecal log10+1eqMCP-1 tissue concentrations (µg/g). Kruskal-Wallis analysis revealed no significant difference in caecal eqMCP-1 tissue concentration between groups ($p=0.059$). (eqMCP-1: equine Mast Cell Proteinase-1; CTMB: Combined Total Mucosal Burden).

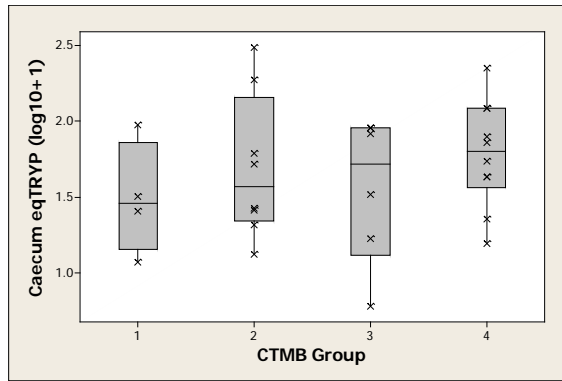


Figure 3.42: Caecal log10+1 eqTRYP tissue concentrations ($\mu\text{g/g}$). Kruskal-Wallis analysis revealed no significant difference in caecal eqTRYP tissue concentration between groups ($p=0.674$). (eqTRYP: equine Tryptase; CTMB: Combined Total Mucosal Burden).

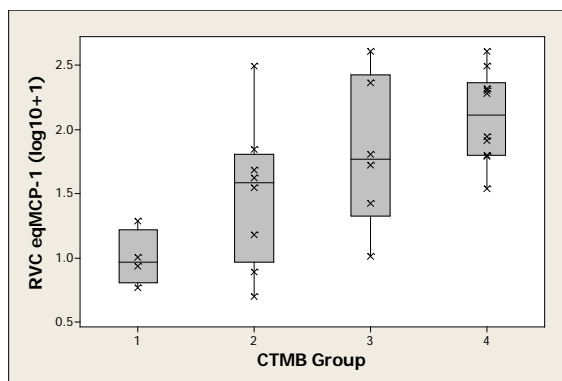


Figure 3.43: RVC log10+1 eqMCP-1 tissue concentrations ($\mu\text{g/g}$). Kruskal-Wallis analysis revealed a significant difference in RVC eqMCP-1 tissue concentration between groups ($p=0.009$). (eqMCP-1: equine Mast Cell Proteinase-1; CTMB: Combined Total Mucosal Burden).

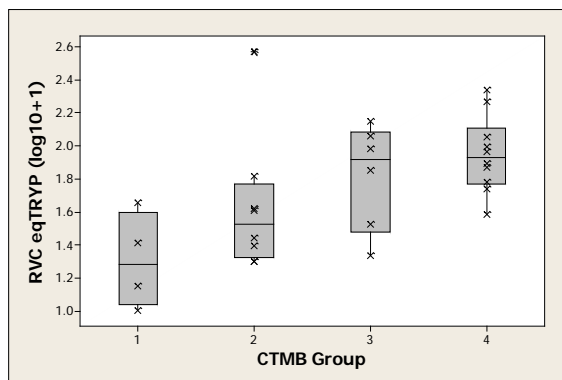


Figure 3.44: RVC log10+1 eqTRYP tissue concentrations ($\mu\text{g/g}$). Kruskal-Wallis analysis revealed a significant difference in RVC eqTRYP tissue concentration between groups ($p=0.019$). (eqTRYP: equine Tryptase; CTMB: Combined Total Mucosal Burden).

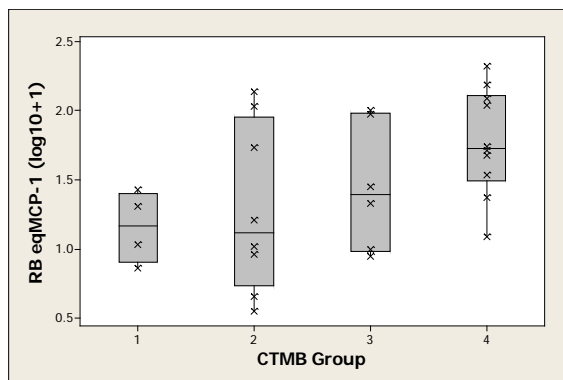


Figure 3.45: RB log10+1 eqMCP-1 tissue concentrations ($\mu\text{g/g}$). Kruskal-Wallis analysis revealed no significant difference in RB eqMCP-1 tissue concentration between groups ($p=0.076$). (eqMCP-1: equine Mast Cell Proteinase-1; CTMB: Combined Total Mucosal Burden. RB: Rectal biopsy).

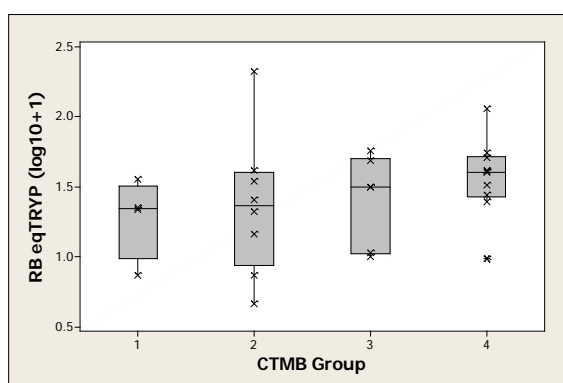


Figure 3.46: RB log10+1 eqTRYP tissue concentrations ($\mu\text{g/g}$). Kruskal-Wallis analysis revealed no significant difference in RB eqTRYP tissue concentration between groups ($p=0.298$). (eqTRYP: equine Tryptase; CTMB: Combined Total Mucosal Burden; RB: Rectal biopsy).

To investigate the relationship between the CTMB or CTLB and tissue proteinase concentrations, linear regression analysis of log10+1 transformed data (with *A. perfoliata* as a confounding variable) was explored. No significant relationship was observed between tissue proteinase concentrations and CTMB in the caecum or rectum (Table 3.20). However, there was a significant positive relationship between both RVC eqMCP-1 (Figure 3.47: $p=0.005$, $r^2=54.3\%$) and RVC eqTRYP (Figure 3.48: $p=0.023$, $r^2=33.1\%$) concentrations and CTMB. A similar significant positive relationship was seen with RVC eqMCP-1 concentrations and CTLB ($p=0.032$, $r^2=47.7$), but not with eqTRYP levels measured in the RVC ($p=0.086$, $r^2=26.7$).

Tissue Proteinase Concentration (µg/ml)	Linear regression analysis with CTMB (p-value)	Linear regression analysis with CTMB (r^2)	Linear regression analysis with CTLB (p-value)	Linear regression analysis with CTLB (r^2)
Caecum eqMCP-1	0.302	46.0	0.134	48.5
RVC eqMCP-1	0.005	54.3	0.032	47.7
RB eqMCP-1	0.255	15.0	0.202	16.2
Caecum eqTRYP	0.851	4.0	0.981	3.8
RVC eqTRYP	0.023	33.1	0.086	26.7
RB eqTRYP	0.927	1.6	0.653	2.4

Table 3.20: Table of p and r^2 values for linear regression analysis of the tissue proteinase concentration of eqMCP-1 and eqTRYP in the caecum, RVC and RB and the combined total mucosal burden (CTMB) or combined total luminal burden (CTLB). Significant p-values are highlighted in yellow. (eqMCP-1: equine Mast Cell Proteinase-1; eqTRYP: equine Tryptase; RVC: Right ventral colon; RB: Rectal biopsy).

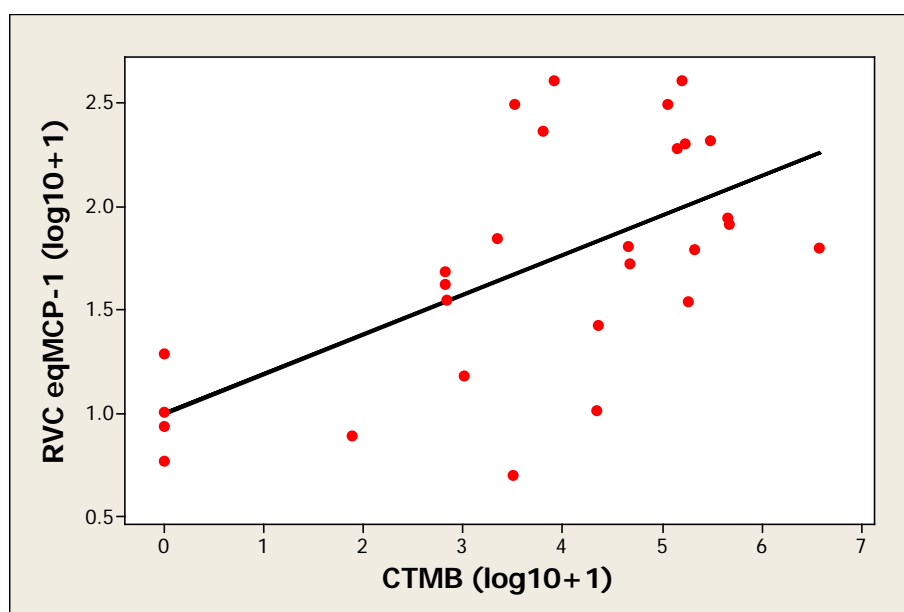


Figure 3.47: Relationship between log10+1 transformed CTMB (x-axis) and RVC eqMCP-1 tissue concentration (µg/g) (y-axis), $p=0.005$, $r^2=54.3\%$ (eqMCP-1: equine Mast Cell Proteinase-1; CTMB: Combined Total Mucosal Burden; RVC: Right ventral colon).

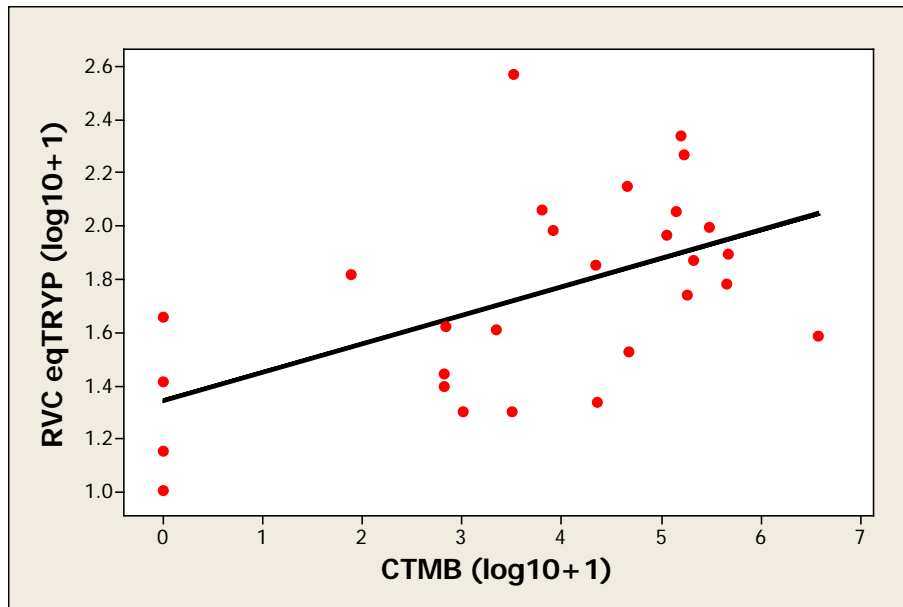


Figure 3.48: Relationship between log10+1 transformed CTMB (x-axis) and RVC eqTRYP tissue concentration ($\mu\text{g/g}$) (y-axis), $p=0.023$, $r^2=33.1\%$ (eqTRYP: equine Tryptase; CTMB: Combined Total Mucosal Burden; RVC: Right ventral colon).

3.4 Discussion

Here, the aim was to further explore the relationship between equine mast cell proteinases and cyathostomin burden. Proteinase-labelled mast cells were stained using immunohistochemistry and the populations of eqMCP-1 and eqTRYP expressing mast cells were enumerated. ELISAs were optimised to measure the concentrations of eqMCP-1 and eqTRYP in serum and tissue. The results were compared to the estimations of the cyathostomin burden from the cohort of horses studied in Chapter 2.

Despite using additional blocking steps, the previously published dual-fluorescence immunohistochemistry technique used to simultaneously label both eqMCP-1 and eqTRYP (Dacre et al. 2010), was incapable of specifically labelling eqMCP-1-positive cells. As a result it was not possible to explore the proportion of mast cells that were positive for both eqMCP-1 and eqTRYP. Thus, this method was replaced with single staining using DAB as a substrate, with eqMCP-1 and eqTRYP expressing cells labelled separately. The results from the enumeration of the single-labelled mast cell populations demonstrated that there were more Toluidine Blue (TB) mast cells (enumerated in Chapter 2) than eqMCP-1-labelled mast cells, and this result was significant in the caecum and RVC. This provides confidence in the combination of labelling and enumeration techniques, as TB stains the total mast cell population and previous studies have indicated that a proportion of TB-stained equine mast cells are chymase-negative and tryptase-positive (du Toit, McGorum et al. 2007; Pickles, Mair et al. 2010). Different mammalian species have differing mast cell population compositions. These populations can either be defined by their location or, more preferably, their proteinase composition (Shimizu, Nagakui et al. 2001). Three mast cell subtypes have previously been described in human (Weidner and Austen 1993), canine (Kube, Audigé et al. 1998), bovine (Küther, Audigé et al. 1998) and equine (Pickles, Mair et al. 2010) tissue: mast cells that contain tryptase only, mast cells that contain chymase only and mast cells that contain both types of proteinases. The immunohistochemistry results here demonstrate a greater number of chymase- (eqMCP-1) compared to tryptase- (eqTRYP) labelled mast cells in the caecum, RVC and rectum. This predominance in chymase expression has also been

observed in parasite-infected intestinal tissues of sheep (Huntley, Gibson et al. 1987) and mice (Wastling, Scudamore et al. 1997; Friend, Ghildyal et al. 1998). The majority of mast cells were eqMCP-1 positive and this finding is in agreement with the most recent equine mast cell proteinase study (Pickles, Mair et al. 2010), which also demonstrated the caecal mast cell population to be predominantly chymase-positive. The results from this study however differ from that reported by du Toit et al. (2007), who found significantly fewer eqMCP-1- compared to eqTRYP-labelled mast cells in the submucosa ($p < 0.024$) and a similar (but non significant, $p < 0.123$) trend in the mucosa (du Toit, McGorum et al. 2007). This discrepancy may be due to the fact that the tissue in the du Toit 2007 study was fixed in formalin and not the optimal fixation solution, Carnoy's (Pickles, Mair et al. 2010). It has been documented in other studies that, despite antigen retrieval techniques, formalin fixation can comprise immunolabelling (Dacre 2005).

There was a significant positive relationship between the numbers of mucosal and submucosal mast cells stained by TB in the three organs examined. This supports the theory of the common mucosal system (van Ginkel, Nguyen et al. 2000); in that stimulation at one mucosal site may provoke a similar immune response at mucosal sites distant to the initial site, and suggests that mast cell activation at one intestinal site results in recruitment of mast cells throughout the intestinal mucosa. EqMCP-1-labelled cells followed a similar pattern to the TB-stained mast cells; caecal eqMCP-1 mucosal cells significantly positively correlated with the right ventral colon (RVC) and rectal biopsy (RB) eqMCP-1 mucosal mast cell labelled populations. EqTRYP-labelled cell numbers had a slightly different pattern; there was a significant positive correlation between the eqTRYP-labelled mucosal cell numbers in the caecum and RVC, but not in the rectum. In the caecum and RVC mucosa, TB MC counts correlated significantly with both eqMCP-1 and eqTRYP MMC counts. However, in the rectum only eqMCP-1-labelled MMC counts correlated with the TB stained MMC counts. EqMCP-1-labelled rectal mucosal mast cells correlated with 11 of the 17 other mast cell populations enumerated. In comparison, rectal eqTRYP-labelled mucosal mast cells only correlated with four of these and these parameters were also measured in the rectum. One hypothesis is that equine intestinal mast cells express

chymase constitutively and tryptase expression is more dynamic and responsive. The chymase expressing cells represent a more stable population. In support of this, caecal eqTRYP has previously demonstrated the strongest relationship with cyathostomin burden, despite the fact that the majority of the equine intestinal mast cell population measured was eqMCP-1-positive and eqTRYP-negative (Pickles, Mair et al. 2010). Measurement of tryptase *in vivo* serves as an overall indicator of mast cell activity (Miller and Schwartz 1988) and tryptase has been implicated as critical to the recruitment of eosinophils into nematode infected murine tissue (Shin, Watts et al. 2008). It has been speculated that tryptase may therefore be expressed in response to encysted cyathostomin larvae (Pickles, Mair et al. 2010).

Rectal mucosal mast cell eqMCP-1 and eqTRYP-labelled cell counts were the only proteinase-labelled populations to correlate significantly with CTMB and CTMB. These results support the hypothesis that rectal tissue mast cell populations correlate with cyathostomin burden, such that they have diagnostic potential for prediction of total burden. Mast cells are resident within tissues that interface with the external environment, such as the rectum, and may play a sentinel role in host defence (Kumar and Sharma 2010). These relationships were not observed with the rectal submucosal proteinase-labelled population counts. The mucosal mast cells are more involved at the site of infection, particular with relation to luminal burden, therefore they are the predominant effector cell population. Differences in mast cell proteinase expression and subtype are linked to cell stage, maturation and activation (Aldenberg and Enerbäck 1994; de Souza, Toso et al. 2012). There is evidence to suggest that mast cells can transform phenotype depending on the local environment interchanging between connective tissue and mucosal mast cells and proteinase expression (Kitamura, Kanakura et al. 1987). Mast cells maturing in different tissue microenvironments can vary in the type and amount of tryptases and chymases expressed (Caughey 2007; Xing, Austen et al. 2011). This could explain the relationship observed here between CTMB and rectal mucosal proteinase-labelled mast cells but not the submucosal mast cell proteinase-labelled population. This is similar to murine mast cell response to *T. spiralis* infection, where the MMC subset undergoes massive hyperplasia but the CTMC population remains sparse (Shin,

Watts et al. 2008). Investigating individual mast cell proteinase expression at one time point may not be representative of current cyathostomin burden and may explain why no relationship was seen in the caecum or RVC. The rectum, with minimal cyathostomin burden, may represent a more stable mast cell population due to reduced local activation and degranulation. As previously mentioned in Chapter 2 degranulated mast cells (such as those seen in Figure 3.12A) are difficult to stain (Sonti 2012) and enumerate, making activated mast cells challenging to quantify. For example, differential mast cell proteinase expression has been demonstrated in mast cells in mice during a defined period post infection (Friend, Ghildyal et al. 1996; Friend, Ghildyal et al. 1998). Thus further work to investigate the kinetics of equine mast cell proteinase expression is warranted and serum measurements of mast cell activation would be of great benefit to study the kinetics of proteinase expression and concentration. However, eqMCP-1 and eqTRYTP proteinase concentrations in serum collected peripherally, from either the jugular vein or a vessel from a lower limb, did not correlate with the concentrations measured in local serum draining the site of interest. When examining this relationship further, through exploring the level of agreement between the sample sites, the limits of agreement for both proteinases were clinically significant. In addition, some individual horses had large differences in the proteinase concentrations measured at the two different sites. Therefore, measuring peripheral proteinase serum concentrations with the ELISA described here, cannot be used to reliably indicate the level of proteinase in serum local to the site of infection. Consistent with this observation, the concentrations of eqTRYTP and eqMCP-1 measured in peripheral serum did not correlate with any of the TB, eqTRYTP or eqMCP-1-labelled MMC or SMMC parameters. This is in comparison to studies in *T. spiralis* infected mice, which demonstrated a correlation between peripheral serum MCP concentration and MMC numbers and also the process of *T. spiralis* expulsion (Huntley, Gooden et al. 1990). Here, linear regression analysis demonstrated no significant relationship between the local eqMCP-1 concentrations measured and CTMB. The relationship was also not significant for local serum eqTRYTP concentrations measured and CTMB. Peripheral serum concentrations of either proteinase did not have a significant positive correlation with CTMB or CTLB.

Therefore the results here indicate that serum MCP concentrations are not a good predictor of cyathostomin burden. When the serum proteinase concentrations were grouped according to the CTMB there was no significant difference between the groups for either eqMCP-1 or eqTRYP levels. The group with the highest CTMB (Group 4) had the highest range of proteinase concentrations and contained the highest proteinase concentration for both eqMCP-1 and eqTRYP, although the relationship was not significant. There was however a significant negative relationship between peripheral serum eqMCP-1 concentrations and the CTMB. An explanation for this could involve the activation and sequestering of proteinases within the gut lumen. During an active infection if proteinases are involved in the host response as hypothesised, they will be recruited to the region required, in this case the intestine, resulting in a potential decrease in peripheral serum concentrations. In mice the intestine is the primary source of peripheral mMCP-1 (Huntley, Gooden et al. 1990; Wastling, Scudamore et al. 1997). MMCP-1 levels increase in the bloodstream and intestinal lumen of *T. spiralis* parasitised mice and are maximal at the time of worm expulsion (Huntley, Gooden et al. 1990). The differences in mast cell proteinase measurement observed here between the mouse and the horse could relate to variance physiology, differences between responses to infection or potentially the fact that proteinase measurements in this study were performed on naturally infected horses rather than synchronous experimental infections. In particular, the hypobiotic stage in which equine cyathostomins can reside for months to years (Gibson 1953; Murphy and Love 1997) could be an important factor in the measurement of mast cell response. As it was not possible to determine the level of cyathostomin infection activity it is difficult to relate the proteinase measurements with active infection. However, these results provide further support for the future investigation of equine mast cell proteinase expression kinetics and serum concentration at different timepoints and stages of infection.

Concentrations of eqMCP-1 and eqTRYP measured locally in serum significantly positively correlated with each other. This demonstrates that the expression and release of these mast cell proteinases is related, which could be due to the fact that some mast cells express both proteinases or that the single mast cell proteinase

expressing populations are responding to the same stimuli and environment. There was no significant positive relationship between local serum proteinase concentrations and CTMB. A factor which may have resulted in this lack of relationship is that mast cell degranulation, causing release of serine proteinases, is not specific to gastrointestinal helminths. Mast cells can be activated in numerous ways, the most well documented of which is activation through IgE bound to high affinity IgE receptor (FcRI) expressed on the mast cell surface (Kinet 1990). Mast cells can also be stimulated by direct injury or activated complement proteins (Erdei, Andrásfalvy et al. 2004) and by pathogens through pattern recognition receptors (Urb and Sheppard 2012). Therefore many stimuli can theoretically increase tissue and serum eqTRYP and eqMCP-1 concentrations. An elevation in bronchial epithelial mast cells and evidence for mast cell degranulation causing tryptase release has been demonstrated in heaves susceptible horses following hay/straw challenge (Dacre, McGorum et al. 2007), however the ELISA used was optimised for BALF fluid and the levels in serum were not measured. Another common equine condition that can potentially cause an IgE mediated mast cell activation is sensitivity to *Culicoides* allergens (Wagner, Miller Jr et al. 2009). In this condition activated mast cells release histamine in the dermis (Morrow, Baker et al. 1987) and such degranulation may also result in the systemic release of serine proteinases, however this has not yet been measured in serum. These could be some of a number of concurrent conditions affecting systemic mast cell proteinase concentrations in the cohort of horses studied here. Concurrent disease is a potential area for further study as it has potential to have an effect on the systemic concentrations of MCPs.

Although there was no significant positive relationship between local serum proteinase concentrations and CTMB for eqTRYP or eqMCP-1, cyathostomin-negative horses had consistently lower levels of eqMCP-1 (mean 0.45 ng/ml) and eqTRYP (mean 0.23 µg/ml). Studies in mice have demonstrated low serum levels of intestinal mast cell proteinase (IMCP) at 0.02 µg/ml in uninfected versus *T. spiralis* infected mice (Huntley, Gooden et al. 1990). The same study demonstrated low intestinal tissue concentrations of IMCP in non-parasitised mice which increased 100-1000 fold in infected mice. Here, tissue from horses with a record of no previous

exposure to cyathostomins was not available. Neither local nor peripheral serum had statistically significant higher eqMCP-1 concentrations; the same was true of eqTRYP concentrations. However serum results were markedly different between the two proteinases; with eqMCP-1 and eqTRYP detected in nanograms and micrograms per millilitre respectively. This was unexpected in light of the significantly greater proportion of eqMCP-1 expressing intestinal mast cells enumerated using immunohistochemistry. The response of intestinal mast cell proteinase systemic release following nematode infection in mice with *T. spiralis* demonstrated peak concentrations of 9.48 µg/ml (Huntley, Gooden et al. 1990). Intravascular challenge of sensitised rats with soluble *Nippostrongylus brasiliensis* antigen demonstrated vascular concentrations of rat mast cell proteinase-II of 6-10 µg/ml after 1 min (Scudamore, Thornton et al. 1995). As eqTRYP was detected in µg/ml compared to ng/ml for eqMCP-1, it is possible that it is being differentially released or potentially differentially cleared, which has been demonstrated in mice (Pemberton, Wright et al. 2006). Mouse mast cell proteinases (mMCP) 1 and 2 have been shown to co-localise in similar quantities in intestinal mucosal mast cells; however, levels of these measured in peripheral blood during nematode infection is very different, with nanograms of mMCP-2 compared to micrograms of mMCP-1 being detected (Pemberton, Wright et al. 2006). This difference is believed to be related to the fact that unlike mMCP-2, mMCP-1 forms complexes with serpins and this prevents its clearance and consequently substantially prolong its half-life (Pemberton, Wright et al. 2006). A similar situation could potentially be occurring here and further investigation in this respect is warranted. Despite the differences between the serum proteinase concentrations, there was no significant difference between the tissue proteinase concentrations in the caecum, RVC or rectum. This provides further evidence to suggest that there is a property of equine serum, such as differential clearance due to serpin complexes, that may be present and affecting the ELISA results here.

Different mast cell population compositions are also found in different tissues (Welle 1997). Although the results here demonstrate eqMCP-1 expressing cells to be more numerous than those expressing eqTRYP in the intestine, this is not the case in all

equine tissues or organs (Pemberton, McEuen et al. 2001). Chymase-expressing cells were found to be scarce in the equine lungs, where tryptase-expressing mast cells predominate (Dacre 2005). This could have an effect on the concentrations of proteinases circulating in the serum. The rat beta chymase mast cell proteinase II is the predominant proteinase expressed in intestinal mucosal mast cells (Gibson, Mackeller et al. 1987; Sture, Huntley et al. 1995). In mice, the soluble beta chymase mouse MCP I is predominantly expressed by mucosal mast cells of the intestine (Wastling, Knight et al. 1998) and in helminth infections predominantly chymase-positive phenotypes were observed (Friend, Ghildyal et al. 1996). However, tryptase expression has been demonstrated at higher levels than chymase in the human intestine (Aldenborg and Enerbäck 1994) and tryptase-positive mast cells have been found to be the most common subtype in bovine intestinal submucosa (Küther, Audigé et al. 1998). Sheep MCP I is abundantly expressed in ovine gastrointestinal cells; however, this proteinase has demonstrated both trypsin and chymotrypsin like activity (Pemberton, Huntley et al. 1997). Systemic concentrations of MCPs are higher in rodents compared to humans (Pemberton, Wright et al. 2006). Following nematode challenge, beta chymases have been detected in micrograms per millilitre in serum from mice (Pemberton, Brown et al. 2003) and rats (Miller, Woodbury et al. 1983). In comparison, human serum levels of tryptase in response to allergic challenge have been measured in the order of nanograms per millilitre (Lin, Schwartz et al. 2000). In ovine studies concentrations of sheep MCP in serum were substantially less than the levels measured in rodents, however they were of a similar order of magnitude to those measured in humans (Huntley, Gibson et al. 1987). The relatively low concentrations of sheep MCP in serum (<1.0 ng/ml) is believed to be due to presence of proteinase inhibitors which interfere with its detection by ELISA (Huntley, Gibson et al. 1987). The binding of endogenous serum inhibitors to the serine proteinases could be masking epitopes and thus affecting their interaction with antibodies in the ELISA (Tate and Ward 2004). This could be a possible complication here and could potentially be responsible for the relatively low concentrations of eqMCP-1 measured in equine serum. The median local serum sample concentration of eqMCP-1 was 1.75 ng/ml compared to 3.16 µg/ml for

eqTRYP. However, using the same capture and detection antibodies for the tissue ELISAs the tissue concentrations were of the same order of magnitude, i.e. the median caecal eqMCP-1 concentrations was 35.78 µg/g compared to 46.47 µg/g for eqTRYP. This provides further evidence for the role of proteinase inhibitors in serum, but not in tissues and this property of equine serum requires further investigation.

For the tissue MCP concentrations there was a significant correlation between the concentration of eqMCP-1 in the caecum, the RVC and the rectum. This was also observed with concentrations of eqTRYP in these organs. In addition, concentrations of eqTRYP significantly positively correlated with the concentrations of eqMCP-1 within each organ. Furthermore, there was a significant relationship between both RVC eqMCP-1 and RVC eqTRYP concentrations and CTMB. Low RVC CTMB was associated with a low tissue proteinase concentration and high CTMB with high proteinase concentration, and this result was significant. Of the three organs examined, the RVC demonstrated the greatest range and highest median of eqMCP-1 and eqTRYP proteinase concentrations. The RVC also had a greater total cyathostomin mucosal burden than the caecum (i.e. caecum: range 0–1,773,047; median 5945. RVC: range 0–2,054,051; median 7028). There were also significantly more luminal worms in the RVC compared to the caecum (Chapter 2). This could explain why the tissue ELISA results were more closely related to the cyathostomin burdens at this site, as the mast cells may be more active due to the higher levels of cyathostomin present. In the case of CTLB, the only significant positive relationship was seen with RVC eqMCP-1 concentration ($p=0.032$, $r^2=47.7$). The lack of relationship in the caecum and RB could also be related to the high assay coefficients of variation (CV). In particular the inter assay CVs for the serum ELISA were both above 30% despite additional optimisation procedures. This high CV could be contributed to by the use of polyclonal antibodies which may be binding non-specifically to a number of epitopes (Lipman, Jackson et al. 2005). Also, the ELISA here used biotinylated versions of the capture antibody as the secondary antibody which is not ideal as these antibodies were raised in the same species (rabbit). As the capture and detections antibodies recognise the same epitopes it is likely that binding

of capture antibody to the proteinase interferes with binding of the detection antibody. This may have prevented antibody recognition and hence affected the level of signal recorded. Dilution errors for the standard curve may also have effected the variation between assays. As previously mentioned substances such as proteinase inhibitors, particularly in the serum, could also have been causing interference by interfering with antibody binding. The effect of this variation could be minimised in the future with the use of monoclonal antibody reagents, as they are produced by only one clone of B cells and therefore recognise only one epitope. Also, chymases are structurally very similar to granzymes and have similar specificities (Trapani 2001). These granzymes are members of a chymotrypsin related family of serine proteinases produced by cytotoxic T-cells and NK cells (Trapani 2001). Due to similarities in the structure of related mast cell chymases and granzymes, it is therefore important to ensure the specificity of the antibodies utilised. The availability of the horse genome allows further investigation into the equine tryptase and chymase loci and this is the basis of Chapter 4.

The work here has provided evidence to support further investigation in to equine mast cell proteinases and their use in diagnostic assays to estimate CTMB. The significant positive relationship demonstrated here between the proteinase-labelled rectal mast cells and CTMB has particular value as rectal biopsy is a viable and accessible sample source. The optimised ELISA demonstrated a significant relationship between both RVC eqMCP-1 and eqTRYP tissue concentrations and CTMB. Currently, in the case of equines, one mast cell chymase and one tryptase have been isolated from an equine mastocytoma (Pemberton, McEuen et al. 2001). However there is evidence for multiple equine chymases (Dacre 2005). Other species not only have varying mast cell population compositions, but express different numbers of both tryptase and chymase types (Caughey 2007). Given the diversity of mast cell proteinases in other species (Puente and López-Otín 2004; Gallwitz and Hellman 2006) there is potential for novel equine mast cell proteinases that have yet to be identified and may be more closely related to cyathostomin burden.

4 Exploration of Novel Equine Mast Cell Proteinases

4.1 Introduction

The recent generation of the horse genome map (Chowdhary and Raudsepp 2008) facilitates further investigation into equine mast cell proteinase sequences and their potential paralogs. This chapter had three broad aims. First to further extend the previous work here on equine mast cell proteinases, which demonstrated the possible existence for multiple equine chymases (Dacre 2005), and thus the aim here was to identify additional mast cell proteinase genes in the equine genome. Second to quantify transcription of four selected mast cell proteinases using quantitative polymerase chain reaction (qPCR). The sequences were chosen on the basis of their presence in equine intestinal tissue and amino acid (aa) at residue 226, an important residue for conferring substrate specificity (Smyth, O'Connor et al. 1996). Third to explore the relationship of the expression of selected proteinases with cyathostomin burden and other mast cell measurements.

Mast cells comprise a heterogeneous population which can be expressed as differences in functional, biochemical and histochemical properties (Welle 1997). For example, there exist functionally distinct mast cell secretory granule subsets that define mast cell populations (Shimizu, Nagakui et al. 2001; Puri and Roche 2008) and like humans (Irani and Schwartz 1994), rats (Le Trong, Neurath et al. 1987) and mice (Miller and Pemberton 2002), horses have mast cell subpopulations that differ in neutral proteinase content (Pickles, Mair et al. 2010). Mast cells also express non-specific proteinases, including granzymes, neurolysin and lysosomal cathepsins (Pejler, Åbrink et al. 2007; Pejler, Ronnberg et al. 2010). As previously mentioned (Chapter 1), the three main mast cell proteinases are tryptase, chymase and carboxypeptidase-A. Tryptase and chymase are classed as serine proteinases, because of the presence of a nucleophilic serine residue at the active site (Hedstrom 2002). The active site cleft is spanned by the catalytic triad with Ser195 on one side and Asp102 and His 57 on the other (Hedstrom 2002). Chymases, one of the major mast cell granule constituents, have chymotrypsin-like cleavage specificity and they cleave substrates on the C-terminal side of aromatic amino acids (Andersson,

Karlson et al. 2008). The chymase family can be subdivided into two groups, alpha and beta chymases, based on phylogenetic analyses (Chandrasekharan, Sanker et al. 1996). Trypsases cleave peptide substrates on the carboxyl side of lysine and arginine residues (Caughey 2007) and are trypsin-like serine proteinases; however, they differ from trypsin in that they are resistant to natural inhibitors of trypsin and have little or no activity against denatured proteins such as casein (Little and Johnson 1995). As discussed in Chapter 3, two neutral serine proteinases have previously been extracted from equine mastocytoma tissue, equine tryptase (eqTRYP) and equine Mast Cell Proteinase-1 (eqMCP-1) which have trypsin-like and chymotrypsin-like specificities, respectively (Pemberton, McEuen et al. 2001). The antibodies used in Chapter 3 for immunolabelling and ELISAs were raised in rabbits using these two equine mastocytoma derived proteins (Pemberton, McEuen et al. 2001). The cloning and sequencing of these proteins has been described (Dacre 2005). The sequence for eqTRYP, referred to here as Tryptase-like Proteinase-1 (TLP1), shares >70 % aa identity with, and is the same length as other mammalian tryptases (Dacre, McAleese et al. 2006).

The situation is more complicated with equine Mast Cell Proteinase-1 (eqMCP-1). When attempting to determine the nucleotide sequence for this chymase from equine intestinal tissue using molecular cloning techniques, the translated aa sequence for the putative eqMCP-1 had an N-terminal aa sequence that differed from that of the mastocytoma derived eqMCP-1 by two aa (Pemberton, McEuen et al. 2001; Dacre 2005). Both sequences shared similar identities with human granzyme H (Pemberton, McEuen et al. 2001; Dacre 2005), however peptide masses of the two sequences, isolated by peptide mass fingerprinting, corresponded poorly with each other (Dacre 2005). Fourteen peptide masses were determined for eqMCP-1 isolated from equine mastocytoma from peptide mass fingerprinting performed on two separate occasions (Dacre 2005). Only three of these corresponded with predicted peptides from putative eqMCP-1 (Dacre 2005). It was therefore hypothesised by Dr. K Pickles et al. (2005) that a similar but novel proteinase had been cloned and sequenced, rather than the original mastocytoma derived chymase that was purified and characterised by Dr A. Pemberton et al. 2001. This new chymase sequence was submitted to NCBI

as putative equine mast cell proteinase-1-like chymase by Dr. K Pickles et al. in 2005 and is referred to as Chymase-like Proteinase-1 (CLP1) in this Chapter.

Granzyme B is the best characterised granzyme and equine granzyme B has been recently isolated and identified (Piuko, Bravo et al. 2007). From preliminary examination of these sequences it is important to note that this sequence shares sequence homology (84% identity) with putative equine MCP-1, and 55% similarity with eqTRYP. Other species express multiple mast cell tryptase and chymase proteinases (Caughey 2007). In particular, the chymase locus has undergone significant evolutionary changes and multiple closely-related chymases are expressed in several mammalian species (McAleese, Pemberton et al. 1998; Miller and Pemberton 2002). The rat genome contains 28 closely related functional chymases (Puente and López-Otín 2004), compared to at least 14 in mice (Gallwitz and Hellman 2006). The finding by K. J Dacre (2005) provides evidence for the presence of multiple, closely related chymases in horses (Dacre 2005). In addition, the expression of specific mast cell proteinases has been demonstrated to correlate closely with intestinal nematode burdens in the mouse and rat (Woodbury, Miller et al. 1984; Huntley, Gooden et al. 1990). EqMCP-1 and eqTRYP tissue ELISA results from Chapter 3 demonstrated a significant positive relationship with cyathostomin burden in the right ventral colon (RVC). However, significant relationships between cyathostomin burden and eqMCP-1 and eqTRYP tissue concentrations were not observed in the caecum or rectum. As there is potential for novel equine mast cell proteinases there is also the potential that the expression of currently unidentified proteinases may be more closely related with cyathostomin burden. Therefore, this chapter aimed to explore this expression further and to examine the final hypothesis:

There are novel equine mast cell proteinases that have not yet been identified. The release of these novel proteinases may be more closely related to worm burden than those previously investigated.

To investigate the discrepancy in eqMCP-1 sequence and to determine whether other equine mast cell proteinases exist, proteomic analysis was performed on the

previously-purified protein products (eqTRYP and eqMCP-1), the equine mastocytoma tissue from which these proteinases were purified, equine intestinal tissue homogenate and serum with the aim of identifying other potential equine mast cell proteinases. Western blot analysis, using the polyclonal antibodies to both purified protein products (Pemberton, McEuen et al. 2001) used in Chapter 3, was performed to identify immunoreactive bands on one dimensional polyacrylamide gels and proteins within these areas were identified by mass-spectrometry with the aim of identifying other proteinases which may also be recognised by these polyclonal antibody reagents. The aa sequences obtained from this proteomic analysis were compared against known sequences for equine tryptase (TLP1) and putative equine Mast Cell Proteinase-1 (CLP1) and the NCBI database. This database includes the recently published equine genome, a bioinformatic resource that facilitates the investigation into predicted equine proteinase sequences. This approach identified seven additional proteinase sequences, of which two (granzyme B-like (GZMBL) and granzyme(BGH)-like GZM(BGH)L) were selected for further investigation. This selection was performed based on their aa residue at position 226, as this is important for conferring substrate specificity (Smyth, O'Connor et al. 1996), and the presence of the proteinase in equine tissue from the Mascot results. Transcription analysis was then performed on four sequences, TLP1, CLP1 GZMBL and GZM(BGH)L, to investigate their expression in the equine cohort described in Chapter 2. Quantitative PCR was optimised and performed on cDNA from 14 horses at three different anatomical sites (the caecum, RVC and rectum) to determine transcript levels of the four proteinases. These results were then compared to mast cell counts and cyathostomin burden data and to immunohistochemistry and ELISA data generated on the two proteinases (eqMCP-1 and eqTRYP) to inform on the relationship of these proteinases with cyathostomin burden and immunological parameters. This work has the potential to provide additional information on equine mast cell proteinase genes and to further investigate their association with cyathostomin infection.

4.2 Materials and methods

4.2.1 Sample Selection for Proteomic analysis

To identify molecules bound by the anti-eqMCP-1 and anti-eqTRYP antibodies used in Chapter 3, serum and tissue homogenate samples were analysed. Sodium dodecyl sulphate polyacrylamide gel electrophoresis, using NuPage Novex Bis-Tris Mini gels (Invitrogen), was performed as per manufacturer's instructions. Lanes containing homogenised equine mastocytoma and previously-purified eqTRYP and eqMCP-1 (Pemberton, McEuen et al. 2001) were included for comparison. Sample 'DV7 Peripheral -80 °C' serum and 'DV12 RVC' tissue homogenate were selected for analysis based on the presence of bands using antibody detection in pilot immunoblot studies. First, 6.5 µl of undiluted tissue homogenate from equine mastocytoma tissue, horse DV12 RVC and peripheral serum from horse DV7 (1:20 PBS) were loaded per lane. Two gels were run in parallel gel using NuPage MES Running Buffer containing 500 µl NuPage Antioxidant (Invitrogen) for 35 min at a constant 200 V. Samples were run in duplicate on two separate gels. One gel was washed three times in deionised water and stained overnight with Simply Blue™ Safe Stain (Invitrogen) to visualise protein bands. An immunoblot was performed on the second gel (see Appendix X) and the blot probed with rabbit anti-eqMCP-1 IgG or rabbit anti-eqTRYP IgG (Chapter 3). Immunoreactive bands were visualised using ECL™ Western Blotting Detection Reagent (GE Healthcare). The blot was aligned with the protein stained gel to identify protein bands of similar size to the immunoreactive band(s). Three 1 mm wide gel slices were obtained for each lane: one slice at approximately the same size as the band, and one above and one below this slice. Each gel slice was analysed separately by mass spectrometry as described below.

4.2.2 Liquid Chromatography- Electrospray Ionisation– Tandem Mass Spectrometry (LC-ESI-MS/MS)

LC-ESI-MS/MS analysis of protein samples was carried out as described previously (Batycka et al. 2006). Briefly, the proteins within each gel slice excised from the sample lane were subjected to standard in-gel destaining, reduction, alkylation and trypsinolysis procedures (Shevchenko et al. 1996). Liquid chromatography (LC) was

then performed on samples of 4 µl from each gel slice, applied by direct injection to a monolithic reverse-phase column (5 cm × 200 µm; Dionex), using an Ultimate 3000 nano-flow HPLC system (Dionex-LC Packings) maintained at 50 °C. Bound peptides were eluted by the application of a 15 min linear gradient of 8-45 % acetonitrile in 0.1 % formic acid and monitored by UV absorbance in a 3 nl UV detector flow cell. LC was interfaced with a 3-D high capacity ion trap mass spectrometer (Esquire HCTplus™, Bruker Daltonics) via a low-volume (<50 µl/min) stainless steel nebulizer (Agilent) and electrospray ionization. Digests were analysed for protein content by LC-ESI-MS/MS in ultrascan mode (26,000 amu/s). MS/MS analysis was initiated on a contact closure signal triggered by Chromeleon chromatography software (Dionex).

4.2.3 Proteomic Analysis of MS/MS Data

Deconvoluted MS/MS data in Mascot Generic Format (mgf) were imported into ProteinScape™ V2.1 (Bruker) proteomics data analysis software for searching against viral and mammalian subsections of the NCBI non-redundant protein sequence databases utilising the Mascot™ V2.2 search algorithm (Matrix Science). A second database containing the two sequences of interest, equine TLP1 and CLP1 was created and the data also searched against this. Mascot search parameters were set in accordance with published guidelines (Taylor & Goodlett, 2005) and to this end, fixed and variable modifications selected were carbamidomethyl (C) and oxidation (M), respectively, while peptide (MS) and fragmentation (MS/MS) tolerance values were set at 1.5 Da and 0.5 Da, respectively. Individual protein candidates identified were inspected manually and considered significant only if: (a) a minimum of two peptides were matched for each protein, and (b) each peptide contained an unbroken “b” or “y” ion series comprising a minimum of four aa residues.

4.2.4 MALDI-TOF-MS for Recombinant Protein Identification

For identification of proteins by MALDI –TOF MS spots were excised from the gels and washed in 50 mM ammonium bicarbonate in 50% acetonitrile (ACN) three times for 15 min each at room temperature on a vortex mixer. The solution was removed and the gel pieces covered with 100 % ACN to dehydrate for 10 min. Supernatant was removed and the gel pieces vacuum-dried for 20 min. The gel spots were then rehydrated in trypsin digest solution (10 ng/μL sequencing grade modified trypsin) in 25 mM ammonium bicarbonate and incubated at 37°C for at least 16 h. Tryptic peptides were applied to a steel MALDI target plate in a solution of 10mg/ml α-cyano-4-hydroxycinnamic acid (CHCA) in 0.1 % TFA and 50 % ACN.

4.2.5 Proteinase Sequence Analysis and Selection

As previously mentioned, each lane was divided into three slices over the region of interest and each slice analysed separately. Two searches were performed using the Mascot™ V2.2 (Matrix Science) search algorithm. The first was performed against the database containing the two initial sequences of interest, TLP1 and CLP1. The second search used the NCBI non-redundant protein sequence databases and gave nine significant proteinase- or granzyme- related hits. After both searches, a database (GranzymeDB) was compiled of the nine protein candidates. From this database, four sequences of interest were selected; TLP1 (NP_001075344.1), GZMBL (XP_001488476.2), CLP1 (NP_001075345.1) and GZM(BGH)L (XP_001488616.3). The sequences were selected based on the aa residue at position 226 as this is important for conferring substrate specificity (Smyth, O'Connor et al. 1996) and the presence of the proteinase in equine tissue either from the Mascot results or, in the case of CLP1, the previous demonstration of this proteinase in equine tissue (Dacre 2005).

4.2.6 Processing and Storage of Tissue Material

Sections were taken in duplicate from tissue adjacent to the samples processed for ELISA analyses and mast cell enumeration from the caecum, RVC and rectum of all

horses during the sampling process (Sections 2.2.6 and 2.2.8). These sections were placed immediately into at least 10 volumes of RNAlater (Invitrogen). The sections were less than 0.5 cm thick to ensure rapid and reliable stabilisation of RNA. Samples were stored for a minimum of 24 h at 4 °C, then transferred to -80 °C.

4.2.7 RNA Extraction from Equine Tissue

RNAlater-preserved tissue was homogenised using a Precellys[®]24 tissue homogeniser (Precellys) as follows: 30-40 mg of tissue were placed into a Precellys CK28 tube (Pqrlab) together with 600 µl Buffer RLT Plus (Qiagen). The tissue was homogenised for five, 23-second cycles at 6200 rpm, with 2 min on ice between each cycle. The homogenised tissue was clarified by centrifugation at 14,000 × *g* for 10 min at 4 °C. The homogenised lysate was passed through QIAshredder column (Qiagen) at 13,000 rpm for 2 min, then processed through a gDNA Eliminator spin column (Qiagen) at 11,000 rpm for 30 sec. RNA was extracted using an RNeasy Plus Mini Kit (Qiagen) with on-column digestion of DNA using an RNase-Free DNase Set (Qiagen) as per the manufacturer's instructions.

4.2.8 RNA Validation

The quantity of the RNA was confirmed using a spectrophotometer (Nanodrop[®] ND-1000 UV-Vis Spectrophotometer) following the manufacturer's instructions. The quality of RNA was assessed using the Agilent RNA 6000 Nano Assay protocol (2100 Bioanalyzer, Agilent Technologies). One µl of heat-treated RNA was added to each prepared well as per the manufacturer's instructions. The 'RNA Integrity Number' for each sample was assessed. Samples with an RNA Integrity Number greater than 8 were accepted and any below this threshold were reprocessed. The mean RNA concentration using the Nanodrop spectrophotometer was 565.96 ng/ml +/- 277.25 (ng/ml +/- SD). The mean RNA concentration using the Agilent RNA 6000 Nano Assay protocol was 803.10 ng/ml +/- 425.92 (ng/ml +/- SD).

4.2.9 Complementary DNA Production

To produce complementary DNA (cDNA), 1 µg of RNA sample was used to synthesise single-stranded cDNA using Sprint™ Powerscript™ PrePrimed Single Shots with Oligo (dT)23 Primers (Sigma O4387). The cDNA was diluted 1:10 with molecular biology grade H₂O before use, divided into aliquots and stored at -20 °C.

4.3 Design of Primers

Primers were designed manually for each of the four selected proteinase sequences; TLP1, GZMBL, CLP1, GZM(BGH)L. Sequences were searched against the equine genome using the NCBI standard nucleotide BLAST function (organism *Equus caballus*) and then aligned against all hits. Areas of unique nucleotide sequence were identified and primers designed to give an amplicon of 117 to 160 base pairs, a melting point of 62 °C and a GC content of between 40 and 65 % (Table 4.1). Once selected, the chosen amplicon sequences were re-verified, using the same BLAST function as above, against the equine NCBI database to ensure their specificity prior to cloning and sequencing.

Gene	Forward Primer Sequence	Reverse Primer Sequence	Product length (bp)
TLP1	5'-AGTCAGTCTGCCACCTCCG-3'	5'-TGCACACAGCATGTCGGCC-3'	139
GZMBL	5'-AGCTGAGGCCTGGAGAGGT-3'	5'-TAATTGCCAAAGTAGGATTCGC-3'	136
CLP1	5'-TCCGAAAGATAAGAAGTCTTCC-3'	5'-AAGGCCTGTGGAATACTCCC-3'	117
GZM(BGH)L	5'-AATTCTAAGAACTTCGCCAACG-3'	5'-CATTTAGGGCAACTCTCCCC-3'	160

Table 4.1: Primer sequences and product length for each of the four amplicons of interest. (bp: base pairs; TLP1: Tryptase-like Proteinase-1; GZMBL: Granzyme B-like; CLP1: Chymase-like Proteinase-1; GZM(BGH)L: Granzyme(BGH)-like).

PCR product generated	Number of significant hits identified on BLASTn search	Percentage of the amplicon sequence that the most similar hit covers	Percentage identity with the most similar hit at the aa level
TLP1	0	0	0
GZMBL	11	97%	93%
CLP1	1	99%	94%
GZM(BGH)L	9	100%	89%

Table 4.2: Table of results from a BLASTn search against the NCBI equine genome database using the PCR products for each gene of interest as the query sequence. The number of similar hits for each PCR product is shown. (TLP1: Tryptase-like Proteinase-1; GZMBL: Granzyme B-like; CLP1: Chymase-like Proteinase-1; GZM(BGH)L: Granzyme(BGH)-like).

4.3.1 Primer Validation and PCR Amplicon Sequencing

Initial PCR was carried out using cDNA from caecal tissue from horse DV11 and RVC tissue from horse DV12. These horses were selected due to high eqTRYP- and eqMCP-1-labelled mast cell counts (DV11 Caecum: eqMCP-1 397 mucosal mast cell (MMC)/mm² and eqTRYP 114 MMC/mm²; DV12 RVC: eqMCP-1 368 MMC/mm² and eqTRYP 162 MMC/mm²). The cDNA was used as a template with specific oligonucleotide primers (Table 4.2) for each of the genes of interest (TLP1, GZMBL, CLP1, GZM(BGH)L) to generate amplicons of 117-160 bp. PCR was performed under the conditions; 94 °C for 5 min, followed by 40 cycles of 94 °C for 30 sec, 55 °C for 30 sec and 72 °C for 30 sec, with a final extension step of 7 min at 72 °C. The PCR products were purified using PCR purification kits (Qiagen), cloned into the pGEM-T easy vector system cloning kit (Promega) and the plasmids were transformed into JM109 High Efficiency Competent Cells (Promega). The transformed plasmids were incubated in SOC medium for 1 h at 37 °C, then spread onto Luria-Bertani (lb) medium plates containing ampicillin at 100 µg/ml. To enable alpha complementation to be used as a screening tool for the plasmids containing DNA, the plates contained 80 µg/ml X-Gal (5-bromo-4-chloro-3-indolyl-β-D-

galactoside, Promega) and 0.5 mM IPTG (Isopropyl β -D-1-Thiogalactopyranoside; Promega). Colony PCR was performed on white colonies using SP6 and T7 primers, with positive colonies selected for culture. Selected plasmid colonies with amplicons of the correct approximate size were purified using the Wizard Plus Miniprep DNA Purification System (Promega) and the inserts sequenced (Eurofins MWG). The PCR was repeated with cDNA from four further horses selected at random (DV3, DV5, DV6, DV10), with cDNA from DV12 and DV11 amplified to act as positive controls. The PCR products from DV3, DV6 and DV10 were also ligated, transformed, purified and sequenced (as above) to examine any differences in nucleotide sequence in the genes of interest between horses and to confirm specificity of the primers.

4.3.2 House Keeping Gene Selection

The geNorm Reference Gene Selection Kit (Primerdesign) was used to establish the optimal reference genes utilising SYBR green detection chemistry. The six reference targets were; beta-actin (ACT β), beta-2-microglobulin (B2M), hypoxanthine phosphoribosyltransferase (HPRT), glyceraldehyde 3-phosphate dehydrogenase (GAPDH), 18s ribosomal RNA (RN18S) and succinate dehydrogenase complex, subunit A, flavoprotein SDHA. Fifteen equine tissue samples were selected at random for preliminary analysis. The samples analysed represented a range of sample sites, genders and ages (Table 4.3).

Sample Number	Horse	Site	Sex	Age (yrs)
1	DV12	C	Male	1
2	DV8	RVC	Male	>15
3	DV6	C	Female	4
4	DV7	C	Male	4
5	DV3	C	Female	3
6	DV12	RB	Male	1
7	DV11	C	Female	25
8	DV7	RVC	Male	4
9	DV6	RB	Female	4
10	DV8	RB	Male	>15
11	DV12	RVC	Male	1
12	DV7	RB	Male	4
13	DV6	RVC	Female	4
14	DV11	RVC	Female	25
15	DV8	C	Male	>15

Table 4.3: Table of the 15 samples of equine tissue selected at random for geNorm analysis. (C: Caecum; RVC: Right ventral colon; RB: Rectal biopsy).

SYBR green *Precision*TM 2X qPCR Mastermix (Primerdesign) was prepared as per manufacturer's instructions. Lyophilised primer was re-suspended in 220 µl RNase free water. A reaction mix (15 µl) containing 1 µl primer suspension, 10 µl PrimerDesign *Precision*TM 2X qPCR Mastermix and 4 µl RNase-free water was added per well. The reactions were performed in quadruplicate. To each well, 5 ng of appropriate cDNA were added to give a final volume of 20 µl. The qPCR was performed using an ABI 7500 machine (Applied Biosystems) under cycling conditions of 10 min at 95 °C, followed by 50 cycles of 15 sec at 95 °C and 60 sec at 60 °C. The geNorm analysis was performed using qbase^{plus} real-time PCR data analysis software (qbase+).

4.3.3 Probe Design for Quantitative PCR for Genes of Interest

Probes were designed for qPCR for each of the four sequences (TLP1, GZMBL, CLP1, GZM(BGH)L) under investigation. Using the blastn suite in NCBI for the equine genome (organism *E. caballus*), each amplicon was aligned with its relevant related sequence results and target areas (highlighted in green) of difference identified (Figures 4.1-4). As the Blastn search for the TLP1 sequence returned no significant related hits, the similarity of TLP1 with the other three selected sequences was assessed (Figure 4.1). Dual-labelled hydrolysis probes (Table 4.4), Taqman (Eurofins MWG), were designed based on the parameters used by Beacon Designer™ and AlleleID®. To comply with these parameters, the probe for sequence GZM(BGH)L was reversed to ensure that the number of G's and C's at the 3' end did not exceed two. Probes were labelled with the fluorescent dye 6-carboxyfluorescein (FAM, Eurofins MWG) at the 3' end and a non-fluorescent quencher, Black Hole Quencher 1 (Eurofins, MWG) at the 5' end.

Gene	Probe Sequence	Probe length (bp)	Probe Melting Temp (°C)	GC Content
TLP1	5'-TGTGACAGGAAATACCACACTGGC-3'	24	72	50%
GZMBL	5'-AGCTGACTGTGCAGCAGGATCAG-3'	23	72	40%
CLP1	5'-TCATCTGTGAGAACGGGCTCCAG-3'	23	72	40%
GZM(BGH)	5'- CTTCGGTAAGCTTGGCCCTTCTC -3'	23	72	40%

Table 4.4: Table of probe sequences and related information for each of the four genes of interest. The bolded sequence for the probe for GZM(BGH)L was reversed in accordance with optimal parameters. (TLP1: Trypsin-like Proteinase-1; GZMBL: Granzyme B-Like; CLP1: Chymase-like Proteinase-1; GZM(BGH)L: Granzyme(BGH)-like).

Mast Cell Recruitment and Activation as Measures of Cyathostomin Burden

```

TLP1      GGGCGATGTCGACAATGGAGTCAGTCTGCCACCTCCGTTCCCTGAAGGAAGTAAAGT
CLP1      GGGGCAACTTGGCCCGAAGGGCAGGTTCACAG-----ACACACTGCAGGAGGTGGAAGT
GZMBL     GGGGAGAGTACACCCCAATGGCAGAGGGTCAG-----ACACCTGCAGGAGGTGGAGCT
GZM(BGH) L GGGGAGAGTTGCCCTAAATGGCAGAGCGTCAG-----ACACTCTGCAGGAGGTGGAGCT
          ***  .: * .*. . . * ***      : . * ***.***.***.***. *

TLP1      CCCCATTTGTGAAACAGCGTTTGTGACAGGAAATACCACACTGGCGTGTCCACGGGGGA
CLP1      GACTGTGCAGCAGGATGAGGTGTGCG-----AATCCTACTTCCGCAATTA-----TTT
GZMBL     GACTGTGCAGCAGGATCAGGTGTGCG-----AATCCTACTTGGCAATTA-----
GZM(BGH) L GACCGTGCAGCAGGACAGGAGTGC-----AATCCTACTTACAAAAGTA-----
          . * . * : * .*. * .: * * *      ***. * ***: . . .: * .

TLP1      CAACATCCGGATTGTCCAAGCCGACATGCTGTGTGCAAGGAATAGGAGGCACGACA----
CLP1      CAACA---G-----T---ACCACCTAGCTGTGTAGGGGATCCGAAAGATAAGGAAGTC
GZMBL     CAACC---G-----T---ACCACCTAGCTGTGTGTGGGGACCCGAAGGAAAAGAGTGC
GZM(BGH) L CAACA---G-----T---ACCACCTAGCTGTGTGTGGGGACCCGAAGGAAAAGAGTGC
          ***.  *      *      .***. .:*****.***. * .***. * . *

```

Figure 4.1: Alignment of the four amplicons of interest with primers (blue) and probe (green) for TLP1 highlighted. (TLP1: Tryptase-like Proteinase-1; GZMBL: Granzyme B-like; CLP1: Chymase-like Proteinase-1; GZM(BGH)L: Granzyme(BGH)-like).

* - indicates positions which have a single, fully conserved residue.

: - indicates conservation between groups of strongly similar properties - scoring > 0.5 in the Gonnet PAM 250 matrix.

. - indicates conservation between groups of weakly similar properties - scoring = < 0.5 in the Gonnet PAM 250 matrix.

```

GZMBL      CAGCCTGCCCTGGGGAACAGCCCCAGCTGAGGCCTGGAGAGGTGTGCAGTGTGGCAGGCTG
gi |194238883|ref|XM_001488635.2| CCGCCTGCCCTGGTCCAAGGCCAGGTGAGGCCCGAGCAGGTGTGCAGTGTGGCGGATG
gi |194207238|ref|XM_001487881.2| CAGCCTGCCCTGGGGCACAGCCCCAGGTGAGGCCTGGAGAGCTGTGCAGTGTGGCCGGCTG
gi |194238887|ref|XM_001915613.1| CAGCCTGCCCTGGGGCACAGCCCCAGGTGAGGCCCGGAGAGCTGTGCAGTGTGGCCGGCTG
gi |194238000|ref|XM_001914653.1| CAGCCTGCCCTGGGGCACAGCCCCAGGTGAGGCCCGGAGAGCTGTGCAGTGTGGCCGGCTG
gi |194207240|ref|XM_001488315.2| CAGCCTGCCCTGGGGAACAGCCCCAGGTGAGGCCTGGAGAGGTGTGCAGTGTGGCAGGCTG
gi |126352429|ref|NM_001081881.1| AAGCCTGCCCAGGGGCCAAGGCCAGGTGAGGCCCGGAGAGGTGTGCAGTGTGGCCGGATG
gi |338717980|ref|XM_001488278.3| AAGCCTGCCCAGGGGCCAAGGCCAGGTGAGGCCCGGAGAGGTGTGCAGTGTGGCCGGATG
gi |338728626|ref|XM_001488566.3| CAACCTGCCCAGGGGCCACAGCCCAGGTGAGGCCCGGAGAGGTGTGCCTGTGGCTGGCTG
gi |338717962|ref|XM_001488193.3| CAGCCTGCCCTGGGGCACAGCCCCAGGTGAGGCCTGGAGAGGTGTGCAGTGTGGCTGGCTG
gi |338717963|ref|XM_001488406.3| CAGCCTGCCCAGGGGCCACAGCCCCAGGTGAGGCCTGGAGAGGTGTGCAGTGTGGCGGGCTG
gi |149692884|ref|XM_001488513.1| CAGCCTGCCCAGGGGCCACAGCCCCAGGTGAGGCCTGGAGAGGTGTGCAGTGTGGCTGGCTG
          ...*****:*** .:..***** .***** ** ** *****:***** ** **

GZMBL      GGGGAGAGTACACCCCAATGGCAGAGGGTCAGACACCTGCAGGAGGTGGAGCTGACTGT
gi |194238883|ref|XM_001488635.2| GGGGTAAGTACACCCCAATGGCAGCTTCTCAGACACACTGCAGGAGGTGGAGCTGACTGT
gi |194207238|ref|XM_001487881.2| GGGGAGAGTCACTTCCAAATGGCACAGGGTCAGACACTCTGCAGGAGGTGGAGCTGACCGT
gi |194238887|ref|XM_001915613.1| GGGGAGAGTACACCCCAATGGCAGAGTGTCAAACTCTGCAGGAGGTGGAGCTGACCGT
gi |194238000|ref|XM_001914653.1| GGGGAGAGTACACCCCAATGGCAGAGTGTCAAACTCTGCAGGAGGTGGAGCTGACCGT
gi |194207240|ref|XM_001488315.2| GGGGAGAGTCACTTCCAAATGGCAGAGGGTCTGACACTCTGCAGGAGGTGGAGTGGAGT
gi |126352429|ref|NM_001081881.1| GGGGAGAGTCTTCCCTGATGGGCAGCTTCTCAGACACCTGCAGGAGGTGGAGCTGACTGT
gi |338717980|ref|XM_001488278.3| GGGGTAAGTCTTCCCGATGGGCAGCTTCTCAGACACCTGCAGGAGGTGGAGCTGACCGT
gi |338728626|ref|XM_001488566.3| GGGGAGAGTGTGCCCTAAATGGCAGAGCTCAGACACTCTGCAGGAGGTGGAGCTGACCGT
gi |338717962|ref|XM_001488193.3| GGGGAGAGTACACCCCAATGGCAGAGCACTCACTTCTGCAGGAGGTGGAGCTGACCGT
gi |338717963|ref|XM_001488406.3| GGGGAGAGTGTGCCCAATGGCAGAGGGTCAGACACCTGCAGGAGGTGGAGCTGACCGT
gi |149692884|ref|XM_001488513.1| GGGGAGTGTGCCCAATTCGGCAGAGCACTCGACACTCTGCAGGAGGTGGAGCTGACCGT
          ***. * : * * * .: .:*** . ** .:*** **********. **** **

GZMBL      GCAGCAGGATCAGGTGTGCGAATCCTACTTTGGCAAT--TACAACCGTACCACCTCAGCT
gi |194238883|ref|XM_001488635.2| GCAGCAGGACAGGTAAGCTGAATCCTACTTACACAATTATCACAACAGTACCACCTCAGCT
gi |194207238|ref|XM_001487881.2| GCAGCAGGACAGGGGTGTGCGAATCCTACTTACGCAAT--TACAACAGTAACACTCAGCT
gi |194238887|ref|XM_001915613.1| GCAGCAGGACAGGGGTGTGCGAATCCTACTTACGCAAT--TACAACAGTAACACGCAGTT
gi |194238000|ref|XM_001914653.1| GCAGCAGGACAGGGGTGTGCGAATCCTACTTACGCAAT--TACAACAGTAACACGCAGTT
gi |194207240|ref|XM_001488315.2| GCAGCAGGACAGGGGTGTGCAATCCTACTTATGCAAT--TACAACAGTACCACCTCAGCT
gi |126352429|ref|NM_001081881.1| GCAGCAGGACAGGGGAATGTGAATCTTACTTACGCAATTATTACAACAGTACCACCTCAGCT
gi |338717980|ref|XM_001488278.3| GCAGCAGGACAGGGATGCGAATCTTACTTACGCAATTATTACAATAGTACCACCTCAGCT
gi |338728626|ref|XM_001488566.3| GCAGCAGGACAGGAGTGGCAATCCTACTTACAAAG--TACAACAGTACCACCTCAGCT
gi |338717962|ref|XM_001488193.3| GCAGCAGGACAGCGTGTGCAATCCTACTTACGCAAT--TACAACAGTACCACCTCAGCT
gi |338717963|ref|XM_001488406.3| GCAGCAGGACAGGGGTGTGCGAATACTACTTTACAAT--TACAACAGTACCACCTCAGCT
gi |149692884|ref|XM_001488513.1| GCAGCAGGACTGGGAGTGGCAATTCTATGGCAAT--TACAACAAGACCACTCAGCT
          ***** .: .: * .*. * : * .: * .:*****.***.*** **

```

Figure 4.2: Alignment of relevant equine proteinase predicted sequences from blastn of granzyme B-like (GZMBL) amplicon (*E. caballus*) with highlighted primer sequences (blue) and selected probe sequence (green). The red areas are nucleotides that match the GZMBL sequence and the yellow are areas of difference.

* - indicates positions which have a single, fully conserved residue.

: - indicates conservation between groups of strongly similar properties - scoring > 0.5 in the Gonnet PAM 250 matrix.

. - indicates conservation between groups of weakly similar properties - scoring = < 0.5 in the Gonnet PAM 250 matrix.

Mast Cell Recruitment and Activation as Measures of Cyathostomin Burden

```

CLP1
gi | 338728628 | ref | XM_001489068.3 AACAGTACCACTCAGCTGTGTGTAGGGGA TCCGAAAGATAAGAAGTCTTCCTTCAGGGT
AACAGTACCACTCAGCTGTGTGTAGGGGA CCGAAGGT TAAGAAGTCTTCCTTCAGGGC
*****_*:*****

CLP1
gi | 338728628 | ref | XM_001489068.3 GACTCTGGGGGCCCTC CATCTGTGAGAACGGGCTCCAG GGCATTGTCTCCTATGGACTA
GACTCTGGGGGCCCTCTCATCTGTGAGAACGGT TCCAGGGGCAATTGTCTCCTATGGACTG
*****_*:*****

CLP1
gi | 338728628 | ref | XM_001489068.3 GATAACGGGAGTATTCCACAGGCCTT CACCAAAGTCTCGAGTTTCTGCCCTGGATAAAG
GATAACGGGAGTCTTCCAG GGCCTT CACCAAAGTCTCGAGTTTCTGCCCTGGATAAAG
*****_*:*****

```

Figure 4.3: Alignment of both equine proteinase predicted sequences from blastn of Chymase-like Proteinase-1 (CLP1) amplicon (*E. caballus*) with highlighted primer sequences (blue) and selected probe sequence (green). The red areas are nucleotides that match the CLP1 sequence and the yellow are areas of difference.

* - indicates positions which have a single, fully conserved residue.

: - indicates conservation between groups of strongly similar properties - scoring > 0.5 in the Gonnet PAM 250 matrix.

. - indicates conservation between groups of weakly similar properties - scoring = < 0.5 in the Gonnet PAM 250 matrix.

```

GZM(BGH)L
gi | 338717963 | ref | XM_001488406 CCACCCAGACTATAATTCTAAGAAGTTCGCCAACGACATCATGTTACTAA
gi | 149692884 | ref | XM_001488513 CCACCCAGACTATAATTCTAAGAAGTTCGCCAACGACATCATGTTACTAA
gi | 126352429 | ref | NM_001081881 ACACCCAGACTATAAACCCTAAGAAGTTCGCCAACGACATCATGTTACTAA
gi | 338717980 | ref | XM_001488278 ACACCCAGACTATAAACCCTAAGAAGTTCGCCAACGACATCATGTTACTAA
gi | 338728628 | ref | XM_001489068 CCACCCAGACTATAATTCTAAGAAGTTCGCCAACGACATCATGTTACTAA
gi | 194238887 | ref | XM_001915613 CCACCCAGACTATAAACCCTAAGAAGTTCGCCAACGACATCATGTTACTAA
gi | 194238000 | ref | XM_001914653 CCACCCAGACTATAAACCCTAAGAAGTTCGCCAACGACATCATGTTACTAA
gi | 338728630 | ref | XM_001489737 CCACCCAGACTATAATTCTAAGAAGTTCGCCAACGACATCATGTTACTAA
gi | 338728709 | ref | XM_003365684 CCACCCAGACTATAATTCTAAGAAGTTCGCCAACGACATCATGTTACTAA
..*****_*:*****

GZM(BGH)L
gi | 338717963 | ref | XM_001488406 AGCTGGAGAGAGAGGCGCAAGCTTACCGAAGCTGTGTGGCCCTCAACCTG
gi | 149692884 | ref | XM_001488513 AGCTGGAGAGAGAGGCGCAAGCTTACCGAAGCTGTGTGGCCCTCAACCTG
gi | 126352429 | ref | NM_001081881 AGCTGGAGAGAGAGGCGCAAGCTTACCGAAGCTGTGTGGCCCTCAACCTG
gi | 338717980 | ref | XM_001488278 AGCTGGAGAGAGAGGCGCAAGCTTACCGAAGCTGTGTGGCCCTCAACCTG
gi | 338728628 | ref | XM_001489068 AGCTGGAGAGAGAGGCGCAAGCTTACCGAAGCTGTGTGGCCCTCAACCTG
gi | 194238887 | ref | XM_001915613 AGCTGGAGAGAGAGGCGCAAGCTTACCGAAGCTGTGTGGCCCTCAACCTG
gi | 194238000 | ref | XM_001914653 AGCTGGAGAGAGAGGCGCAAGCTTACCGAAGCTGTGTGGCCCTCAACCTG
gi | 338728630 | ref | XM_001489737 AGCTGGAGAGAGAGGCGCAAGCTTACCGAAGCTGTGTGGCCCTCAACCTG
gi | 338728709 | ref | XM_003365684 AGCTGGAGAGAGAGGCGCAAGCTTACCGAAGCTGTGTGGCCCTCAACCTG
****_*:*****

GZM(BGH)L
gi | 338717963 | ref | XM_001488406 CCCAGGGGCACAGCCAGGTGAGGCCCGGAGAGGTGTGCCGTGTGGCTGG
gi | 149692884 | ref | XM_001488513 CCCAGGGGCACAGCCAGGTGAGGCCCTGGAGAGGTGTGCCGTGTGGCTGG
gi | 126352429 | ref | NM_001081881 CCCAGGGGCACAGCCAGGTGAGGCCCGGAGAGGTGTGCCGTGTGGCTGG
gi | 338717980 | ref | XM_001488278 CCCAGGGGCACAGCCAGGTGAGGCCCGGAGAGGTGTGCCGTGTGGCTGG
gi | 338728628 | ref | XM_001489068 CCCAGGGGCACAGCCAGGTGAGGCCCGGAGAGGTGTGCCGTGTGGCTGG
gi | 194238887 | ref | XM_001915613 CCCAGGGGCACAGCCAGGTGAGGCCCGGAGAGGTGTGCCGTGTGGCTGG
gi | 194238000 | ref | XM_001914653 CCCAGGGGCACAGCCAGGTGAGGCCCGGAGAGGTGTGCCGTGTGGCTGG
gi | 338728630 | ref | XM_001489737 CCCAGGGGCACAGCCAGGTGAGGCCCGGAGAGGTGTGCCGTGTGGCTGG
gi | 338728709 | ref | XM_003365684 CCCAGGGGCACAGCCAGGTGAGGCCCGGAGAGGTGTGCCGTGTGGCTGG
***:***_*:*****

GZM(BGH)L
gi | 338717963 | ref | XM_001488406 CTGGGGGAGAGTTCGCCCTAAATGGCAGAGCGTCAGACACTCTGCAGGAGG
gi | 149692884 | ref | XM_001488513 CTGGGGGAGAGTTCGCCCTAAATGGCAGAGCGTCAGACACTCTGCAGGAGG
gi | 126352429 | ref | NM_001081881 ATGGGGGAGAGTCTCCCTGATGGGACGCTTCTCAGACACGCTGCAGGAGG
gi | 338717980 | ref | XM_001488278 ATGGGGGAGAGTCTCCCTGATGGGACGCTTCTCAGACACGCTGCAGGAGG
gi | 338728628 | ref | XM_001489068 CTGGGGGCAACTTGGCCCCAAAGGGCAGGTTCCGAGACACACTGCAGGAGG
gi | 194238887 | ref | XM_001915613 CTGGGGGAGAGTCAACCCAAATGGCAGAGTGTCAAACACTCTGCAGGAGG
gi | 194238000 | ref | XM_001914653 CTGGGGGAGAGTCAACCCAAATGGCAGAGTGTCAAACACTCTGCAGGAGG
gi | 338728630 | ref | XM_001489737 CTGGAGGCTAATTCGGCCCAATGGCATAATTTCCAACACACTGCGGGAGG
gi | 338728709 | ref | XM_003365684 TTGGAGGCTAATTCGGCCCTAAAGGCATAATTTCCAACACACTGTGGGAGG
***_*:*****

```

Figure 4.4: Alignment of relevant equine proteinase predicted sequences from blastn of Granzyme(BGH)-like (GZM(BGH)L) amplicon (*E. caballus*) with highlighted primer sequences (blue) and selected probe sequence (green). The red areas are nucleotides that match the GZM(BGH)L sequence and the yellow are areas of difference.

* - indicates positions which have a single, fully conserved residue.

: - indicates conservation between groups of strongly similar properties - scoring > 0.5 in the Gonnet PAM 250 matrix.

. - indicates conservation between groups of weakly similar properties - scoring = < 0.5 in the Gonnet PAM 250 matrix.

4.3.4 Probe design for Quantitative PCR housekeeping genes

Probes were designed for the two chosen housekeeping genes, selected from the geNORM results, GAPDH and SDHA (Primerdesign). Probes were verified using cDNA from samples DV8 C and DV12 RVC. For consistency, the housekeeping probes were also labelled with FAM and Black Hole Quencher1.

4.3.5 Generation of Plasmid Standards for Quantitative PCR

Plasmids containing inserts purified from amplicons of the four sequences of interest (TLP1, GZMBL, CLP1, GZM(BGH)L) were purified. A spectrophotometer was used to determine the concentration of DNA in preparations of the purified plasmids and, from this value, the number of copies calculated using the formula:

$$\text{Number of copies} = \frac{\text{quantity (ng)} \times 6.022 \times 10^{23}}{\text{length (bp)} \times 1 \times 10^9 \times 650}$$

The qPCR reaction was performed under the conditions; 94 °C for 5 min, followed by 45 cycles of 94 °C for 30 sec, 55 °C for 30 sec and a data collection step of 72 °C for 32 sec.

4.3.6 Probe Verification

Combinations of primers and probes were tested. Each primer set was tested in duplicate with each of the four different probes, 0.5 µl of the relevant forward and reverse primers (10 µM each), 0.25 µl of relevant probe (10 µM) and 5 µl of template (cDNA diluted 1:10). Because the experiment required a large amount of cDNA, samples from four horses were selected at random, one for each primer set. DV10 RVC was used for TLP1, DV7 caecum for GZMBL, DV12 caecum for CLP1 and DV9 caecum for GZM(GBH)L. The qPCR was performed using a ABI 7500 cycler under conditions of 94 °C for 5 min, followed by 45 cycles of 94 °C for 30 sec, 55 °C for 30 sec and a data collection step of 72 °C for 32 sec.

4.3.7 Quantitative PCR of Equine Tissue Samples

Proteinase transcript levels were measured by relative qPCR using the standard curve method. For each plate standard curves were generated using plasmids containing the DNA sequence of the relevant genes of interest or the reference genes. Amplifications for the standard curve were performed in triplicate and diluted over a range of 10^5 copies/ μ l to 1 copy/ μ l. All cDNA samples were analysed in duplicate. Negative controls were prepared using an identical mastermix, but with 5 μ l of PCR-grade water instead of cDNA. Each qPCR reaction consisted of 6.2 μ l PCR grade H_2O , 12.5 μ l mastermix (Invitrogen), 0.05 μ l reference dye (ROX), 0.5 μ l of the relevant forward and reverse primers (10 μ M each), 0.25 μ l of relevant probe (10 μ M) and 5 μ l of template (cDNA diluted 1:10). The qPCR was performed using the ABI 7500 cyclor under conditions of 94 °C for 5 min, followed by 45 cycles of 94 °C for 30 sec, 55 °C for 30 sec and a data collection step of 72 °C for 32 sec. Levels of gene transcript in each sample were evaluated using ABI 7500 software (Applied Biosystems), and the results normalised to the two selected reference genes, GAPDH and SDHA. This was performed by calculating the geometric mean of the reference genes and, subsequently, deriving a normalisation coefficient for each cDNA sample by dividing the geometric mean of the reference genes by the average geometric mean from all the reference samples. The individual genes of interest were then normalised by dividing the copies/ μ l of cDNA by the normalisation coefficient for the same cDNA sample. All plates were run with a plasmid standard curve for absolute quantification. Samples were repeated if the difference between the duplicate results was greater than 1.5 Ct (threshold cycle).

4.3.8 Re-annotation of Equine Genome

The horse genome was re-annotated and this was made public in September 2013 (version EquCab 2.0) (Personal Communication: Wayne Matten, PhD). The four mast cell proteinase sequences were assessed and compared with the re-annotated entries in order to assure their accuracy.

4.3.9 Data Analysis

As the data were not normally distributed, non-parametric tests were selected. For optimal graphical representation, log transformed ($\log_{10}+1$) data is sometimes presented here. Statistical analyses and graphical displays were performed using R Studio (V 0.97.551), Minitab 15 statistical software and GraphPad Prism5. To investigate the relationships between mast cell measures, including Toluidine blue stained mast cell counts, eqMCP-1- and eqTRYP-labelled mast cell counts, ELISA serum and tissue values and qPCR results, correlations were assessed using the Spearman rank test. Standard linear regression analysis was used to explore the relationships between $\log_{10}+1$ transformed normalised proteinase results and $\log_{10}+1$ transformed combined total mucosal burdens (CTMB). The presence of *A. perfoliata* was added as a confounding variable. The associations were considered as statistically significant at $p<0.05$.

4.4 Results

4.4.1 Sequence Selection for Identification of Additional Proteinases

Protein stained SDS PAGE gels and immunoblots were performed in parallel on mastocytoma tissue, serum and mucosal tissue to identify proteins within regions recognised by the anti-eqMCP-1 and anti-eqTRYP antibodies for subsequent mass spectrometry analysis. The images are shown in Figures 4.5A and B for eqTRYP and 4.6A and B for eqMCP-1, respectively. Bands bound by the antibodies were used to guide excision of the protein bands of interest on the corresponding protein stained gel. Each lane was separated into three slices (Figures 4.5A and 4.6A), and each of these analysed separately. Two searches were performed on the deconvoluted MS/MS data, firstly using the NCBI non-redundant protein sequence databases and Mascot™ V2.2 (Matrix Science) search algorithm, followed by the second database containing the two initial sequences of interest, TLP1 and CLP1, which had previously been submitted to NCBI by Dacre et al. 2005. These searches identified seven novel predicted equine sequences and confirmed the presence of TLP1 and CLP1. After both searches a final database was compiled of nine candidates (GranzymeDB). This database included the proteins TLP1 and CLP1. The NCBI sequence identifiers for the nine sequences were gi126352403 (TLP1), gi126352661 (CLP1), gi338728629, gi338728627, gi194238001, gi194207243, gi149692885, gi194207249 and gi194207247 respectively.

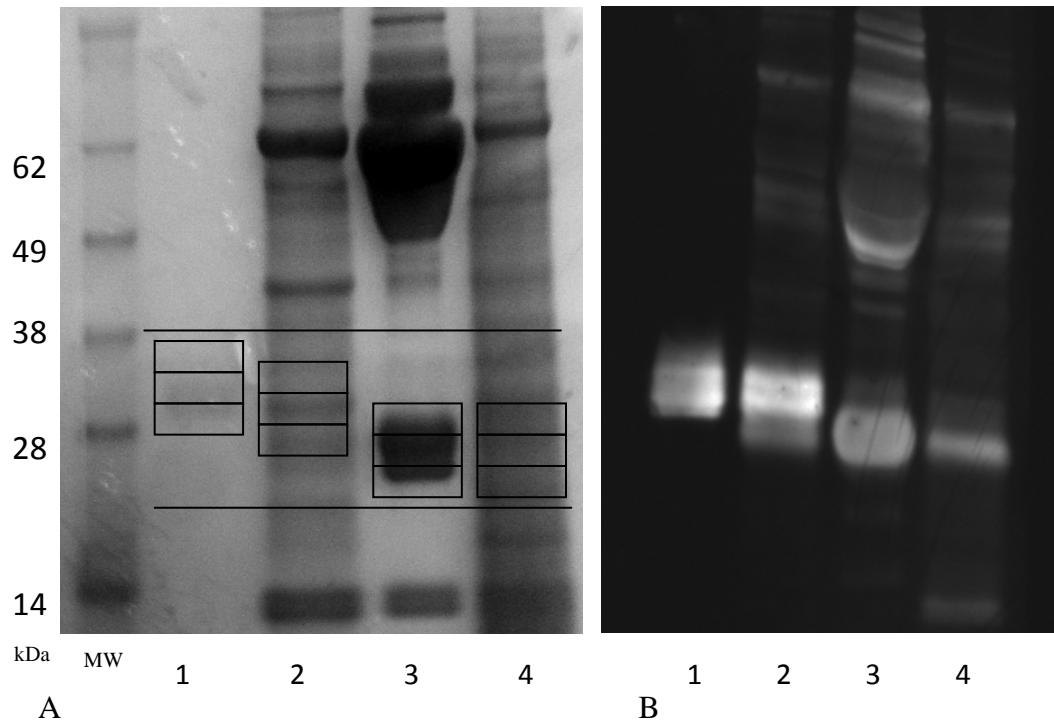


Figure 4.5: A: EqTRYP SDS PAGE gel showing the three slices each lane was divided into. B: The corresponding Western blot probed with rabbit IgG anti-eqTRYP (1 µg/ml) and developed with ECL. Lane 1: Purified eqTRYP. Lane 2: Equine mastocytoma tissue homogenate. Lane 3: Equine serum. Lane 4: Equine right ventral colon tissue homogenate.

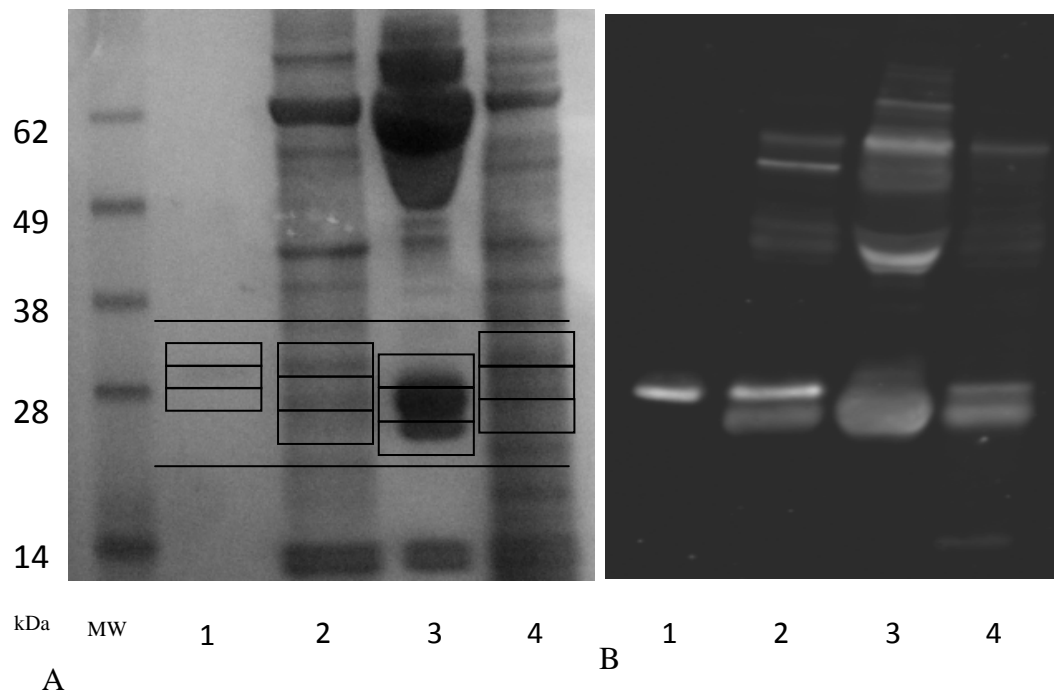


Figure 4.6: A: EqMCP-1 SDS PAGE gel showing the three slices each lane was divided into. B: The corresponding eqMCP-1 western blot probed with rabbit IgG anti-eqMCP-1 (1 µg/ml) and developed with ECL. Lane 1: Purified eqMCP-1. Lane 2: Equine mastocytoma tissue homogenate. Lane 3: Equine serum. Lane 4: Equine right ventral colon tissue homogenate.

Mast Cell Recruitment and Activation as Measures of Cyathostomin Burden

[illegible]

Figure 4.7: Alignment of the nine novel proteinase candidates in granzymeDB identified by Mascot database search. The areas highlighted in red are peptide sequences defined from the Mascot results that are unique to the proteins of interest. The pink highlighted area denotes the start and end of each unique sequence. The areas highlighted in yellow are peptide sequences that are not unique and match one or more of the granzymeDB protein sequences.

The sequences within the GranzymeDB database were aligned using Clustal Omega (Goujon, McWilliam et al. 2010; Sievers, Wilm et al. 2011) and examined to identify unique peptide sequences from the Mascot results (Figure 4.7). The nine sequences of GranzymeDB were also aligned and compared to ovine MCP1, and human and mouse GZMB (Figure 4.8) to identify aa residues at position 226 as this is important for conferring specificity (Smyth, O'Connor et al. 1996). GranzymeDB sequences were grouped according to this residue. Group 1 had a glycine at 226 (blue), Group 2, like mouse and human GZMB, had an arginine (pink) and Group 3 had a glutamine (green). These proteins are listed in Table 4.5 and were classified as granzyme or mast cell proteinase related. The slices of gel (Figure 4.5 and 4.6) were analysed to identify the proteinase sequences in each lane. In lane 1 of the eqTRYP gel, which contained purified eqTRYP (Figure 4.5), the only identified sequence from the GranzymeDB database was TLP1. In lane 1 of the eqMCP-1 gel, containing purified eqMCP-1 (Figure 4.6), GZM(GBH)L was the only proteinase identified. The equine mastocytoma (Lanes 2: Figures 4.5 and 4.6) contained TLP1, GZMBL, GZM(BGH)L and CLP1 as well as two other sequences categorised alongside GZMBL in Group 2, gi338728629 and gi194207243. From the analysis of eqTRYP and eqMCP-1 slices derived from equine serum lanes (Lanes 3: Figures 4.5 and 4.6), no significant matches against any of the sequences in the GranzymeDB sequences in any slices were identified. The most abundant equine protein in all six slices from lanes in which serum was loaded was immunoglobulin lambda light chain. GZMBL, GZM(BHG)L, TLP1 and gi194207247 (Group 2) were confirmed in the lanes containing equine intestinal tissue (Lanes 4: Figures 4.5 and 4.6). CLP1 was not confirmed in any of the equine intestinal tissue sections however its presence in equine tissue (bronchus, bronchiole, colon, liver and skin) has been previously confirmed (Dacre 2005). In addition, the equine genome was investigated using the NCBI and ensemble databases. The chymase locus was found to be situated on chromosome 1 and the tryptase locus on chromosome 13.

Four sequences were selected for further analyses (Table 4.5: highlighted in yellow) on the following basis. First, Tryptase-like Proteinase-1 (TLP1) was the tryptase sequence previously sequenced from equine tissue (Dacre, McAleese et al. 2006) and was selected due to its presence in equine mastocytoma and tissue. Chymase-like Proteinase-1 (CLP1) was the sequence of the putative eqMCP-1 cloned and characterised previously (Dacre 2005). This sequence was selected also due to its previously confirmed presence in equine tissue (Dacre 2005). Due to a combination of identification of unique peptides not identified in the other proteinase sequences and presence, identified here, in equine tissue, two further sequences were identified and selected. One of these was a sequence from Group 2, Granzyme B-like (GZMBL) and the second was a sequence from Group 3, Granzyme(BGH)-like (GZM(BGH)L).

Group 1	gi 126352403	ref NP_001075344.1	TLP1	CQGDSSGGPLVCKVKGTWLQAGVVSANSCAQPNRPGIYTRVTYYLDW
Group 1	gi 194207247	ref XP_001488456.2		YKGDSSGGPLMCKNM----IQGIVSYGRRGG--IPPGAFATKVVSSFLPW
Group 2	gi 338728629	ref XP_001489118.3		FQGDSSGGPLICENG----LQGIVSYGLDNG--SPPRAFTKVSSFLPW
Group 2	gi 194207243	ref XP_001488243.2		FKGDSSGGPLVCNNL----IQGLVSYGRGNG--TPPRAFTKVSSFLPW
Group 2	gi 194207249	ref XP_001488476.2	GZMBL	YKGDSSGGPLVCKNV----IQGIVSYGRSGG--LPPRAFTKVSSFLPW
Group 3	gi 126352661	ref NP_001075345.1	CLP1	FQGDSSGGPLICENG----LQGIVSYGLDNG--SIDRAFTKVSSFLPW
Group 3	gi 338728627	ref XP_001488616.3	GZMBGHL	FKGDSRGTLVCKNV----IQGIVSYGRIGG--IPPRAFATKVSSFLPW
Group 3	gi 194238001	ref XP_001914688.1		FKGDSSGGPLVCENV----IQGLVSYGRRDG--TPPRAFTKVSSFLPW
Group 3	gi 149692885	ref XP_001488563.1		YKGDSSGGPLVCKNV----IQGIVSYGRIGG--IPPRAFATKVSSFLPW
		MCP1 ovis aries		FSGDSSGGPLVCNGV----AQGIVSYGKDDG--TPPDVYTRISSFLSW
		GZMB Mus musculus		FRGDSSGGPLVCKKV----AAGIVSYGYKDG--SPPRAFTKVSSFLSW
		GZMB Homo Sapiens		FKGDSSGGPLVCNKV----AQGIVSYGRNNG--MPPRACTKVSSFVHW
				*** * * *: * : * : * : * : * : * : * : * : * : * : * : * : *

Figure 4.8: Alignment of the nine sequences in the granzymeDB. The sequences were grouped according to the residue at 226 (highlighted). Group 1 (Blue: glycine), Group 2 (Pink: arginine), Group 3 (Green: glutamine). Results are compared to the sequences for MCP1 *Ovis Aries*, GZMB *Mus Muscularis* and GZMB *Homo Sapiens* (Yellow) with known specificity. (TLP1: Tryptase-like Proteinase-1; GZMBL: Granzyme B-Like; CLP1: Chymase-like Proteinase-1; GZM(BGH)L: Granzyme(BGH)-like).

Mast Cell Recruitment and Activation as Measures of Cyathostomin Burden

	Sequence	Residue at 226	No. Unique Peptides	Purified eqMCP1	Equine Mastocytoma	Equine Tissue	Purified eqTRYP	Equine Serum
Group 1								
	gi126352403 TLP1	G	10	No	Yes	Yes	Yes	No
	gi194207247	G	0	No	No	No	No	No
Group 2								
	gi194207249 GZMBL	R	2	No	Yes	Yes	No	No
	gi338728629	R	3	No	Yes	No	No	No
	gi194207243	R	3	No	Yes	No	No	No
Group 3								
	gi338728627 GZM(BG)HL	Q	6	Yes	Yes	Yes	No	No
	gi126352661	Q	3	No	Yes	No	No	No
	gi149692885	Q	1	No	No	No	No	No
	gi194238001	Q	1	No	No	No	No	No

Table 4.5: Table of the nine GranzymeDB sequences grouped according to their aa at residue 226. Group 1 (G: glycine), Group 2 (R: arginine), Group 3 (Q: glutamine). The number of unique peptides from the MASCOT results are shown. The presence or absence of each sequence in purified eqMCP-1, equine mastocytoma, equine tissue and purified eqTRYP are also shown. The four sequences highlighted in yellow were selected for further analysis. (TLP1: Trypsin-like Proteinase-1; GZMBL: Granzyme B-like; CLP1: Chymase-like Proteinase-1; GZM(BGH)L: Granzyme(BGH)-like).

The four sequences selected for subsequent analyses are aligned in Figure 4.9 with the sequences for sheep mast cell proteinase-1, mouse GZMB and human GZMB for comparison. These were selected for sequence comparison due to their known specificity. All seven sequences share the conserved catalytic triad, with a histidine at residue 57, aspartic acid at 102 and serine at 195 (highlighted in red). Equine TLP1 contains an aspartate at residue 189 (shown in blue), whereas in the equine other sequences, (CLP1, GZMBL and GZM(BGH)L) there is a serine at this site (shown in green). The sheep, mouse and human sequences all differ at residue 189 (shown in yellow). At residue 216, six of the sequences have a glycine (shown in pink and yellow); however, TLP1 differs here as it has an alanine. At residue 226 TLP1 has a glycine, where CLP1 and GZM(BGH)L both have a glutamine, GZMBL

and the human and murine sequences have an arginine. The TLP1 sequence has identity of about 50% identical amino acids across the entire granzyme-like and CLP1 sequences. CLP1, GZMBL and GZM(BGH)L are more similar and have approximately 80% sequence identity across their entire sequence.

Mast Cell Recruitment and Activation as Measures of Cyathostomin Burden

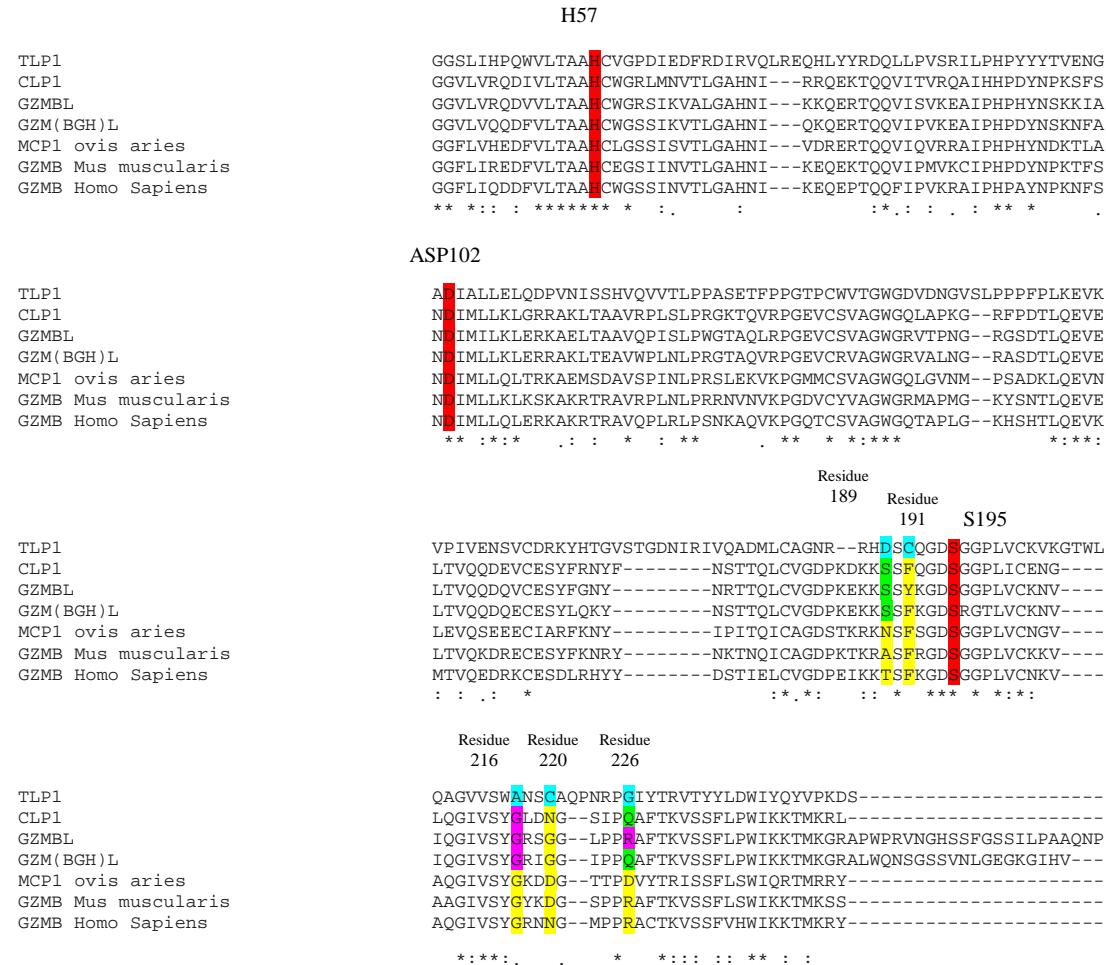


Figure 4.9: Alignment of the four selected sequences, TLPl, CLPl, GZMBL and GZM(BGH)L with MCP1 ovis aries, GZMB Mus Muscularis and GZMB Homo Sapiens for comparison and highlighted residues and important bases. (TLPl: Tryptase-like Proteinase-1; GZMBL: Granzyme B-like; CLPl: Chymase-like Proteinase-1; GZM(BGH)L: Granzyme(BGH)-like).

4.4.1.1 Comparison of N-terminal Amino Acid Sequence

The N-terminal aa sequences for each of the nine sequences in the GranzymeDB were aligned (Figure 4.10) to facilitate comparison between these sequences and those previously generated by Pemberton et al. (Pemberton, McEuen et al. 2001). This region was compared here as it had been previously described and determined to 20 residues (Pemberton, McEuen et al. 2001). As mentioned, two proteolytic components from equine mastocytoma tissue were previously purified and characterised (Pemberton, McEuen et al. 2001). The N-terminal aa sequence of TLP1 (Pemberton, McEuen et al. 2001), was found to be very similar to human beta and bovine tryptase (85% - 17 out of 20 aa) and to a lesser extent, to sheep tryptase 1 and tryptase 2 (75% - 15 out of 20 aa) (Figure 4.11). In these studies eqMCP-1 was found to be 95% identical to human granzyme H and 84% identical to bovine duodenase and SMCP-1. In the case of N-terminal aa sequencing for eqMCP-1 (Pemberton, McEuen et al. 2001), residue number 10 could not be assigned unambiguously, indicating both Pro and His (Table 4.12). It is probable that this ambiguity was due to carry-over from incomplete hydrolysis at residue 9 which would indicate that residue 10 is a His, similar to other MCP enzymes (Pemberton, McEuen et al. 2001). The N-terminal aa sequence of the mastocytoma derived eqMCP-1 differed from that of cloned putative eqMCP-1 (CLP1) by 2 aa (highlighted in yellow: Figure 4.12). This was hypothesised to be a similar but novel equine chymase (Dacre 2005). The N-terminal aa sequence for GZM(BGH)L (annotated by NCBI) has a matching sequence to that of the mastocytoma derived sequence, eqMCP-1 published previously (Pemberton, McEuen et al. 2001). As it is the most abundant granzyme from the purified equine chymase (Section 4.4.1) it is possible that GZM(GBH)L is the same protein (eqMCP-1) characterised previously (Pemberton, McEuen et al. 2001).

Mast Cell Recruitment and Activation as Measures of Cyathostomin Burden

TLP1			IVGGQEASGSKWPQVSLRK
CLP1			IIGGHEAKPHSRPYMALVQF
GZMBL			IIGGHEARPHSRPYMAFVQI
GZM(BGH)L			IIGGHEARPHSRPYMAFVQF
gi 338728629	ref XP_001489118.3		IIGGHEAWPHSRPYMALVQF
gi 194238001	ref XP_001914688.1		IIGGHEAKPHSRPYMVFVQC
gi 194207243	ref XP_001488243.2		IIGGHEARPHSRPYMAFVQF
gi 149692885	ref XP_001488563.1		IIGGHEAWPHSRPYMAFVLS
gi 194207247	ref XP_001488456.2		IIGGHEAWPHSRPYMAFVQI
			*:***:*** . *: . :

Figure 4.10: N terminal aa sequence of the 9 proteins in the granzymeDB database. (TLP1: Tryptase-like Proteinase-1; GZMBL: Granzyme B-like; CLP1: Chymase-like Proteinase-1; GZM(BGH)L: Granzyme(BGH)-like).

	1	10	20
TLP1	I V G G Q E A S G S K W P W Q V S L R K		
Human Tryptase-β	I V G G Q E A P R S K W P W Q V S L R V		
Sheep Tryptase-1	I I G G K E A P G S R W P W Q V S L R V		
Bovine Tryptase	I V G G Q E A P G S Q W P W Q V S L R V		

Figure 4.11: N terminal aa sequences from TLP1 compared with the sequences from human tryptase-β (Miller, Moxley et al. 1990), sheep tryptase-1 (Pemberton, McAleese et al. 2000) and bovine tryptase (Pallaoro, Gambacurta et al. 1996). (TLP1: Tryptase-like Proteinase-1).

	1	10	20
EqMCP-1	I I G G H E A R P X S R P Y M A F V Q F		
CLP1	I I G G H E A K P H S R P Y M A L V Q F		
GZMBL	I I G G H E A R P H S R P Y M A F V Q I		
GZM(BGH)L	I I G G H E A R P H S R P Y M A F V Q F		
Human granzyme H	I I G G H E A K P H S R P Y M A F V Q F		
SMCP-1	I I G G H E A K P H S R P Y M A F L Q I		
Bovine duodenase	I I G G H E A K P H S R P Y M A F L L F		

Figure 4.12: N terminal aa sequences from EQMCP-1, CLP1 and predicted sequences for GZMBL and GZMBGHL compared with the sequences human granzyme H (Haddad, Jenne et al. 1991), sheep mast cell proteinase-1 (McAleese, Pemberton et al. 1998) and bovine duodenase (Zamolodchikova, Vorotyntseva et al. 1995). (GZMBL: Granzyme B-like; CLP1: Chymase-like Proteinase-1; GZM(BGH)L: Granzyme(BGH)-like).

4.4.2 Sequence Analysis of PCR Products

PCR was performed using cDNA from caecal tissue from horse DV11 and RVC tissue from horse DV12 as template with specific oligonucleotide primers for each gene of interest (TLP1, GZMBL, CLP1 and GZM(BGH)L) designed from nucleotide sequences derived proteomic analysis to generate amplicons of 100-170 bp. The gel (Figure 4.13) shows amplicons at the expected length for each of the four sequences: 139 bp for TLP1, 136 bp for GZMBL, 117 bp for CLP1 and 160 bp for GZM(BGH)L.

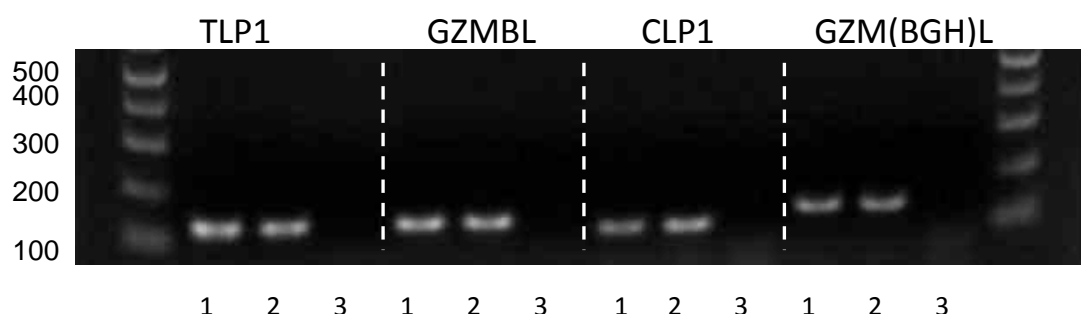


Figure 4.13: Agarose gel image showing the PCR products using the four primer sets generated from cDNA from horses DV11 and DV12. The size of the 1kb plus ladder (Invitrogen) is shown in bp. 1: DV11 Caecum; 2: DV12 RVC; 3: Negative Control. (RVC: Right ventral colon; TLP1: Tryptase-like Proteinase-1; GZMBL: Granzyme B-like; CLP1: Chymase-like Proteinase-1; GZM(BGH)L: Granzyme BGH LikeGranzyme(BGH)-like).

To ensure that the primers were able to amplify specific sequences from tissue derived from different horses, PCR was performed using cDNA from additional horses DV3, DV5, DV6, DV10, DV11 and DV12. The specific oligonucleotide primers were used for each of the genes of interest; TLP1 (Figure 4.14A), GZMBL (Figure 4.14B), CLP1 (Figure 4.14C), and GZM(BGH)L (Figure 4.14D). These figures show the PCR products generated. Amplicons of the expected size were produced from each of the six horses for all four genes. No PCR product was present in any of the negative control samples (no template control).

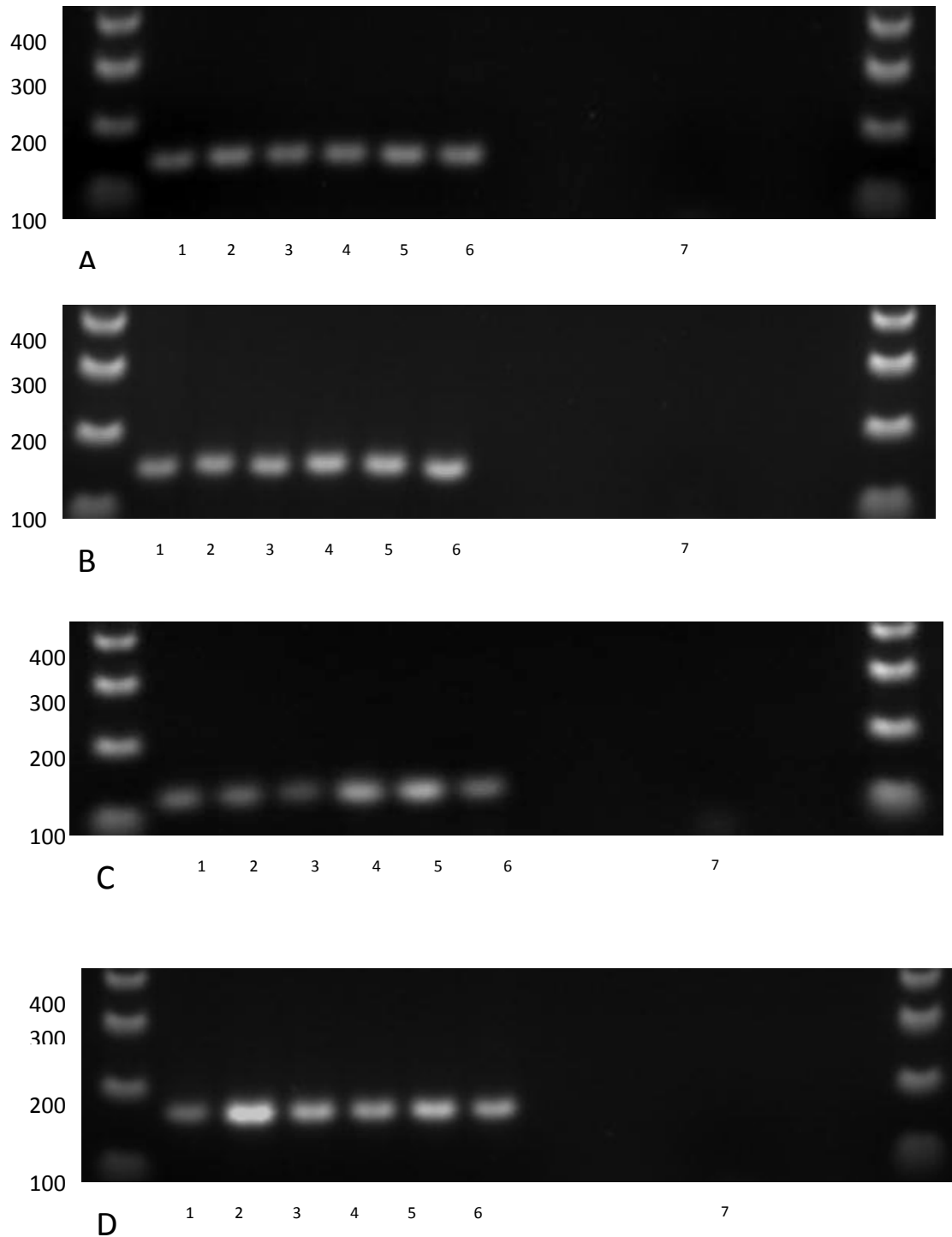


Figure 4.14: A-D: Agarose gel image showing the PCR products from caecal tissue from horse DV3, DV5, DV6, DV10, DV12 and DV11. The size of the 1kb plus ladder (Invitrogen) is shown in bp. A: TLP1 B: GZMBL C: CLP1 D: GZM(BGH)L. 1: DV3 caecum; 2: DV12 caecum; 3: DV6 caecum; 4: DV11 caecum; 5: DV10 caecum; 6: DV5 caecum; 7: Negative control. (TLP1: Tryptase-like Proteinase-1; GZMBL: Granzyme B-like; CLP1: Chymase-like Proteinase-1; GZM(BGH)L: Granzyme(BGH)-like.)

PCR products (two clones) from each horse, representing each of the four genes were submitted for sequencing. Sequences derived from these PCR products were compared with the original sequences used to design the primers, referred to here as ‘query’ sequences. The TLP1 amplicon nucleotide (Figure 4.15) and protein sequence (Figure 4.16) were identical to the query TLP1 sequence for all five horses. There were a number of differences in the nucleotide sequences between the five horses and the query GZMBL sequence. These were mainly seen in sequences from DV10 and DV12 which each had the same five single nucleotide polymorphisms (SNPs) when compared to the query sequence (Figure 4.17). Only two of these differences altered the translated sequence (Figure 4.18) resulting in the substitution of a glutamine from a glycine and an arginine from a glutamine (Fig 4.18). The CLP1 nucleotide sequences (Figure 4.19) showed two differences (highlighted in pink). Sequences from all horses had a cytosine in place of a thymidine at amplicon nucleotide position 32 which did not translate to any difference in the derived aa sequence (Figure 4.20). Sequence from horse DV3 had a SNP: a cytosine in place of a thymidine, which translated to a change from a serine to a proline at residue 214 (Figure 4.20). The GZM(BGH)L amplicon nucleotide sequences (Figure 4.21) showed two differences (highlighted in pink). Both were seen in sequences from horse DV3. There was cytosine in place of a thymidine, which translated to a difference in the aa sequence as a change from isoleucine to threonine at residue 103 (Figure 4.22). Sequence from horse DV3 also had a SNP at the end of the reverse primer sequence, an adenine in place of a guanine. This did not alter the protein sequence (Figure 4.22).

Mast Cell Recruitment and Activation as Measures of Cyathostomin Burden

```

QueryTLP1      AGTCAGTCTGCCACCTCCGTTTCCCCTGAAGGAAGTAAAAGTCCCCATGTGGAAAACAG
DV3TLP1        AGTCAGTCTGCCACCTCCGTTTCCCCTGAAGGAAGTAAAAGTCCCCATGTGGAAAACAG
DV6TLP1        AGTCAGTCTGCCACCTCCGTTTCCCCTGAAGGAAGTAAAAGTCCCCATGTGGAAAACAG
DV10TLP1       AGTCAGTCTGCCACCTCCGTTTCCCCTGAAGGAAGTAAAAGTCCCCATGTGGAAAACAG
DV11TLP1       AGTCAGTCTGCCACCTCCGTTTCCCCTGAAGGAAGTAAAAGTCCCCATGTGGAAAACAG
DV12TLP1       AGTCAGTCTGCCACCTCCGTTTCCCCTGAAGGAAGTAAAAGTCCCCATGTGGAAAACAG
*****

QueryTLP1      CGTTTGTGACAGGAAATACCACACTGGCGTGTCCACGGGGGACAACATCCGGATTGTCCA
DV3TLP1        CGTTTGTGACAGGAAATACCACACTGGCGTGTCCACGGGGGACAACATCCGGATTGTCCA
DV6TLP1        CGTTTGTGACAGGAAATACCACACTGGCGTGTCCACGGGGGACAACATCCGGATTGTCCA
DV10TLP1       CGTTTGTGACAGGAAATACCACACTGGCGTGTCCACGGGGGACAACATCCGGATTGTCCA
DV11TLP1       CGTTTGTGACAGGAAATACCACACTGGCGTGTCCACGGGGGACAACATCCGGATTGTCCA
DV12TLP1       CGTTTGTGACAGGAAATACCACACTGGCGTGTCCACGGGGGACAACATCCGGATTGTCCA
*****

QueryTLP1      GGCCGACATGCTGTGTGCA
DV3TLP1        GGCCGACATGCTGTGTGCA
DV6TLP1        GGCCGACATGCTGTGTGCA
DV10TLP1       GGCCGACATGCTGTGTGCA
DV11TLP1       GGCCGACATGCTGTGTGCA
DV12TLP1       GGCCGACATGCTGTGTGCA
*****

```

Figure 4.15: Alignment of nucleotide sequence of TLP1 amplicons from DV3 Caecum, DV6 Caecum, DV10 Caecum, DV11 Caecum and DV12 RVC. The primer sequences are highlighted in yellow and the probe sequence in green. (TLP1: Trypsin-like Proteinase-1).

```

QueryTLP1      VSLPPFPLKEVKVPIVENSVC DRKYHTGVSTGDNIRIVQADMLCA
DV3TLP1        VSLPPFPLKEVKVPIVENSVC DRKYHTGVSTGDNIRIVQADMLCA
DV6TLP1        VSLPPFPLKEVKVPIVENSVC DRKYHTGVSTGDNIRIVQADMLCA
DV10TLP1       VSLPPFPLKEVKVPIVENSVC DRKYHTGVSTGDNIRIVQADMLCA
DV11TLP1       VSLPPFPLKEVKVPIVENSVC DRKYHTGVSTGDNIRIVQADMLCA
DV12TLP1       VSLPPFPLKEVKVPIVENSVC DRKYHTGVSTGDNIRIVQADMLCA
*****

```

Figure 4.16: Alignment of predicted protein sequence of TLP1 amplicons from DV3 Caecum, DV6 Caecum, DV10 Caecum, DV11 Caecum and DV12 RVC using reading frame 2 direct. (TLP1: Trypsin-like Proteinase-1).

```

QueryGZMBL      AGCTGAGGCCTGGAGAGGTGTGCAGTGTGGCAGGCTGGGGGAGAGTCACCCCAAATGGCA
DV10GZMBL       AGCTGAGGCCTGGAGAGGTGTGCAGTGTGGCAGGCTGGGGGAGAGTCACCCCAAATGGCA
DV12GZMBL       -----GGCCTGGAGAGGTGTGCAGTGTGGCAGGCTGGGGGAGAGTCACCCCAAATGGCA
DV3GZMBL        TGTGAGGCCTGGAGAGGTGTGCAGTGTGGCAGGCTGGGGGAGAGTCACCCCAAATGGCA
DV11GZMBL       AGCTGAGGCCTGGAGAGGTGTGCAGTGTGGCAGGCTGGGGGAGAGTCACCCCAAATGGCA
DV6GZMBL        AGCTGAGGCCTGGAGAGGTGTGCAGTGTGGCAGGCTGGGGGAGAGTCACCCCAAATGGCA
*****

QueryGZMBL      GAGGGTCAGACACCTGCAGGAGGTGGAGCTGACTGTGCAGCAGGATCAGGTGTGCGAAT
DV10GZMBL       GAGAGTCAGACACTCTGCAGGAGGTGGAGCTGACCGTGCAGCAGGACCGGGTGTGCGAAT
DV12GZMBL       GAGAGTCAGACACTCTGCAGGAGGTGGAGCTGACCGTGCAGCAGGACCGGGTGTGCGAAT
DV3GZMBL        GAGGGTCAGACACCTGCAGGAGGTGGAGCTGACCGTGCAGCAGGATCAGGTGTGCGAAT
DV11GZMBL       GAGGGTCAGACACCTGCAGGAGGTGGAGCTGACTGTGCAGCAGGATCAGGTGTGCGAAT
DV6GZMBL        GAGGGTCAGACACCTGCAGGAGGTGGAGCTGACCGTGCAGCAGGATCAGGTGTGCGAAT
***.*****.*****.*****.*****.*****.*****.*****.*****

QueryGZMBL      CCTACTTTGGCAATTA
DV10GZMBL       CCTACTTTGGCAATTA
DV12GZMBL       CCTACTTTGGCAATTA
DV3GZMBL        CCTACTTTGGCAATTA
DV11GZMBL       CCTACTTTGGCAATTA
DV6GZMBL        CCTACTTTGGCAATTA
*****

```

Figure 4.17: Alignment of nucleotide sequence of GZMBL amplicons from DV3 Caecum, DV6 Caecum, DV10 Caecum, DV11 Caecum and DV12 RVC. The primer sequences are highlighted in yellow and the probe sequence in green. Nucleotides that differ from the query sequence are highlighted in pink. (GZMBL: Granzyme B-like).

Mast Cell Recruitment and Activation as Measures of Cyathostomin Burden

```

QueryGZMBL      LRPGEVCSVAGWGRVTPNGRGSDDLQEVLELTVQQDQVCESYFGN
DV3GZMBL        LRPGEVCSVAGWGRVTPNGRGSDDLQEVLELTVQQDQVCESYFGN
DV6GZMBL        LRPGEVCSVAGWGRVTPNGRGSDDLQEVLELTVQQDQVCESYFGN
DV11GZMBL       LRPGEVCSVAGWGRVTPNGRGSDDLQEVLELTVQQDQVCESYFGN
DV10GZMBL       LRPGEVCSVAGWGRVTPNGRGSDDLQEVLELTVQQDQVCESYFGN
DV12GZMBL       --PGEVCSVAGWGRVTPNGRGSDDLQEVLELTVQQDRVCESYFGN
                  *****:*****

```

Figure 4.18: Alignment of predicted protein sequence of GZMBL amplicons from DV3 Caecum, DV6 Caecum, DV10 Caecum, DV11 Caecum and DV12 RVC using reading frame 3 direct. Aa that differ from the query sequence are highlighted in pink. (GZMBL: Granzyme B-like).

```

QueryCLP1      TCCGAAAGATAAGAAGTCTTCCCTTCAGGGTGACTCTGGGGGCCCTCTCATCTGTGAGAA
DV3CLP1        TCCGAAAGATAAGAAGTCTTCCCTTCAGGGTGACTCTGGGGGCCCTCTCATCTGTGAGAA
DV6CLP1        TCCGAAAGATAAGAAGTCTTCCCTTCAGGGTGACTCTGGGGGCCCTCTCATCTGTGAGAA
DV10CLP1       TCCGAAAGATAAGAAGTCTTCCCTTCAGGGTGACTCTGGGGGCCCTCTCATCTGTGAGAA
DV11CLP1       TCCGAAAGATAAGAAGTCTTCCCTTCAGGGTGACTCTGGGGGCCCTCTCATCTGTGAGAA
DV12CLP1       TCCGAAAGATAAGAAGTCTTCCCTTCAGGGTGACTCTGGGGGCCCTCTCATCTGTGAGAA
                  *****

QueryCLP1      CGGGCTCCAGGCATTGTCTCCTATGGACTAGATAACGGGAGTATTCCACAGGCCTT
DV3CLP1        CGGGCTCCAGGCATTGTCTCCTATGGACTAGATAACGGGAGTATTCCACAGGCCTT
DV6CLP1        CGGGCTCCAGGCATTGTCTCCTATGGACTAGATAACGGGAGTATTCCACAGGCCTT
DV10CLP1       CGGGCTCCAGGCATTGTCTCCTATGGACTAGATAACGGGAGTATTCCACAGGCCTT
DV11CLP1       CGGGCTCCAGGCATTGTCTCCTATGGACTAGATAACGGGAGTATTCCACAGGCCTT
DV12CLP1       CGGGCTCCAGGCATTGTCTCCTATGGACTAGATAACGGGAGTATTCCACAGGCCTT
                  *****

```

Figure 4.19: Alignment of nucleotide sequence of CLP1 amplicons from Horse samples DV3 Caecum, DV6 Caecum, DV10 Caecum, DV11 Caecum and DV12 RVC. The primer sequences are highlighted in yellow and the probe sequence in green. Nucleotides that differ from the query sequence are highlighted in pink. (CLP1: Chymase-like Proteinase-1).

```

QueryCLP1      PKDKKSSFQGDSSGPLICENLQGIVSYGLDNGSIPQA
DV6CLP1        PKDKKSSFQGDSSGPLICENLQGIVSYGLDNGSIPQA
DV10CLP1       PKDKKSSFQGDSSGPLICENLQGIVSYGLDNGSIPQA
DV11CLP1       PKDKKSSFQGDSSGPLICENLQGIVSYGLDNGSIPQA
DV12CLP1       PKDKKSSFQGDSSGPLICENLQGIVSYGLDNGSIPQA
DV3CLP1        PKDKKSSFQGDSSGPLICENLQGIYGLDNGSIPQA
                  *****

```

Figure 4.20: Alignment of predicted protein sequence of CLP1 amplicons from Horse samples DV3 Caecum, DV6 Caecum, DV10 Caecum, DV11 Caecum and DV12 RVC using reading frame 2 direct. Aa that differ from the query sequence are highlighted in pink. (CLP1: Chymase-like Proteinase-1).

QueryGZMBGHL	AATTCTAAGAACTTCGCCAACGACATCATGTTACTAAAGCTGGA
DV6GZMBGHL	AATTCTAAGAACTTCGCCAACGACATCATGTTACTAAAGCTGGA
DV10GZMBGHL	AATTCTAAGAACTTCGCCAACGACATCATGTTACTAAAGCTGGA
DV11GZMBGHL	AATTCTAAGAACTTCGCCAACGACATCATGTTACTAAAGCTGGA
DV12GZMBGHL	AATTCTAAGAACTTCGCCAACGACATCATGTTACTAAAGCTGGA
DV3GZMBGHL	AATTCTAAGAACTTCGCCAACGACATCATGTTACTAAAGCTGGA
QueryGZMBGHL	ACCGAAGCTGTGTGGCCCCCTCAACCTGCCCAGGGGCACAGCCAGGTGAGGCCCGGAGAG
DV6GZMBGHL	ACCGAAGCTGTGTGGCCCCCTCAACCTGCCCAGGGGCACAGCCAGGTGAGGCCCGGAGAG
DV10GZMBGHL	ACCGAAGCTGTGTGGCCCCCTCAACCTGCCCAGGGGCACAGCCAGGTGAGGCCCGGAGAG
DV11GZMBGHL	ACCGAAGCTGTGTGGCCCCCTCAACCTGCCCAGGGGCACAGCCAGGTGAGGCCCGGAGAG
DV12GZMBGHL	ACCGAAGCTGTGTGGCCCCCTCAACCTGCCCAGGGGCACAGCCAGGTGAGGCCCGGAGAG
DV3GZMBGHL	ACCGAAGCTGTGTGGCCCCCTCAACCTGCCCAGGGGCACAGCCAGGTGAGGCCCGGAGAG
QueryGZMBGHL	GTGTGCCGTGTGGCTGGCTGGCTGGGGAGAGTTGCCCTAAATG
DV6GZMBGHL	GTGTGCCGTGTGGCTGGCTGGCTGGGGAGAGTTGCCCTAAATG
DV10GZMBGHL	GTGTGCCGTGTGGCTGGCTGGGGAGAGTTGCCCTAAATG
DV11GZMBGHL	GTGTGCCGTGTGGCTGGCTGGGGAGAGTTGCCCTAAATG
DV12GZMBGHL	GTGTGCCGTGTGGCTGGCTGGGGAGAGTTGCCCTAAATG
DV3GZMBGHL	GTGTGCCGTGTGGCTGGCTGGGGAGAGTTGCCCTAAATG

Figure 4.21: Alignment of nucleotide sequence of GZMBGHL amplicons from DV3 Caecum, DV6 Caecum, DV10 Caecum, DV11 Caecum and DV12 RVC. The primer sequences are highlighted in yellow and the probe sequence in green. Nucleotides that differ from the query sequence are highlighted in pink. (GZM(BGH)L: Granzyme(BGH)-like).

QueryGZMBGHL	NSKNFANDIMLLKLERRAKLTEAVWPLNLPRGTAQVRPGEVCRVAGWGRVALN
DV6GZMBGHL	NSKNFANDIMLLKLERRAKLTEAVWPLNLPRGTAQVRPGEVCRVAGWGRVALN
DV10GZMBGHL	NSKNFANDIMLLKLERRAKLTEAVWPLNLPRGTAQVRPGEVCRVAGWGRVALN
DV11GZMBGHL	NSKNFANDIMLLKLERRAKLTEAVWPLNLPRGTAQVRPGEVCRVAGWGRVALN
DV12GZMBGHL	NSKNFANDIMLLKLERRAKLTEAVWPLNLPRGTAQVRPGEVCRVAGWGRVALN
DV3GZMBGHL	NSKNFANDIMLLKLERRAKLTEAVWPLNLPRGTAQVRPGEVCRVAGWGRVALN

Figure 4.22: Alignment of predicted protein sequence of GZMBGHL amplicons from DV3 Caecum, DV6 Caecum, DV10 Caecum, DV11 Caecum and DV12 RVC using reading frame 1 direct. Aa that differ from the query sequence are highlighted in pink. (GZM(BGH)L: Granzyme(BGH)-like).

4.4.2.1 Re-annotation of the equine genome

The horse genome was re-annotated (version EquCab 2.0) and this was made public in September 2013 after the primer and probe design and qPCR analysis here. The NCBI annotation for TLP1 and CLP1 was not altered; the sequences entered by K. J Dacre (2005) remained the same. After reannotation GZMBL sequence (XP_001488476.2), was replaced with XP_005603467.1 (XM_005603410.1) and XP_005603468.1 (XM_005603411.1). These two predicted proteins have been

annotated as granzyme H-like isoform X1 and granzyme H-like isoform X2 respectively. The nucleotide sequence over the amplicon area used for qPCR for GZMBL, is identical to the same area of sequence for granzyme H-like isoform X1 and granzyme H-like isoform X2. The sequence GZM(BGH)L (XP_001488616.3), was removed during the re-annotation process and replaced with XM_005613502.1: XP_005613559.1. This protein has been annotated as granzyme H-like. The nucleotide sequence over the amplicon area used for qPCR for GZM(BGH)L was also identical to the same area of granzyme H-like.

Granzyme specificity is determined by the aa residue at 226. Figure 4.23 shows an alignment of the two re-annotated sequences of interest (GZMBL and GZM(BGH)L) with the residue at 226 highlighted. The sequences are aligned with human and rat granzyme H, both of which have a glycine at 226. The equine sequences did not share this residue. Which suggests that the original nomenclature of granzyme B-like and granzyme-(BGH)-like is more accurate than the granzyme H-like re-annotation.

```

GZMBL          ---IQGIVSYGRSGG--LPPPAFTKVSSFLPWIKKTMKGRAPWP
GZM(BGH)L      ---IQGIVSYGRIGG--IPPPAFTKVSSFLPWIKKTMKGRALWQ
Granzyme H (brown rat) ---AYGVVSYGKNGT--ISSGVFTKVYVFLPWISRNMKLL----
Granzyme H precursor (Human) ---AQGILSYGNKKG--TPPGVYIKVSHFLPWIKRTMKRL----
                * * * * *          . * * * * .

```

Figure 4.23: Alignment of GZMB(L), GZM(BGH)L and human and rat granzyme H. Residue 226 is highlighted. (GZMBL: Granzyme B-like; GZM(BGH)L: Granzyme(BGH)-like).

4.4.3 Reference Gene Selection

GeNorm analysis was performed on 15 samples using the six available equine reference targets. These targets were ACT β , B2M, HPRT, GAPDH, RN18S and SDHA. Reference target stability was high (average geNorm $M \leq 0.5$) as indicated by the average expression stability value (M) of reference genes at each step during stepwise exclusion of the least stably expressed reference gene. Starting with the least stable gene at the left, RN18S, the genes are ranked according to increasing expression stability; with SDHA and GAPDH appearing as the most stable (Figure 4.24).

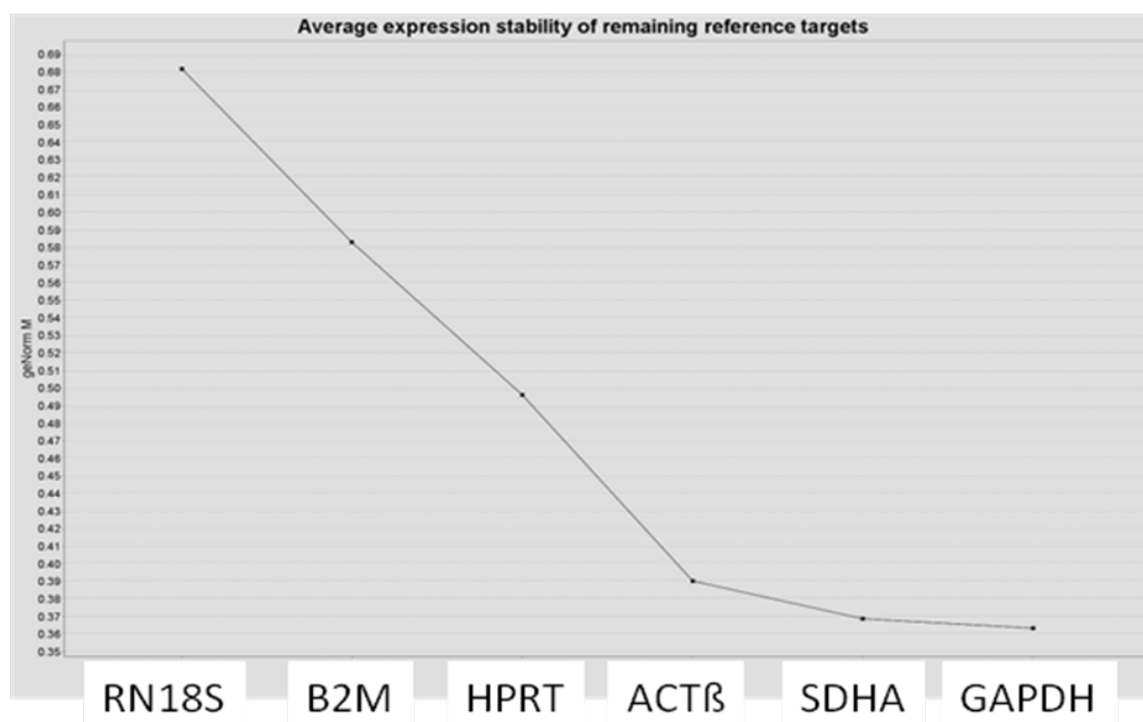


Figure 4.24: Graph of average expression stability of reference target genes. (ACTβ: beta-actin; B2M: beta-2-microglobulin; HPRT: hypoxanthine phosphoribosyltransferase; GAPDH: glyceraldehyde 3-phosphate dehydrogenase; RN18S: 18s ribosomal RNA; SDHA: succinate dehydrogenase complex, subunit A, flavoprotein)

The bar chart (Figure 4.25), geNorm V, shows the optimum number of reference genes required as it illustrates the variation in average stability of each. The chart demonstrates sequential addition of each reference gene beginning on the left with the two most stably-expressed genes (SDHA and GAPDH) then moving to the right with the inclusion of a third, fourth and fifth gene respectively. The optimal number of reference genes is observed when $V(n/n+1)$, the pairwise variation, drops below the threshold 0.15 (Vandesompele, De Preter et al. 2002). The optimal number of reference targets in this experimental situation is two (geNorm V < 0.15, when comparing a normalisation factor based on the two or three most stable targets). As such, the optimal normalisation factor can be calculated as the geometric mean of the reference targets, SDHA and GAPDH.

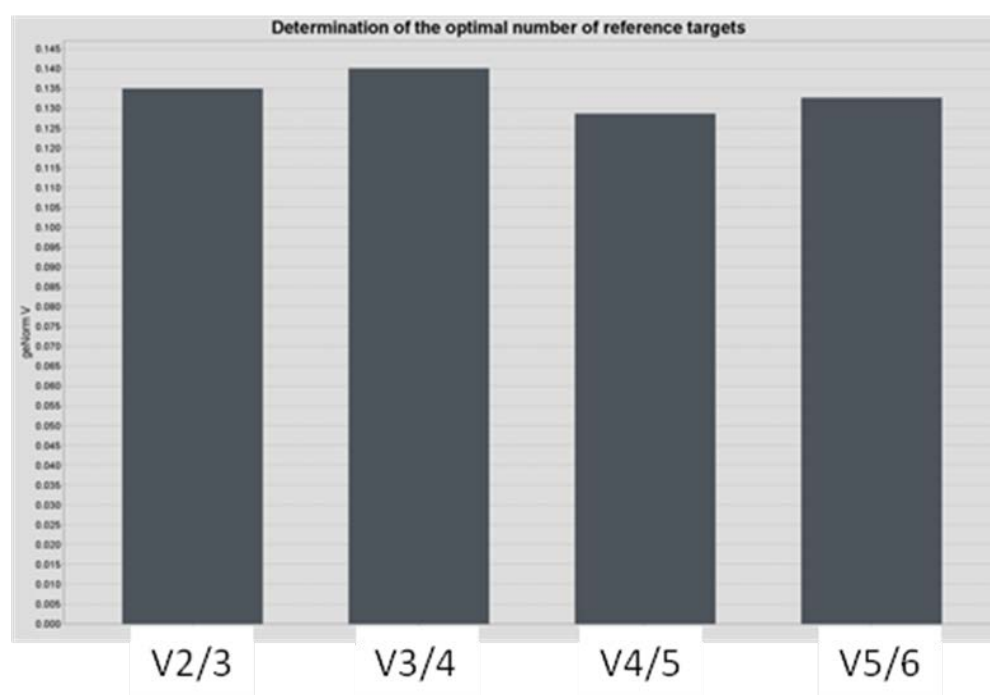


Figure 4.25: Bar chart to determine optimal number of reference targets. The chart demonstrates sequential addition of each reference gene beginning on the left with the two most stably expressed genes then moving to the right with the inclusion of a third, fourth and fifth gene respectively.

4.4.4 Probe Validation

Combinations of primers and probes were tested. Each primer set was tested in duplicate with each of the four different probes. The probes were specific to the amplicons produced from the PCR reaction. For each of the four genes of interest a positive result in the form of a measureable Ct value (cycle threshold defined as the number of cycles required for the signal to exceed the background level (Vargas and Vivas-Mejia 2013)) was only observed with the correct combination of primer and probe (Table 4.6).

Primers	Probe	cDNA	Ct
TLP1	TLP1	DV10 RVC	32.3
TLP1	GZMBL	DV10 RVC	>40.0
TLP1	CLP1	DV10 RVC	>40.0
TLP1	GZM(BGH)L	DV10 RVC	>40.0
GZMLBL	TLP1	DV7 Caecum	>40.0
GZMLBL	GZMBL	DV7 Caecum	37.8
GZMLBL	CLP1	DV7 Caecum	>40.0
GZMLBL	GZM(BGH)L	DV7 Caecum	>40.0
CLP1	TLP1	DV12 Caecum	>40.0
CLP1	GZMBL	DV12 Caecum	>40.0
CLP1	CLP1	DV12 Caecum	32.8
CLP1	GZM(BGH)L	DV12 Caecum	>40.0
GZM(BGH)L	TLP1	DV9 Caecum	>40.0
GZM(BGH)L	GZMBL	DV9 Caecum	>40.0
GZM(BGH)L	CLP1	DV9 Caecum	>40.0
GZM(BGH)L	GZM(BGH)L	DV9 Caecum	33.3

Table 4.6: Table of Ct values from Primer/Probe combinations. The assay used 40 cycles and a positive Ct result was only obtained from the correct combination of primer set and probe. (TLP1: Trypsin-like Proteinase-1; GZMBL: Granzyme B-like; CLP1: Chymase-like Proteinase-1; GZM(BGH)L: Granzyme(BGH)-like).

4.4.5 Quantitative PCR Efficiency

The qPCR reactions were optimised and the range of efficiencies from each of the assays is shown in Table 4.7. The primary step of every qPCR is the extraction and purification of RNA. The quality of template is very important for the reproducibility and reliability of assay results (Bustin and Nolan 2004). The qPCR efficiency is also dependent on the assay, the master mix performance, and sample quality. It is important that assays are reliable and of optimum efficiency for comparison of the data. Efficiency between 90 and 110% is generally considered optimal (D'haene, Vandesompele et al. 2010). Figure 4.26 shows the standard curves for each of the four genes of interest.

Gene	Efficiency Range (%)
TLP1	96 - 103
GZMBL	91 - 110
CLP1	94 - 104
GZM(BGH)L	88 - 94
GAPDH	93 - 102
SDHA	88 - 99

Table 4.7: Table of the range of efficiencies for each qPCR reaction. (TLP1: Trypsin-like Proteinase-1; GZMBL: Granzyme-B-like; CLP1: Chymase-like Proteinase1; GZM(BGH)L: Granzyme (BGH) like; GAPDH: Glyceraldehyde 3-phosphate dehydrogenase; SDHA: Succinate Dehydrogenase subunit A).

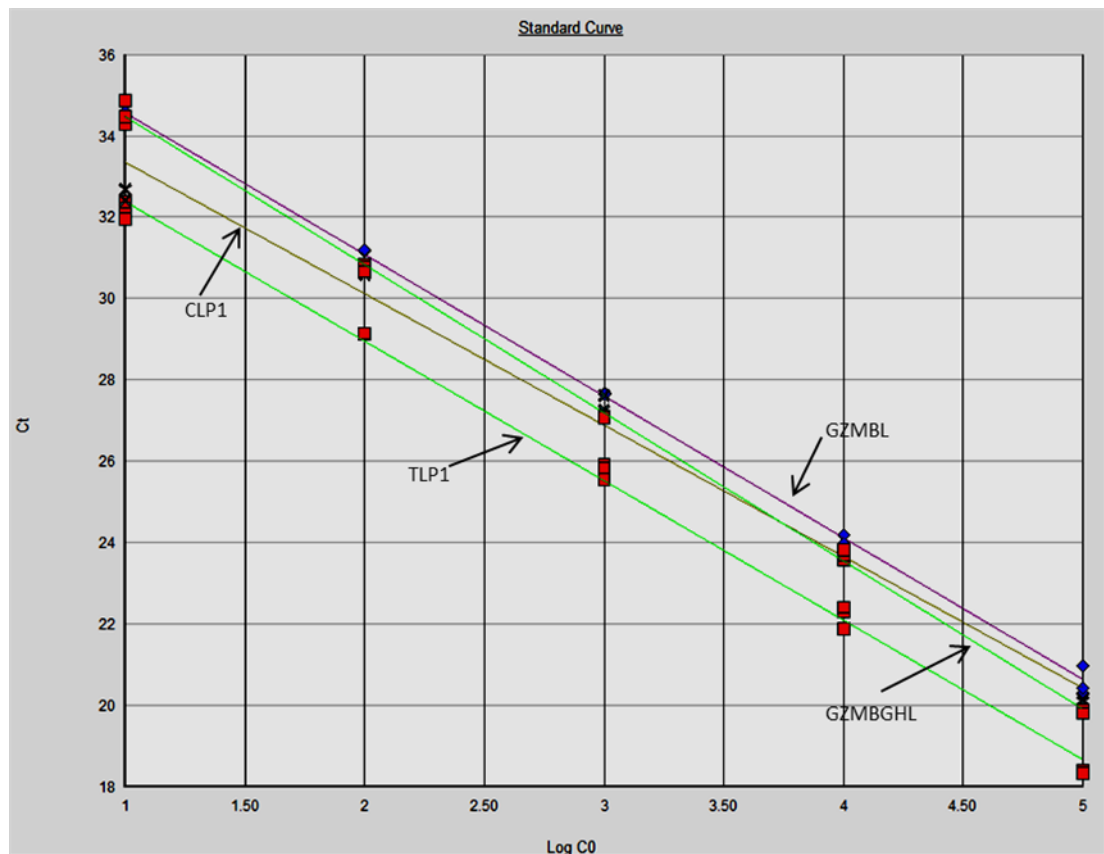


Figure 4.26: Plasmid standard curves from qPCR for each of the four genes of interest. (TLP1: Trypsin-like Proteinase-1; GZMBL: Granzyme B-like; CLP1: Chymase-like Proteinase-1; GZM(BGH)L: Granzyme(BGH)-like).

4.4.6 Tissue Transcript Levels from Quantitative PCR

The levels of transcript in the 42 tissue samples were evaluated using ABI 7500 software, normalising all results to the two selected reference genes, GAPDH and SDHA. The normalised number of copies per μl of TLP1, GZMBL, CLP1, GZM(BGH)L in each of the organs sampled are shown (Figure 4.27A-C). The levels of the four proteinases in each of the three organs were compared. Although the range of proteinase levels varied by organ, there was no significant difference when comparing the expression of each gene individually in the three different organs (Figure 4.28A-D).

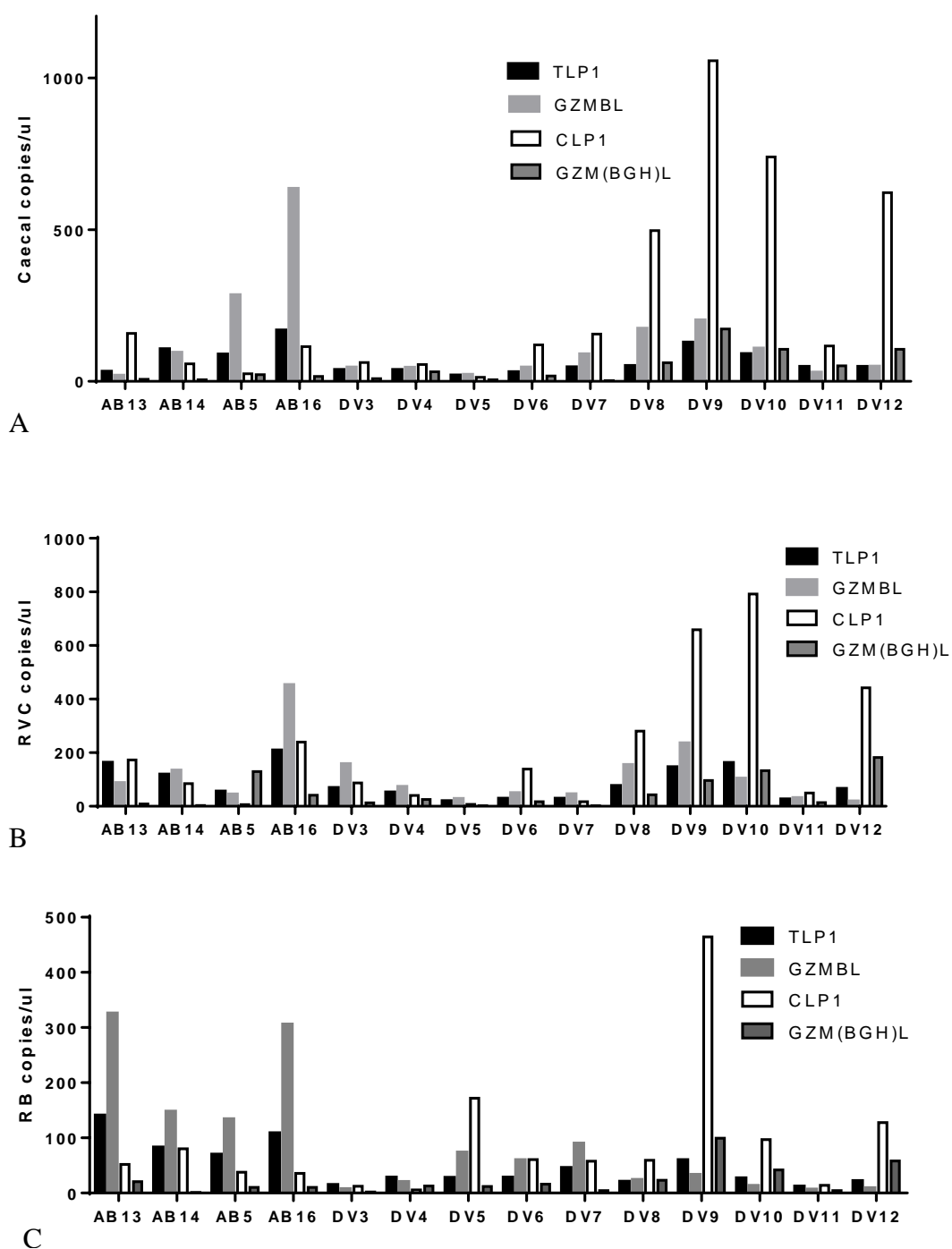


Figure 4.27: Bar charts of the normalised number of copies per µl of TLP1, GZMBL, CLP1, GZM(BGH)L in each of the organs sampled. A: Caecum. B: RVC. C: RB. (RVC: Right ventral colon; RB: Rectal biopsy; TLP1: Tryptase-like Proteinase-1; GZMBL: Granzyme B-Like; CLP1: Chymase-like Proteinase-1; GZM(BGH)L: Granzyme(BGH)-like).

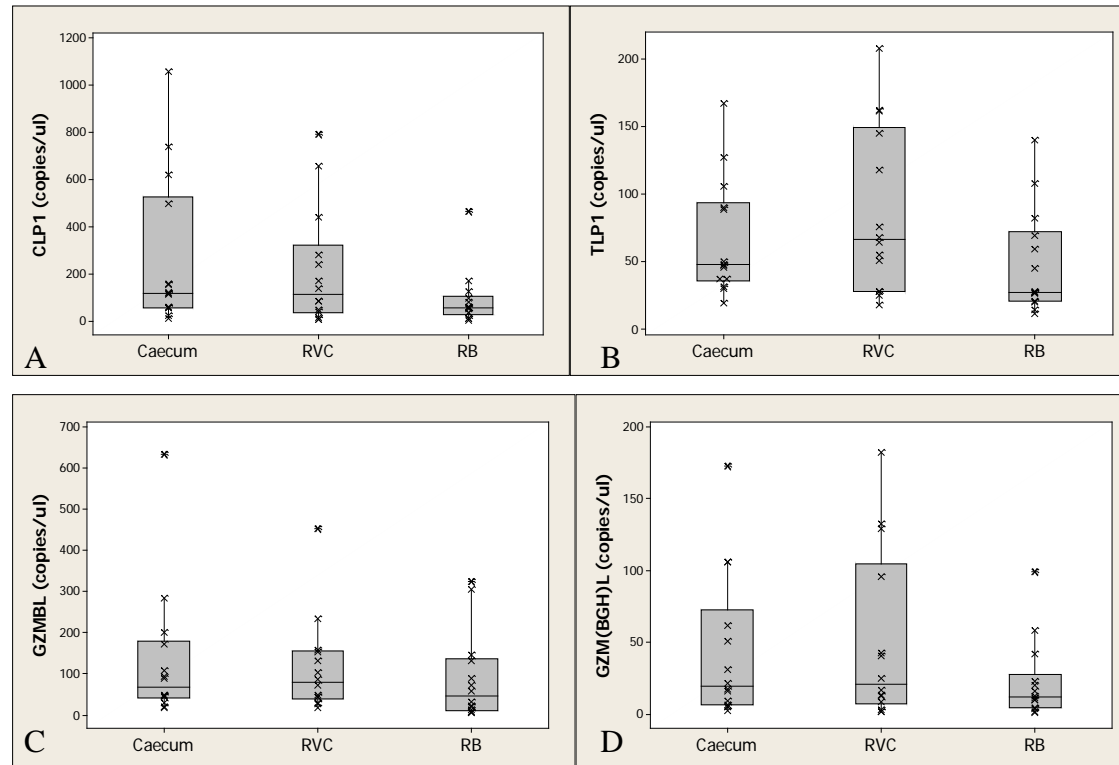


Figure 4.28. Box plots of individual proteinase transcript levels divided by organ.

A: Friedman analysis revealed no significant difference in CLP1 copies/ μ l between organs ($p=0.146$). B: Friedman analysis revealed no significant difference in TLP1 copies/ μ l between organs ($p=0.103$). C: Friedman analysis revealed no significant difference in GZMBL copies/ μ l between organs ($p=0.410$). D: Friedman analysis revealed no significant difference in GZM(BGH)L copies/ μ l between organs ($p=0.411$). (RVC: Right ventral colon; RB: Rectal biopsy; TLP1: Tryptase-like Proteinase-1; GZMBL: Granzyme B-like; CLP1: Chymase-like Proteinase-1; GZM(BGH)L: Granzyme(BGH)-like).

4.4.6.1 Transcript Levels in the Caecum

The median and range of transcript levels in the caecum are shown in Table 4.8. Friedman analysis revealed a significant difference in caecal copies/ μ l between proteinases ($p<0.001$). CLP1 had the highest median (118.7) and the greatest range (13.2 – 1057.0) of copies/ μ l. The relationships between caecal transcript levels are displayed as a matrix scatter plot in Figure 4.29, and the p and ρ values for each correlation in Table 4.9. There was a significant correlation between the levels of TLP1 and GZMBL ($p<0.001$, $\rho=0.860$), and the levels of CLP1 and GZM(BGH)L ($p=0.033$, $\rho=0.578$).

Caecum	TLP1	GZMBL	CLP1	GZM(BGH)L
Median	47.8	68.9	118.7	19.9
Range	19.6 - 167.5	18.8 - 634.7	13.2 - 1057.0	2.3 - 173.0

Table 4.8: Median and range of Caecal TLP1, GZMBL, CLP1 and GZM(BGH)L transcript levels expressed as copies/ μ l. (TLP1: Tryptase-like Proteinase-1; GZMBL: Granzyme B-like; CLP1: Chymase-like Proteinase-1; GZM(BGH)L: Granzyme(BGH)-like).

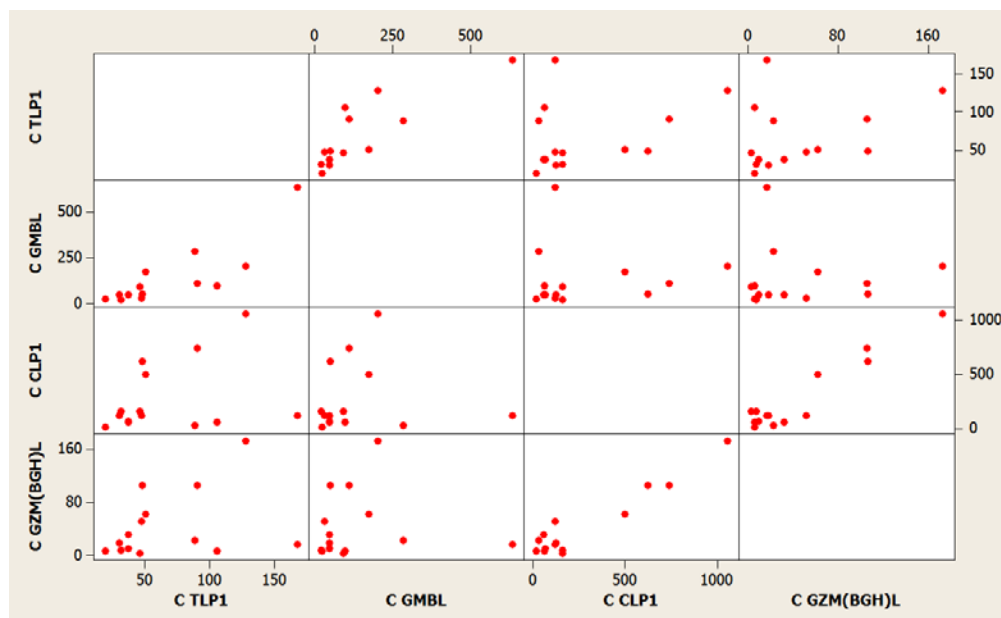


Figure 4.29: Matrix scatter plot of caecal transcript levels of TLP1, GZMBL, CLP1 and GZM(BGH)L. (C: Caecum; TLP1: Tryptase-like Proteinase-1; GZMBL: Granzyme B-like; CLP1: Chymase-like Proteinase-1; GZM(BGH)L: Granzyme(BGH)-like).

Caecum	TLP1	GZMBL	CLP1	GZM(BGH)L
TLP1	-	0.860	0.310	0.376
GZMBL	<0.001	-	0.220	0.301
CLP1	<i>0.280</i>	<i>0.450</i>	-	0.578
GZM(BGH)L	<i>0.185</i>	<i>0.295</i>	0.033	-

Table 4.9: Table of rho values (bold) and p values (in italics) for correlations between genes of interest in the caecum. Significant p-values are highlighted in yellow. (TLP1: Tryptase-like Proteinase-1; GZMBL: Granzyme B-like; CLP1: Chymase-like Proteinase-1; GZM(BGH)L: Granzyme(BGH)-like).

4.4.6.2 Transcript Levels in the RVC

The median and range of transcript levels in the RVC are shown in Table 4.10. For the RVC, Friedman analysis showed a significant difference in RVC copies/ μ l between the proteinases ($p < 0.01$). The proteinase with the highest median was CLP1 (112.6 copies/ μ l) and CLP1 also had the greatest range (6.4 – 792.4 copies/ μ l). The relationships between RVC transcript levels are displayed as a matrix scatter plot in Figure 4.30, and the p and rho values for each correlation in Table 4.11. As in the caecum, there were significant correlations between the levels of TLP1 and GZMBL ($p = 0.003$, $\rho = 0.754$), and the levels of CLP1 and GZM(BGH)L ($p = 0.032$, $\rho = 0.582$).

RVC	TLP1	GZMBL	CLP1	GZM(BGH)L
Median	66.4	79.2	112.6	21.1
Range	18.4 - 208.1	18.0 - 452.4	6.4 - 792.4	1.8 - 182.4

Table 4.10: Median and range of RVC TLP1, GZMBL, CLP1 and GZM(BGH)L transcript levels expressed as copies/ μ l. (TLP1: Tryptase-like Proteinase-1; GZMBL: Granzyme B-like; CLP1: Chymase-like Proteinase-1; GZM(BGH)L: Granzyme(BGH)-like).

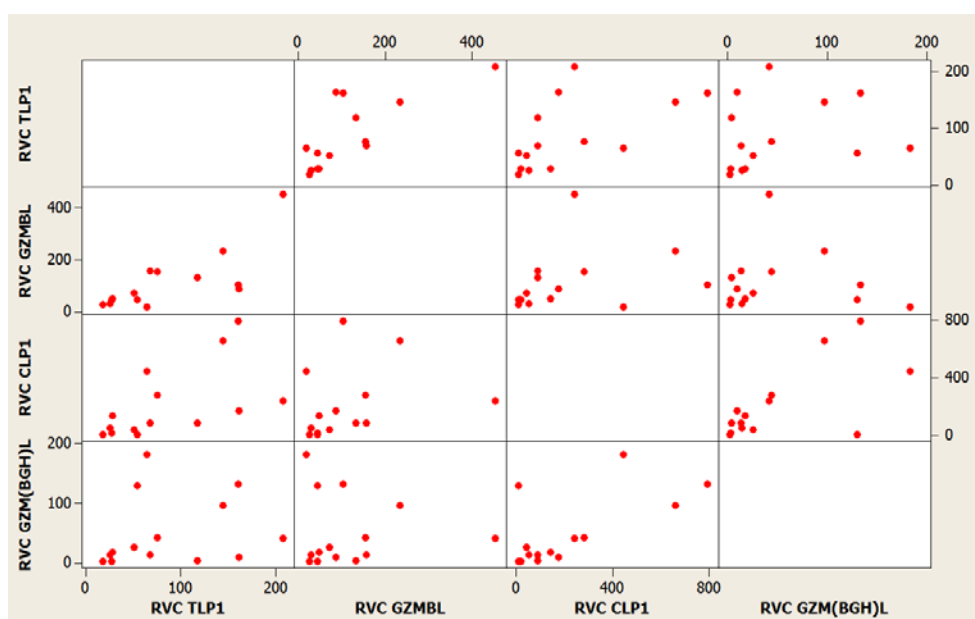


Figure 4.30: Matrix scatter plot of RVC transcript levels of TLP1, GZMBL, CLP1 and GZM(BGH)L. (RVC: Right ventral colon; TLP1: Tryptase-like Proteinase-1; GZMBL: Granzyme B-like; CLP1: Chymase-like Proteinase-1; GZM(BGH)L: Granzyme(BGH)-like).

RVC	TLP1	GZMBL	CLP1	GZM(BGH)L
TLP1	-	0.754	0.697	0.371
GZMBL	0.003	-	0.486	0.090
CLP1	<i>0.007</i>	<i>0.081</i>	-	0.582
GZM(BGH)L	<i>0.192</i>	<i>0.762</i>	0.032	-

Table 4.11: Table of rho values (bold) and p values (in italics) for correlations between genes of interest in the RVC. Significant p-values are highlighted in yellow. (TLP1: Tryptase-like Proteinase-1; GZMBL: Granzyme B-like; CLP1: Chymase-like Proteinase-1; GZM(BGH)L: Granzyme(BGH)-like).

4.4.6.3 Transcript Levels in the Rectum

The median and range of transcript levels in the rectum are shown in Table 4.12. Friedman analysis revealed a significant difference in RB transcript copies/ μ l between proteinases ($p < 0.05$). Levels of CLP1 had the highest median (58.6 copies/ μ l) and the greatest range (5.6 – 464.2 copies/ μ l). The relationships between rectal transcript levels for the four different proteinases is displayed as a matrix scatter plot in Figure 4.31, and the p and rho values for each correlation in

Table 4.13. There was a significant correlation between the levels of TLP1 and GZMBL ($p<0.001$, $\rho=0.7925$) at this site.

RB	TLP1	GZMBL	CLP1	GZM(BGH)L
Median	27.8	46.0	58.6	12.3
Range	11.5 - 140.2	6.0 - 325.2	5.6 - 464.2	1.2 - 99.5

Table 4.12: Median and range of RB TLP1, GZMBL, CLP1 and GZM(BGH)L transcript levels expressed as copies/ μ l. (TLP1: Tryptase-like Proteinase-1; GZMBL: Granzyme B-like; CLP1: Chymase-like Proteinase-1; GZM(BGH)L: Granzyme(BGH)-like).

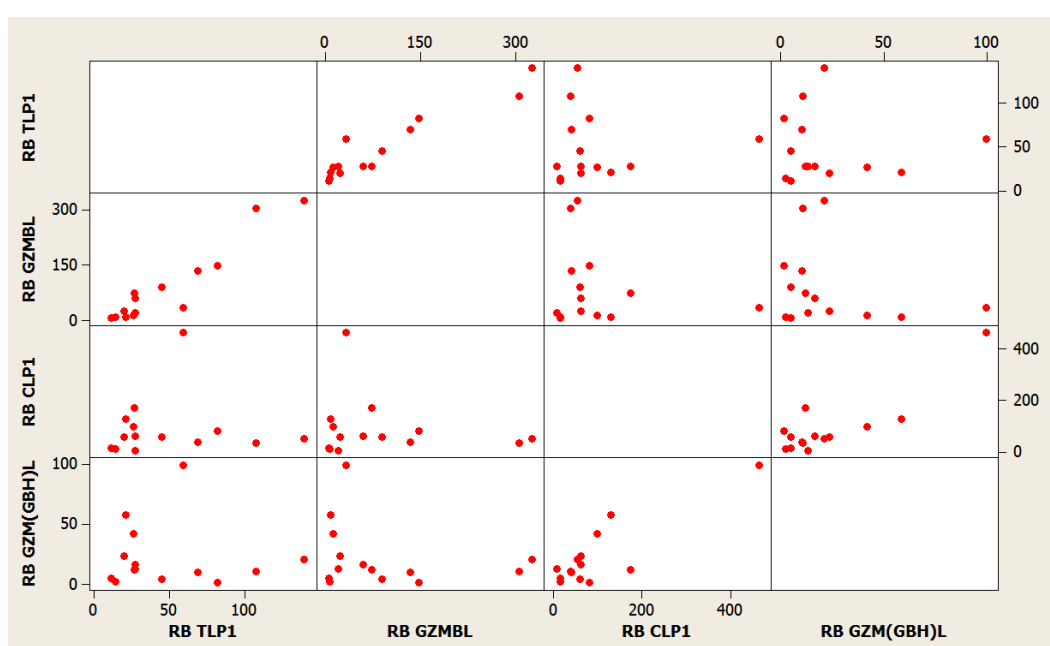


Figure 4.31: Matrix scatter plot of RB transcript levels of TLP1, GZMBL, CLP1 and GZM(BGH)L. (RB: Rectal biopsy; TLP1: Tryptase-like Proteinase-1; GZMBL: Granzyme B-like; CLP1: Chymase-like Proteinase-1; GZM(BGH)L: Granzyme(BGH)-like).

RB	TLP1	GZMBL	CLP1	GZM(BGH)L
TLP1	-	0.925	0.077	-0.055
GZMBL	<0.001	-	0.090	-0.169
CLP1	<i>0.797</i>	<i>0.762</i>	-	0.530
GZM(BGH)L	<i>0.856</i>	<i>0.563</i>	<i>0.054</i>	-

Table 4.13: Table of rho values (bold) and p values (in italics) for correlations between genes of interest in the rectum from rectal biopsy (RB). Significant p-values are highlighted in yellow. (TLP1: Tryptase-like Proteinase-1; GZMBL: Granzyme B-like; CLP1: Chymase-like Proteinase-1; GZM(BGH)L: Granzyme(BGH)-like).

4.4.7 Relationship between Mast Cell Proteinase Transcripts and Mucosal Cyathostomin Burdens

4.4.7.1 Caecum Transcript Levels and Combined Total Mucosal Burden

The relationship between caecal transcript levels and combined total mucosal burden (CTMB) are displayed in Figures 4.32A-D. Standard linear regression analysis with the presence of *A. perfoliata* as a confounding variable showed that there was no significant relationship between the log10+1 transformed CTMB and the caecal transcript levels of any of the proteinases under study.

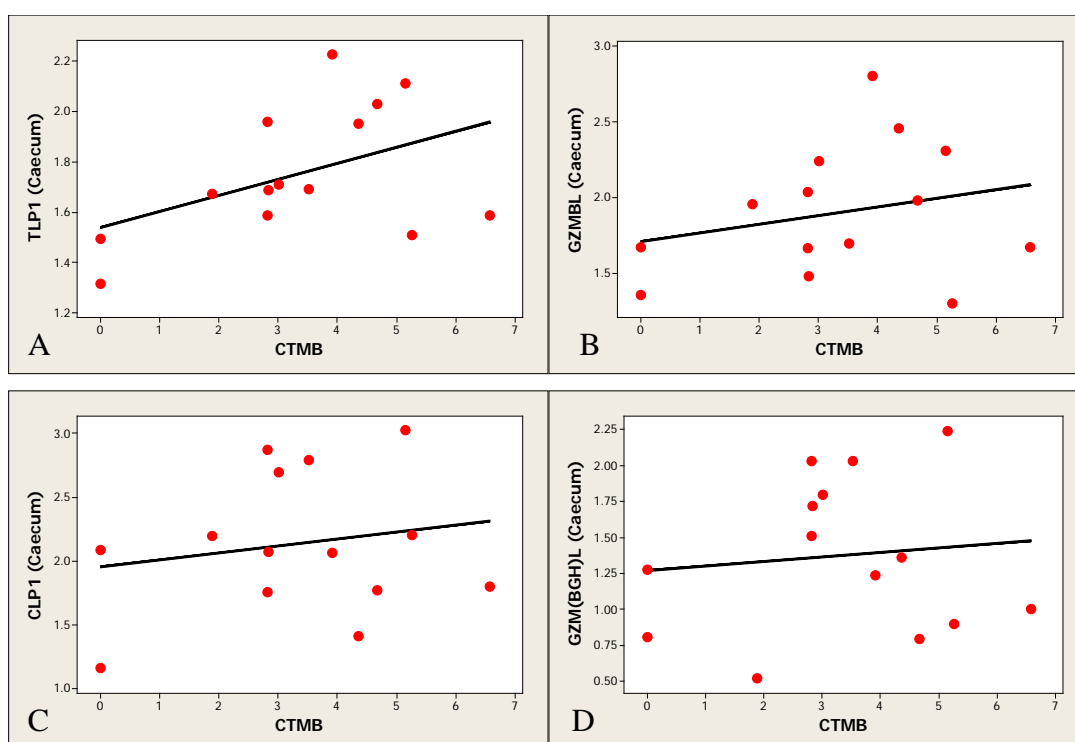


Figure 4.32.A: Relationship between log10+1 transformed Caecal TMB (x-axis) and Caecal TLP1 (y-axis), $p=0.093$, $r^2=34.0\%$. B: Relationship between log10+1 transformed Caecal TMB (x-axis) and Caecal GZMBL (y-axis), $p=0.419$, $r^2=28.3\%$. C: Relationship between log10+1 transformed Caecal TMB (x-axis) and Caecal CLP1 (y-axis), $p=0.534$, $r^2=0.0\%$. D: Relationship between log10+1 transformed Caecal TMB (x-axis) and Caecal GZM(BGH)L (y-axis), $p=0.698$, $r^2=0.0\%$. (CTMB: Combined Total Mucosal Burden; TLP1: Tryptase-like Proteinase-1; GZMBL: Granzyme B-like; CLP1: Chymase-like Proteinase-1; GZM(BGH)L: Granzyme(BGH)-like).

4.4.7.2 RVC Transcript Levels and Combined Total Mucosal Burden

The relationship between transcript levels of proteinases in the RVC and CTMB is shown in Figures 4.34A-D. Standard linear regression analysis with the presence of *A. perfoliata* as a confounding variable showed a significant relationship between log10+1 transformed CTMB and log10+1 transformed RVC TLP1 levels ($p=0.007$, $r^2=51.2\%$) (Figure 4.33A) and GZMBL levels ($p=0.042$, $r^2=45.4\%$) (Figure 4.34B).

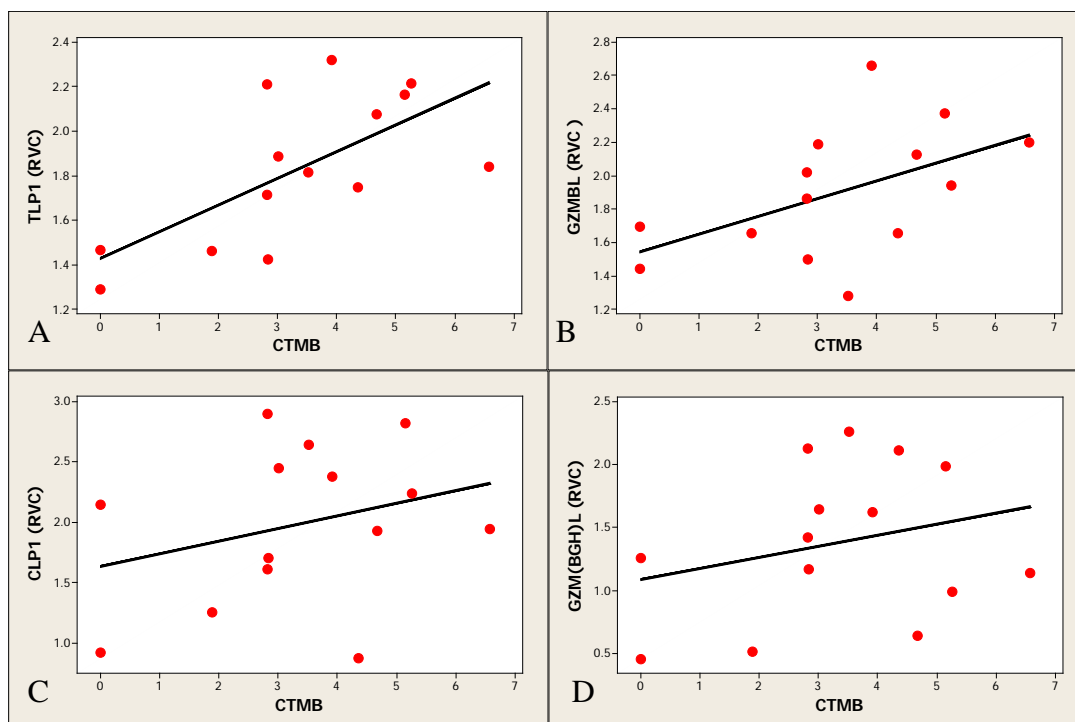


Figure 4.33. A Relationship between log10+1 transformed RVC TMB (x-axis) and RVC TLP1 (y-axis), $p=0.007$, $r^2=51.2\%$. B: Relationship between log10+1 transformed RVC TMB (x-axis) and RVC GZMBL (y-axis), $p=0.042$, $r^2=45.4\%$. C: Relationship between log10+1 transformed RVC TMB (x-axis) and RVC CLP1 (y-axis), $p=0.336$, $r^2=0.0\%$. D: Relationship between log10+1 transformed RVC TMB (x-axis) and RVC GZM(BGH)L (y-axis), $p=0.385$, $r^2=0.0\%$. (CTMB: Combined Total Mucosal Burden; TLP1: Trypsin-like Proteinase-1; GZMBL: Granzyme B-like; CLP1: Chymase-like Proteinase-1; GZM(BGH)L: Granzyme(BGH)-like).

4.4.7.3 Rectal Transcript Levels and Combined Total Mucosal Burden

The relationship between proteinase transcript expression in the rectum and CTMB is shown in Figure 4.34A-D. Standard linear regression analysis with the presence of *A. perfoliata* as a confounding variable showed that there was no significant relationship between the log10+1 transformed CTMB and expression of any of the four transcripts in the rectum.

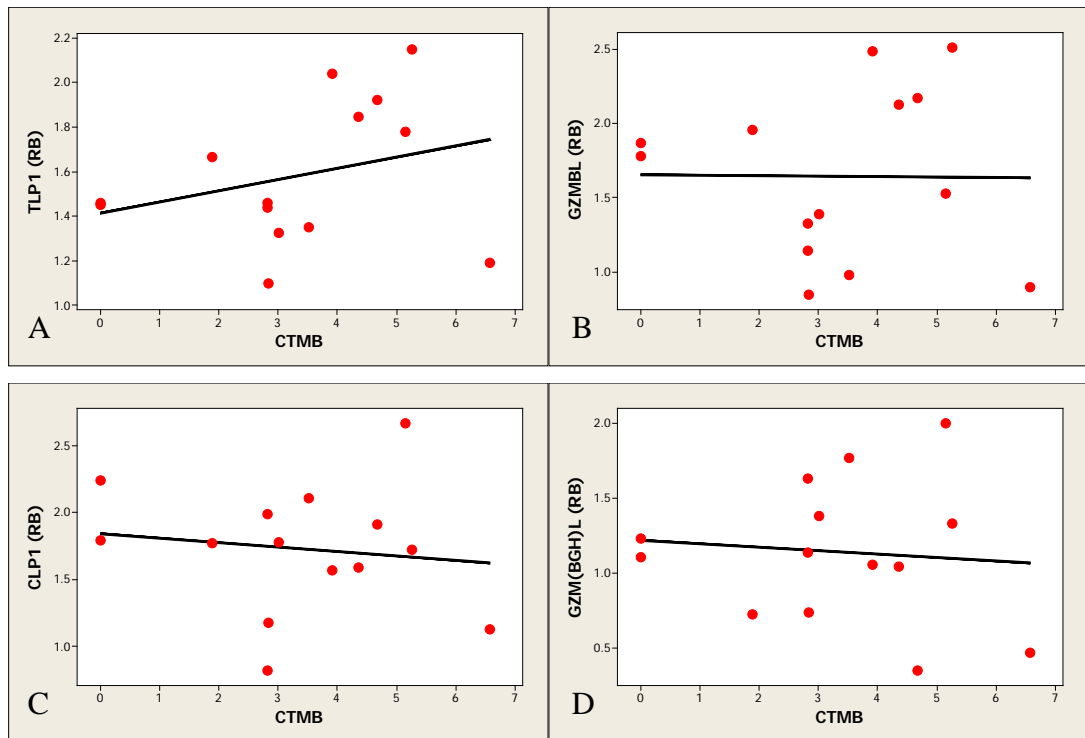


Figure 4.34: A: Relationship between log₁₀+1 transformed CTMB (x-axis) and Rectal TLP1 (y-axis), $p=0.344$, $r^2=9.5\%$. B: Relationship between log₁₀+1 transformed CTMB (x-axis) and Rectal GZMBL (y-axis), $p=0.862$, $r^2=3.5\%$. C: Relationship between log₁₀+1 transformed CTMB (x-axis) and Rectal CLP1 (y-axis), $p=0.685$, $r^2=0.0\%$. D: Relationship between log₁₀+1 transformed CTMB (x-axis) and Rectal GZM(BGH)L (y-axis), $p=0.781$, $r^2=0.0\%$. (CTMB: Combined Total Mucosal Burden; TLP1: Tryptase-like Proteinase-1; GZMBL: Granzyme B-like; CLP1: Chymase-like Proteinase-1; GZM(BGH)L: Granzyme(BGH)-like).

4.4.8 Relationship between Tissue Transcript Expression and Mast Cell Populations

The relationships between caecal transcript levels and mast cell populations (Toluidine Blue (TB), eqMCP-1-labelled and eqTRYP-labelled mucosal mast cells (MMC) and submucosal mast cells (SMMC)) in the caecum are displayed as a matrix scatter plot in Figure 4.35. The p and ρ values for each correlation are in Table 4.14. There were significant correlations between the levels of CLP1 transcripts and TB MMC, eqMCP-1 MMC and eqTRYP MMC (Table 4.14) in the caecum. No other significant correlations were seen in the caecum.

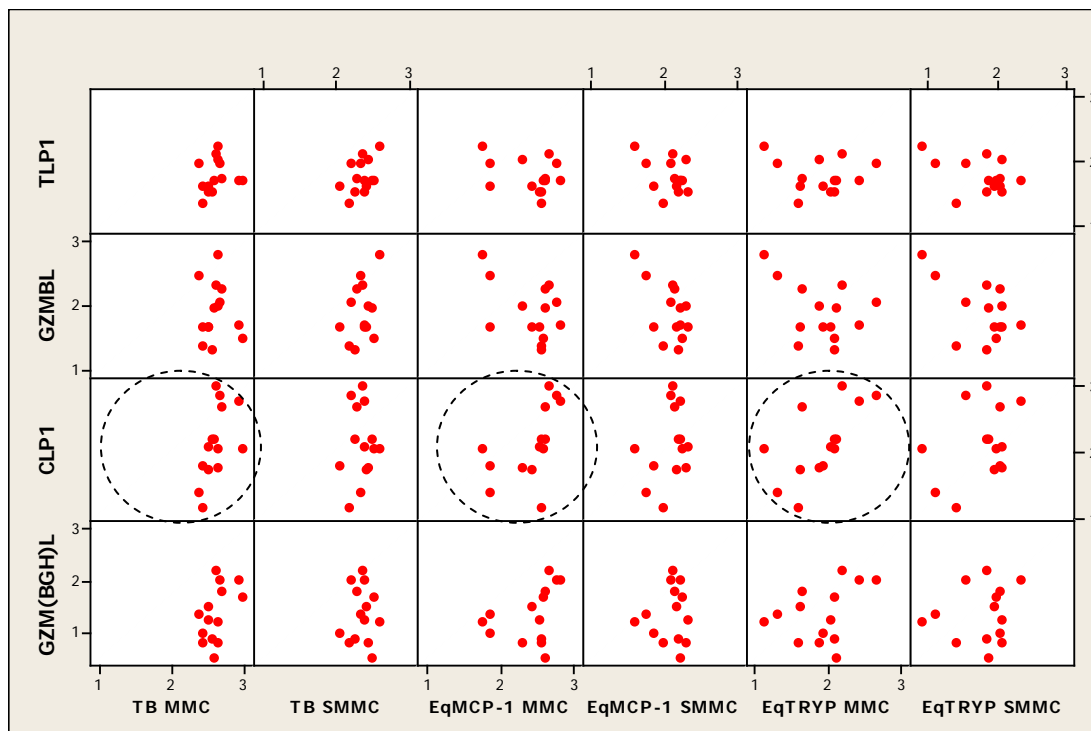


Figure 4.35: Matrix scatter plot of log10+1 transformed counts for caecal mast cell counts (x-axis) and caecal transcript levels (y-axis). Significant relationships are circled. (TLP1: Tryptase-like Proteinase-1; GZMBL: Granzyme B-like; CLP1: Chymase-like Proteinase-1; GZM(BGH)L: Granzyme(BGH)-like).

Caecum		TB MMC	TB SMMC	EqMCP-1 MMC	EqMCP-1 SMMC	EqTRYP MMC	EqTRYP SMMC
TLP1	rho	0.473	0.343	0.019	-0.268	0.040	-0.225
	p	<i>0.088</i>	<i>0.230</i>	<i>0.949</i>	<i>0.354</i>	<i>0.893</i>	<i>0.440</i>
GZMBL	rho	0.184	0.213	-0.080	-0.422	-0.141	-0.288
	p	<i>0.529</i>	<i>0.464</i>	<i>0.785</i>	<i>0.132</i>	<i>0.631</i>	<i>0.319</i>
CLP1	rho	0.623	-0.051	0.748	0.226	0.793	0.187
	p	0.017	<i>0.868</i>	0.002	<i>0.436</i>	0.001	<i>0.522</i>
GZM(BGH)L	rho	0.464	-0.081	0.506	-0.055	0.393	0.084
	p	<i>0.095</i>	<i>0.785</i>	<i>0.065</i>	<i>0.856</i>	<i>0.165</i>	<i>0.776</i>

Table 4.14: Table of rho values (bold) and p values (in italics) for correlations between genes of interest in the caecum and caecal TB, eqMCP-1 and eqTRYP MMC and SMMC. Significant p-values are highlighted in yellow. (TLP1: Tryptase-like Proteinase-1; GZMBL: Granzyme B-like; CLP1: Chymase-like Proteinase-1; GZM(BGH)L: Granzyme(BGH)-like).

The relationships between proteinase transcript levels and mast cell populations in the RVC are displayed as a matrix scatter plot in Figure 4.36. The p and rho values for each correlation are shown in Table 4.15. There was a significant correlation between the levels of CLP1 and TB MMC ($p=0.024$, $\rho=0.609$) at this site. No other significant correlations were seen in the RVC.

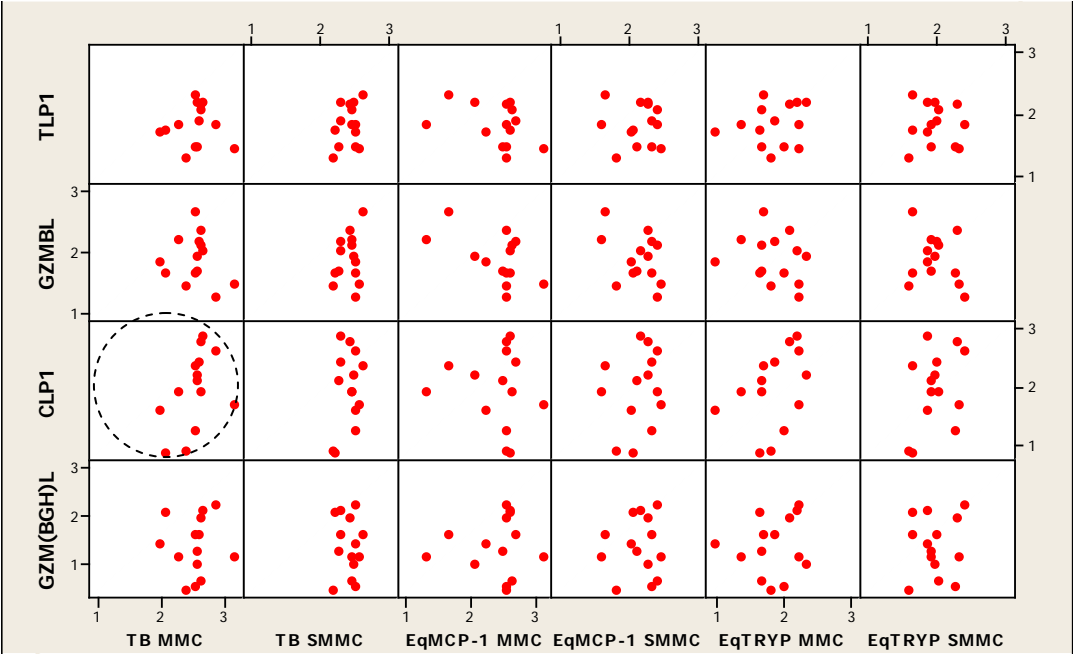


Figure 4.36: Matrix scatter plot of $\log_{10}+1$ transformed counts for RVC mast cell counts (x-axis) and RVC transcript levels (y-axis). Significant relationships are circled. (TLP1: Trypsin-like Proteinase-1; GZMBL: Granzyme B-like; CLP1: Chymase-like Proteinase-1; GZM(BGH)L: Granzyme(BGH)-like).

RVC		TB MMC	TB SMMC	EqMCP-1 MMC	EqMCP-1 SMMC	EqTRYP MMC	EqTRYP SMMC
TLP1	rho	0.191	0.191	-0.218	-0.086	0.191	-0.026
	p	<i>0.512</i>	<i>0.512</i>	<i>0.454</i>	<i>0.771</i>	<i>0.512</i>	<i>0.929</i>
GZMBL	rho	-0.059	0.077	-0.332	-0.271	-0.227	-0.095
	p	<i>0.844</i>	<i>0.797</i>	<i>0.246</i>	<i>0.349</i>	<i>0.436</i>	<i>0.747</i>
CLP1	rho	0.609	0.147	0.020	0.178	0.491	0.322
	p	0.024	<i>0.616</i>	<i>0.952</i>	<i>0.542</i>	<i>0.075</i>	<i>0.262</i>
GZM(BGH)L	rho	0.292	0.020	0.222	0.051	0.147	0.077
	p	<i>0.310</i>	<i>0.952</i>	<i>0.445</i>	<i>0.864</i>	<i>0.615</i>	<i>0.793</i>

Table 4.15: Table of rho values (bold) and p values (in italics) for correlations between genes of interest in the RVC and RVC TB, eqMCP-1 and eqTRYP MMC and SMMC. Significant p-values are highlighted in yellow. (TLP1: Tryptase-like Proteinase-1; GZMBL: Granzyme B-like; CLP1: Chymase-like Proteinase-1; GZM(BGH)L: Granzyme(BGH)-like).

The relationships between proteinase transcript levels and mast cell populations in the rectum are displayed as a matrix scatter plot in Figure 4.37. The p and rho values for each correlation are shown in Table 4.16. There was a significant correlation between the levels of GZM(BGH)L and eqMCP-1 MMC and eqTRYP SMMC (Table 4.16). No significant relationships were seen with the levels of CLP1.

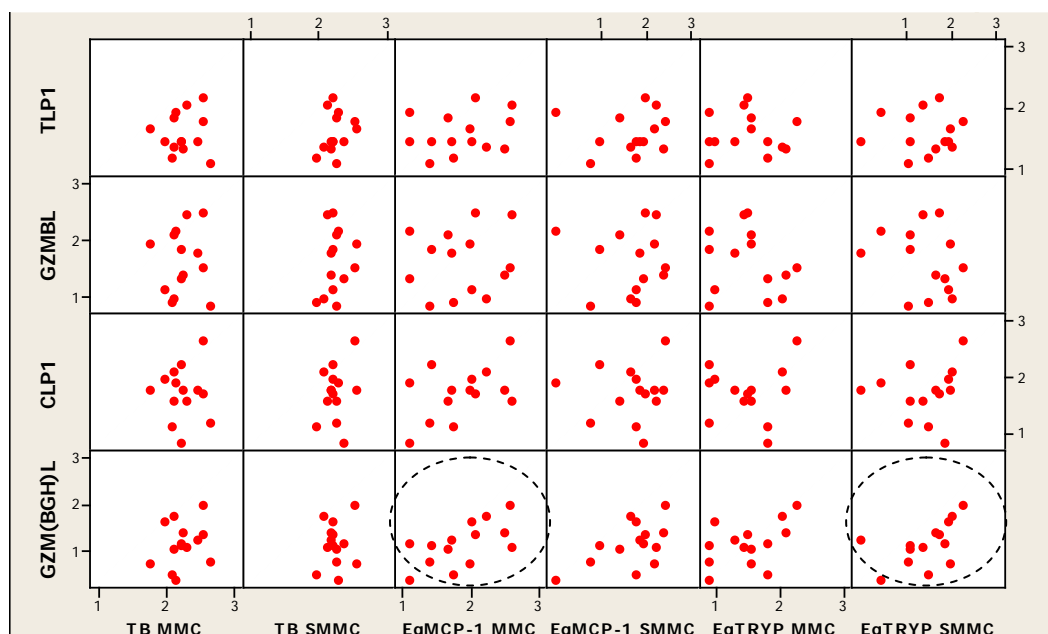


Figure 4.37: Matrix scatter plot of log10+1 transformed counts for RB mast cell counts (x-axis) and RB transcript levels (y-axis). Significant relationships are circled. (TLP1: Tryptase-like Proteinase-1; GZMBL: Granzyme B-like; CLP1: Chymase-like Proteinase-1; GZM(BGH)L: Granzyme(BGH)-like. RB: Rectal biopsy).

RB		TB MMC	TB SMMC	EqMCP-1 MMC	EqMCP-1 SMMC	EqTRYP MMC	EqTRYP SMMC
TLP1	rho	0.154	0.270	0.150	0.235	-0.086	-0.040
	p	<i>0.599</i>	<i>0.349</i>	<i>0.610</i>	<i>0.418</i>	<i>0.770</i>	<i>0.893</i>
GZMBL	rho	0.112	0.174	0.123	0.182	-0.203	-0.200
	p	<i>0.703</i>	<i>0.553</i>	<i>0.675</i>	<i>0.532</i>	<i>0.486</i>	<i>0.493</i>
CLP1	rho	-0.033	0.095	0.282	-0.029	-0.016	0.240
	p	<i>0.911</i>	<i>0.750</i>	<i>0.329</i>	<i>0.928</i>	<i>0.958</i>	<i>0.409</i>
GZM(BGH)L	rho	0.251	-0.160	0.581	0.446	0.471	0.574
	p	<i>0.387</i>	<i>0.584</i>	0.029	<i>0.112</i>	<i>0.089</i>	0.032

Table 4.16: Table of rho values (bold) and p values (in italics) for correlations between genes of interest in the rectum and rectal TB, eqMCP-1 and eqTRYP MMC and SMMC from rectal biopsy. Significant p-values are highlighted in yellow. (TLP1: Tryptase-like Proteinase-1; GZMBL: Granzyme B-like; CLP1: Chymase-like Proteinase-1; GZM(BGH)L: Granzyme(BGH)-like. RB: Rectal biopsy).

4.5 Relationship between Tissue Transcript Levels and Tissue Proteinase Concentration

The relationships between caecal transcript levels and caecal tissue proteinase concentrations are displayed as a matrix scatter plot in Figure 4.38. The p and rho values for each correlation are in Table 4.17. There was no significant correlation between the levels of transcript and the tissue proteinase concentrations at this site.

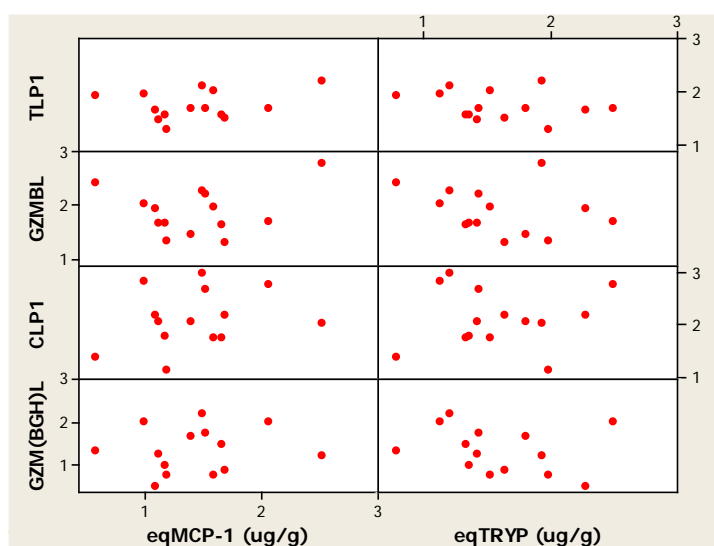


Figure 4.38: Matrix scatter plot of log10+1 transformed data for the amount of caecal eqMCP-1 and eqTRYP from Tissue ELISA (x-axis) and caecal transcript levels (y-axis). (TLP1: Tryptase-like Proteinase-1; GZMBL: Granzyme B-like; CLP1: Chymase-like Proteinase-1; GZM(BGH)L: Granzyme(BGH)-like).

Caecum		TLP1	GZMBL	CLP1	GZM(BGH)L
eqMCP-1(μ g/g)	rho	0.169	-0.088	0.103	0.086
	p	<i>0.563</i>	<i>0.765</i>	<i>0.727</i>	<i>0.773</i>
eqTRYP(μ g/g)	rho	-0.229	-0.326	-0.002	-0.371
	p	<i>0.431</i>	<i>0.256</i>	<i>1.000</i>	<i>0.192</i>

Table 4.17: Table of rho values (bold) and p values (in italics) for correlations between Caecal genes of interest and Caecal eqMCP-1 and eqTRYP Tissue ELISA results. (TLP1: Tryptase-like Proteinase-1; GZMBL: Granzyme B-like; CLP1: Chymase-like Proteinase-1; GZM(BGH)L: Granzyme(BGH)-like).

The relationships between RVC transcript levels and RVC tissue proteinase concentrations are displayed as a matrix scatter plot in Figure 4.40. The p and rho values for each correlation are shown in Table 4.18. There was a significant correlation between the levels of TLP1 transcript and eqMCP-1 tissue concentrations (Table 4.18: $p=0.032$, $\rho=0.582$) at this site.

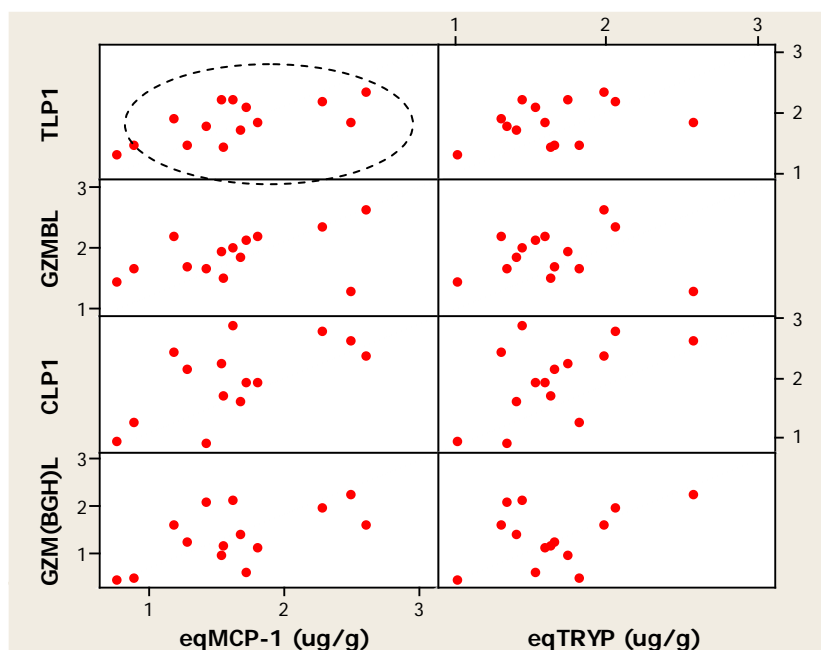


Figure 4.39: Matrix scatter plot of log10+1 transformed data for the amount of RVC eqMCP-1 and eqTRYP from Tissue ELISA (x-axis) and RVC transcript levels (y-axis). Significant relationships are circled. (TLP1: Tryptase-like Proteinase-1; GZMBL: Granzyme B-like; CLP1: Chymase-like Proteinase-1; GZM(BGH)L: Granzyme(BGH)-like).

RVC		TLP1	GZMBL	CLP1	GZM(BGH)L
eqMCP-1 (µg/g)	rho	0.582	0.451	0.512	0.451
	p	0.032	<i>0.186</i>	<i>0.064</i>	<i>0.108</i>
eqTRYP (µg/g)	rho	0.306	0.130	0.451	0.174
	p	<i>0.288</i>	<i>0.660</i>	<i>0.108</i>	<i>0.553</i>

Table 4.18: Table of rho values (bold) and p values (in italics) for correlations between RVC genes of interest and RVC eqMCP-1 and eqTRYP Tissue ELISA results. Significant p-values are highlighted in yellow. (TLP1: Tryptase-like Proteinase-1; GZMBL: Granzyme B-like; CLP1: Chymase-like Proteinase-1; GZM(BGH)L: Granzyme(BGH)-like).

The relationships between rectal transcript levels and rectal tissue proteinase concentrations are displayed as a matrix scatter plot in Figure 4.40. The p and rho values for each correlation are displayed in Table 4.19. There was a significant correlation between levels of GZM(BGH)L transcript and the eqMCP-1 tissue concentration in the rectum (Table 4.19: $p=0.005$, $\rho=0.723$).

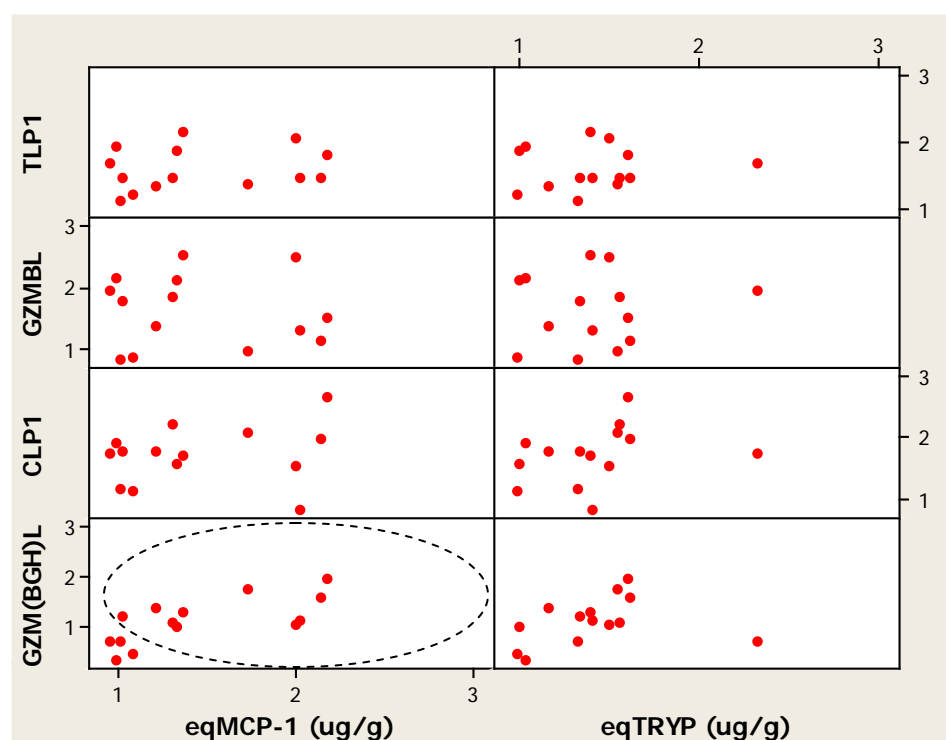


Figure 4.40: Matrix scatter plot of log10+1 transformed data for the amount of RB eqMCP-1 and eqTRYP from Tissue ELISA (x-axis) and RB transcript levels (y-axis). Significant relationships are circled. (TLP1: Tryptase-like Proteinase-1. GZMBL: Granzyme B-like. CLP1: Chymase-like Proteinase-1. GZM(BGH)L: Granzyme(BGH)-like. RB: Rectal biopsy).

RB		TLP1	GZMBL	CLP1	GZM(BGH)L
eqMCP-1(μ g/g)	rho	0.160	-0.055	0.187	0.723
	p	<i>0.584</i>	<i>0.856</i>	<i>0.522</i>	0.005
eqTRYP(μ g/g)	rho	0.112	0.042	0.499	0.468
	p	<i>0.704</i>	<i>0.892</i>	<i>0.072</i>	<i>0.094</i>

Table 4.19: Table of rho values (bold) and p values (in italics) for correlations between RB genes of interest and RB eqMCP-1 and eqTRYP Tissue ELISA results. Significant p-values are highlighted in yellow. (TLP1: Tryptase-like Proteinase-1; GZMBL: Granzyme B-like; CLP1: Chymase-like Proteinase-1; GZM(BGH)L: Granzyme(BGH)-like. RB: Rectal biopsy).

4.6 Relationship between Tissue Transcript Levels and Serum Proteinase Concentration

The relationships between caecal transcript levels and local serum eqMCP-1 and eqTRYP concentrations were explored and are displayed as a matrix scatter plot in Figure 4.41. The p and rho values for each correlation are shown in Table 4.20. There was a significant correlation between the caecal levels of CLP1 transcript and the local serum concentration of eqMCP-1 (Table 4.20: $p=0.028$, $\rho=0.596$). There was also a significant correlation between the caecal levels of GZM(BGH)L transcript and the concentration of eqMCP-1 in the local serum (Table 4.20: $p=0.044$, $\rho=0.552$).

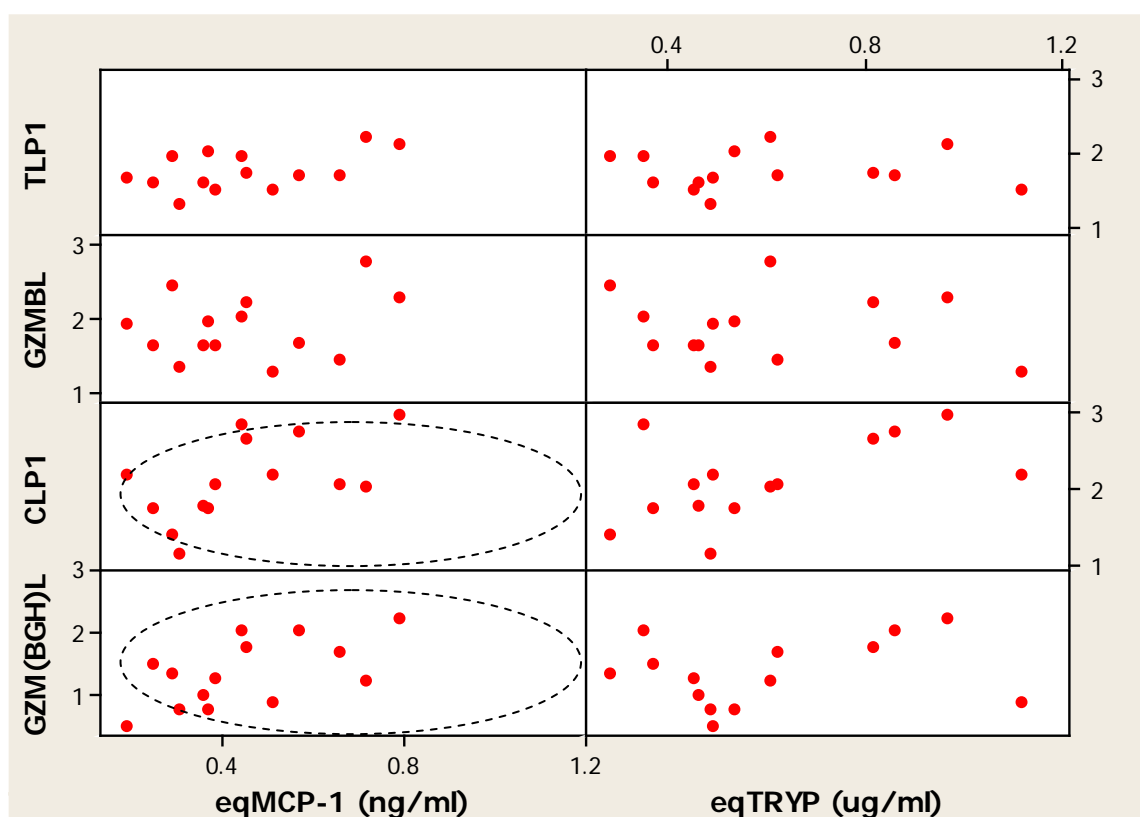


Figure 4.41: Matrix scatter plot of log10+1 transformed data for the amount of caecal eqMCP-1 and eqTRYP from -20°C Serum ELISA (x-axis) and caecal transcript levels (y-axis). Significant relationships are circled. (TLP1: Tryptase-like Proteinase-1; GZMBL: Granzyme B-like; CLP1: Chymase-like Proteinase-1; GZM(BGH)L: Granzyme(BGH)-like).

Caecum		TLP1	GZMBL	CLP1	GZM(BGH)L
eqMCP-1 (ng/ml) (-20°C)	rho	0.462	0.209	0.596	0.552
	p	<i>0.096</i>	<i>0.473</i>	0.028	0.044
eqTRYP (µg/ml) (-20°C)	rho	0.152	-0.097	0.521	0.152
	p	<i>0.604</i>	<i>0.742</i>	<i>0.059</i>	<i>0.605</i>

Table 4.20: Table of rho values (bold) and p values (in italics) for correlations between genes of interest from Caecal tissue and eqMCP-1 and eqTRYP serum ELISA results. Significant p-values are highlighted in yellow. (TLP1: Tryptase-like Proteinase-1; GZMBL: Granzyme B-like; CLP1: Chymase-like Proteinase-1; GZM(BGH)L: Granzyme(BGH)-like).

The relationships between RVC transcript levels local serum eqMCP-1 and eqTRYP concentrations are displayed as a matrix scatter plot in Figure 4.42. The p and rho values for each correlation are shown in Table 4.21. There was a significant

correlation between the RVC levels of CLP1 transcript and the concentration of eqMCP-1 in the serum (Table 4.21: $p=0.004$, $\rho=0.732$).

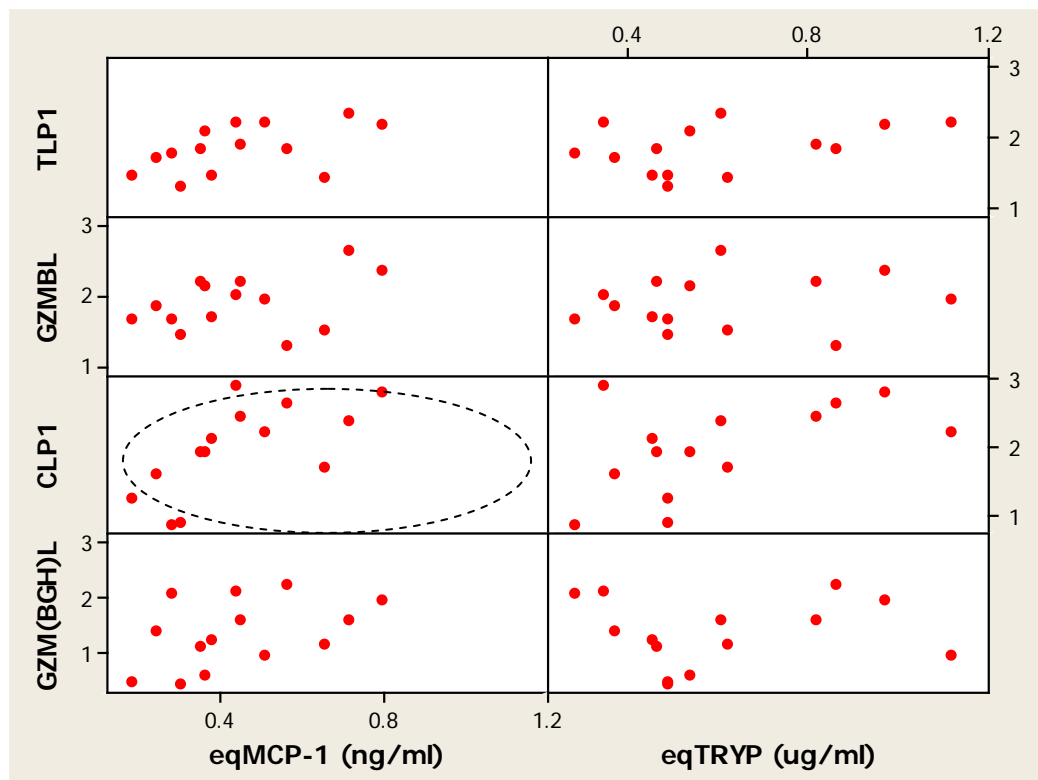


Figure 4.42: Matrix scatter plot of log10+1 transformed data for the amount of RVC eqMCP-1 and eqTRYP from -20°C Serum ELISA (x-axis) and RVC transcript levels (y-axis). Significant relationships are circled. (TLP1: Tryptase-like Proteinase-1; GZMBL: Granzyme B-like; CLP1: Chymase-like Proteinase-1; GZM(BGH)L: Granzyme(BGH)-like).

RVC		TLP1	GZMBL	CLP1	GZM(BGH)L
eqMCP-1 (ng/ml) (-20°C)	rho	0.525	0.332	0.732	0.411
	p	<i>0.057</i>	<i>0.246</i>	0.004	<i>0.146</i>
eqTRYP(μg/ml) (-20°C)	rho	0.328	0.160	0.446	-0.046
	p	<i>0.253</i>	<i>0.584</i>	<i>0.112</i>	<i>0.880</i>

Table 4.21: Table of rho values (bold) and p values (in italics) for correlations between genes of interest from RVC tissue and eqMCP-1 and eqTRYP serum ELISA results. Significant p-values are highlighted in yellow. (TLP1: Tryptase-like Proteinase-1; GZMBL: Granzyme B-like; CLP1: Chymase-like Proteinase-1; GZM(BGH)L: Granzyme(BGH)-like).

The relationships between rectal transcript levels and local serum eqMCP-1 and eqTRYP serum proteinase concentrations are displayed as a matrix scatter plot in Figure 4.43. The p and rho values for each correlation are shown in Table 4.22. There were no significant correlations between the levels of transcript of each of the proteinases and serum concentrations of either eqMCP-1 or eqTRYP.

RB		TLP1	GZMBL	CLP1	GZMBGHL
eqMCP-1 (ng/ml) (-20°C)	rho	0.011	-0.099	0.253	0.499
	p	<i>0.976</i>	<i>0.739</i>	<i>0.383</i>	<i>0.072</i>
eqTRYP (µg/ml) (-20°C)	rho	0.112	0.108	0.262	0.332
	p	<i>0.704</i>	<i>0.716</i>	<i>0.366</i>	<i>0.246</i>

Table 4.22: Table of rho values (bold) and p values (in italics) for correlations between genes of interest from rectal biopsy and eqMCP-1 and eqTRYP -20°C serum ELISA results. (TLP1: Tryptase-like Proteinase-1; GZMBL: Granzyme B-like; CLP1: Chymase-like Proteinase-1; GZM(BGH)L: Granzyme(BGH)-like. RB: Rectal biopsy).

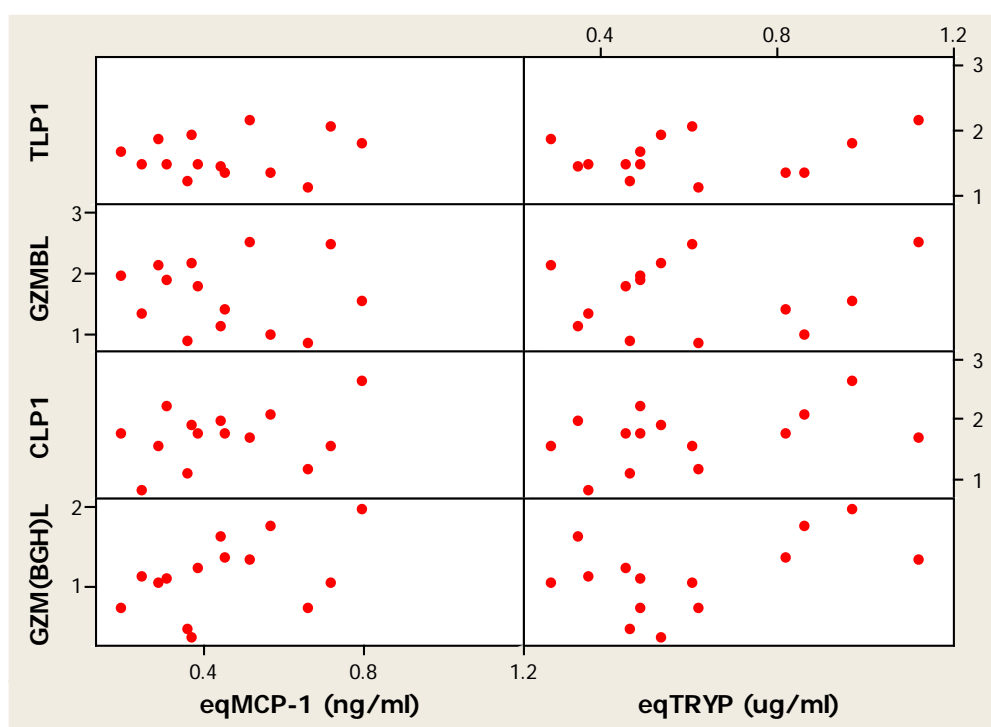


Figure 4.43: Matrix scatter plot of log10+1 transformed data for the amount of rectal eqMCP-1 and eqTRYP from -20 °C Serum ELISA (x-axis) and RB transcript levels (y-axis). (TLP1: Tryptase-like Proteinase-1; GZMBL: Granzyme B-like; CLP1: Chymase-like Proteinase-1; GZM(BGH)L: Granzyme(BGH)-like. RB: Rectal biopsy).

4.7 Discussion

The first aim here was to investigate the ambiguity surrounding previous work on equine mast cell proteinases. The equine genome was utilised as a tool to further clarify the situation and to explore novel equine mast cell proteinases. Observations were made using the archetypal chymotrypsinogen numbering system based on the alignment of amino acid sequences with chymotrypsinogen (Hartley and Neurath 1970; Hedstrom 2002). The second aim was quantitative analysis for further investigation into proteinase expression and the relationship of these proteinases with cyathostomin burden and mast cell response.

The two neutral serine proteinases previously extracted from equine mastocytoma tissue, equine tryptase (eqTRYP) and equine Mast Cell Proteinase-1 (eqMCP-1), had been used to raise antibodies in rabbits. The cloning and sequencing of these equine mastocytoma derived proteins has been previously investigated. EqTRYP has been cloned and sequenced (Dacre, McAleese et al. 2006) and is referred to in this chapter as Tryptase-like Proteinase-1 (TLP1). At the time of study, exploration into the equine genome did not demonstrate any further predicted tryptase-like equine mast cell proteinase sequences. TLP1 was also the only tryptase-like sequence identified from the MASCOT results. Therefore the results here suggest that there is only one equine tryptase gene, however full mapping of the equine tryptase locus would be necessary to confirm this.

Enzymic activity of granzymes depends on the presence of three highly conserved aa: His57, Asp102 and Ser195 (chymotrypsinogen numbering), otherwise known as the catalytic triad (Hedstrom 2002). Other highly conserved sites include aa residues 189, 216 and 226, which are important in determining the specificity pocket, and cysteine residues required for disulphide bridge formation (Hedstrom 2002). The S1 site, a polypeptide binding site adjacent to Ser195, is formed by residues 189-192, 214-216 and 224-228 (Hedstrom 2002). Granzyme specificity is determined by the aa residue at 226. This is in contrast to tryptase enzymes, in which the residue of primary importance for specificity is at position 189 (Zamolodchikova, Sokolova et al. 2003). Ser195 is the catalytic residue in all serine proteinases and is adjacent to the S1 substrate recognition site (Hedstrom 2002).

Equine TLP1, like all trypsin-like proteinases, contains an aspartate at residue 189 (Dacre, McAleese et al. 2006). Other conserved trypsin-like proteinase features present in the TLP1 sequence are the activation site region IVGG (residues 31-34) and cysteine residues at 191 and 220 (Dacre 2005). Unusually for a trypsin-like proteinase, equine tryptase contains an alanine, rather than glycine, at residue 216, as seen here (Figure 4.9) and in previous studies (Dacre, McAleese et al. 2006). This is of importance because this forms part of the substrate binding pocket wall and is considered a critical determinant of substrate specificity (Perona, Hedstrom et al. 1995). This substitution may alter substrate specificity as alanine has a larger side chain (CH₃) than glycine (H) and will therefore protrude further into the substrate-binding pocket. The biological significance of this substitution could be that it may restrict fibrinogenolysis (Dacre, McAleese et al. 2006) as, unlike equivalents in humans (human β tryptase) (Thomas, Wheelless et al. 1998) and sheep (sheep mast cell proteinase-1) (Pemberton, Huntley et al. 1997), equine tryptase lacks the ability to cleave fibrinogen (Dacre, McAleese et al. 2006). This theory is supported by the fact that the aspartate substitution at residue 216 (Fiorucci and Ascoli 2004) in human alpha tryptase is implicated in this proteinase's reduced activity (Selwood, Wang et al. 2002) and inability to cleave substrates including fibrinogen (Huang, Li et al. 1999). Further work is required to confirm the relevance of this substitution.

Multiple closely related chymases are expressed by many mammalian species (McAleese, Pemberton et al. 1998; Miller and Pemberton 2002). The genome of the rat contains 28 closely related functional chymases (Puente and López-Otín 2004), compared to at least 14 in the mouse (Gallwitz and Hellman 2006) and four in the human (Caughey, Schaumberg et al. 1993; Gallwitz and Hellman 2006). When Pickles et al. (2005) attempted to obtain the chymase nucleotide sequence from equine tissue, the deduced aa sequence for the putative equine Mast Cell Proteinase-1 had an N-terminal aa sequence that differed from the mastocytoma derived eqMCP-1 sequence by two aa. The peptide mass fingerprints of these chymases were poorly matched and it was hypothesised that a similar, but novel, proteinase was cloned and sequenced (CLP1), rather than the original mastocytoma derived chymase (eqMCP-1) (Dacre 2005). Proteomic analysis in this chapter demonstrated that the

most abundant proteinase in the purified eqMCP-1 was in fact GZM(BGH)L. In addition this sequence also had the highest number of unique peptide hits (6). Also, the predicted N-terminal aa sequence of GZM(GBH)L was identical to the N-terminal aa sequence of eqMCP-1 (Pemberton, McEuen et al. 2001). Due to this sequence similarity and the abundance of this proteinase it is hypothesised that the sequence GZM(BGH)L is the original sequence of mast cell chymase characterised and isolated by Pemberton et al. (2001) and that the chymase measured in previous chapters is in fact GZM(BGH)L. The NCBI annotation GZM(BGH)L is potentially misleading as there is no official gene nomenclature for equids, hence gene and protein names originate from a number of sources including annotation on GenBank (INSDC) records, literature, and Swiss-Prot. Both CLP1 and GZM(BGH)L have a glutamine at residue 226 which suggests that they have a similar activity. This provides further evidence of the presence of multiple equine mast cell chymases as the predicted nucleotide sequence of GZM(BGH)L shares <85% identity with the NCBI entry for putative equine mast cell proteinase-1 (CLP1). Full sequence analysis of the proteinase GZM(BGH)L would be necessary to confirm this in conjunction with experiments to deduce its biological activity and functional specificity.

Investigation into the equine genome here has shown that the mast cell chymase locus is situated on equine chromosome 1. This locus contains one or two alpha chymases and additional serine proteinases including lymphocyte-derived granzymes (Gallwitz, Enoksson et al. 2007). Granzymes can be grouped according to their specificity; their subfamilies have tryptase-like, chymotrypsin-like and elastase-like properties (Smyth, O'Connor et al. 1996). In humans and mice, granzymes are grouped into three clusters among three different chromosomes; GrA, GrB and GrM (Ewen, Kane et al. 2012). The subfamily with chymotrypsin-like specificity (GrB) is grouped on the chymase locus and includes mouse granzyme B, C, D, E, F and G and granzyme B and H in the human (Trapani 2001). Equine granzyme B (eqGrzmB) has been identified and characterized (Piuko, Bravo et al. 2007) and is also located on equine chromosome 1. At the time of this study, eqGrzmB was the only

sequenced equine granzyme in the NCBI database; TLP1 and CLP1 were the only previously identified equine mast cell proteinases.

The database GranzymeDB was compiled of nine protein candidates selected from the MASCOT results from the equine mastocytoma and tissue homogenate and comprised eqTRYP/TLP1, CLP1 and an additional seven predicted sequences. Two of the predicted sequences were selected for further analysis and quantification, granzyme B-like (GZMBL) and Granzyme(BGH)-like (GZM(BGH)L). Although these sequences were termed granzyme B-like and Granzyme(BGH)-like, as previously mentioned there is no official gene nomenclature for equids. Therefore, for these predicted sequences their assigned ‘granzyme-like’ names are potentially misleading as their cellular origin is yet to be determined. Also, these sequences were re-named when the equine genome was re-annotated. The re-annotated gene and protein name for both sequences, granzyme H-like, was generated automatically by NCBI’s genome annotation pipeline. The sequences were aligned with human and rat granzyme H, both of which have a glycine at 226. This glycine has a critical role for substrate specificity of human granzyme H (Wang, Zhang et al. 2012). The sequences do not share this residue, with GZMBL displaying an arginine and GZM(BGH)L displaying a glutamine. This suggests that they do not share the same specificity and hence their re-annotation as granzyme H-like is potentially inaccurate. Interestingly, like human, mouse and rat granzyme B, GZMBL has an arginine at residue 226 (Cullen, Adrain et al. 2007) suggesting that the original NCBI nomenclature is more accurate. Despite the significant similarities in sequence, human and murine granzyme B have been demonstrated to have divergent substrate preferences (Cullen, Adrain et al. 2007). Full sequence analysis and specificity studies on these proteins would be necessary to confirm the correct annotation for these proteinases. Furthermore, as the RNA was extracted from a tissue homogenate with a mixed cell population, it is not possible to definitively state the cellular origin of the proteinases. It is possible that they may be lymphocyte derived; granzymes are members of a chymotrypsin related family of serine proteinases produced by cytotoxic T-cells and NK cells (Trapani 2001). However, granzymes are not always limited to a single cellular origin. In mice, granzyme D is expressed by both mucosal

mast cells and T cells (Rönnberg, Calounova et al. 2013). *In situ* hybridisation would be necessary to confirm the cellular locations of these proteinases in equine tissue.

Here, cDNA created from RNA extracted from the intestinal tissue of five horses, was used to compare the nucleotide and translated protein sequences of TLP1, GZMBL, CLP1 and GZM(BGH)L across a region of interest unique to that gene. The RNA quality of all horses, even those in a known diseased state, such as horse DV3, was high; all RIN values were greater than 8. Full sequence analysis was not performed as it was outwith the scope of the project. Due to the highly conserved nature of the proteinase sequences it was necessary to design the primer and probes manually to ensure that selected regions were specific to the sequences of interest. The primers were verified using cDNA from five horses and the amplicons from samples compared to ensure that the primers were specific. Due to the highly similar nucleotide sequences of the genes of interest, probes were used to increase the reaction specificity. The primers and probes were also tested in a matrix; this experiment was successful in demonstrating specificity, as all probes were specific to their designed primer set. All TLP1 sequences were identical to the query TLP1 sequence. Although there were a number of differences in the nucleotide sequences between the five horses and the query GZMBL sequence, only two differences altered the derived aa sequence. The CLP1 amplicon nucleotide sequences demonstrated only one translated difference between the query sequence and sequences derived from the equine tissue here. The GZM(BGH)L amplicon nucleotide sequences showed two differences, both of which were seen in a single horse. Only one of these translated to a difference in the derived protein sequence.

Although it was outwith the scope of this project to analyse the full sequences it is interesting to observe that horse DV3, a case of larval cyathostominosis, had a number of sequence polymorphisms over the area compared in the protein sequence of both CLP1 and GZM(BGH)L. This could potentially have an effect on protein structure and function (Ng and Henikoff 2001). In the case of GZM(BGH)L this difference was at residue 103. The aspartate residue at position 102 is of importance because as mentioned above, along with His57 and Ser195, it is part of the catalytic triad which is a complex network of hydrogen bonds (Hedstrom 2002). In the case of

CLP1, the difference in protein sequence was at residue 214. Residue 216 is of importance because, along with residues 189 and 226, it forms the substrate specificity pocket. Potentially of greater importance is that Ser214 (replaced with a proline in horse DV3) forms a hydrogen bond with Asp102 (Hedstrom 2002). Ser214 has been considered the fourth member of the catalytic triad (McGrath, Vasquez et al. 1992; Krem and Di Cera 2001; Hedstrom 2002). Although some studies have suggested it is non-essential for enzyme catalytic function (Epstein and Abeles 1992; McGrath, Vasquez et al. 1992) Ser214 is highly conserved due to its role in substrate recognition (Krem, Prasad et al. 2002) and contributes to the S1 binding pocket (Perona, Hedstrom et al. 1995). As these two substitutions in horse DV3 for the CLP1 (residue 214) and GZM(BGH)L (residue 103) sequences are closely related to residues affecting proteinase specificity, further work is warranted to explore the full protein sequences and the enzymic activity of the derived enzymes.

In mice the absence of the chymase mMCP-1 gene has been demonstrated to affect the kinetics of *Nippostrongylus brasiliensis* infection (Wastling, Knight et al. 1998) and this knockout also had a negative effect on the clearance of *Trichinella spiralis* worms from the intestine (Knight, Wright et al. 2000). A hypothesis that requires further investigation is that alterations in mast cell proteinase aa sequence has a deleterious effect on the proteinase structure and function. SNPs are the most abundant and widespread form of genetic sequence variation (Marth, Korf et al. 1999). An equine SNP genotyping array has been developed and evaluated (Wade, Giulotto et al. 2009; McCue, Bannasch et al. 2012). Exploring the chymase locus on equine chromosome 1, particularly investigating the minority of horses that are carrying high cyathostomin burdens, would be a valuable way of determining the significance of these SNPs. The results from this Chapter provide a preliminary framework for this: however, further sequence analysis at the genetic and functional levels must be performed.

It is becoming increasingly important to analyse the appropriate housekeeping gene as it has been shown that commonly used housekeeping genes are not always suitable choices due to variation in their own expression profiles (Dheda, Huggett et al. 2004; Barber, Harmer et al. 2005; Cappelli, Felicetti et al. 2008). In the case of the horse, a

number of studies have utilised different housekeeping genes in BALF (Beekman, Tohver et al. 2011), peripheral blood mononuclear cells (Cappelli, Felicetti et al. 2008; Figueiredo, Salter et al. 2009) and colon, heart, kidney, liver, lung, lymph node, small intestine and spleen (Zhang, Davis et al. 2009), skin and sarcoid tissue (Bogaert, Van Poucke et al. 2006). Also, of relevance here, intestinal regions have been shown to differ in their gene expression (Comelli, Lariani et al. 2009). The computer programme geNorm, minimises errors caused by inappropriate reference gene selection by enabling analysis of a selection of reference genes and providing information on the best possible combination for the experimental conditions (Vandesompele, De Preter et al. 2002). GeNorm provides a gene expression normalisation factor that can be calculated for each sample based on the geometric mean of a defined number of reference genes. The optimal normalisation factor for this study was calculated as the geometric mean of reference targets SDHA and GAPDH. GAPDH is a commonly used reference gene in intestinal samples of horses (Hjertner, Olofsson et al. 2013 ; Southwood, Lindermann et al. 2006; Woodward, Holcombe et al. 2010; Fossum, Hjertner et al. 2012). GAPDH is also used as an intestinal reference gene in rats (Bulut, Felderbauer et al. 2008) and humans (Pizarro, Michie et al. 1999). There are fewer reports of SDHA as a reference gene; however SDHA was the optimal small intestinal housekeeping gene in sheep infected with gastrointestinal nematodes (Zaros, Coutinho et al. 2010). Efficiency between 90 and 110% is generally considered optimal (D'haene, Vandesompele et al. 2010) and encouragingly, all the reactions were within an efficiency range of 88 to 110%.

There was a significant difference in the levels of transcript of TLP1, GZMBL, CLP1 and GZM(BGH)L in each organ. Transcript levels of CLP1 consistently displayed the highest median and greatest range at all sites. The elevated levels of CLP1 supports the previous immunolabelled-cell counts (Chapter 3) as the majority of mast cells enumerated were chymase-positive. The level of transcript of each protein between organs was not significantly different. In the caecum, RVC and rectum, transcript levels of TLP1 and GZMBL were significantly positively correlated. Levels of CLP1 and GZM(BGH)L positively correlated significantly in the caecum and RVC, and approached significance ($p=0.054$, $\rho=0.530$) in the rectum. This

could be due to two predominant subsets of mast cells; one that is producing TLP1 and GZMBL and another subset generating CLP1 and GZM(BGH)L. Alternatively, production of these proteinases could be from individual cell populations that are responding to the environment, including the cyathostomin burden, in a similar way. As mentioned, the GZMBL sequence contains an arginine at residue 226 as do human, mouse and rat granzyme B (Cullen, Adrain et al. 2007). This strict requirement at this residue confers specificity at the P1 site (Vaughn, Harris et al. 2000; Hedstrom 2002; Ruggles, Fletterick et al. 2004). As previously mentioned, granzymes can be expressed by more than one cell type; murine granzyme D is expressed by both T cells and mucosal mast cells (Rönnerberg, Calounova et al. 2013) and mast cells have the ability to both express multiple chymases and adjust their proteinase phenotype to their environment (Friend, Ghildyal et al. 1998). Furthermore, granzyme and chymase sequences show high identity at the nucleotide level; hence it would be necessary to perform *in situ* hybridisation to confirm the cellular origin of these genes and further characterise the intestinal mast cell populations at these sites.

The results presented here provide evidence that serum concentrations of eqMCP-1, measured by ELISA (Chapter 3), correlate with transcript expression of certain chymases in the large intestine. The closest relationship was observed with CLP1. Caecal transcript levels of CLP1 and GZM(GBH)L significantly positively correlated with the eqMCP-1 measured in serum from veins draining the large intestine. In the RVC, a similar correlation was observed between CLP1 transcript levels and eqMCP-1 serum concentrations. There were no significant correlations between local serum proteinase concentrations and any of these transcripts measured in the rectum. The conclusions that can be drawn from this data are limited without full knowledge of the specificity of the antibodies utilised in the ELISA. As the sequences are homologous and the antibodies polyclonal there is potential for the recognition of multiple epitopes leading to cross-reactivity. Further studies are warranted, such as immunoaffinity chromatography, to assess the specificity of the rabbit anti-eqMCP-1 and -eqTRYP IgG reagents used earlier in this study.

When comparing transcript levels and mast cell counts, significant positive correlations were seen between mucosal TB-stained mast cell levels, eqMCP-1-positive and eqTRYP positive cells with CLP1 transcript levels in the caecum. In the RVC, significant positive correlations were observed only between CLP1 transcript levels and TB-stained mucosal mast cells levels ($p=0.024$, $\rho=0.609$). In the rectum relationships were seen between GZM(BGH)L transcript levels and eqMCP-1-positive mucosal mast cell ($p=0.029$, $\rho=0.581$) and eqTRYP positive submucosal mast cells ($p=0.032$, $\rho=0.574$). The relationships between GZM(BGH)L and chymase measures could be explained by the proteomic results here. These have demonstrated that the previously purified chymase was predominantly GZM(BGH)L, and therefore the antibodies raised against this chymase used here may actually be largely recognising GZM(BGH)L. There was a significant positive correlation between tissue transcript levels of GZM(BGH)L and eqMCP-1 tissue concentrations in the rectum ($p=0.005$, $\rho=0.723$). This relationship is further supported by the ELISA results which demonstrated a significant positive relationship between rectal eqMCP-1 mucosal mast cell counts and rectal eqMCP-1 concentration, ($p=0.002$, $\rho=0.564$). This is of interest due to the significant positive linear relationship between the eqMCP-1-labelled MMC in the rectal biopsy tissue and the combined CTMB ($p=0.018$, $r^2=43.1\%$). However, there was no significant relationship between the log10+1 transformed CTMB and any of the four transcript levels in the rectum.

In the mouse the constitutive expression of the chymase mast cell proteinase-1 (mMCP-1) in the jejunum has been demonstrated, as well as the up-regulation of this proteinase during *N. brasiliensis* infection (Wastling, Scudamore et al. 1997). The altered expression of this proteinase has also been demonstrated to delay expulsion of *T. spiralis* (Knight, Wright et al. 2000). Linear regression analysis here demonstrated a statistically significant positive relationship between transcript levels of TLP1 and the CTMB, ($p=0.007$, $r^2=51.2\%$) in the RVC. In this organ, there was also a statistically significant positive relationship between transcript levels of GZMBL and the CTMB, ($p=0.042$, $r^2=45.4\%$). This result supports the relationship observed between tissue eqTRYP concentrations and the RVC CTMB in Chapter 3. It also provides support for the hypothesis that there are previously unidentified

novel equine mast cell proteinases. The cellular origin of GZMBL requires verification; however the fact that its presence was identified in equine mastocytoma tissue is support for the hypothesis that this novel equine proteinase is mast cell derived. The strong relationship between GZMBL and TLP1 expression in all three organs examined provides further support for this.

The relationship between TLP1 and RVC CTMB also supports previous equine studies which demonstrated that tryptase-labelled mast cells had the strongest relationship with cyathostomin burden, with total cyathostomin burden accounting for 57% of the variation in tryptase-labelled mast cell counts in the caecal mucosa (Pickles, Mair et al. 2010). Although in the cohort studied here these relationships were not verified in the caecum and rectum the results from the RVC are encouraging. As was demonstrated here, the equine genome provides a valuable tool for further investigation. Preliminary investigation using this resource has shown that the equine chymase expressing genes are located around chromosome 1. The work described here has provided evidence of multiple equine mast cell proteinase-like gene sequences that are expressed in equine intestinal tissue and a foundation for their characterisation. Two transcripts that were analysed here, GZMBL and GZM(BGH)L, have close homology to the putative equine Mast Cell Proteinase-1 sequence (CLP1). There was strong evidence to suggest that the predicted sequence GZM(BGH)L is the same as the initial equine mast cell proteinase originally purified from an equine mastocytoma. This proteinase was used to generate many of the immunological reagents used in this study (Pemberton, McEuen et al. 2001). This requires further verification but it may mean that the antibodies used in the ELISAs and immunohistochemistry in Chapter 3 were predominantly picking up signals for GZM(BGH)L.

This chapter has therefore provided useful insight into the potential for novel equine mast cell proteinases. The previous ambiguity surrounding equine mast cell proteinase-1 has been clarified through the proteomic work and the identification of GZM(BGH)L as the previously isolated and characterised eqMCP-1 proteinase. Full sequence analysis is required to investigate the four sequences examined in this chapter further, in conjunction with *in situ* hybridisation to examine the cellular

origin of these proteinases. The expression of TLP1 was closely correlated with GZMBL expression, and linear regression analysis has demonstrated a statistically significant positive relationship between both TLP1 and GZMBL transcript levels and total mucosal cyathostomin in the RVC. This work has therefore provided a good foundation for further exploration into the role of equine mast cell proteinases in the immune response to equine cyathostomins.

5 General Discussion

As a result of their prevalence and pathogenicity cyathostomins are considered the most important equine nematode (Matthews 2014; Love, Murphy et al. 1999; Matthews 2008). With the growing concern over the development of anthelmintic resistance, and no new therapeutic options on the horizon, it is important to investigate the potential for diagnostic assays to facilitate targeted treatment (Matthews 2014; McWilliam, Nisbet et al. 2010). In particular, encysted larvae play an important role in the epidemiology and pathogenesis of cyathostominosis (Giles, Urquhart et al. 1985) and to date there is no accurate way to assess an individual's infection status. An increase in caecal mast cells expressing proteinases has been demonstrated during cyathostomin infection (du Toit, McGorum et al. 2007; Pickles, Mair et al. 2010) and ELISAs have been used with some success to measure the systemic release of mast cell proteinases into blood during nematode infections in other species (Miller, Woodbury et al. 1983; Woodbury, Miller et al. 1984; Huntley, Gibson et al. 1987; Huntley, Gooden et al. 1990). By increasing the knowledge of the relationship between immune effector cells, such as mast cells, and cyathostomins the potential for their use as predictors of burden can be explored. This thesis has further investigated the involvement of mast cells and their proteinases, equine mast cell proteinase-1 (eqMCP-1) and equine tryptase (eqTRYP) in natural equine cyathostomin infection, and evaluated the potential for mast cell proteinase assays to be used in minimally invasive diagnostic tests to estimate encysted cyathostomin larval burden. Knowledge of an individual's larval cyathostomin status would be beneficial to inform strategic and targeted treatments, especially in young horses that are more susceptible to clinical disease (Traversa, Milillo et al. 2010). Prerequisites for a cyathostomin diagnostic assay include identification of cyathostomins at their encysted and pathogenic stage and an assay that quickly becomes negative following effective therapy to allow the monitoring of treatment protocols (Andersen, Howe et al. 2013). A diagnostic assay for clinical use must be robust and practically applicable in the field (Matthews 2014), hence the focus here was on serum and rectal tissue biopsy samples. A diagnostic IgG(T) serum ELISA using recombinant versions of cyathostomin gut associated larval antigen (Cy-GALA) generated for a

number of common cyathostomin species is currently being assessed (Matthews 2011). However, the dynamics of antigen specific IgG(T) responses, particularly following treatment, are a concern when considering this assay's utility. Mast cell proteinase tissue expression and concentrations in serum and tissue were therefore investigated in this study as potential biomarkers of active infection. The usefulness of a diagnostic assay can be described by its sensitivity, specificity, and positive and negative predictive value (Akobeng 2006). This study was limited in its ability to assess these factors, as the horses examined were carrying natural infections. A complete history of anthelmintic treatment and cyathostomin burden was not available. Due to this, horses could not be reliably placed into positive and negative groups, limiting the assessment of the aforementioned properties. Whilst these factors could not be assessed here at this stage, due to the limitations in study design, the relationship between proteinase expression and cyathostomin burden was explored here as a necessary step in the process of evaluating the potential for these proteinase to be used as biomarkers for active infection. The requirement for a diagnostic test that will provide information on an individual's cyathostomin larval infection status has been illustrated here. Only three of the 28 horses (11%) had faecal egg counts (FEC) above the commonly used treatment cut off of 200 eggs per gram (Nielsen, Haaning et al. 2006; Larsen, Ritz et al. 2011); however 50% of the horses had combined total mucosal burdens (CTMBs) greater than 20,000 encysted larvae. Furthermore, the case of larval cyathostominosis here had caecal and right ventral colon (RVC) mucosal burdens to the order of several million, yet the FEC was negative.

The common mucosal immune system has the potential to evoke mucosal immune responses throughout the gut, including the rectum (Lycke 2012) and is a key determinant of the success of rectal biopsies and mast cell activity at this site as diagnostic tests. This thesis provided evidence to support the theory of mast cell recruitment as part of the common mucosal system in equines. The Toluidine blue (TB) mast cell mucosal and submucosal populations significantly correlated at each site and significant correlations were also observed between mucosal and submucosal mast cells across sites: the caecum and RVC, the caecum and the rectum,

and the rectum and RVC. This result is supported by a previous study which examined the mast cell response in naturally cyathostomin infected horses and demonstrated correlations between the large intestinal (caecum, ventral and dorsal colon) mast cell counts (Collobert-Laugier, Hoste et al. 2002). The rectum was not investigated in the latter study; therefore the results from this thesis are novel in their explorations of this anatomical location. These results support the theory that mast cells are recruited throughout the intestinal mucosa so that stimulation at one site, such as the caecum, has potential to provoke a response at a distant site.

A more complex relationship was observed when examining the composition of the mast cell serine proteinase-labelled populations. The majority of mast cells were eqMCP-1-positive, a finding in agreement with Pickles et al. 2010 and the eqMCP-1-labelled mast cell populations followed a similar pattern to the TB stained cells. The eqTRYP-labelled mast cell enumerations were less consistent; for example, the rectal eqTRYP-labelled mucosal mast cells only correlated with other rectal based cell counts. Mast cells maturing in different tissue microenvironments can vary in the type and amount of the proteinases they express (Caughey 2007; Xing, Austen et al. 2011). One hypothesis to explain the findings here is that the chymase-like expressing cells comprise the majority of the mast cell population and therefore their numbers are more closely related throughout the intestinal tract. The expression of eqTRYP may be more dependent on the local environment. This hypothesis is supported by the fact that caecal eqTRYP has previously demonstrated the strongest relationship with cyathostomin burden, despite the majority of the equine intestinal mast cell population being eqMCP-1-positive and eqTRYP-negative (Pickles, Mair et al. 2010).

Previous work has demonstrated strong positive linear relationships between cyathostomin burden and the production of both equine tryptase and eqMCP-1 within the caecal wall of naturally infected horses (Pickles, Mair et al. 2010). In this thesis the rectal mucosal populations of both eqTRYP- and eqMCP-1-labelled cells were significantly positively correlated with both CTMB and combined total luminal burden (CTLB). Standard linear regression analysis, performed with the presence of *A. perfoliata* as a confounding variable, demonstrated a significant positive linear

relationship between both eqMCP-1- and eqTRYP-labelled MMC in the rectal biopsy tissue and CTMB ($p=0.018$, $r^2=43.1\%$ and $p=0.048$, $r^2=24.4\%$ respectively). Similar significant positive relationships were also seen with CTLB (eqMCP-1: $p=0.009$, $r^2=41.5$; eqTRYP: $p=0.007$, $r^2=28.9$). These results provide support for rectal biopsy and determination of proteinase-labelled mast cells as a diagnostic predictor of total cyathostomin burden.

Of the three anatomical sites explored, the RVC demonstrated the most consistent relationship with cyathostomin larval burden. This may have future diagnostic value for investigation of weight loss during exploratory laparotomy. Significant results in the RVC included a positive relationship between TB submucosal mast cells (SMMC) and CTMB, and between CTMB and eqMCP-1 and eqTRYP tissue concentrations. The RVC was the only organ in which linear regression analysis demonstrated a statistically significant positive relationship between transcript levels of tryptase-like proteinase-1 (TLP1) and the CTMB, and in this anatomical location there was also a statistically significant positive relationship between transcript levels of granzyme B-like (GZMBL) and the CTMB. Of the three locations examined, the RVC demonstrated the greatest range and highest median of both eqMCP-1 and eqTRYP proteinase concentration. Interestingly, the RVC (range 0 – 2,054,051; median 7028) had a greater total cyathostomin mucosal burden than the caecum (range 0 – 1,773,047; median 5945). There were also significantly more luminal worms in the RVC compared to the caecum. This increased cyathostomin challenge could possibly explain the more consistent relationship with cyathostomin burden in the RVC seen here.

Larval cyathostominosis is associated with diarrhoea and colic; however these are common gastrointestinal symptoms and present the veterinarian with a clinical challenge (Ricketts 1996). Additional clinical signs ascribed to this condition include weight loss, anorexia, oedema and pyrexia (Love, Murphy et al. 1999; Smets, Shaw et al. 1999; Bodecek, Jahn et al. 2010). Here, and in previous studies (Pickles, Mair et al. 2010), mast cell proteinase expression has been linked to cyathostomin infection. However, it is unclear as to the exact nature of the relationship. The association between intestinal pathology and immune expulsion of gastrointestinal

helminths has yet to be elucidated and remains controversial in other species (Lawrence, Paterson et al. 2004). Altered gastrointestinal motility is considered an important feature of equine colic and it is thought that the inflammatory changes within the mucosa due to encysted larvae may be the cause (Love, Murphy et al. 1999). Despite the fact that mast cells were discovered over a century ago, there is no consensus regarding their physiologic role (Abraham and Malaviya 1997). Whilst the classic mastocytosis and systemic release of chymase is a hallmark of infection, mast cells have also been shown to play a role in the amplification of the T helper 2 (Th2) associated immune response, which is required for parasite loss but also results in an associated enteropathy (Lawrence, Paterson et al. 2004). In equines, the findings to date are supportive of a Th2 type immune response to cyathostomin challenge (du Toit, McGorum et al. 2007), however the precise role of Th2 derived cytokines in the horse has not been defined. Whilst it is hypothesised that they are protective in the host immune response to parasites the factors driving these Th2 cytokines and their downstream mechanisms have yet to be thoroughly investigated (Davidson, Hodgkinson et al. 2005). In the mouse Th2 responses have been demonstrated to generate muscle hypercontractility with the roles of individual cytokines differing according to the type of nematode infection (Khan, Richard et al. 2003). Increases in interleukin-9 (IL-9) levels accelerate worm clearance and are required for optimal response to *Trichuris muris* infection; in contrast IL-9 is not required for the hypermotility associated with *Trichinella spiralis* infection, as IL-3 and IL-4 are sufficient (Khan, Richard et al. 2003). In addition, mouse mMCP1 has been demonstrated to induce intestinal inflammation (Lawrence, Paterson et al. 2004) and it may be the case that the release of mast proteinases is partly responsible for the clinical signs ascribed to larval cyathostominosis. As such, mast cell proteinases may be a measure of immunity as opposed to a marker of infection. Further studies are warranted to investigate the role of mast cells in immunity to nematodes in horses; these may provide information about those animals that harbour high burdens.

Mast cells appear to have a dual role in the innate immune system, as both sentinels for invading pathogens and also regulatory cells through the course of acute inflammation (St. John and Abraham 2013). There is also evidence to support the

role of mast cell activation in response to chronic pathogen infection (Shin, Watts et al. 2008), although this is not well understood. In the mouse, tryptase has been demonstrated to be involved in the modulation of the immune response to the chronic colonisation phase of *T. spiralis* infection. This role has also been demonstrated to be mast cell subset and proteinase specific, as it is the tryptase mouse mast cell proteinase-6 (mMCP-6), not mMCP-7 (another murine tryptase), that has been shown to be critical to eosinophil recruitment in this chronic infection phase (Shin, Watts et al. 2008). This highlights the importance of the effector role for mast cells in the adaptive immune system. The host/parasite interaction in equine cyathostomiasis is complicated by the lengthy period of encystment, thought to last for months to years (Gibson 1953; Murphy and Love 1997). An improved understanding of the mechanism controlling encystment would be beneficial to gain a better understanding of the role of mast cells in this chronic phase of infection.

Serum mast cell proteinase concentrations in mice, rats and sheep, measured by ELISA have been demonstrated to be associated with gastrointestinal mastocytosis and intestinal nematode infections (Woodbury, Miller et al. 1984; Huntley, Gibson et al. 1987; Huntley, Gooden et al. 1990; Miller 1996). Encouragingly in this study, local serum concentrations of eqTRYP and eqMCP-1 were significantly positively correlated ($p=0.006$, $\rho=0.665$) and serum from cyathostomin-negative horses gave consistently low readings for eqMCP-1 (mean 0.45 ng/ml) and eqTRYP (mean 0.23 μ g/ml) serum ELISA. Peripheral serum is relatively easy to obtain and would be a more accessible sample for diagnostic assay than serum sourced from the intestinal tract. However, both eqMCP-1 and eqTRYP proteinase concentrations in peripheral serum did not correlate with concentrations in local serum suggesting that they cannot be used to indicate the level of proteinase in the serum local to the site of infection, and thus limiting the diagnostic potential of this assay in horses. There was a significant negative relationship observed between peripheral serum eqMCP-1 concentrations and the CTMB, which could be a result of activation and sequestering of proteinases within the gut lumen. However, linear regression analysis demonstrated no significant relationship between local proteinase concentrations measured in these tests with the CTMB. This could relate to the differences in the

exact cyathostomin stage of infection between animals, which may have affected the local responses at the time of assay. In addition, proteinases may have been released and sequestered into the gut lumen as occurs in other species (Huntley, Gooden et al. 1990; Scudamore, Thornton et al. 1995; Miller 1996), which was not measured here. With the antibodies currently available this serum assay is of little diagnostic value in cyathostomin infection.

With regards to assessing the clinical application of a diagnostic assay, biological markers should be robust enough to be unaffected by season, breed and common history. However, as this was a study of natural infection, the analysis of the relationships between all mast cell measures and cyathostomin burden was limited by a lack of knowledge of infection and treatment history of the horses studied. Differences in horse management, particularly between the two sampling locations, stage of infection and also the phase of immune response may be confounding factors and could explain why the relationships observed here in the caecum were not as significant when compared to previous studies performed by K. Dacre et al. 2010. The results here may also have been affected by age, variations in levels of pasture contamination, treatment frequency and external stresses such as nutrition, travelling or concurrent diseases (Collobert-Laugier, Hoste et al. 2002). In addition, the antibodies previously validated and used in this study and by Dacre et al (2010) were polyclonal. This may have resulted in a loss of sensitivity, particularly when considering the sequence homology between chymases and granzymes, and may also have contributed to the high coefficients of variation seen in the optimised ELISA. Although the serum levels of eqTRYP and eqMCP-1 correlated with each other there was no correlation between local serum proteinase and CTMB. A lack of specificity may have caused a lack of sensitivity due to cross-reactivity, as the polyclonal antibodies may have been binding to a number of epitopes (Lipman, Jackson et al. 2005). This may have resulted in subtle relationships being missed and could explain why the results were more significant in the RVC where the cyathostomin larval burden in individuals was greater. Previous work has highlighted the potential for other equine mast cell proteinases (Dacre 2005) and that expression of these proteinase may be more related to cyathostomin burden, or a lack of sensitivity to

specific proteinases may be hindering analysis. In an attempt to address the limitations of the antibodies available, this thesis explored previously undescribed mast cell proteinases using the equine genome as a bioinformatic resource. In addition, the proteinases recognised by the previously purified antibodies were investigated. The results provided evidence for the presence of multiple equine chymases isoforms. Subsequently, the transcription of three such chymases was explored and a further five potential chymase sequences were identified here. It was outside the scope of this project to investigate all related predicted sequences, but the results provided encouraging preliminary data. Results from the qPCR experiments demonstrated that CLP1 was the most abundant of the four proteinase transcripts measured in the caecum, RVC and in rectal tissue. This result was supported by the significant positive correlations between the caecal and RVC CLP1 transcript levels and the eqMCP-1 concentrations in the local serum. The antibodies that were used in the serum ELISA were purified from equine mastocytoma tissue (Pemberton, McEuen et al. 2001). Granzyme(BGH)-like (GZM(BGH)L) was the most abundant chymase-like proteinase in the equine mastocytoma and also had an identical N-terminal aa sequence to the previously described equine mast cell proteinase-1 sequence (Pemberton, McEuen et al. 2001; Dacre 2005). This suggests that the predicted sequence (GZM(BGH)L) is the same as the original equine mast cell proteinase that was purified from equine mastocytoma (Pemberton, McEuen et al. 2001), although full sequence analysis and assessment of substrate specificity are required to confirm this.

There are many elements of the research presented here that would be beneficial to continue exploring. One interesting area would be clarification of the heterogeneity of mast cell expression in the horse. The initial mast cell proteinase expression results described provides the basis for this work. To take this further would require a thorough examination of the equine genome, with a particular focus on chromosome 1 where the mast cell chymase locus is situated (Chapter 4). As mentioned above, this thesis has provided further evidence for multiple, closely-related equine chymases. Full sequence analysis on all identified sequences alongside *in situ* hybridisation to confirm their cellular origin would clarify the level of heterogeneity

further. This would provide an insight into the correlation between the proteinases (TLP1 with GZMBL, CLP1 with GZM(BGH)L) identified here. There could potentially be a number of mast cell subsets expressing various combinations of serine proteinases. A greater understanding of the origin of these sequences would aid in interpreting their expression and defining equine mast cell heterogeneity.

Following confirmation of the cellular origin of all identified potential mast cell sequences, a further step of great benefit would be the production of monoclonal antibodies that are specific to an individual proteinase. Monoclonal antibodies would produce less background signal and less cross-reactivity as they target a single epitope (Lipman, Jackson et al. 2005). This would allow the development of optimised ELISAs that could reliably measure concentrations of known sequences for direct comparison. This would be valuable due to the high sequence homology between serine proteinases, especially chymases. The chymase-like sequences investigated in this study, CLP1, GZMBL and GZM(BGH)L, are highly homologous and this may cause cross reactivity in the ELISA. There is also potential for other closely related proteinases expressed by mast cells or lymphocytes that may be recognised by the polyclonal antibody available. It would be very interesting to optimise an ELISA specific to CLP1 in equine serum using a monoclonal antibody. As this proteinase has been demonstrated to be more abundant in the tissue, this may also be the case in serum. This would allow investigation into which proteinases are at higher concentrations in serum to assess the potential for differential release, as noted in other species, and also to further investigate the relationship between tissue transcript proteinase levels and cyathostomin infection. A further benefit of specific monoclonal antibodies would be to assess mast cell labelled populations in detail according to their specific proteinase expression and allow exploration of the kinetics of mast cell response. Differential mast cell proteinase expression has been demonstrated in the mouse during the inflammatory response to nematode infection (Friend, Ghildyal et al. 1996; Friend, Ghildyal et al. 1998) and it would be interesting to investigate this in the equine. Here, immunolabelled mast cells in sections of rectal tissue taken using rectal biopsy demonstrated significant positive relationships with

CTMB. Rectal biopsies may be a practical method for investigating the dynamics of the mast cell response to cyathostomin infection.

In summary, this thesis has further explored and characterised large intestinal mast cell recruitment and proteinase expression in response to cyathostomin infection in naturally infected horses. Serum and tissue mast cell proteinase concentrations have been estimated using optimised ELISAs. The ambiguity surrounding the previously purified mastocytoma-derived proteinases and the antibodies raised against them have been investigated. Additionally, the identification and quantification of novel equine mast cell proteinase-related sequences has been successfully performed, providing a foundation for future exploration and investigation.

6 References

- Abonia, J. P., K. F. Austen, et al. (2005). Constitutive homing of mast cell progenitors to the intestine depends on autologous expression of the chemokine receptor CXCR2.
- Abraham, S. N. and R. Malaviya (1997). "Mast cells in infection and immunity." *Infection and Immunity* 65(9): 3501-3508.
- Akin, C., D. Soto, et al. (2007). "Tryptase haplotype in mastocytosis: Relationship to disease variant and diagnostic utility of total tryptase levels." *Clinical Immunology* 123(3): 268-271.
- Akobeng, A. (2006). "Understanding diagnostic tests 1: sensitivity, specificity and predictive values." *Acta Pædiatrica* 2006 96: 338–341
- Al-Zghoul, M., R. Al-Rukibat, et al. (2009). "Distribution and density of mast cells in camel small intestine and influence of fixation techniques." *European Journal of Histochemistry* 2009 52(4).
- Aldenberg, F. and L. Enerbäck (1994). "The immunohistochemical demonstration of chymase and tryptase in human intestinal mast cells." *The Histochemical Journal* 26(7): 587-596.
- Andersen, U. V., D. K. Howe, et al. (2013). "Recent advances in diagnosing pathogenic equine gastrointestinal helminths: The challenge of prepatent detection." *Veterinary Parasitology* 192(1–3): 1-9.
- Andersson, M. K., U. Karlson, et al. (2008). "The extended cleavage specificity of the rodent β -chymases rMCP-1 and mMCP-4 reveal major functional similarities to the human mast cell chymase." *Molecular Immunology* 45(3): 766-775.
- Arolas, J. L., J. Vendrell, et al. (2007). "Metalloprotease: emerging drug targets in biomedicine." *Curr Pharm Des* 13(4): 349-366.
- Bairden, K., S. R. Brown, et al. (2001). "Efficacy of moxidectin 2 per cent gel against naturally acquired strongyle infections in horses, with particular reference to larval cyathostomes." *Veterinary Record* 148(5): 138-141.
- Bairden, K., H. S. Davies, et al. (2006). "Efficacy of moxidectin 2 per cent oral gel against cyathostomins, particularly third-stage inhibited larvae, in horses." *Veterinary Record* 158(22): 766-768.
- Barber, R. D., D. W. Harmer, et al. (2005). "GAPDH as a housekeeping gene: analysis of GAPDH mRNA expression in a panel of 72 human tissues." *Physiological Genomics* 21(3): 389-395.
- Barnes, P. J. (1983). "Calcium-channel blockers and asthma." *Thorax* 38(7): 481-485.
- Bartley, D. J., A. A. Donnan, et al. (2006). "A small scale survey of ivermectin resistance in sheep nematodes using the faecal egg count reduction test on

- samples collected from Scottish sheep." *Veterinary Parasitology* 137(1-2): 112-118.
- Baudena, M. A., M. R. Chapman, et al. (2000). "Seasonal development and survival of equine cyathostome larvae on pasture in south Louisiana." *Vet Parasitol* 88(1-2): 51-60.
- Beekman, L., T. Tohver, et al. (2011). "Evaluation of suitable reference genes for gene expression studies in bronchoalveolar lavage cells from horses with inflammatory airway disease." *BMC Mol Biol* 12: 5.
- Befus, A. D., F. L. Pearce, et al. (1982). "Unique functional characteristics of mucosal mast cells." *Advances in Experimental Medicine and Biology* 149: 521-527.
- Bhattacharyya, S. P., I. Drucker, et al. (1998). "Activated T lymphocytes induce degranulation and cytokine production by human mast cells following cell-to-cell contact." *Journal of Leukocyte Biology* 63(3): 337-341.
- Blank, U. (2011). "The mechanisms of exocytosis in mast cells." *Adv Exp Med Biol* 716: 107-122.
- Bodecek, S., P. Jahn, et al. (2010). "Equine cyathostomosis: case reports." *Veterinari Medicina* 55(4): 187-193.
- Bogaert, L., M. Van Poucke, et al. (2006). "Selection of a set of reliable reference genes for quantitative real-time PCR in normal equine skin and in equine sarcoids." *BMC Biotechnol* 6: 24.
- Borgsteede, F. H. M., J. H. Boersma, et al. (1993). "The reappearance of eggs in faeces of horses after treatment with ivermectin." *Veterinary Quarterly* 15(1): 24-26.
- Brooks, S. A. and E. Bailey (2010). "RT-qPCR comparison of mast cell populations in whole blood from healthy horses and those with laminitis." *Anim Genet* 41 Suppl 2: 16-22.
- Bueno, L., Y. Ruckebusch, et al. (1979). "Disturbances of digestive motility in horses associated with strongyle infection." *Veterinary Parasitology* 5(2-3): 253-260.
- Bulut, K., P. Felderbauer, et al. (2008). "Increased duodenal expression of transforming growth factor-alpha and epidermal growth factor during experimental colitis in rats." *Eur J Gastroenterol Hepatol* 20(10): 989-994.
- Bustin, S. A. and T. Nolan (2004). "Pitfalls of quantitative real-time reverse-transcription polymerase chain reaction." *J Biomol Tech* 15(3): 155-166.
- Cappelli, K., M. Felicetti, et al. (2008). "Exercise induced stress in horses: selection of the most stable reference genes for quantitative RT-PCR normalization." *BMC Mol Biol* 9: 49.
- Caughey, G. H. (2007). "Mast cell tryptases and chymases in inflammation and host defense." *Immunol Rev* 217: 141-154.

- Caughey, G. H., W. W. Raymond, et al. (2000). "Characterization of human gamma-tryptases, novel members of the chromosome 16p mast cell tryptase and proctasin gene families." *J Immunol* 164(12): 6566-6575.
- Caughey, G. H., T. H. Schaumberg, et al. (1993). "The Human Mast Cell Chymase Gene (CMA1): Mapping to the Cathepsin G/Granzyme Gene Cluster and Lineage-Restricted Expression." *Genomics* 15(3): 614-620.
- Chandrasekharan, U. M., S. Sanker, et al. (1996). "Angiotensin II-Forming Activity in a Reconstructed Ancestral Chymase." *Science* 271(5248): 502-505.
- Chapman, M. R., D. D. French, et al. (2002). "One season of pasture exposure fails to induce a protective resistance to cyathostomes but increases numbers of hypobiotic third-stage larvae." *Journal of Parasitology* 88(4): 678-683.
- Chapman, M. R., M. T. Kearney, et al. (1999). "An experimental evaluation of methods used to enumerate mucosal cyathostome larvae in ponies." *Veterinary Parasitology* 1999 86: 3.
- Chowdhary, B. and T. Raudsepp (2008). "The Horse Genome Derby: racing from map to whole genome sequence." *Chromosome Research* 16(1): 109-127.
- Christie, M. and F. Jackson (1982). "Specific identification of strongyle eggs in small samples of sheep feces" *Research in Veterinary Science* 32(1): 113-117.
- Church, S., D. F. Kelly, et al. (1986). "Diagnosis and successful treatment of diarrhea in horses caused by immature small strongyles apparently insusceptible to anthelmintics." *Equine Veterinary Journal* 18(5): 401-403.
- Clayton, H. M. and J. L. Duncan (1979). "Development of immunity to *Parascaris Equorum* infection in the foal." *Research in Veterinary Science* 26(3): 383-384.
- Cobb, R. and A. Boeckh (2009). "Moxidectin: a review of chemistry, pharmacokinetics and use in horses." *Parasites & Vectors* 2.
- Collobert-Laugier, C., H. Hoste, et al. (2002). "Mast cell and eosinophil mucosal responses in the large intestine of horses naturally infected with cyathostomes." *Veterinary Parasitology* 2002 107: 3.
- Collobert-Laugier, C., H. Hoste, et al. (2002). "Prevalence, abundance and site distribution of equine small strongyles in Normandy, France." *Veterinary Parasitology* 110(1-2): 77-83.
- Comelli, E. M., S. Lariani, et al. (2009). "Biomarkers of human gastrointestinal tract regions." *Mamm Genome* 20(8): 516-527.
- Corning, S. (2009). "Equine cyathostomins: a review of biology, clinical significance and therapy." *Parasites & Vectors* 2.
- Cruse, G., V. E. Fernandes, et al. (2010). "Human lung mast cells mediate pneumococcal cell death in response to activation by pneumolysin." *J Immunol* 184(12): 7108-7115.

- Cullen, S. P., C. Adrain, et al. (2007). "Human and murine granzyme B exhibit divergent substrate preferences." *The Journal of Cell Biology* 176(4): 435-444.
- Czapinska, H. and J. Otlewski (1999). "Structural and energetic determinants of the S₁-site specifically in serine proteases." *European Journal of Biochemistry* 260(3): 571.
- D'haene, B., J. Vandesompele, et al. (2010). "Accurate and objective copy number profiling using real-time quantitative PCR." *Methods* 50(4): 262-270.
- Dacre, K. J. (2005). "The Role of Mast Cells and Mast Cell Serine Proteinases in Equine Heaves." PhD Thesis ().
- Dacre, K. J., S. M. McAleese, et al. (2006). "cDNA cloning and substrate specificity of equine tryptase, a possible mediator in equine heaves." *Clin Exp Allergy* 36(10): 1303-1309.
- Dacre, K. J., B. C. McGorum, et al. (2007). "Organic dust exposure increases mast cell tryptase in bronchoalveolar lavage fluid and airway epithelium of heaves horses." *Clinical and Experimental Allergy* 37(12): 1809-1818.
- Davidson, A. J., J. E. Hodgkinson, et al. (2005). "Cytokine responses to Cyathostominae larvae in the equine large intestinal wall." *Research in Veterinary Science* 2005 78: 2.
- De Jonge, F., L. Van Nassauw, et al. (2002). "Temporal distribution of distinct mast cell phenotypes during intestinal schistosomiasis in mice." *Parasite Immunology* 24(5): 225-231.
- de Souza, D. A., Jr., V. D. Toso, et al. (2012). "Expression of Mast Cell Proteases Correlates with Mast Cell Maturation and Angiogenesis during Tumor Progression." *PLoS ONE* 7(7): e40790.
- Demeulenaere, D., J. Vercruysse, et al. (1997). "Comparative studies of ivermectin and moxidectin in the control of naturally acquired cyathostome infections in horses." *Veterinary Record* 141(15): 383-386.
- Dheda, K., J. F. Huggett, et al. (2004). "Validation of housekeeping genes for normalizing RNA expression in real-time PCR." *Biotechniques* 37(1): 112-114, 116, 118-119.
- Dorny, P., I. Meijer, et al. (2000). "A survey of anthelmintic resistance on Belgian horse farms." *Vlaams Diergeneeskundig Tijdschrift* 2000 69: 5.
- dos Santos, C. N., L. S. de Souza, et al. (2011). "Seasonal dynamics of cyathostomin (Nematoda – Cyathostominae) infective larvae in *Brachiaria humidicola* grass in tropical southeast Brazil." *Veterinary Parasitology* 180(3–4): 274-278.
- Douch, P. G. C., R. S. Green, et al. (1996). "Serum mast cell proteinase responses of sheep to challenge with *Trichostrongylus colubriformis* and the effect of dexamethasone treatment." *International Journal for Parasitology* 26(1): 91-95.

- Dowdall, S. M. J., J. B. Matthews, et al. (2002). "Antigen-specific IgG(T) responses in natural and experimental cyathostominae infection in horses." *Veterinary Parasitology* 2002 106: 3.
- Dowdall, S. M. J., C. J. Proudman, et al. (2004). "Characterisation of IgG(T) serum antibody responses to two larval antigen complexes in horses naturally- or experimentally-infected with cyathostomins." *International Journal for Parasitology* 2004 34: 1.
- Dowdall, S. M. J., C. J. Proudman, et al. (2003). "Purification and analyses of the specificity of two putative diagnostic antigens for larval cyathostomin infection in horses." *Research in Veterinary Science* 2003 75: 3.
- Drudge, J. H. and E. T. Lyons (1966). "Control of Internal Parasites of the Horse." *Journal of the American Veterinary Medical Association* 148: 378-383.
- du Toit, N., B. C. McGorum, et al. (2007). "The involvement of mast cells and mast cell proteinases in the intestinal response to equine cyathostomin infection." *Veterinary Immunology and Immunopathology* 115(1-2): 35-42.
- Duncan, J. L. (1985). "Internal parasites of the horse and their control." *Equine Veterinary Journal* 17(2): 79-82.
- Duncan, J. L., K. Bairden, et al. (1998). "Elimination of mucosal cyathostome larvae by five daily treatments with fenbendazole." *Veterinary Record* 1998 142: 11.
- Duncan, J. L. and S. Love (1991). "Preliminary observations on an alternative strategy for the control of horse strongyles." *Equine Veterinary Journal* 23(3): 226-228.
- Dutta, N. K. and K. G. A. Narayanan (1954). "Release of histamine from skeletal muscle by snake venoms." *British Journal of Pharmacology and Chemotherapy* 9(4): 408-412.
- Echtenacher, B., D. N. Mannel, et al. (1996). "Critical protective role of mast cells in a model of acute septic peritonitis." *Nature* 381(6577): 75-77.
- Edwards, G. B. (1986). "Surgical management of intussusception in the horse." *Equine Veterinary Journal* 18(4): 313-321.
- Else, K. J., F. D. Finkelman, et al. (1994). "Cytokine-mediated regulation of chronic intestinal helminth infection." *J Exp Med* 179(1): 347-351.
- Else, K. J. and R. K. Grencis (1991). "Cellular immune responses to the murine nematode parasite *Trichuris muris* I. Differential cytokine production during acute or chronic infection." *Immunology* 72(4): 508-513.
- Else, K. J., L. Hültner, et al. (1992). "Cellular immune responses to the murine nematode parasite *Trichuris muris*: II. Differential induction of the Th cell subsets in resistant versus susceptible mice." *Immunology* 75(2): 232-237.
- Epstein, D. M. and R. H. Abeles (1992). "Role of serine 214 and tyrosine 171, components of the S2 subsite of .alpha.-lytic protease, in catalysis." *Biochemistry* 31(45): 11216-11223.

- Erdei, A., M. Andrásfalvy, et al. (2004). "Regulation of mast cell activation by complement-derived peptides." *Immunology Letters* 92(1–2): 39-42.
- Ewen, C. L., K. P. Kane, et al. (2012). "A quarter century of granzymes." *Cell Death Differ* 19(1): 28-35.
- Eysker, M., J. Bakker, et al. (2008). "The use of age-clustered pooled faecal samples for monitoring worm control in horses." *Veterinary Parasitology* 151(2–4): 249-255.
- Eysker, M., J. H. Boersema, et al. (1997). "Controlled dose confirmation study of a 2% moxidectin equine gel against equine internal parasites in The Netherlands." *Veterinary Parasitology* 70(1-3): 165-173.
- Eysker, M., J. H. Boersema, et al. (1992). "The effect of ivermectin treatment against inhibited early 3rd stage, late 3rd stage and 4th stage larvae and adult stages of the cyathostomes in Shetland ponies and spontaneous expulsion of these helminths." *Veterinary Parasitology* 42(3-4): 295-302.
- Eysker, M. and T. R. Klei (1999). "Mucosal larval recovery techniques of cyathostomes: can they be standardized?" *Veterinary Parasitology* 85(2-3): 137-144.
- Figueiredo, M. D., C. E. Salter, et al. (2009). "Validation of a reliable set of primer pairs for measuring gene expression by real-time quantitative RT-PCR in equine leukocytes." *Veterinary Immunology and Immunopathology* 131(1–2): 65-72.
- Fiorucci, L. and F. Ascoli (2004). "Mast cell tryptase, a still enigmatic enzyme." *Cellular and Molecular Life Sciences CMLS* 61(11): 1278-1295.
- Fjeldsgaard, B. E. and B. S. Paulsen (1993). "Comparison of IgE-binding antigens in horse dander and a mixture of horse hair and skin scrapings." *Allergy* 48(7): 535-541.
- Fogarty, U., F. del Piero, et al. (1994). "Incidence of *Anoplocephala perfoliata* in horses examined at an Irish abattoir." *Veterinary Record* 134(20): 515-518.
- Fossum, C., B. Hjertner, et al. (2012). "Expression of tlr4, md2 and cd14 in equine blood leukocytes during endotoxin infusion and in intestinal tissues from healthy horses." *Vet Immunol Immunopathol* 150(3-4): 141-148.
- Friend, D. S., N. Ghildyal, et al. (1996). "Mast cells that reside at different locations in the jejunum of mice infected with *Trichinella spiralis* exhibit sequential changes in their granule ultrastructure and chymase phenotype." *Journal of Cell Biology* 135(1): 279-290.
- Friend, D. S., N. Ghildyal, et al. (1998). "Reversible expression of tryptases and chymases in the jejunal mast cells of mice infected with *Trichinella spiralis*." *Journal of Immunology* 160(11): 5537-5545.
- Fukuoka, Y., M. R. Hite, et al. (2013). "Human Skin Mast Cells Express Complement Factors C3 and C5." *The Journal of Immunology*.

- Galli, S. J., S. Nakae, et al. (2005). "Mast cells in the development of adaptive immune responses." *Nature Immunology* 6(2): 135-142.
- Gallwitz, M., M. Enoksson, et al. (2007). "Expression profile of novel members of the rat mast cell protease (rMCP)-2 and (rMCP)-8 families, and functional analyses of mouse mast cell protease (mMCP)-8." *Immunogenetics* 59(5): 391-405.
- Gallwitz, M. and L. Hellman (2006). "Rapid lineage-specific diversification of the mast cell chymase locus during mammalian evolution." *Immunogenetics* 58(8): 641-654.
- Gallwitz, M. and L. Hellman (2006). "Rapid lineage-specific diversification of the mast cell chymase locus during mammalian evolution." *Immunogenetics* 58(8): 641-654.
- Gallwitz, M., J. M. Reimer, et al. (2006). "Expansion of the mast cell chymase locus over the past 200 million years of mammalian evolution." *Immunogenetics* 58(8): 655-669.
- Gasser, R. B., R. M. C. Williamson, et al. (2005). "Anoplocephala perfoliata of horses - significant scope for further research improved diagnosis and control." *Parasitology* 131: 1-13.
- Gawor, J. J. (1995). "The prevalence and abundance of internal parasites in working horses autopsied in Poland." *Veterinary Parasitology* 58(1-2): 99-108.
- Ghildyal, N., D. S. Friend, et al. (1993). "Reversible expression of mouse mast cell protease 2 mRNA and protein in cultured mast cells exposed to IL-10." *The Journal of Immunology* 151(6): 3206-3214.
- Gibson, S., A. Mackeller, et al. (1987). "Phenotypic expression of mast cell granule proteinases. Distribution of mast cell proteinases I and II in the rat digestive system." *Immunology* 62(4): 621-627.
- Gibson, S. and H. R. Miller (1986). "Mast cell subsets in the rat distinguished immunohistochemically by their content of serine proteinases." *Immunology* 58(1): 101-104.
- Gibson, T. E. (1953). "The Effect of Repeated Anthelmintic Treatment with Phenothiazine on the Faecal Egg Counts of Housed Horses, with Some Observations on the Life Cycle of *Trichonema* spp. in the Horse." *Journal of Helminthology* 27(1-2): 29-40.
- Giles, C. J., K. A. Urquhart, et al. (1985). "Larval cyathostomiasis (immature trichonema induced enteropathy) a report of 15 clinical cases." *Equine Veterinary Journal* 17(3): 196-201.
- Gokbulut, C., A. M. Nolan, et al. (2001). "Plasma pharmacokinetics and faecal excretion of ivermectin, doramectin and moxidectin following oral administration in horses." *Equine Veterinary Journal* 33(5): 494-498.
- Goujon, M., H. McWilliam, et al. (2010). "A new bioinformatics analysis tools framework at EMBL-EBI." *Nucleic Acids Research* 38(suppl 2): W695-W699.

- Gurish, M. F. and J. A. Boyce (2006). "Mast cells: Ontogeny, homing, and recruitment of a unique innate effector cell." *Journal of Allergy and Clinical Immunology* 117(6): 1285-1291.
- Gurish, M. F., H. Tao, et al. (2001). "Intestinal Mast Cell Progenitors Require CD49d β 7 (α 4 β 7 Integrin) for Tissue-specific Homing." *The Journal of Experimental Medicine* 194(9): 1243-1252.
- Haddad, P., D. Jenne, et al. (1991). "Structure and evolutionary origin of the human granzyme H gene." *Int Immunol* 3(1): 57-66.
- Hamilton, M. J., M. J. Sinnamon, et al. (2011). "Essential role for mast cell tryptase in acute experimental colitis." *Proceedings of the National Academy of Sciences* 108(1): 290-295.
- Hartley, B. S. and H. Neurath (1970). "Homologies in Serine Proteinases [and Discussion]." *Philosophical Transactions of the Royal Society of London. Series B, Biological Sciences* 257(813): 77-87.
- He, S., M. D. Gaca, et al. (1998). "A role for tryptase in the activation of human mast cells: modulation of histamine release by tryptase and inhibitors of tryptase." *J Pharmacol Exp Ther* 286(1): 289-297.
- He, S. H. and H. Xie (2004). "Modulation of tryptase secretion from human colon mast cells by histamine." *World J Gastroenterol* 10(3): 323-326.
- He, S. H., H. Xie, et al. (2005). "Inhibition of tryptase release from human colon mast cells by histamine receptor antagonists." *Asian Pac J Allergy Immunol* 23(1): 35-39.
- Hedstrom, L. (2002). "Serine Protease Mechanism and Specificity." *Chemical Reviews* 102(12): 4501-4524.
- Heib, V., M. Becker, et al. (2008). "Advances in the understanding of mast cell function." *British Journal of Haematology* 142(5): 683-694.
- Herd, R. P. (1986). "Epidemiology and control of equine strongylosis at Newmarket." *Equine Veterinary Journal* 18(6): 447-452.
- Herd, R. P. and A. A. Gabel (1990). "Reduced efficacy of anthelmintics in young compared with adult horses." *Equine Veterinary Journal* 22(3): 164-169.
- Herd, R. P., T. B. Miller, et al. (1981). "A field evaluation of pro-benzimidazole, benzimidazole, and non-benzimidazole anthelmintics in horses." *Journal of the American Veterinary Medical Association* 179(7): 686-691.
- Hinney, B., N. C. Wirtherle, et al. (2011). "Prevalence of helminths in horses in the state of Brandenburg, Germany." *Parasitology Research* 108(5): 1083-1091.
- Hjertner, B., K. M. Olofsson, et al. (2013). "Expression of reference genes and T helper 17 associated cytokine genes in the equine intestinal tract." *The Veterinary Journal* (0).
- Hodgkinson, J. E. (2006). "Molecular diagnosis and equine parasitology." *Veterinary Parasitology* 136(2): 109-116.

- Hodgkinson, J. E., J. R. Lichtenfels, et al. (2003). "A PCR-ELISA for the identification of cyathostomin fourth-stage larvae from clinical cases of larval cyathostominosis." *International Journal for Parasitology* 2003 33: 12.
- Hogan, A. D. and L. B. Schwartz (1997). "Markers of mast cell degranulation." *Methods* 13(1): 43-52.
- Huang, C., L. Li, et al. (1999). "Human Trypsases α and β /II Are Functionally Distinct Due, in Part, to a Single Amino Acid Difference in One of the Surface Loops That Forms the Substrate-binding Cleft." *Journal of Biological Chemistry* 274(28): 19670-19676.
- Hunt, J. E., D. S. Friend, et al. (1997). "Mouse mast cell protease 9, a novel member of the chromosome 14 family of serine proteases that is selectively expressed in uterine mast cells." *J Biol Chem* 272(46): 29158-29166.
- Huntley, J. F., S. Gibson, et al. (1987). "Systemic release of a mast-cell proteinase following nematode infections in sheep." *Parasite Immunology* 9(5): 603-614.
- Huntley, J. F., S. Gibson, et al. (1987). "Systemic release of a mast cell proteinase following nematode infections in sheep." *Parasite Immunology* 9(5): 603-614.
- Huntley, J. F., C. Gooden, et al. (1990). "Distribution of intestinal mast-cell proteinase in blood and tissue of normal and *Trichinella*-infected mice." *Parasite Immunology* 12(1): 85-95.
- Huntley, J. F., G. F. J. Newlands, et al. (1992). "The influence of challenge dose, duration of immunity, or steroid treatment on mucosal mast cells and on the distribution of sheep mast cell proteinase in *Haemonchus*-infected sheep." *Parasite Immunology* 14(4): 429-440.
- Irani, A. A., N. M. Schechter, et al. (1986). "Two types of human mast cells that have distinct neutral protease compositions." *Proceedings of the National Academy of Sciences* 83(12): 4464-4468.
- Irani, A. M. and L. B. Schwartz (1994). "Human mast cell heterogeneity." *Allergy Proc* 15(6): 303-308.
- Jackson, F. and R. L. Coop (2000). "The development of anthelmintic resistance in sheep nematodes." *Parasitology* 120 Suppl: S95-107.
- Jarrett, E. E. E. and H. R. P. Miller (1982). "Production and activities of IgE in helminth infection." *Progress in Allergy* 31: 178-233.
- Kaplan, R. M. (2002). "Anthelmintic resistance in nematodes of horses." *Veterinary Research* 33(5): 491-507.
- Kaplan, R. M. (2004). "Drug resistance in nematodes of veterinary importance: a status report." *Trends in Parasitology* 20(10): 477-481.
- Kaplan, R. M., T. R. Klei, et al. (2004). "Prevalence of anthelmintic resistant cyathostomes on horse farms." *Journal of the American Veterinary Medical Association* 204 225: 6.

- Kaplan, R. M. and M. K. Nielsen (2010). "An evidence-based approach to equine parasite control: It ain't the 60s anymore." *Equine Veterinary Education* 22(6): 306-316.
- Khan, W. I., M. Richard, et al. (2003). "Modulation of Intestinal Muscle Contraction by Interleukin-9 (IL-9) or IL-9 Neutralization: Correlation with Worm Expulsion in Murine Nematode Infections." *Infection and Immunity* 71(5): 2430-2438.
- Khatri, M. J., R. S. Desai, et al. (2013). "Immunohistochemical Expression of Mast Cells Using c-Kit in Various Grades of Oral Submucous Fibrosis." *ISRN Pathology* 2013: 5.
- Kinet, J. P. (1990). "The high-affinity receptor for IgE." *Current Opinion in Immunology* 2(4): 499-505.
- King, C. L., X. L. Jia, et al. (1997). "Mice with a targeted deletion of the IgE gene have increased worm burdens and reduced granulomatous inflammation following primary infection with *Schistosoma mansoni*." *Journal of Immunology* 158(1): 294-300.
- King, S. J. and H. R. P. Miller (1984). "Anaphylactic release of mucosal mast cell protease and its relationship to gut permeability in *Nippostrongylus*-primed rats." *Immunology* 51(4): 653-660.
- Kingston, D. and J. R. Pearson (1981). "The use of the peroxidase reaction to obliterate staining of eosinophils by fluorescein-labelled conjugates." *J Immunol Methods* 44(2): 191-198.
- Kingston, D. and J. R. Pearson (1981). "The use of the peroxidase reaction to obliterate staining of eosinophils by fluorescein-labelled conjugates." *Journal of Immunological Methods* 44(2): 191-198.
- Kitamura, Y., Y. Kanakura, et al. (1987). "Mutual Phenotypic Changes between Connective Tissue Type and Mucosal Mast Cells." *International Archives Of Allergy And Immunology* 82(3-4): 244-248.
- Kiyono, H., M.-N. Kweon, et al. (2001). "The mucosal immune system: from specialized immune defense to inflammation and allergy." *Acta Odontologica Scandinavica* 59(3): 145-153.
- Klei, T. R. and M. R. Chapman (1999). "Immunity in equine cyathostome infections." *Veterinary Parasitology* 1999 85: 2/3.
- Klei, T. R., M. R. Chapman, et al. (1993). "Evaluation of ivermectin at an elevated dose against encysted equine cyathostome larvae." *Veterinary Parasitology* 47(1-2): 99-106.
- Knight, P. A., S. H. Wright, et al. (2000). "Delayed expulsion of the nematode *Trichinella spiralis* in mice lacking the mucosal mast cell-specific granule chymase, mouse mast cell protease-1." *Journal of Experimental Medicine* 192(12): 1849-1856.

- Kornas, S., J. Cabaret, et al. (2010). "Horse infection with intestinal helminths in relation to age, sex, access to grass and farm system." *Veterinary Parasitology* 174(3-4): 285-291.
- Krem, M. M. and E. Di Cera (2001). "Molecular markers of serine protease evolution." *The EMBO Journal* 20(12): 3036-3045.
- Krem, M. M., S. Prasad, et al. (2002). "Ser(214) is crucial for substrate binding to serine proteases." *J Biol Chem* 277(43): 40260-40264.
- Kruger, P. G. and D. Lagunoff (1981). "Mast cell restoration. A study of the rat peritoneal mast cells after depletion with polymyxin B." *Int Arch Allergy Appl Immunol* 65(3): 278-290.
- Kube, P., L. Audigé, et al. (1998). "Distribution, density and heterogeneity of canine mast cells and influence of fixation techniques." *Histochemistry and Cell Biology* 110(2): 129-135.
- Kumar, V. and A. Sharma (2010). "Mast cells: Emerging sentinel innate immune cells with diverse role in immunity." *Molecular Immunology* 48(1-3): 14-25.
- Küther, K., L. Audigé, et al. (1998). "Bovine mast cells: distribution, density, heterogeneity, and influence of fixation techniques." *Cell and Tissue Research* 293(1): 111-119.
- Lagunoff, D. and E. P. Benditt (1960). "Mast cell degranulation and histamine release observed in a new invitro system." *Journal of Experimental Medicine* 112(4): 571-&.
- Lagunoff, D., T. W. Martin, et al. (1983). "Agents that release histamine from mast-cells." *Annual Review of Pharmacology and Toxicology* 23: 331-351.
- Larsen, M. L., C. Ritz, et al. (2011). "Determination of ivermectin efficacy against cyathostomins and *Parascaris equorum* on horse farms using selective therapy." *The Veterinary Journal* 188(1): 44-47.
- Laugier, C., C. Sevin, et al. (2012). "Prevalence of *Parascaris equorum* infection in foals on French stud farms and first report of ivermectin-resistant *P. equorum* populations in France." *Veterinary Parasitology* 188(1-2): 185-189.
- Lawrence, C. E., J. C. M. Paterson, et al. (1998). "IL-4-regulated enteropathy in an intestinal nematode infection." *European Journal of Immunology* 28(9): 2672-2684.
- Lawrence, C. E., Y. Y. W. Paterson, et al. (2004). "Mouse mast cell protease-1 is required for the enteropathy induced by gastrointestinal helminth infection in the mouse." *Gastroenterology* 127(1): 155-165.
- Le Trong, H., H. Neurath, et al. (1987). "Substrate specificity of the chymotrypsin-like protease in secretory granules isolated from rat mast cells." *Proceedings of the National Academy of Sciences of the United States of America* 84(2): 364-367.

- Lester, H. E., D. J. Bartley, et al. (2013). "A cost comparison of faecal egg count-directed anthelmintic delivery versus interval programme treatments in horses." *Veterinary Record* 173(15): 371.
- Lester, H. E., J. Spanton, et al. (2013). "Anthelmintic efficacy against cyathostomins in horses in Southern England." *Veterinary Parasitology* 197(1-2): 189-196.
- Li, W. W., T. Z. Guo, et al. (2012). "Substance P signaling controls mast cell activation, degranulation, and nociceptive sensitization in a rat fracture model of complex regional pain syndrome." *Anesthesiology* 116(4): 882-895.
- Lichtenfels, J. R., L. M. Gibbons, et al. (2002). "Recommended terminology and advances in the systematics of the Cyathostominea (Nematoda : Strongyloidea) of horses." *Veterinary Parasitology* 107(4): 337-342.
- Lin, R. Y., L. B. Schwartz, et al. (2000). "Histamine and tryptase levels in patients with acute allergic reactions: An emergency department-based study." *Journal of Allergy and Clinical Immunology* 106(1, Part 1): 65-71.
- Lind, E. O., J. Höglund, et al. (1999). "A field survey on the distribution of strongyle infections of horses in Sweden and factors affecting faecal egg counts." *Equine Veterinary Journal* 31(1): 68-72.
- Lindberg, R., A. Nygren, et al. (1996). "Rectal biopsy diagnosis in horses with clinical signs of intestinal disorders: A retrospective study of 116 cases." *Equine Veterinary Journal* 28(4): 275-284.
- Lipman, N. S., L. R. Jackson, et al. (2005). "Monoclonal Versus Polyclonal Antibodies: Distinguishing Characteristics, Applications, and Information Resources." *ILAR Journal* 46(3): 258-268.
- Little, S. S. and D. A. Johnson (1995). "Human mast cell tryptase isoforms: separation and examination of substrate-specificity differences." *Biochem. J.* 307(2): 341-346.
- Lorenz, D., B. Wiesner, et al. (1998). "Mechanism of peptide-induced mast cell degranulation - Translocation and patch-clamp studies." *Journal of General Physiology* 112(5): 577-591.
- Love, S. and J. L. Duncan (1992). "The development of naturally acquired cyathostome infection in ponies." *Veterinary Parasitology* 44(1-2): 127-142.
- Love, S., J. L. Duncan, et al. (1995). "Efficacy of oral ivermectin paste against mucosal stages of cyathostomes." *Veterinary Record* 136(1): 18-19.
- Love, S. and J. B. McKeand (1997). "Cyathostomosis: practical issues of treatment and control." *Equine Veterinary Education* 1997 9: 5.
- Love, S., D. Murphy, et al. (1999). "Pathogenicity of cyathostome infection." *Veterinary Parasitology* 1999 85: 2/3.
- Lützelshwab, C., M. R. Huang, et al. (1998). "Characterization of mouse mast cell protease-8, the first member of a novel subfamily of mouse mast cell serine proteases, distinct from both the classical chymases and tryptases." *European Journal of Immunology* 28(3): 1022-1033.

- Lycke, N. (2012). "Recent progress in mucosal vaccine development: potential and limitations." *Nature Reviews Immunology* 12(8): 592-605.
- Lyons, E. T., S. C. Tolliver, et al. (1999). "Historical perspective of cyathostomes: prevalence, treatment and control programs." *Veterinary Parasitology* 85(2-3): 97-111.
- Lyons, E. T., S. C. Tolliver, et al. (1996). "Critical test evaluation (1977–1992) of drug efficacy against endoparasites featuring benzimidazole-resistant small strongyles (Population S) in Shetland ponies." *Veterinary Parasitology* 66(1–2): 67-73.
- Lyons, E. T., S. C. Tolliver, et al. (1996). "A study (1977–1992) of population dynamics of endoparasites featuring benzimidazole-resistant small strongyles (Population S) in Shetland ponies." *Veterinary Parasitology* 66(1–2): 75-86.
- Mair, T. S. and G. R. Pearson (1995). "Multifocal non-strangulating intestinal infarction associated with larval cyathostomiasis in a pony." *Equine Veterinary Journal* 27(2): 154-155.
- Malaviya, R., T. Ikeda, et al. (1996). "Mast cell modulation of neutrophil influx and bacterial clearance at sites of infection through TNF-[alpha]." *Nature* 381(6577): 77-80.
- Marshall, J. S. and D. M. Jawdat (2004). "Mast cells in innate immunity." *Journal of Allergy and Clinical Immunology* 114(1): 21-27.
- Marth, G. T., I. Korf, et al. (1999). "A general approach to single-nucleotide polymorphism discovery." *Nature Genetics* 23(4): 452.
- Matthews, J. (2010). "Clinical forum - Drug resistance in cyathostomins." *Companion Animal* 15(3): 9-17.
- Matthews, J. B. (2014) "Anthelmintic resistance in equine nematodes." *International Journal for Parasitology: Drugs and Drug Resistance*(0). 310-315.
- Matthews, J. B. (2008). "An update on cyathostomins: anthelmintic resistance and worm control." *Equine Veterinary Education* 2008 20: 10.
- Matthews, J. B. (2008). "An update on cyathostomins: Anthelmintic resistance and worm control." *Equine Veterinary Education* 20(10): 552-560.
- Matthews, J. B. (2011). "Facing the threat of equine parasitic disease." *Equine Veterinary Journal* 43(2): 126-132.
- Matthews, J. B., J. E. Hodgkinson, et al. (2004). "Recent developments in research into the Cyathostominae and Anoplocephala perfoliata." *Vet Res* 35(4): 371-381.
- Mayrhofer, G. and R. Fisher (1979). "Mast-cells in severely T-cell depleted rats and the response to infestation with *Nippostrongylus brasiliensis*." *Immunology* 37(1): 145-155.
- McAleese, S. M., A. D. Pemberton, et al. (1998). "Sheep mast-cell proteinases-1 and -3: cDNA cloning, primary structure and molecular modelling of the enzymes and further studies on substrate specificity." *Biochem J* 333 (Pt 3): 801-809.

- McCue, M. E., D. L. Bannasch, et al. (2012). "A high density SNP array for the domestic horse and extant Perissodactyla: utility for association mapping, genetic diversity, and phylogeny studies." *PLoS Genet* 8(1): e1002451.
- McCurdy, J. D., T. J. Lin, et al. (2001). "Toll-like receptor 4-mediated activation of murine mast cells." *J Leukoc Biol* 70(6): 977-984.
- McDermott, J. R., R. E. Bartram, et al. (2003). "Mast cells disrupt epithelial barrier function during enteric nematode infection." *Proceedings of the National Academy of Sciences of the United States of America* 100(13): 7761-7766.
- McGhee, J. R., J. Mestecky, et al. (1992). "The mucosal immune system: from fundamental concepts to vaccine development." *Vaccine* 10(2): 75-88.
- McGrath, M. E., J. R. Vasquez, et al. (1992). "Perturbing the polar environment of Asp102 in trypsin: consequences of replacing conserved Ser214." *Biochemistry* 31(12): 3059-3064.
- McKellar, Q. A. and F. Jackson (2004). "Veterinary anthelmintics: old and new." *Trends in Parasitology* 20(10): 456-461.
- McWilliam, H. E. G., A. J. Nisbet, et al. (2010). "Identification and characterisation of an immunodiagnostic marker for cyathostomin developing stage larvae." *International Journal for Parasitology* 2010 40: 3.
- Metcalfe, D. D., D. Baram, et al. (1997). "Mast cells." *Physiological Reviews* 77(4): 1033-1079.
- Metz, M. and M. Maurer (2007). "Mast cells - key effector cells in immune responses." *Trends in Immunology* 28(5): 234-241.
- Metz, M., A. M. Piliponsky, et al. (2006). "Mast Cells Can Enhance Resistance to Snake and Honeybee Venoms." *Science* 313(5786): 526-530.
- Mfitilodze, M. W. and G. W. Hutchinson (1990). "Prevalence and Abundance of Equine Strongyles (Nematoda: Strongyloidea) in Tropical Australia." *The Journal of Parasitology* 76(4): 487-494.
- Miller, H. R. P. (1996). "Mucosal mast cells and the allergic response against nematode parasites." *Veterinary Immunology and Immunopathology* 54(1-4): 331-336.
- Miller, H. R. P., J. F. Huntley, et al. (1988). "Granule proteinases define mast cell heterogeneity in the serosa and the gastrointestinal mucosa of the mouse." *Immunology* 65(4): 559-566.
- Miller, H. R. P. and A. D. Pemberton (2002). "Tissue-specific expression of mast cell granule serine proteinases and their role in inflammation in the lung and gut." *Immunology* 105(4): 375-390.
- Miller, H. R. P., R. G. Woodbury, et al. (1983). "Systemic release of mucosal mast-cell protease in primed rats challenged with *Nippostrongylus brasiliensis*." *Immunology* 49(3): 471-479.
- Miller, J. S., G. Moxley, et al. (1990). "Cloning and characterization of a second complementary DNA for human tryptase." *J Clin Invest* 86(3): 864-870.

- Miller, J. S. and L. B. Schwartz (1988). "Human mast cell proteases and mast cell heterogeneity." *Current Opinion in Immunology* 1(4): 637-642.
- Molento, M. B., J. Antunes, et al. (2008). "Anthelmintic resistant nematodes in Brazilian horses." *Veterinary Record* 162(12): 384-385.
- Molento, M. B., M. K. Nielsen, et al. (2012). "Resistance to avermectin/milbemycin anthelmintics in equine cyathostomins – Current situation." *Veterinary Parasitology* 185(1): 16-24.
- Monahan, C. M., M. R. Chapman, et al. (1995). "Dose titration of moxidectin oral gel against gastrointestinal parasites of ponies." *Veterinary Parasitology* 59(3-4): 241-248.
- Monahan, C. M., M. R. Chapman, et al. (1996). "Comparison of moxidectin oral gel and ivermectin oral paste against a spectrum of internal parasites of ponies with special attention to encysted cyathostome larvae." *Veterinary Parasitology* 63(3-4): 225-235.
- Monahan, C. M., M. R. Chapman, et al. (1998). "Experimental cyathostome challenge of ponies maintained with or without benefit of daily pyrantel tartrate feed additive: comparison of parasite burdens, immunity and colonic pathology." *Veterinary Parasitology* 74(2-4): 229-241.
- Morrow, A. N., K. P. Baker, et al. (1987). "Skin Lesions of Sweet Itch and the Distribution of Dermal Mast Cells in the Horse." *Journal of Veterinary Medicine, Series B* 34(1-10): 347-355.
- Murphy, D., M. P. Keane, et al. (1997). "Cyathostome-associated disease in the horse: investigation and management of four cases." *Equine Veterinary Education* 1997 9: 5.
- Murphy, D. and S. Love (1997). "The pathogenic effects of experimental cyathostome infections in ponies." *Veterinary Parasitology* 1997 70: 1/3.
- N. K, D. and N. K. G. A (1952). "Release of Histamine from Rat Diaphragm by Cobra Venom." *Nature* 169(4312): 1064-1065.
- Nakano, T., T. Sonoda, et al. (1985). "Fate of bone-marrow derived cultured mast-cells after intracutaneous, intraperitoneal, and intravenous transfer into genetically mast cell deficient W/WV mice - evidence that cultured mast-cells can give rise to both connective-tissue type and mucosal mast-cells." - *Journal of Experimental Medicine* 162(3): 1025-1043.
- Ng, P. C. and S. Henikoff (2001). "Predicting Deleterious Amino Acid Substitutions." *Genome Research* 11(5): 863-874.
- Nielsen, M. K., N. Haaning, et al. (2006). "Strongyle egg shedding consistency in horses on farms using selective therapy in Denmark." *Veterinary Parasitology* 135(3-4): 333-335.
- Nielsen, M. K., R. M. Kaplan, et al. (2007). "Climatic influences on development and survival of free-living stages of equine strongyles: Implications for worm control strategies and managing anthelmintic resistance." *The Veterinary Journal* 174(1): 23-32.

- Nielsen, M. K., J. Monrad, et al. (2006). "Prescription-only anthelmintics—A questionnaire survey of strategies for surveillance and control of equine strongyles in Denmark." *Veterinary Parasitology* 135(1): 47-55.
- Nielsen, M. K., A. N. Vidyashankar, et al. (2012). "Strongylus vulgaris associated with usage of selective therapy on Danish horse farms—Is it reemerging?" *Veterinary Parasitology* 189(2–4): 260-266.
- Ogbourne, C. P. (1976). "The prevalence, relative abundance and site distribution of nematodes of the subfamily Cyathostominae in horses killed in Britain." *Journal of Helminthology* 50(03): 203-214.
- Owen, C. F. (2009). *Mast Cell Stabilizers to Prevent or Treat Laminitis*, Google Patents.
- Owen, R., D. Jagger, et al. (1989). "Caecal intussusceptions in horses and the significance of *Anoplocephala perfoliata*." *Veterinary Record* 124(2): 34-37.
- Pallaoro, M., A. Gambacurta, et al. (1996). "cDNA cloning and primary structure of trypsin from bovine mast cells, and evidence for the expression of bovine pancreatic trypsin inhibitor mRNA in the same cells." *Eur J Biochem* 237(1): 100-105.
- Pejler, G., M. Åbrink, et al. (2007). *Mast Cell Proteases*. *Advances in Immunology*. K. F. A. T. H. F. M. J. W. U. Frederick W. Alt and R. U. Emil, Academic Press. Volume 95: 167-255.
- Pejler, G., S. D. Knight, et al. (2009). "Novel insights into the biological function of mast cell carboxypeptidase A." *Trends in Immunology* 30(8): 401-408.
- Pejler, G., E. Ronnberg, et al. (2010). "Mast cell proteases: multifaceted regulators of inflammatory disease." *Blood* 115(24): 4981-4990.
- Pemberton, A., J. Brown, et al. (2003). "Purification and characterization of mouse mast cell proteinase-2 and the differential expression and release of mouse mast cell proteinase-1 and -2 in vivo." *Clinical & Experimental Allergy* 33(7): 1005-1012.
- Pemberton, A. D., J. F. Huntley, et al. (1997). "Sheep mast cell proteinase-1: characterization as a member of a new class of dual-specific ruminant chymases." *Biochem. J.* 321(3): 665-670.
- Pemberton, A. D., S. M. McAleese, et al. (2000). "cDNA sequence of two sheep mast cell trypsinases and the differential expression of trypsinase and sheep mast cell proteinase-1 in lung, dermis and gastrointestinal tract." *Clinical and Experimental Allergy* 30(Article): 818-832.
- Pemberton, A. D., S. M. McAleese, et al. (2000). "cDNA sequence of two sheep mast cell trypsinases and the differential expression of trypsinase and sheep mast cell proteinase-1 in lung, dermis and gastrointestinal tract." *Clinical and Experimental Allergy* 30(6): 818-832.
- Pemberton, A. D., A. R. McEuen, et al. (2001). "Characterisation of trypsinase and a granzyme H-like chymase isolated from equine mastocytoma tissue." *Veterinary Immunology and Immunopathology* 83(3-4): 253-267.

- Pemberton, A. D., S. H. Wright, et al. (2006). "Anaphylactic release of mucosal mast cell granule proteases: role of serpins in the differential clearance of mouse mast cell proteases-1 and -2." *J Immunol* 176(2): 899-904.
- Peregrine, A. S., B. McEwen, et al. (2006). "Larval cyathostominosis in horses in Ontario: An emerging disease? (vol 47, pg 80, 2006)." *Canadian Veterinary Journal-Revue Veterinaire Canadienne* 47(2): 161-161.
- Pereira, P. J. B., A. Bergner, et al. (1998). "Human beta-tryptase is a ring-like tetramer with active sites facing a central pore." *Nature* 392(6673): 306.
- Perona, J. J., L. Hedstrom, et al. (1995). "Structural origins of substrate discrimination in trypsin and chymotrypsin." *Biochemistry* 34(5): 1489-1499.
- Pickles, K. J., J. A. Mair, et al. (2010). "Large intestinal mast cell count and proteinase expression is associated with larval burden in cyathostomin-infected horses." *Equine Veterinary Journal* 42(7): 652-657.
- Piuko, K., I. G. Bravo, et al. (2007). "Identification and characterization of equine granzyme B." *Veterinary Immunology and Immunopathology* 118(3-4): 239-251.
- Pizarro, T. T., M. H. Michie, et al. (1999). "IL-18, a Novel Immunoregulatory Cytokine, Is Up-Regulated in Crohn's Disease: Expression and Localization in Intestinal Mucosal Cells." *The Journal of Immunology* 162(11): 6829-6835.
- Polosa, R., S. Rorke, et al. (2002). "Evolving concepts on the value of adenosine hyperresponsiveness in asthma and chronic obstructive pulmonary disease." *Thorax* 57(7): 649-654.
- Proudman, C. J., N. P. French, et al. (1998). "Tapeworm infection is a significant risk factor for spasmodic colic and ileal impaction colic in the horse." *Equine Vet J* 30(3): 194-199.
- Puente, X. S. and C. López-Otín (2004). "A Genomic Analysis of Rat Proteases and Protease Inhibitors." *Genome Research* 14(4): 609-622.
- Puri, N. and P. A. Roche (2008). "Mast cells possess distinct secretory granule subsets whose exocytosis is regulated by different SNARE isoforms." *Proceedings of the National Academy of Sciences of the United States of America* 105(7): 2580-2585.
- Puri, N. and P. A. Roche (2008). "Mast cells possess distinct secretory granule subsets whose exocytosis is regulated by different SNARE isoforms." *Proceedings of the National Academy of Sciences* 105(7): 2580-2585.
- Reid, S. W. J., T. S. Mair, et al. (1995). "Epidemiological risk factors associated with a diagnosis of clinical cyathostomiasis in the horse." *Equine Veterinary Journal* 27(2): 127-130.
- Reimer, J. M., P. B. Samollow, et al. (2010). "High degree of conservation of the multigene tryptase locus over the past 150-200 million years of mammalian evolution." *Immunogenetics* 62(6): 369-382.

- Reinemeyer, C. (2009). "Diagnosis and control of anthelmintic-resistant *Parascaris equorum*." *Parasites & Vectors* 2(Suppl 2): S8.
- Reinemeyer, C. R. and R. P. Herd (1986). "Comparison of two techniques for quantitation of encysted cyathostome larvae in the horse." *American Journal of Veterinary Research* 1986 47: 3.
- Reinemeyer, C. R., S. A. Smith, et al. (1984). "The prevalence and intensity of internal parasites of horses in the U.S.A." *Veterinary Parasitology* 15(1): 75-83.
- Relf, V. E., H. E. Lester, et al. (2014). "Anthelmintic efficacy on UK Thoroughbred stud farms." *International Journal for Parasitology* 44(8): 507-514.
- Ricketts, S. W. (1996). "Rectal biopsy - A piece of the diagnostic jigsaw puzzle." *Equine Veterinary Journal* 28(4): 254-255.
- Romagnani, S. (1999). "Th1/Th2 cells." *Inflammatory Bowel Diseases* 5(4): 285-294.
- Rönneberg, E., G. Calounova, et al. (2013). "Granzyme D Is a Novel Murine Mast Cell Protease That Is Highly Induced by Multiple Pathways of Mast Cell Activation." *Infection and Immunity* 81(6): 2085-2094.
- Rossano, M. G., A. R. Smith, et al. (2010). "Shortened strongyle-type egg reappearance periods in naturally infected horses treated with moxidectin and failure of a larvicidal dose of fenbendazole to reduce fecal egg counts." *Veterinary Parasitology* 173(3-4): 349-352.
- Rouleau, A., M. Garbarg, et al. (1994). "Molecular cloning of rat mast cell protease 1 and development of specific probes for its gene transcript." *Biochem Biophys Res Commun* 199(2): 593-602.
- Ruggles, S. W., R. J. Fletterick, et al. (2004). "Characterization of Structural Determinants of Granzyme B Reveals Potent Mediators of Extended Substrate Specificity." *Journal of Biological Chemistry* 279(29): 30751-30759.
- Salminen, S., C. Bouley, et al. (1998). "Functional food science and gastrointestinal physiology and function." *British Journal of Nutrition* 80(SupplementS1): S147-S171.
- Sangster, N. (2003). "A practical approach to anthelmintic resistance." *Equine Veterinary Journal* 35(3): 218-219.
- Sangster, N. C. (1999). "Pharmacology of anthelmintic resistance in cyathostomes: will it occur with the avermectin/milbemycins?" *Veterinary Parasitology* 85(2-3): 189-201.
- Sarin, S. K., V. Malhotra, et al. (1987). "Significance of eosinophil and mast cell counts in rectal mucosa in ulcerative colitis." *Digestive Diseases and Sciences* 32(4): 363-367.

- Schopf, L. R., K. F. Hoffmann, et al. (2002). "IL-10 is critical for host resistance and survival during gastrointestinal helminth infection." *Journal of Immunology* 168(5): 2383-2392.
- Schumacher, J. and J. Taintor (2008). "A review of the use of moxidectin in horses." *Equine Veterinary Education* 20(10): 546-551.
- Schwartz, L. B. (2001). "Clinical utility of tryptase levels in systemic mastocytosis and associated hematologic disorders." *Leukemia Research* 25(7): 553-562.
- Schwartz, L. B., A. M. Irani, et al. (1987). "Quantitation of histamine, tryptase, and chymase in dispersed human T and TC mast cells." *The Journal of Immunology* 138(8): 2611-2615.
- Schwartz, L. B., D. D. Metcalfe, et al. (1987). "Tryptase Levels as an Indicator of Mast-Cell Activation in Systemic Anaphylaxis and Mastocytosis." *New England Journal of Medicine* 316(26): 1622-1626.
- Scudamore, C. L., M. A. Jepson, et al. (1998). "The rat mucosal mast cell chymase, RMCP-11, alters epithelial cell monolayer permeability in association with altered distribution of the tight junction proteins ZO-1 and occludin." *European Journal of Cell Biology* 75(4): 321-330.
- Scudamore, C. L., L. McMillan, et al. (1997). "Mast cell heterogeneity in the gastrointestinal tract - Variable expression of mouse mast cell protease-1 (mMCP-1) in intraepithelial mucosal mast cells in nematode-infected and normal BALB/c mice." *American Journal of Pathology* 150(5): 1661-1672.
- Scudamore, C. L., E. M. Thornton, et al. (1995). "Release of the mucosal mast-cell granule chymase, rat mast-cell protease-II, during anaphylaxis is associated with the rapid development of paracellular permeability to macromolecules in rat jejunum." *Journal of Experimental Medicine* 182(6): 1871-1881.
- Selwood, T., Z.-M. Wang, et al. (2002). "Diverse Stability and Catalytic Properties of Human Tryptase α and β Isoforms are Mediated by Residue Differences at the S1 Pocket[†]." *Biochemistry* 41(10): 3329-3340.
- Shelburne, C. P. and J. J. Ryan (2001). "The role of Th2 cytokines in mast cell homeostasis." *Immunol Rev* 179: 82-93.
- Sheoran, A. S., J. F. Timoney, et al. (2000). "Immunoglobulin isotypes in sera and nasal mucosal secretions and their neonatal transfer and distribution in horses." *American Journal of Veterinary Research* 61(9): 1099-1105.
- Shimizu, H., Y. Nagakui, et al. (2001). "Demonstration of Chymotryptic and Tryptic activities in Mast Cells of Rodents: Comparison of 17 Species of the Family Muridae." *Journal of Comparative Pathology* 125(1): 76-79.
- Shin, K., G. F. M. Watts, et al. (2008). "Mouse mast cell tryptase mMCP-6 is a critical link between adaptive and innate immunity in the chronic phase of *Trichinella spiralis* infection." *Journal of Immunology* 180(7): 4885-4891.
- Shoop, W. L., H. Mrozik, et al. (1995). "Structure and activity of avermectins and milbemycins in animal health." *Vet Parasitol* 59(2): 139-156.

- Sievers, F., A. Wilm, et al. (2011). "Fast, scalable generation of high-quality protein multiple sequence alignments using Clustal Omega." *Mol Syst Biol* 7: 539.
- Slocombe, J. O., J. F. Cote, et al. (2008). "The persistence of benzimidazole-resistant cyathostomes on horse farms in Ontario over 10 years and the effectiveness of ivermectin and moxidectin against these resistant strains." *Can Vet J* 49(1): 56-60.
- Slocombe, J. O. and R. V. de Gannes (2006). "Cyathostomes in horses in Canada resistant to pyrantel salts and effectively removed by moxidectin." *Vet Parasitol* 140(1-2): 181-184.
- Slocombe, J. O. D. (1979). "Prevalence and treatment of tapeworms in horses." *Canadian Veterinary Journal-Revue Veterinaire Canadienne* 20(5): 136-140.
- Smets, K., D. J. Shaw, et al. (1999). "Diagnosis of larval cyathostominosis in horses in Belgium." *Veterinary Record* 1999 144: 24.
- Smyth, M. J., M. D. O'Connor, et al. (1996). "Granzymes: a variety of serine protease specificities encoded by genetically distinct subfamilies." *Journal of Leukocyte Biology* 60(5): 555-562.
- Sonti, S. (2012). "A study on the mast cells in appendicitis." *Journal of Clinical and Diagnostic Research* 6(7): 1276.
- Southwood, L. L., J. Lindermann, et al. (2006). "Growth factor and receptor mRNA expression in the intestine of horses with large colon volvulus: a pilot study." *Equine Veterinary Journal* 38(6): 532-537.
- St. John, A. L. and S. N. Abraham (2013). "Innate Immunity and Its Regulation by Mast Cells." *The Journal of Immunology* 190(9): 4458-4463.
- Stancampiano, L., L. M. Gras, et al. (2010). "Spatial niche competition among helminth parasites in horse's large intestine." *Veterinary Parasitology* 170(1-2): 88-95.
- Steinbach, T., C. Bauer, et al. (2006). "Small strongyle infection: Consequences of larvicidal treatment of horses with fenbendazole and moxidectin." *Veterinary Parasitology* 139(1-3): 115-131.
- Stevens, R. L., D. S. Friend, et al. (1994). "Strain-specific and tissue-specific expression of mouse mast cell secretory granule proteases." *Proc Natl Acad Sci U S A* 91(1): 128-132.
- Stratford, C. H., B. C. McGorum, et al. (2011). "An update on cyathostomins: Anthelmintic resistance and diagnostic tools." *Equine Veterinary Journal* 43: 133-139.
- Strobel, S., H. R. P. Miller, et al. (1981). "Human intestinal mucosal mast-cells - Evaluation of fixation and staining techniques." *Journal of Clinical Pathology* 34(8): 851-858.
- Sture, G. H., J. F. Huntley, et al. (1995). "Ovine mast cell heterogeneity is defined by the distribution of sheep mast cell proteinase." *Veterinary Immunology and Immunopathology* 48(3-4): 275-285.

- Tate, J. and G. Ward (2004). "Interferences in immunoassay." *Clin Biochem Rev* 25(2): 105-120.
- Tchougounova, E., G. Pejler, et al. (2003). "The Chymase, Mouse Mast Cell Protease 4, Constitutes the Major Chymotrypsin-like Activity in Peritoneum and Ear Tissue. A Role for Mouse Mast Cell Protease 4 in Thrombin Regulation and Fibronectin Turnover." *The Journal of Experimental Medicine* 198(3): 423-431.
- Tertian, G., Y. P. Yung, et al. (1981). "Long-term invitro culture of murine mast-cells .1. Description of a growth factor-dependent cluture technique." *Journal of Immunology* 127(2): 788-794.
- Theoharides, T. C., P. Patra, et al. (2000). "Chondroitin sulphate inhibits connective tissue mast cells." *British Journal of Pharmacology* 131(6): 1039-1049.
- Thomas, V. A., C. J. Wheelless, et al. (1998). "Human mast cell tryptase fibrinogenolysis: kinetics, anticoagulation mechanism, and cell adhesion disruption." *Biochemistry* 37(8): 2291-2298.
- Torbert, B. J., T. R. Klei, et al. (1986). "A Survey in Louisiana of Intestinal Helminths of Ponies with Little Exposure to Anthelmintics." *The Journal of Parasitology* 72(6): 926-930.
- Trapani, J. A. (2001). "Granzymes: a family of lymphocyte granule serine proteases." *Genome Biol* 2(12): REVIEWS3014.
- Traver, D. S. and H. L. Thacker (1979). "Malabsorption-syndromes in the horse - Use of rectal mucosal biopsy in differential-diagnosis." *Journal of Equine Medicine and Surgery* 3(3): 144-144.
- Traversa, D., G. Castagna, et al. (2012). "Efficacy of major anthelmintics against horse cyathostomins in France." *Veterinary Parasitology* 188(3-4): 294-300.
- Traversa, D., R. Iorio, et al. (2007). "New Method for Simultaneous Species-Specific Identification of Equine Strongyles (Nematoda, Strongylida) by Reverse Line Blot Hybridization." *Journal of Clinical Microbiology* 45(9): 2937-2942.
- Traversa, D., T. R. Klei, et al. (2007). "Occurrence of anthelmintic resistant equine cyathostome populations in central and southern Italy." *Preventive Veterinary Medicine* 82(3-4): 314-320.
- Traversa, D., P. Milillo, et al. (2010). "Distribution and species-specific occurrence of cyathostomins (Nematoda, Strongylida) in naturally infected horses from Italy, United Kingdom and Germany." *Veterinary Parasitology* 168(1-2): 84-92.
- Traversa, D., G. von Samson-Himmelstjerna, et al. (2009). "Anthelmintic resistance in cyathostomin populations from horse yards in Italy, United Kingdom and Germany." *Parasites & Vectors* 2.
- Tremaine, W. J., A. Brzezinski, et al. (2002). "Treatment of mildly to moderately active ulcerative colitis with a tryptase inhibitor (APC 2059): an open-label pilot study." *Alimentary Pharmacology & Therapeutics* 16(3): 407-413.

- Trivedi, N. N. and G. H. Caughey (2010). "Mast cell peptidases: chameleons of innate immunity and host defense." *Am J Respir Cell Mol Biol* 42(3): 257-267.
- Trivedi, N. N., Q. Tong, et al. (2007). "Mast Cell α and β Tryptases Changed Rapidly during Primate Speciation and Evolved from γ -Like Transmembrane Peptidases in Ancestral Vertebrates." *The Journal of Immunology* 179(9): 6072-6079.
- Trotz-Williams, L., P. Physick-Sheard, et al. (2008). "Occurrence of *Anoplocephala perfoliata* infection in horses in Ontario, Canada and associations with colic and management practices." *Veterinary Parasitology* 153(1–2): 73-84.
- Tshori, S. and E. Razin (2010). "Editorial: Mast cell degranulation and calcium entry—the Fyn-calcium store connection." *Journal of Leukocyte Biology* 88(5): 837-838.
- Urb, M. and D. C. Sheppard (2012). "The Role of Mast Cells in the Defence against Pathogens." *PLoS Pathog* 8(4): e1002619.
- van Ginkel, F. W., H. H. Nguyen, et al. (2000). "Vaccines for mucosal immunity to combat emerging infectious diseases." *Emerging Infectious Diseases* 6(2): 123-132.
- Vandesompele, J., K. De Preter, et al. (2002). "Accurate normalization of real-time quantitative RT-PCR data by geometric averaging of multiple internal control genes." *Genome Biol* 3(7): Research 0034.
- Vargas, I. M. and P. E. Vivas-Mejia (2013). "Assessment of mRNA splice variants by qRT-PCR." *Methods Mol Biol* 1049: 171-186.
- Vercruysse, J., M. Eysker, et al. (1998). "Persistence of the efficacy of a moxidectin gel on the establishment of cyathostominae in horses." *Veterinary Record* 143(11): 307-309.
- Wade, C. M., E. Giulotto, et al. (2009). "Genome Sequence, Comparative Analysis, and Population Genetics of the Domestic Horse." *Science* 326(5954): 865-867.
- Wagner, B., W. H. Miller Jr, et al. (2009). "Sensitization of skin mast cells with IgE antibodies to *Culicoides* allergens occurs frequently in clinically healthy horses." *Veterinary Immunology and Immunopathology* 132(1): 53-61.
- Wallace, J. L. and D. N. Granger (1996). "The cellular and molecular basis of gastric mucosal defense." *The FASEB Journal* 10(7): 731-740.
- Walls, A. F., D. B. Jones, et al. (1990). "Immunohistochemical identification of mast cells in formaldehyde-fixed tissue using monoclonal antibodies specific for tryptase." *The Journal of Pathology* 162(2): 119-126.
- Wang, L., K. Zhang, et al. (2012). "Structural Insights into the Substrate Specificity of Human Granzyme H: The Functional Roles of a Novel RKR Motif." *The Journal of Immunology* 188(2): 765-773.

- Wastling, J. M., P. Knight, et al. (1998). "Histochemical and Ultrastructural Modification of Mucosal Mast Cell Granules in Parasitized Mice Lacking the β -Chymase, Mouse Mast Cell Protease-1." *The American Journal of Pathology* 153(2): 491-504.
- Wastling, J. M., C. L. Scudamore, et al. (1997). "Constitutive expression of mouse mast cell protease-1 in normal BALB/c mice and its up-regulation during intestinal nematode infection." *Immunology* 90(2): 308-313.
- Waugh, S. M., J. L. Harris, et al. (2000). "The structure of the pro-apoptotic protease granzyme B reveals the molecular determinants of its specificity." *Nature Structural Biology* 7(9): 762.
- Weber, A., J. Knop, et al. (2003). "Pattern analysis of human cutaneous mast cell populations by total body surface mapping." *British Journal of Dermatology* 148(2): 224-228.
- Weidner, N. and K. F. Austen (1993). "Heterogeneity of Mast Cells at Multiple Body Sites: Fluorescent Determination of Avidin Binding and Immunofluorescent Determination of Chymase, Tryptase, and Carboxypeptidase Content." *Pathology - Research and Practice* 189(2): 156-162.
- Welle, M. (1997). "Development, significance, and heterogeneity of mast cells with particular regard to the mast cell-specific proteases chymase and tryptase." *Journal of Leukocyte Biology* 61(3): 233-245.
- Welle, M. M., L. Audige, et al. (1997). "The equine endometrial mast cell during the puerperal period: evaluation of mast cell numbers and types in comparison to other inflammatory changes." *Vet Pathol* 34(1): 23-30.
- Williamson, R. M. C., R. B. Gasser, et al. (1997). "The distribution of *Anoplocephala perfoliata* in the intestine of the horse and associated pathological changes." *Veterinary Parasitology* 73(3-4): 225-241.
- Wong, G. W., S. Yasuda, et al. (2004). "Mouse Chromosome 17A3.3 Contains 13 Genes That Encode Functional Tryptic-like Serine Proteases with Distinct Tissue and Cell Expression Patterns." *Journal of Biological Chemistry* 279(4): 2438-2452.
- Woodbury, R. G., M. Everitt, et al. (1978). "A major serine protease in rat skeletal muscle: Evidence for its mast cell origin." *Proceedings of the National Academy of Sciences* 75(11): 5311-5313.
- Woodbury, R. G., G. M. Gruzenski, et al. (1978). "Immunofluorescent localization of a serine protease in rat small intestine." *Proceedings of the National Academy of Sciences* 75(6): 2785-2789.
- Woodbury, R. G., H. R. P. Miller, et al. (1984). "Mucosal mast-cells are functionally active during spontaneous expulsion of intestinal nematode infections in rat." *Nature* 312(5993): 450-452.
- Woodward, A. D., S. J. Holcombe, et al. (2010). "Cationic and neutral amino acid transporter transcript abundances are differentially expressed in the equine intestinal tract." *Journal of Animal Science* 88(3): 1028-1033.

- Xiang, Z., M. Block, et al. (2001). "IgE-mediated mast cell degranulation and recovery monitored by time-lapse photography." *Journal of Allergy and Clinical Immunology* 108(1): 116-121.
- Xiao, L., R. P. Herd, et al. (1994). "Comparative efficacy of moxidectin and ivermectin against hypobiotic and encysted cyathostomes and other equine parasites." *Veterinary Parasitology* 53(1-2): 83-90.
- Xiao, L., R. P. Herd, et al. (1994). "Comparative efficacy of moxidectin and ivermectin against hypobiotic and encysted cyathostomes and other equine parasites." *Veterinary Parasitology* 53(1-2): 83-90.
- Xing, W., K. F. Austen, et al. (2011). "Protease phenotype of constitutive connective tissue and of induced mucosal mast cells in mice is regulated by the tissue." *Proc Natl Acad Sci U S A* 108(34): 14210-14215.
- Zamolodchikova, T. S., E. A. Sokolova, et al. (2003). "Graspases - A special group of serine proteases of the chymotrypsin family that has lost a conserved active site disulfide bond." *Biochemistry-Moscow* 68(3): 309-316.
- Zamolodchikova, T. S., T. I. Vorotyntseva, et al. (1995). "Duodenase, a new serine protease of unusual specificity from bovine duodenal mucosa. Primary structure of the enzyme." *Eur J Biochem* 227(3): 873-879.
- Zaros, L. G., L. L. Coutinho, et al. (2010). "Evaluation of reference genes for real-time PCR studies of Brazilian Somalis sheep infected by gastrointestinal nematodes." *Genet Mol Biol* 33(3): 486-490.
- Zhang, Y. W., E. G. Davis, et al. (2009). "Determination of internal control for gene expression studies in equine tissues and cell culture using quantitative RT-PCR." *Veterinary Immunology and Immunopathology* 130(1-2): 114-119.

7 Appendix A: Additional Data

Horse	MMC Caecum (MC/mm ²)	SMMC Caecum (MC/mm ²)	MMC RVC (MC/mm ²)	SMMC RVC (MC/mm ²)	MMC RB (MC/mm ²)	SMMC RB (MC/mm ²)
AB 1	397	254	467	320	93	266
AB 2	518	299	704	373	420	235
AB 3	208	130	317	110	99	70
AB 4	794	286	749	405	461	229
AB 5	181	194	157	158	98	93
AB 6	407	275	429	389	314	200
AB 7	398	224	381	254	40	166
AB 8	592	317	546	326	288	318
AB 9	1,062	355	789	357	315	218
AB 10	795	437	738	413	414	242
AB 11	787	413	832	349	307	283
AB 12	637	312	731	387	541	330
AB 13	386	184	382	304	352	163
AB 14	448	269	437	299	144	200
AB 15	240	216	120	170	134	182
AB 16	451	395	362	432	205	133
DV 1	22	158	34	170	19	102
DV 2	594	293	517	445	395	206
DV 3	285	110	197	296	122	94
DV 4	336	268	101	328	170	243
DV 5	285	150	250	150	170	166
DV 6	341	250	394	184	298	157
DV 7	390	315	350	325	59	383
DV 8	526	195	423	193	174	150
DV 9	440	229	428	281	354	355
DV 10	473	162	473	196	96	166
DV 11	1,035	331	1,470	364	467	183
DV 12	874	248	738	334	131	118

Table 7.1: Results of mucosal and submucosal mast cell counts from the caecum, RVC and rectum of all horses (AB1-16, DV1-12). Cells expressed as MC per mm². (MMC: Mucosal mast cell; SMMC: Submucosal mast cell; RVC: Right ventral colon; RB: Rectal biopsy)

Mast Cell Recruitment and Activation as Measures of Cyathostomin Burden

	Mucosa	Submucosa	Mucosa	Submucosa	Mucosa	Submucosa
	Caecum	Caecum	RVC	RVC	RB	RB
	(EC/mm²)	(EC/mm²)	(EC/mm²)	(EC/mm²)	(EC/mm²)	(EC/mm²)
DV6	270	144	166	134	8	83
DV7	928	734	624	605	94	778
DV8	218	80	237	106	6	42
DV9	355	405	302	315	19	248
DV10	501	606	570	510	34	435
DV11	376	552	403	270	8	174
DV12	1178	419	875	389	88	106

Table 7.2: Results of mucosal and submucosal eosinophil cell counts (EC/mm²) from the caecum, RVC and rectum of R(D)SVS horses (DV6-12). (RVC: Right ventral colon).

Mast Cell Recruitment and Activation as Measures of Cyathostomin Burden

Horse	eqMCP-1 MMC Caecum (MC/mm ²)	eqMCP-1 SMMC Caecum (MC/mm ²)	eqMCP-1 MMC RVC (MC/mm ²)	eqMCP-1 SMMC RVC (MC/mm ²)	eqMCP-1 MMC RB (MC/mm ²)	eqMCP-1 SMMC RB (MC/mm ²)
AB 1	333	179	211	160	125	50
AB 2	542	146	432	165	328	186
AB 3	290	98	250	107	30	35
AB 4	395	152	344	213	106	74
AB 5	70	14	118	56	19	2
AB 6	632	178	565	224	613	32
AB 7	96	14	483	246	136	128
AB 8	363	230	442	222	392	158
AB 9	1027	224	966	205	136	25.6
AB 10	638	192	634	179	256	78
AB 11	627	171	366	149	371	40
AB 12	507	77	621	138	558	46
AB 13	371	150	117	187	115	90
AB 14	205	187	450	262	11	0
AB 15	70	54	400	110	46	24
AB 16	54	38	43	43	395	155
DV 1	56	64	56	50	3	8
DV 2	301	98	272	213	85	19
DV 3	70	69	19	38	59	58
DV 4	264	146	176	107	11	86
DV 5	376	94	360	62	26	8
DV 6	339	210	320	125	51	72
DV 7	419	160	346	218	96	141
DV 8	408	131	509	218	309	226
DV 9	464	125	354	189	381	258
DV 10	598	122	418	146	101	54
DV 11	397	173	1323	288	24	5
DV 12	686	165	368	259	171	42

Table 7.3: Table of eqMCP-1 labelled mast cells in the mucosa (MMC) and submucosa (SMMC) in the caecum, RVC and rectum from horses sampled from the abattoir and the R(D)SVS. Cells expressed as MC per mm². (eqMCP-1: equine mast cell proteinase-1. MMC: mucosal mast cell. SMMC: submucosal mast cell. RVC: Right ventral colon. RB: Rectal biopsy).

Mast Cell Recruitment and Activation as Measures of Cyathostomin Burden

Horse	eqTRYP MMC Caecum (MC/mm ²)	eqTRYP SMMC Caecum (MC/mm ²)	eqTRYP MMC RVC (MC/mm ²)	eqTRYP SMMC RVC (MC/mm ²)	eqTRYP MMC RB (MC/mm ²)	eqTRYP SMMC RB (MC/mm ²)
AB 1	29	11	38	13	154	38
AB 2	118	37	77	37	59	13
AB 3	24	21	34	30	11	6
AB 4	130	106	219	171	40	80
AB 5	21	2	34	50	2	0
AB 6	218	93	235	51	85	56
AB 7	35	8	94	34	19	32
AB 8	102	27	45	43	83	38
AB 9	150	11	220	45	22	3
AB 10	93	3	94	27	27	5
AB 11	181	51	98	6	64	3
AB 12	230	75	261	72	83	8
AB 13	112	66	202	88	29	50
AB 14	72	115	43	99	6	2
AB 15	18	11	40	40	34	11
AB 16	11	6	46	40	24	21
DV 1	6.4	37	19	21	14	2
DV 2	69	37	21	14	26	11
DV 3	78	109	21	78	59	30
DV 4	38	86	8	66	62	69
DV 5	35	24	59	35	6	11
DV 6	102	115	43	77	18	0
DV 7	126	74	94	179	34	90
DV 8	40	107	67	94	122	42
DV 9	149	66	117	190	174	181
DV 10	432	34	144	66	8	80
DV 11	114	96	160	197	6	10
DV 12	256	214	162	245	107	98

Table 7.4: Table of eqTRYP labelled mast cells in the mucosa (MMC) and submucosa (SMMC) in the caecum, RVC and rectum from horses sampled from the abattoir and the R(D)SVS. Cells expressed as MC per mm². (eqTRYP: equine tryptase. MMC: mucosal mast cell. SMMC: Submucosal mast cell. RVC: Right ventral colon. RB: Rectal biopsy).

Mast Cell Recruitment and Activation as Measures of Cyathostomin Burden

Sample	Serum at -20°C	SEM (+/- ng/ml)	Serum at -80°C	SEM (+/- ng/ml)
AB13 L	2.25	0.13	1.64	0.37
AB14 L	1.32	0.05	1.07	0.19
AB15 L	0.93	0.13	0.93	0.11
AB16 L	4.18	0.29	3.86	0.34
DV1 L	2.26	0.22	1.99	0.20
DV1 P	2.27	0.25	2.04	0.29
DV2 L	1.33	0.15	1.32	0.42
DV2 P	1.00	0.08	0.93	0.20
DV3 L	1.26	0.14	0.96	0.33
DV3 P	1.25	0.12	0.96	0.33
DV4 L	0.75	0.13	0.58	0.18
DV5 L	1.01	0.25	0.70	0.13
DV5 P	2.77	0.19	2.02	0.60
DV6 L	1.40	0.10	1.65	0.90
DV6 P	1.60	0.68	0.81	0.22
DV7 L	0.54	0.05	0.54	0.27
DV7 P	0.98	0.32	0.53	0.20
DV8 L	1.82	0.20	1.34	0.28
DV8 P	1.45	0.02	1.62	0.37
DV9 L	5.21	0.63	3.84	0.36
DV9 P	1.55	0.05	1.60	0.31
DV10 L	1.75	0.17	1.35	0.16
DV10 P	1.31	0.07	1.15	0.13
DV11 L	3.54	1.68	1.74	0.27
DV11 P	2.15	0.50	1.65	0.14
DV12 L	2.68	0.61	1.92	0.21
DV12 P	2.05	0.50	1.31	0.03
NEG	0.45	0.02	0.56	0.12

Table 7.5: Table of mean serum eqMCP-1 ELISA concentration results from serum collected from a local (L) or peripheral site (P) and stored at -20 °C or -80 °C. (eqMCP-1: equine mast cell proteinase-1. NEG: serum from cyathostomin negative ponies. SEM: Standard Error of the Mean).

Mast Cell Recruitment and Activation as Measures of Cyathostomin Burden

Sample	Serum at -20°C	SEM (+/-µg/ml)	Serum at -80°C	SEM (+/-µg/ml)
AB13 L	12.14	5.29	17.43	4.29
AB14 L	2.42	0.72	5.74	0.34
AB15 L	0.91	0.18	1.08	0.09
AB16 L	3.02	0.95	7.29	0.87
DV1 L	3.55	1.31	1.98	0.21
DV1 P	1.64	0.40	1.44	0.16
DV2 L	3.91	1.40	5.62	0.80
DV2 P	0.51	0.11	0.39	0.05
DV3 L	1.89	0.71	2.01	0.55
DV3 P	0.73	0.11	0.88	0.13
DV4 L	1.33	0.37	1.11	0.15
DV5 L	2.05	0.61	3.06	0.27
DV5 P	14.25	4.42	14.84	3.48
DV6 L	1.83	0.43	2.61	0.17
DV6 P	5.77	0.70	4.89	1.23
DV7 L	2.07	0.71	2.40	0.27
DV7 P	2.38	0.97	2.10	0.20
DV8 L	5.54	2.08	4.11	0.98
DV8 P	1.37	0.37	2.10	0.37
DV9 L	8.31	2.96	10.03	1.06
DV9 P	0.53	0.06	0.76	0.18
DV10 L	1.22	0.41	1.43	0.17
DV10 P	0.42	0.12	0.47	0.03
DV11 L	3.16	0.98	3.53	0.89
DV11 P	2.63	1.05	4.50	1.35
DV12 L	6.27	1.96	19.62	5.24
DV12 P	1.22	0.33	1.46	0.13
NEG	0.23	0.04	0.21	0.04

Table 7.6: Table of mean serum eqTRYP ELISA concentration results from serum collected from a local (L) or peripheral site (P) and stored at -20 °C or -80 °C (eqTRYP: equine tryptase. P: Peripheral. L: Local. NEG: serum from cyathostomin negative ponies. SEM: Standard Error of the Mean).

Mast Cell Recruitment and Activation as Measures of Cyathostomin Burden

Horse	Caecum (µg/g)	SEM (+/-µg/g)	RVC (µg/g)	SEM (+/-µg/g)	RB (µg/g)	SEM (+/-µg/g)
AB1	115.73	33.39	81.47	15.83	54.01	9.97
AB2	220.90	35.61	200.02	37.87	50.57	10.54
AB3	21.75	5.04	7.59	3.89	25.84	4.38
AB4	34.13	8.08	229.26	36.40	93.37	21.70
AB5	4.97	0.68	3.96	0.82	3.52	0.56
AB6	167.07	33.43	206.03	43.05	108.46	32.57
AB7	61.98	11.14	87.03	19.74	46.18	7.68
AB8	10.79	2.48	9.28	1.66	7.83	2.50
AB9	63.66	9.23	63.23	11.19	27.18	7.71
AB10	39.71	11.36	60.49	9.13	33.06	4.53
AB11	386.26	69.52	404.85	62.84	209.49	45.62
AB12	248.54	42.34	313.26	67.72	121.43	26.39
AB13	46.27	8.07	33.46	6.01	22.54	2.45
AB14	37.43	4.58	52.20	6.44	8.86	2.97
AB15	2.74	0.59	25.65	7.82	20.42	5.67
AB16	328.09	38.07	404.14	33.09	100.04	19.57
DV1	13.80	1.70	9.10	2.74	6.30	1.53
DV2	68.46	8.61	68.81	10.46	2.54	0.35
DV3	13.56	1.79	62.05	11.27	11.21	1.79
DV4	43.11	4.36	47.27	6.07	106.24	19.13
DV5	13.88	1.49	4.83	1.75	19.30	1.48
DV6	12.00	2.10	18.38	3.27	9.74	0.55
DV7	11.03	0.95	6.80	1.56	8.12	1.90
DV8	31.75	4.82	14.10	1.14	15.27	1.50
DV9	29.83	3.42	190.90	30.46	152.36	38.44
DV10	8.76	2.07	41.17	6.15	137.28	16.25
DV11	23.31	6.82	34.17	4.04	9.43	0.82
DV12	113.72	43.09	312.75	46.05	53.25	7.04

Table 7.7: Table of mean eqMCP-1 ELISA results from caecal, RVC and RB tissue (eqMCP-1: equine mast cell proteinase-1. SEM: Standard Error of the Mean. RVC: Right ventral colon. RB: Rectal biopsy).

Mast Cell Recruitment and Activation as Measures of Cyathostomin Burden

Horse	Caecum ($\mu\text{g/g}$)	SEM ($\pm\mu\text{g/g}$)	RVC ($\mu\text{g/g}$)	SEM ($\pm\mu\text{g/g}$)	RB ($\mu\text{g/g}$)	SEM ($\pm\mu\text{g/g}$)
AB1	71.44	22.72	77.02	9.18	49.85	10.58
AB2	224.22	46.30	185.40	26.62	31.57	6.96
AB3	30.88	3.22	24.95	5.00	21.49	6.09
AB4	15.89	3.98	113.54	27.37	47.25	11.59
AB5	24.92	6.23	19.08	4.39	3.59	6.79
AB6	77.69	25.82	97.31	15.76	113.34	44.01
AB7	53.86	7.16	59.66	0.42	26.44	7.72
AB8	90.00	1.15	70.41	28.80	56.11	4.39
AB9	89.70	11.79	140.44	32.11	30.57	6.72
AB10	41.83	5.74	73.44	3.73	39.96	5.47
AB11	120.11	17.01	215.95	1.68	54.25	11.25
AB12	120.54	14.07	91.79	6.37	39.80	3.58
AB13	42.17	16.15	54.07	13.54	23.74	7.05
AB14	31.92	6.82	32.60	6.19	9.73	4.04
AB15	5.00	0.87	20.76	6.31	8.93	2.52
AB16	82.03	25.38	94.89	32.08	30.54	6.17
DV1	10.83	1.31	13.21	1.69	6.36	2.30
DV2	50.77	3.01	39.71	5.20	6.31	0.42
DV3	21.50	2.63	37.50	2.63	8.68	0.95
DV4	19.83	2.41	23.84	2.91	24.34	2.15
DV5	93.89	30.07	9.08	1.02	34.63	5.09
DV6	24.68	6.43	44.52	9.86	20.63	4.32
DV7	187.11	115.71	64.71	27.13	209.55	126.94
DV8	25.62	3.08	18.87	3.70	13.48	5.20
DV9	14.68	3.80	112.51	49.74	38.72	5.23
DV10	12.32	2.43	26.59	3.77	40.42	4.85
DV11	60.81	12.94	41.07	17.73	20.07	5.27
DV12	306.19	223.65	371.40	187.99	33.81	6.53

Table 7.8: Table of mean eqTRYP ELISA results from caecal, RVC and RB tissue. (eqTRYP: equine trypsinase. SEM: Standard Error of the Mean. RVC: Right ventral colon. RB: Rectal biopsy).

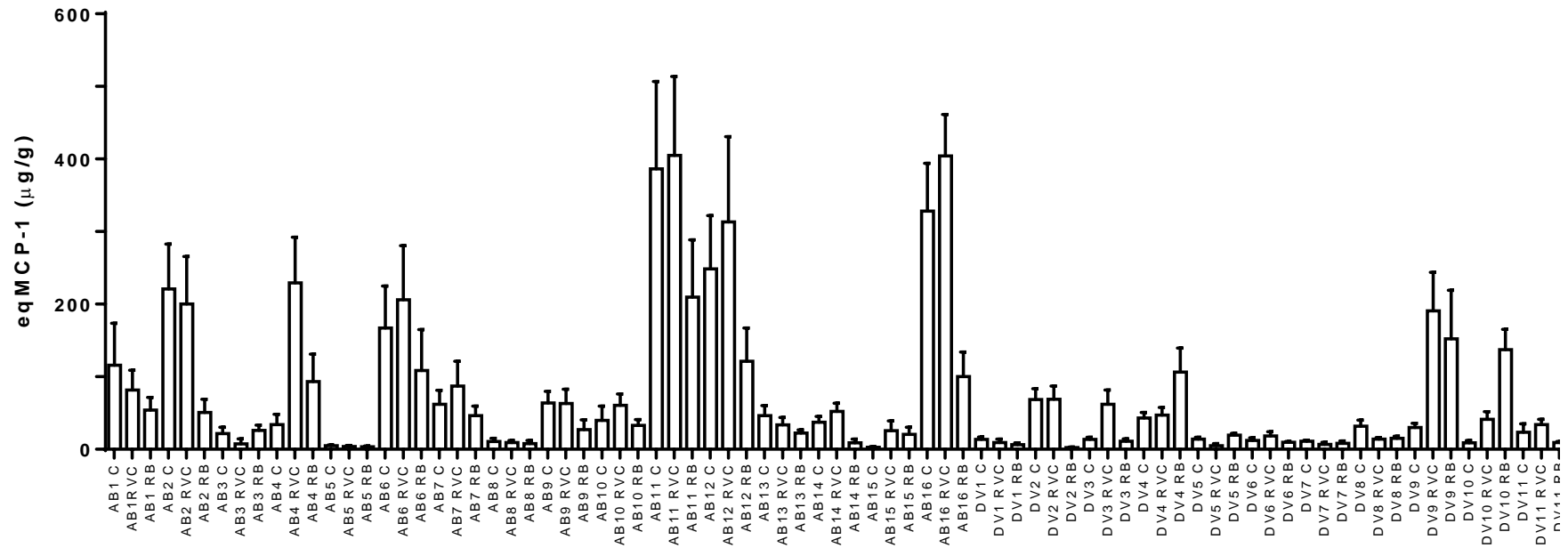


Figure 7.1: Barchart of mean eqMCP-1 tissue concentrations (µg/g). Error bars show standard error of the mean. (eqMCP-1: equine Mast Cell Proteinase-1; C: Caecum; RVC: Right ventral colon; RB: Rectal biopsy).

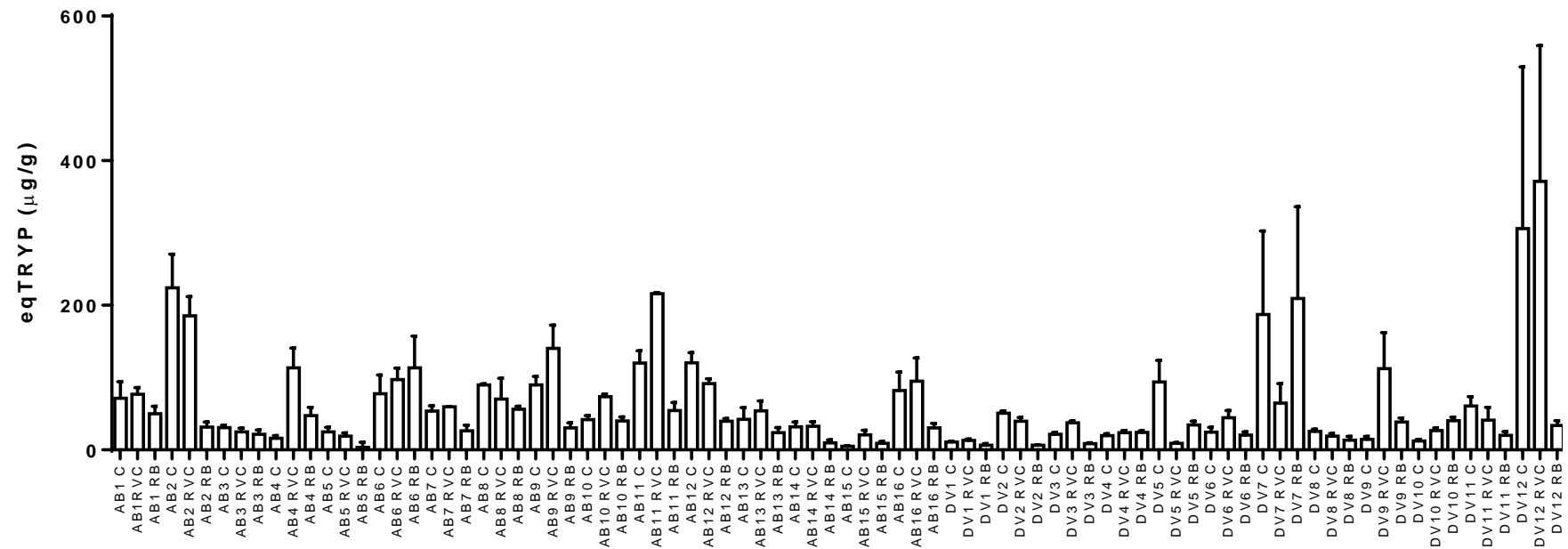


Figure 7.2: Barchart of mean eqTRYP tissue concentrations (µg/g). Error bars show standard error of the mean. (eqTRYP: equine Tryptase; C: Caecum; RVC: Right ventral colon; RB: Rectal biopsy).

8 Appendix B: Nucleotide and Protein Sequences

8.1 Nucleotide Sequences

8.1.1 Tryptase-like Proteinase-1(TLP1)

GCAGCAGGGACCAGCCAAGATGCCAAATCTGCTGGTGCTGGCACTGGCCCTCTGGTGA
 ACCTGGGCCACGCGGCCCTGCCCCAGGCCAGGCCCTGGAGCGAGAGGGCATCGTAGGA
 GGACAGGAGGCCTCTGGGAGCAAGTGGCCCTGGCAGGTGAGCCTGAGAAAGAACTG
 AATACTGGAAACACTTCTGCGGGGGCTCCCTAATCCACCCCCAGTGGGTGCTGACGGCGG
 CGCACTGTGTTGGACCGGACATTGAAGATTTAGAGACATCAGGGTGCAGCTGCGAGAG
 CAGCACCTCTATTATCGAGACCAGCTGCTGCCCCGTCAGCAGGATCCTCCCCACCCCTAC
 TACTACACAGTTGAGAACGGGGCCGACATTGCCCTGCTGGAGCTCCAGGACCCTGTCAAC
 ATCTCCAGCCATGTCCAGGTGGTCACTCTGCCCCCTGCCTCTGAGACCTTCCCCCGGGG
 ACGCCGTGCTGGGTGACAGGCTGGGGCGATGTCGACAATGGAGTCAGTCTGCCACCTCC
 GTTTCCTGAAAGGAAGTAAAGTCCCCATTGTGGAAAACAGCGTTTGTGACAGGAAAT
 ACCCACTGGCGTGTCCACGGGGGACAACATCCGGATTGTCCAGGCCGACATGCTGTGT
 GCAGGGAATAGGAGGCACGACAGCTGCCAGGGCGACTCTGGAGGACCCCTGGTGTGCAA
 GGTGAAGGGCACCTGGCTGCAGGCGGGCGTGGTCAGCTGGGCCAACAGCTGTGCTCAGC
 CCAACCGGCCGGGCATCTATACCCGTGTACCTACTACTTGGACTGGATCTACCAGTATG
 TCCCCAAGGACTCTTGAGCCCCGTCCCCAGGGCTGCCACCTGGATCAGCAGAGAAGCCA
 GCCCCCTCCTGTCTCACACCACTGCTTCCTGTCCAGGTGGTGTCTTCCCGTCCCTGCC
 CAGAGCCACCTCCCTGCACGGCCCAGGGAGCAGGCATGGACACTGGTCTCATTAAAGAG
 CATGGAAA

8.1.2 Granzyme B-like (GZMBL)

ATGCAGCCTCTCCTGTTCTGCTGGCGTTTTTACTATCCCCCTGGGCCAGAGGCAGGGGAG
 ATCATCGGGGGACATGAGGCCAGGCCCCACTCTCGCCCCTACATGGCATTGTGTCAAATT
 CTGATTGAACAAAAATGGAAGAGCTGCGGTGGTGTACTCGTGCGACAGGATGTTGTTCTG
 ACAGCTGCTCACTGCTGGGGAAGGTCAATCAAGGTGGCCCTGGGGGGCCACAACATTAA
 GAAGCAGGAGAGGACCCAGCAGGTCATCTCTGTGAAGGAAGCCATCCCCACCCACACT
 ATAATTCTAAGAAGATAGCCAACGACATCATGATACTAAAGCTGGAGAGAAAGGCCGAG
 CTGACTGCAGCTGTGCAGCCCATCAGCCTGCCCTGGGGAACAGCCCAGCTGAGGCCTGG
 AGAGGTGTGCAGTGTGGCAGGCTGGGGGAGAGTCACCCCAAATGGCAGAGGGTCAGAC
 ACCCTGCAGGAGGTGGAGCTGACTGTGCAGCAGGATCAGGTGTGCGAATCCTACTTTGG
 CAATTACAACCGTACCACTCAGCTGTGTGTGGGGGACCCGAAGGAAAAGAAGTCTTCCT
 ATAAGGGGGACTCCGGGGGGCCCTCTCGTGTGTAAGAACGTGATTCAGGGCATTGTCTCCT
 ATGGACGATCAGGCGGGCTTCCTCCACGGGCCTTCACCAAAGTCTCTAGTTTCCTGCCCT
 GGATAAAGAAAACCATGAAGGGGGCGGGCCCCATGGCCGAGGGTCAATGGGCACAGCAG
 CTTTGGCAGCTCTATCTTGCTGTGCTCAGAACCTACCAGGACTATCCCAACCTACCCC
 CCTCAGAGGCTAACTGGGAGCCATTCTTTGGGCAGACAAGACATTTAGTGGGCACCTAC
 GACCTATCAGGCTCAAGCAGATACAGAGCAAACACAGCCCAGCATCTTGAGCTCATGTT
 CCGAACATTACAGACCAGCAGACCAGTGAGGTCTGGAAAAGAAGAGAGGGGAGAGGAC
 TCAGAGAACATCAGGGAAAGGATTTTCCAGGATCCACCAGACCTTCAACGCTTGTTCCAA
 ACACCATTCTGTCTGCCACCCATGTGCCTGCAGCAGGAATTAAGGAATGA

8.1.3 Chymase-like Proteinase-1 (CLP1)

GTAACACCAGCAGCTGTGACCCCGGCAGACCTTCGGGAAAGATGCGGCCACTCCTGCTTT
TGTTAGCGTTTCTTCTGCCTCCTGAGGCTGGGACAGAGGACATCATCGGAGGACATGAGG
CCAAGCCCCACTCCCGTCCCTACATGGCATTGGTTCAATTTCTGTTTGAAGAGATACTGC
ACAGTTGTGGTGGTGTCTCGTGCGACAGGACATTGTTCTGACGGCAGCTCACTGCTGGG
GAAGATTAATGAATGTCACCCTTGGGGCCCAACATCAGGAGGCAGGAGAAGACCCAG
CAAGTCATCACTGTAAGACAAGCCATACACCACCCAGACTATAATCCTAAGAGCTTCTCC
AACGACATCATGTTACTAAAGCTGGGGAGAAGGGCCAAGCTGACTGCAGCTGTGCGGCC
CCTCAGCCTGCCAGGGGCAAGACCCAGGTGAGGCCCCGAGAGGTGTGCAGTGTGGCTG
GCTGGGGGCAACTTGCCCCGAAGGGCAGGTTCCCAGACACACTGCAGGAGGTGGAAGT
ACTGTGCAGCAGGATGAGGTGTGCGAATCCTACTTCCGCAATTATTTCAACAGTACCACT
CAGCTGTGTGTAGGGGATCCGAAAGATAAGAAGTCTTCCTTTTCAGGGTGACTCTGGGGG
CCTCTCATCTGTGAGAACGGGCTCCAGGGCATTGTCTCCTATGGACTAGATAACGGGAGT
ATTCCACAGGCCTTACCAAAGTCTCGAGTTTCTGCCCTGGATAAAGAAAACCATGAAA
AGGCTCTAACTGTGGGAGCCAGCCCACCAGCTCTGGAGCTGATCCAGAAACACCCAGC
AACTAAATAA

8.1.4 Granzyme(BGH)-like (GZM(BGH)L)

ATGCAGCCTCTTCTGCTCCTGCTGGCCATTTTAGTGCCCCCTGGGGCAGGGAGATCATCG
GGGGACATGAGGCCAGGCCCACTCTCGACCCTACATGGCATTCTGTTCAATTTCTGGTTG
AAGAGGCAAAGGACGGCTGTGGCGGTGTCTTGTGCAACAGGACTTTGTTCTGACGGCT
GCTCACTGCTGGGGAAGCTCAATCAAGGTGACCCTGGGGGCCCAACATCCAGAAGCA
GGAGAGGACCCAGCAGGTATCCCTGTGAAGGAAGCCATCCCCACCCAGACTATAATT
CTAAGAACTTCGCCAACGACATCATGTTACTAAAGCTGGAGAGAAGGGCCAAGCTTACC
GAAGCTGTGTGGCCCCTCAACCTGCCAGGGGCACAGCCAGGTGAGGCCCCGAGAGGT
GTGCCGTGTGGCTGGCTGGGGGAGAGTTGCCCTAAATGGCAGAGCGTCAGACACTCTGC
AGGAGGTGGAGCTGACCGTGCAGCAGGACCAGGAGTGCGAATCCTACTTACAAAAGTAC
AACAGTACCACTCAGCTGTGTGTGGGGGACCCGAAGGAAAAGAAGTCTTCCTTTAAGGG
GGACTCCAGGGGCACTCTTGTGTGTAAGAACGTGATCCAGGGCATTGTCTCCTATGGACG
AATAGGCGGGATTCTCCACAGGCCTTACCAAAGTCTCGAGTTTCTGCCCTGGATAAA
GAAAACCATGAAGGGGCGGGCCCTGTGGCAGAATTCAGGAAGCTCAGTGAACCTCGGGG
AGGGCAAAGGAATCCATGTGTAA

8.2 Protein Sequences

8.2.1 Tryptase-like Proteinase-1(TLP1)

MPNLLVLALALLVNLGHAAPAPGQALEREGIVGGQEASGSKWPWQVSLRKNTHEYWKHFCG
GSLHPQWVLTAACHCVGPDIEDFRDIRVQLREQHLYYRDQLLPVSRILPHPYYYTVENGADIA
LLELQDPVNISSHVQVVTLPASETFFPGTPCWVTGWGDVDNGVSLPPFPLKEVKVPIVENS
VCDRKYHTGVSTGDNIRIVQADMLCAGNRRHDSCQDSSGGPLVCKVKGTWLQAGVVSWA
NSCAQPNRPGIYTRVTYYLDWIYQYVPKDS

8.2.2 Granzyme B-like (GZMBL)

MQPLLFLLAFLSPGPEAGEIIGGHEARPHSRPYMAFVQILIEQKWKSCGGVLVRQDVVLTA
HCWGRSIKVALGAHNIKKQERTQQVISVKEAIPHPHYNSKKIANDIMILKLERKAELTAAVQP
ISLPWGTAQLRPGEVCSVAGWGRVTPNGRGSDDLQVELTVQQDQVCESYFGNYNRTTQLC
VGDPKEKKSSYKGDSSGGLVCKNVIQIVSYGRSGGLPPRAFTKVSSFLPWIKKTMKGRAPW
PRVNGHSSFGSSILPAAQNPTRTIPTYPQRLTGSHSFGQTRHLVGTIDLSGSSRYRANTAQHL
ELMFRTLQTSRPVRSKGKEERGEDSENIRERIFQDPPDLQRLFQTPFLSATHVPAAGIKE

8.2.3 Chymase-like Proteinase-1 (CLP1)

MRPLLLLLAFLPPPEAGTEDIIGGHEAKPHSRPYMALVQFLFEEILHSCGGVLVRQDIVLTA
CWGRLMNVTLGAHNIRREQKTQQVITVRQAIHHPDYNPKSFSNDIMLLKLGRRAKLTA
PLSLPRGKTQVRPGEVCSVAGWGQLAPKGRFPDDLQVELTVQQDEVCEYFRNYFNSTTQL
CVGDPKDKKSSFQGDSSGPLICENGLQGIVSYGLDNGSIPQAFTKVSSFLPWIKKTMKRL

8.2.4 Granzyme(BGH)-like (GZM(BGH)L)

MQPLLLLLAILVPPGAEEIIGGHEARPHSRPYMAFVQFLVEEAKDGCGGVLVQQDFVLTA
CWGSSIKVTLGAHNIQKQERTQQVIPVKEAIPHPDYNPKNFANDIMLLKLERRAKLTEAVWP
LNLPRGTAQVRPGEVCRVAGWGRVALNGRASDDLQVELTVQQDQECESYLQKYNSTTQL
CVGDPKEKKSSFQGDSSRGTLVCKNVIQIVSYGRIGGIPPQAFTKVSSFLPWIKKTMKGRALW
QNSGSSVNLGEGKGIHV

9 Appendix C: General Laboratory Solutions and Procedures

9.1.1 Carnoy's Solution

150 ml chloroform

300 ml absolute alcohol

50ml glacial acetic acid

9.1.2 Peptic Digestion Solution

10 g pepsin (Fisher)

15ml HCL

1L warm water

The pepsin was dissolved in a small volume of the warm water before being added to the acid and the rest of the water.

9.1.3 0.5% Toluidine Blue Solution

Toluidine Blue powder

HCL

Distilled water

The Toluidine blue stain was prepared by adding Toluidine blue powder to distilled water, concentrated hydrochloric acid was added to give an acidity of pH 0.5. The solution was made up to final volume with distilled water to give a 0.5% w/v solution. It was left overnight on a magnetic stirrer and filtered before use.

9.1.4 0.1% Eosin Solution

Eosin

70% ethanol

9.1.5 ELISA Coating buffer

5.3g Na₂CO₃ (anhydrous)

4.2g NaHCO₃

The above were combined and made up to 1 L with dH₂O and the pH adjusted to 9.6 using HCl.

9.1.6 Western Transfer Buffer

850 ml Distilled water

100 ml Methanol

50 ml NuPAGE transfer buffer (20 x; Invitrogen)

The above were combined and stored at room temperature.

9.1.7 TNTT

50 ml 1 M Tris

146.1 g NaCl

2.5 ml Tween 20

0.5 g Thimerasol

The above were combined and made up to 5 litres with dH₂O and the pH adjusted to 7.4 using HCl.

9.1.8 Tris-acetate-EDTA (TAE) Buffer (50X)

242 g Tris base

57.1 ml Glacial acetic acid

100 ml 0.5M EDTA (pH 8)

The above were combined and made up to 1 L with dH₂O to make a 50 X solution.

9.1.9 1 % Agarose Gel

2 g agar

4 ml 50 x TAE

20 µL 10,000 x Gel Red

The above were combined and the volume made up to 200ml with dH₂O. The solution was heated in a microwave on full power for approximately 3 min and then allowed to cool to 45 °C. The gel was then poured into a gel electrophoresis tank with a comb pre-positioned to give the correct number and size of wells. Once the gel had set, the comb was removed and 1 x TAE poured over to submerge the gel. The samples were loaded alongside a Ready-Load™ 1 kb DNA Ladder (Invitrogen) and the tank attached to a power supply. 100 V were applied for approximately 40 mins and the gel visualised using UV.

9.1.10 DNA Loading Buffer

0.25 % Bromophenol blue

0.25 % Xylene cyanol FF

40 % (w/v) Sucrose in water

A 6 X gel loading buffer was made by combining the above and stored at 4 °C.

9.1.11 Western Blot

The gel was transferred to a nitrocellulose membrane using the Iblot blotting system as per the manufacturer's instructions (Thermo Fisher). After removal of the ladder (which was placed in distilled water) TNTT was used to block the membrane overnight at room temperature. The primary antibody was diluted 1/100 in TNTT, poured onto the membrane and left to rock gently. After 1 h the antibody was washed off and three 10 min washes with TNTT were performed. The secondary antibody was also diluted 1/1000 TNTT and the same process was repeated. The bands were visualised using the ECL system (GE Healthcare) followed by the SigmaFast 3,3'-diaminobenzidine tablet set (Sigma) as per the manufacturers' instructions and the reaction stopped with distilled water.